

Studies Towards the Total Synthesis of the Chivosazoles

This dissertation is submitted for the degree of Doctor of Philosophy at University of
Cambridge

Jialu Jin

Sidney Sussex College

December 2017

Acknowledgement

First and foremost, I would like to thank my PhD supervisor Professor Ian Paterson for giving me the opportunity to work on such a challenging and interesting project in his group. This project could not have been completed smoothly without his unfailing support. Thank Professor Jonathan Goodman for being my supervisor at the end of my PhD and giving me tremendous motivation and encouragement for writing my thesis and helped me revise it.

A massive thank you to Simon Williams, who is really talented and always helpful. Working with him was quite a pleasant experience. Thank Mike Housden, who was always happy to answer my questions about my research project and never failed to tell “educational” jokes. Thank you to Mengyang Xuan, who helped me get familiar with everything when I first came to Cambridge. I am grateful to previous group members who worked on this project and made amazing contributions: Lisa Gibson, Jennifer Kan and Mungyuen Li.

Thank you to Melvyn Oriss, Matt Pond, Nic Davies and Naomi Hobbs who provided invaluable technical support. Thank Jennifer Kan, Mungyuen Li and Professor Gordon Florence for solving the problems of my project through emails. My gratitude also goes to Simon Williams, Talia Pettigrew and Nelson Lam for proofreading this thesis. I would like to pay tribute to lab 122 members for running NMR, sharing reagents and creating a lovely working environment. Thank Nick Bampos and Deborah Longbottom for regularly checking if everything goes well with me during my writing.

Personally, I would like to thank Isabel Wilkinson, Talia Pettigrew and Andrew Philips, who always took time to talk to me and cheer me up when I felt upset in the lab. I am really grateful to my flatmate Thomas Choi who sorts out everything in the house and keeps the flat a cosy place. Many thanks to my parents, who have been supporting and encouraging me. Special thanks go to Cambridge Trust and Sidney Sussex College for helping me survive in UK by offering me the scholarships.

Declaration

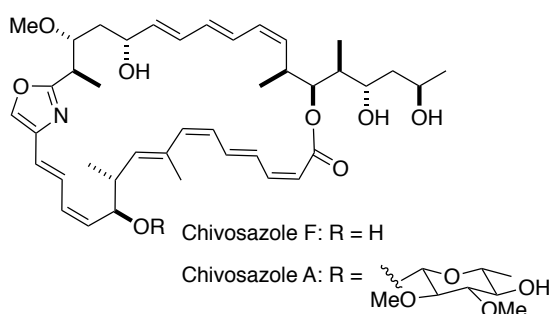
This dissertation is the result of my own work and contains nothing that is the outcome of work in collaboration with others, except as specified in the text or by conventional references. It is not substantially the same as any that I have submitted, or, is being concurrently submitted for a degree or diploma or other qualification at the University of Cambridge or any other University or similar institution except as declared in the preface and specified in the text. I further state that no substantial part of my dissertation has already been submitted, or, is being concurrently submitted for any such degree, diploma or other qualification at the University of Cambridge or any other University or similar institution except as declared in the Preface and specified in the text. In accordance with regulations, this dissertation does not exceed 60,000 words in length.

Jialu Jin

Cambridge, December 2017

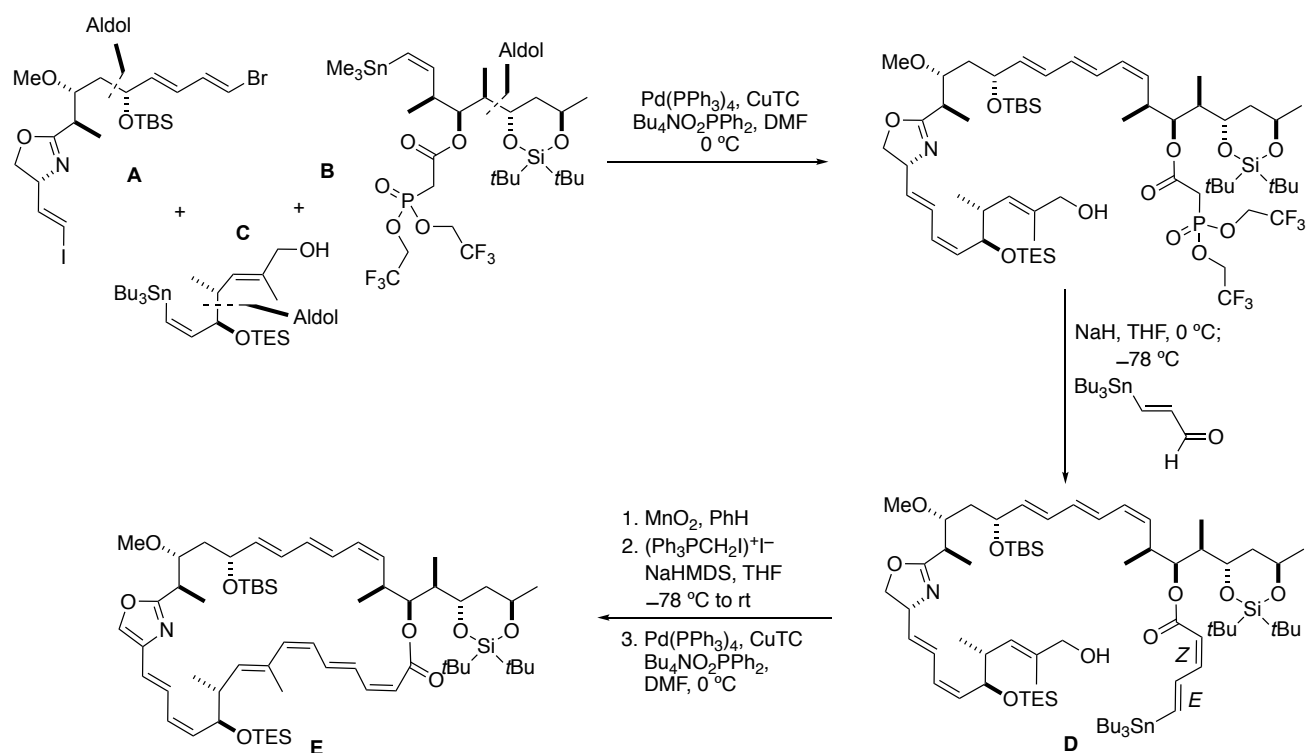
Summary

First isolated from the myxobacterium *Sorangium cellulosum* So Ce12 in 1994, the chivosazoles have been reported to possess antiproliferative activity against human cancer cell lines, as well as antifungal activity. This thesis focuses on studies towards the total synthesis of chivosazole F. Some developments towards the total synthesis of chivosazole A are also discussed.

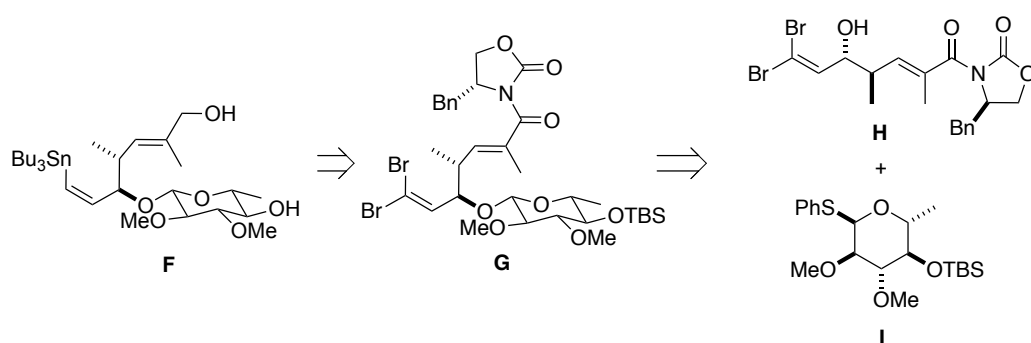


Chapter 1 discusses the isolation, characterisation and biological activity of the chivosazoles, as well as the first total synthesis of chivosazole F reported by the Kalesse group and the previous work towards synthesising chivosazole F in our group.

Chapter 2 describes the synthesis of the three key fragments **A**, **B** and **C**, their coupling reactions and subsequent modifications for assembling the backbone of chivosazole F. Paterson boron aldol methodology and Evans-Tishchenko reduction were utilised to construct the 1,4-*syn* and 1,3-*anti* stereochemical relationships within both fragment **A** and fragment **B**. Di-*tert*-butyl silyl group was used for the efficient and precise protection of the terminal diol of **B**. The key stereochemistry of fragment **C** was defined with a vinylogous Mukaiyama aldol reaction. Site-selective Stille cross-coupling reactions of the three fragments, *via* a one-pot process, rapidly installed the requisite stereodefined polyene motifs within chivosazole F. Optimised Still-Gennari-type HWE olefination conditions were applied to install the (2*Z*,4*E*)-dienoate in **D**. MnO₂-mediated double oxidation of **D** turned the terminal alcohol into an aldehyde and the oxazoline into an oxazole, followed by a Stork-Zhao olefination transforming the aldehyde to a *Z*-vinyl iodide for a macro-Stille coupling reaction, which achieved the ring closure to afford macrocycle **E**.



Chapter 3 discusses the developments towards the synthesis of the southern fragment **F** of chivosazole **A**. Sugar **I** was prepared first and conditions were screened for the glycosylation of **H** and **I** to afford **G**.



Chapter 4 outlines the achievements of this research and points out some future issues that need to be tackled.

TABLE OF CONTENTS

Nomenclature

Abbreviations

Chapter 1 Introduction	1
1.1 Natural products in drug discovery	1
1.2 Myxobacteria	3
1.3 Chivosazoles	4
1.4 Kalesse's synthesis of chivosazole F.....	7
1.5 Synthetic strategy evolution.....	11
1.5.1 The first-generation endgame strategy.....	11
1.5.2 The second-generation endgame strategies.....	18
1.5.3 The third-generation endgame strategies	21
Chapter 2 Results and discussion on Chivosazole F	30
2.1 Synthesis of the C14-C26 north-western fragment.....	31
2.2 Synthesis of the C27-C35 north-eastern fragment	41
2.2.1 Modifications of the C27-C35 Fragment	41
2.2.2 Installation of the dienyl stannane motif.....	49
2.3 Synthesis of the C7-C13 Southern fragment	58
2.4 Fragment coupling and endgame strategy	61
2.4.1 One-pot Stille cross-coupling	61
2.4.2 Construction of the macrocycle	64
2.5 Conclusions.....	69
Chapter 3 Results and discussion on glycosylation.....	70
3.1 Glycosyl fluoride synthesis.....	72
3.2 Glycosylation	75
3.2.1 Glycosylation with glycosyl fluoride.....	75
3.2.2 Glycosylation with thioglycoside	76
Chapter 4 Conclusions and future work	78

Chapter 5 Experimental	82
5.1 General and analytical procedures	82
5.2 Preparation of Reagents.....	84
5.3 Detailed experimental procedures.....	85

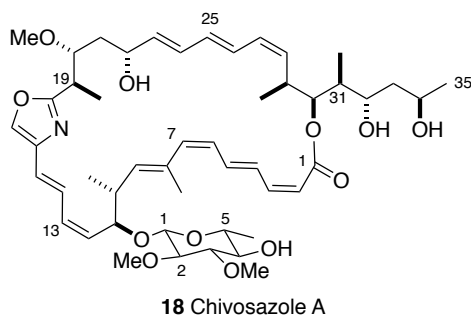
References

Appendix

Nomenclature

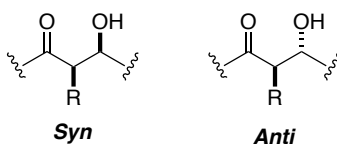
Compound numbering

The numbering system used for any structurally related compounds will be with reference to the numbering of the carbon chain of chivosazole A (**18**). This numbering is given on the structure and is used in ^1H NMR assignments. When atoms on the macrocycle and the sugar are both referred to, the sugar numbering will be primed e.g. C1', C2' etc.



Syn and *Anti* diastereomers

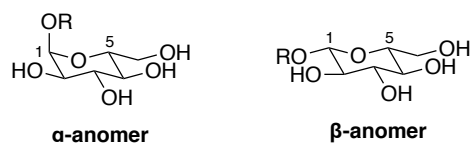
The *syn* and *anti* convention for assigning the stereochemistry of acyclic compounds is used in this dissertation.



α and β anomers

The α and β convention in carbohydrate nomenclature is used to describe the relative configurational relationship between the anomeric centre (C1) and the anomeric reference centre

(C5).



The naming of compounds follows the IUPAC convention.

Abbreviations

Ac	acetyl
AIBN	azobisisobutyronitrile
Ar	aryl
App	apparent
Bn	benzyl
br	broad
brsm	based on recovered starting material
Bu	butyl
BAIB	iodobenzene diacetate
BINAP	2,2'-bis(diphenylphosphino)-1,1'-binaphthyl
CuTC	Copper(I) thiophene-2-carboxylate
COSY	¹ H- ¹ H correlation spectroscopy
d	doublet
dba	dibenzylideneacetone
dr	diastereomeric ratio
DAST	(diethylamino)sulphurtrifluoride
DCM	dichloromethane
DCC	<i>N,N'</i> -dicyclohexylcarbodiimide
DDQ	2,3-dichloro-5,6-dicyano-1,4-benzoquinone
DIBAL-H	diisobutylaluminium hydride
DMAP	4- <i>N,N</i> -dimethyaminopyridine
DMB	3,4-dimethoxybenzyl
DMBTCA	3,4-dimethoxybenzyl trichloroacetimidate
DMF	dimethylformamide
DMP	Dess-Martin periodinane
DMSO	dimethylsulphoxide

EDC	1-ethyl-3-(3-dimethylaminopropyl) carbodiimide
ee	enantiomeric excess
eq.	equivalent(s)
Et	ethyl
g	gram(s)
h	hour(s)
HMPA	hexamethylphosphoramide
HOBt	hydroxybenzotriazole
HPLC	high-performance liquid chromatography
HRMS	high resolution mass spectroscopy
HWE	Horner-Wadsworth-Emmons
Hz	Hertz
IC ₅₀	median inhibition constant that reduces the effect by 50%
Ipc	<i>iso</i> -pinocampheyl
IUPAC	International Union of Pure and Applied Chemistry
IR	infrared spectroscopy
<i>J</i>	¹ H- ¹ H coupling constant
LLS	longest linear sequence
m	multiplet
M	moles per litre
MS	molecular sieves
Me	methyl
mg	milligram(s)
MHz	Mega-Hertz
min	minute(s)
mL	millilitre(s)
mmol	millimole(s)
MTPA	α-methoxy-α-(trifluoromethyl)phenylacetic acid

NBS	<i>N</i> -bromosuccinimide
nm	nanometre(s)
NMR	nuclear magnetic resonance
nOe	nuclear Overhauser effect
PE	petroleum ether
Ph	phenyl
pin	pinacol
PMB	4-methoxybenzyl
PMBTCA	4-methoxybenzyl trichloroacetimidate
PPTS	pyridinium <i>p</i> -toluenesulfonate
<i>i</i> Pr	isopropyl
ppm	parts per million
py.	pyridine
q	quartet
qn	quintet
R	unspecified substituent
R _f	TLC retention factor
rt	room temperature
s	singlet
So ce	<i>Sorangium cellulosum</i>
t	triplet
TBAF	tetra- <i>n</i> -butylammonium fluoride
TBME	methyl <i>tert</i> -butyl ether
TBS	<i>tert</i> -butyldimethylsilyl
TCBC	trichlorobenzyl chloride
TEMPO	2,2,6,6-tetramethyl-1-piperidinyloxy
TES	triethylsilyl
Tf	trifluoromethane sulfonyl
TFA	trifluoroacetic acid

THF	tetrahydrofuran
TIPS	triisopropylsilyl
TMS	trimethylsilyl
TLC	thin layer chromatography
UV	ultra violet

Chapter 1 Introduction

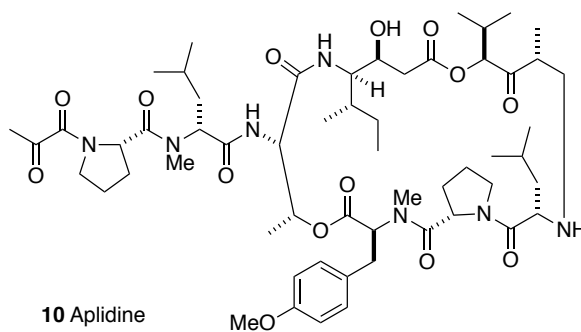
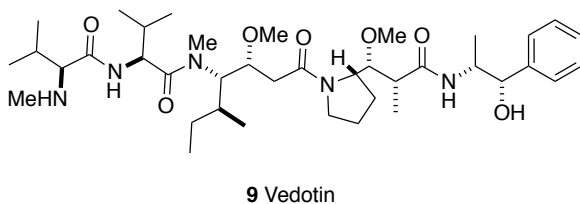
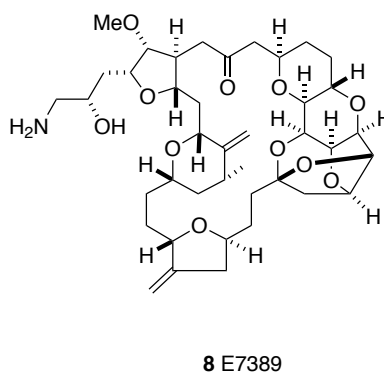
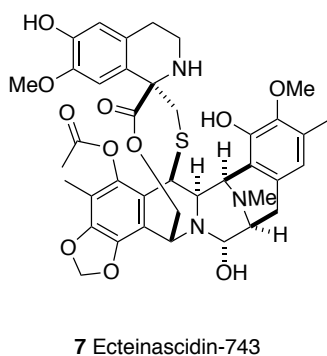
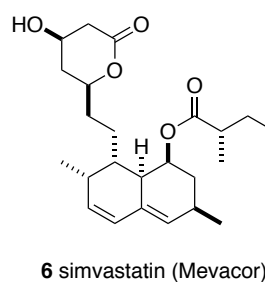
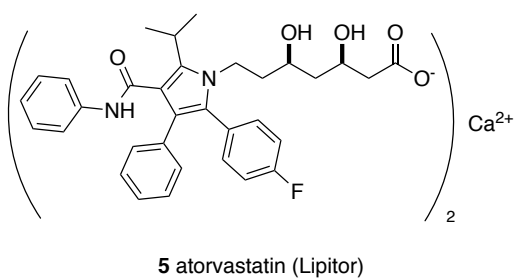
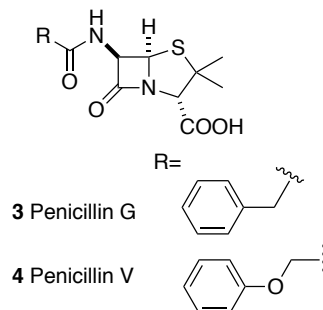
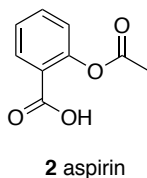
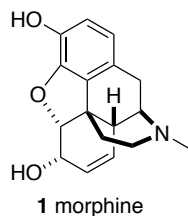
1.1 Natural products in drug discovery

Natural products have been a research focus for drug discovery since the early 1800s. The development of the first commercialised natural product, morphine (**1**), by E. Merck in 1826 and the promotion of the first semi-synthetic, natural product-derived drug, aspirin (**2**), by Bayer in 1899 started a new age in which medicines could be isolated from plants and then utilised independently from the original sources.^{1,2}

The landmark discovery of penicillin (**3**, **4**) by Fleming in 1929 extended the research focus from plants to microbes as sources of novel compounds possessing antibacterial, antifungal or antiparasitic activities.^{1,3} Other important properties of microbial natural products include antitumour and anticholesterolemic activities. The latter were exploited in the development of atorvastatin (Lipitor, **5**) and simvastatin (Mevacor, **6**) from the fungal metabolites mevastatin and lovastatin, inhibitors of HMG-CoA reductase. These drugs are among the best-selling class of all time.^{3,4} During investigation of microbes for the production of antibiotics, research on plants has mainly focused on anticancer drug discovery as in the case of Taxol and the vinca alkaloids.^{5,6}

In this context, marine organisms did not receive much attention until the latter part of the 20th century. Considering that over 90% of macro-organism phyla originate from the seafloor and that marine micro-organisms are much more diverse compared to macro-organisms, marine organisms can be regarded as an invaluable source of secondary metabolites, often having novel structures and biochemical modes of action.⁷ Particular attention has been paid to the anticancer properties of many marine natural products. To date, several marine-derived drugs have been approved for commercial use, including Ecteinascidin-743 (ET-743/trabectedin/Yondelis, **7**), eribulin mesylate (E7389/Halaven, **8**) and monomethylauristatin E (Vedotin, **9**). Some marine-derived agents in

clinical trials include aplidine (plitidepsin/dehydrodidemnin B, **10**), kahalalide F (**11**), PM10450 (zalypsis, **12**) and PM1183 (lurbinctedin, **13**).⁸



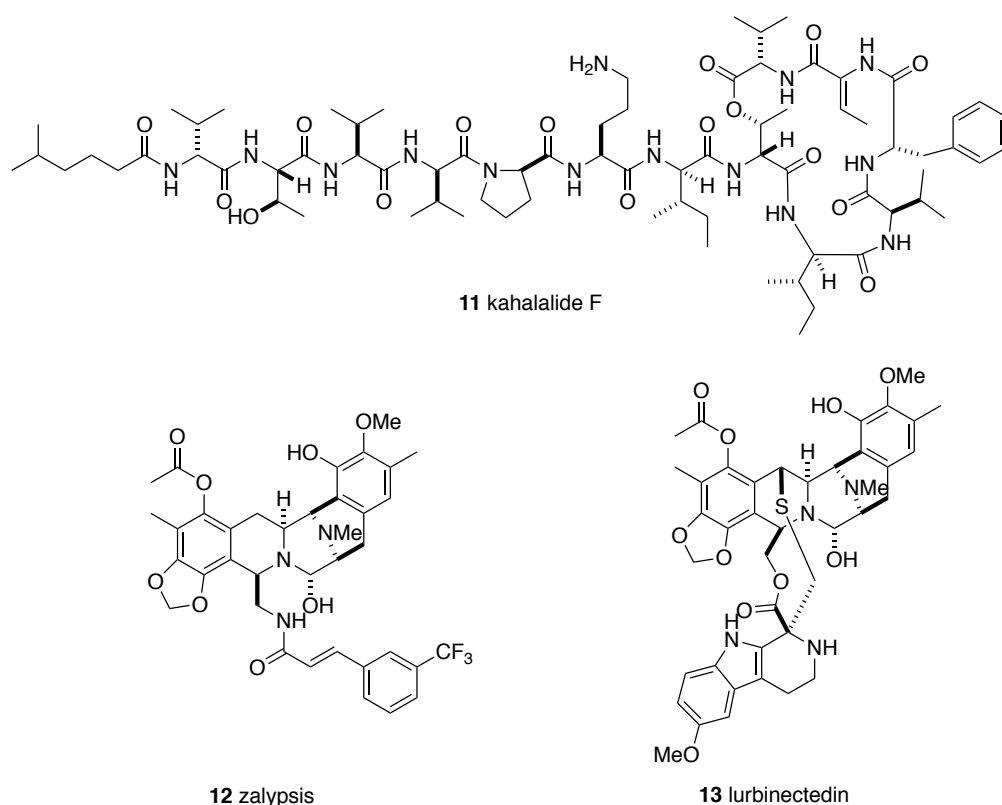


Figure 1.1: Commercialised or in trial natural products and natural product-derived drugs

1.2 Myxobacteria

After an intensive study on actinomycetes over the last century, the potential of this class of bacteria for providing new bioactive structures has been shrinking. As a promising alternative, myxobacteria have become a novel research focus. Among Gram-negative bacteria, myxobacteria are special because of their ability to move by gliding and creeping on surfaces and to form fruiting bodies, a property similar to eukaryotic organisms or fungi, which distinguishes them from other prokaryotic bacteria.⁹ Of great interest to natural product chemists are their bioactive secondary metabolites based on novel molecular scaffolds.¹⁰ Among the genres of myxobacteria, *Sorangium* is of special interest, having provided nearly half of the known secondary metabolites of myxobacterial origin.¹¹ For example, five compound families have been characterised from *S. cellulosum*: tubulin destabilizers disorazoles (**14**), eubacterial RNA polymerase inhibitors sorangicins (**15**), bactericidal sorangiolides (**16**), the sulfangolides (**17**), and the antifungal and anticancer chivosazoles

(18).^{12,13,14,15,16}

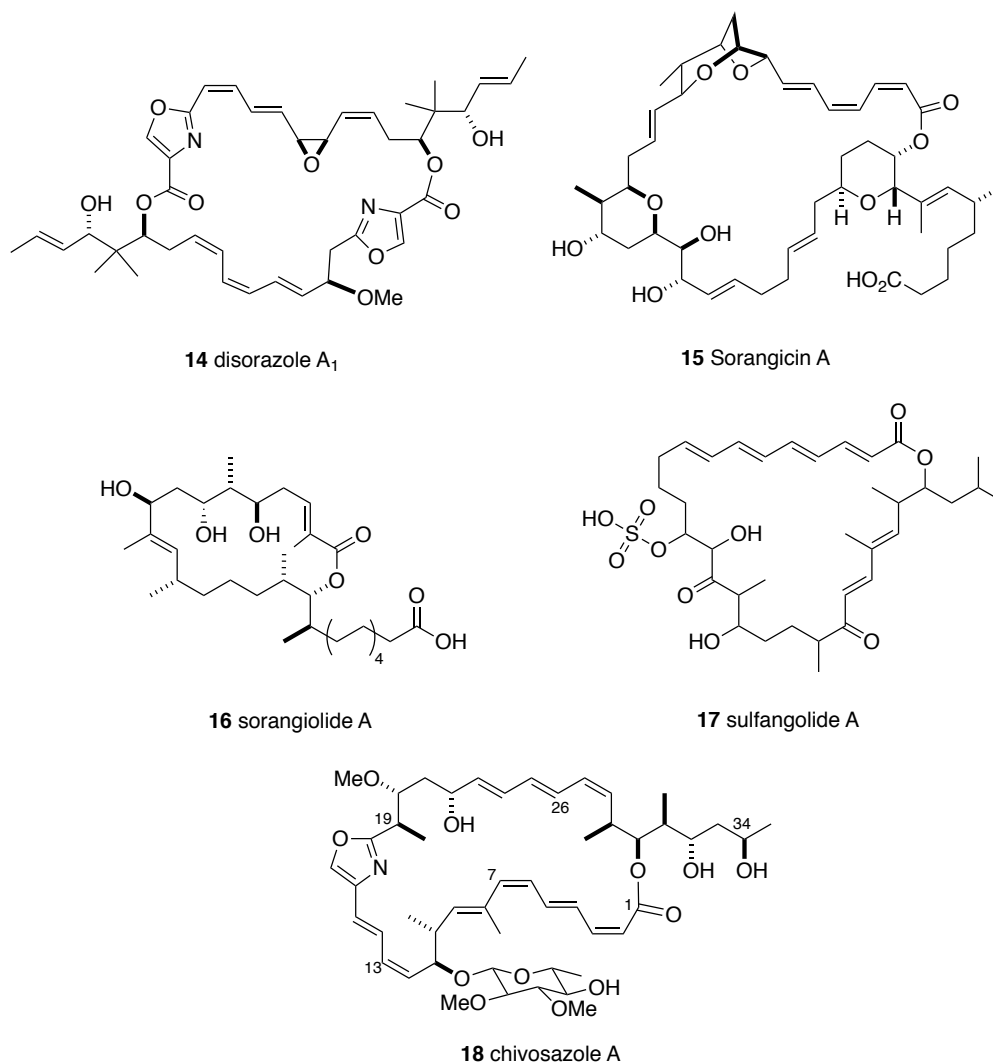


Figure 1.2: Five compounds from different families characterised from *So ce12*

1.3 Chivosazoles

The chivosazoles were first isolated from the myxobacterium *So ce12* in 1994 during research on the disorazoles.¹³ Subsequently, several other strains of *S. cellulorum* were also reported to be sources of chivosazoles. Strain *So ce192* was chosen for the purpose of isolation of the chivosazoles as it only contains soraphens as co-metabolites. Separation of chivosazoles A-E was achieved by a sequence of purification steps: elution from adsorber resin, partition between methanol and *n*-heptane, silica-gel

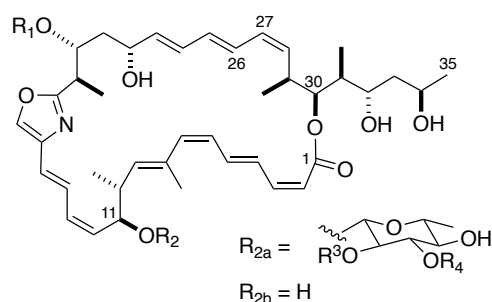
flash chromatography, and a combination of normal-phase and reversed-phase HPLC.¹⁶

Chivosazoles are potent and selective modulators of actin, which is the most abundant protein in eukaryotic cells and accounts for about 10% of the total protein mass.¹⁷ F-actin is the constituent of microfilaments, which provide structural support for cells and mediate many essential processes such as cell motility, cell division and many more.¹⁸ The binding of chivosazoles to actin causes inhibition of actin polymerisation and depolymerisation of F-actin, resulting in a cytostatic effect on cells. Chivosazole A was reported to possess potent antiproliferative activity against human cancer cell lines ($IC_{50} = 2.9$ nM for K-562; $IC_{50} = 3.5$ nM for KB-3-1; $IC_{50} = 8.1$ nM for A-549).¹⁹ Chivosazole F is similar to latrunculin A²⁰ as they both interact with actin by direct binding, and the binding sites for chivosazole F and latrunculin A partially overlap. Latrunculin A has proven its usefulness in interrogating actin-related processes. As a microbial metabolite, chivosazole F is potentially more useful, because collection of chivosazole F is more convenient compared to the tedious isolation or complicated synthesis of latrunculin A.²¹

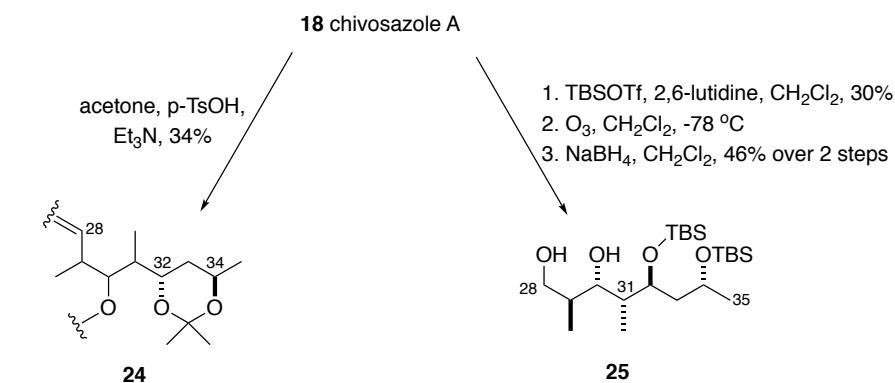
The planar structure of chivosazole A was elucidated based on mass spectrometry and NMR methods that confirmed the oxazole-containing 31-membered macrocycle, three conjugated polyene regions, ten stereocentres and a 6-deoxyglucose derivative. The structures of chivosazoles B-E were identified by comparing their MS and NMR data with that of chivosazole A. Chivosazole F was isolated from *So ce885* as the only chivosazole without the glycosyl side-chain at C11.¹⁶ The relative and absolute configuration of chivosazole A was elucidated in 2007 through a combination of chemical degradation, partial synthesis, NMR spectroscopy and genetic analysis.²²

Table 1.1: Structures of chivosazole A-F

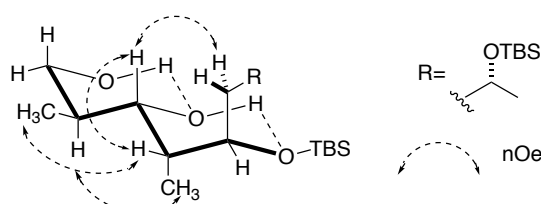
Chivosazoles		R ₁	R ₂	R ₃	R ₄
18	A	Me	R _{2a}	Me	Me
19	B	H	R _{2a}	Me	Me
20	C	Me	R _{2a}	H	H
21	D	H	R _{2a}	H	Me
22	E	H	R _{2a}	H	H
23	F	Me	R _{2b}	—	—



The double bond geometries in chivosazole A were deduced from their vicinal coupling constants ($^3J = 14\text{--}15\text{ Hz}$ for *E*-alkenes; $10\text{--}12\text{ Hz}$ for *Z*-alkenes). The 1,3-*anti* relationship between the alcohols at C32 and C34 was established by formation of the acetonide derivative **24** (Scheme 1.1) and use of the ^{13}C NMR method described by Rychnovsky and Evans.²³ To identify the configuration at the C29, C30 and C31 stereocentres, TBS-protected chivosazole A was degraded into fragment **25** (Figure 1.3). NOESY analysis of fragment **25**, together with the established 1,3-*anti* relationship of the C32-C34 diol allowed the relative stereochemistry of the whole fragment to be deduced. Subsequently, fragment **25** was synthesised independently to confirm the proposed relative stereochemistry and to determine the absolute configuration by comparison of NMR data and $[\alpha]_D$ values.



Scheme 1.1: Formation of acetonide derivative **24** and chemical degradation of chivosazole A



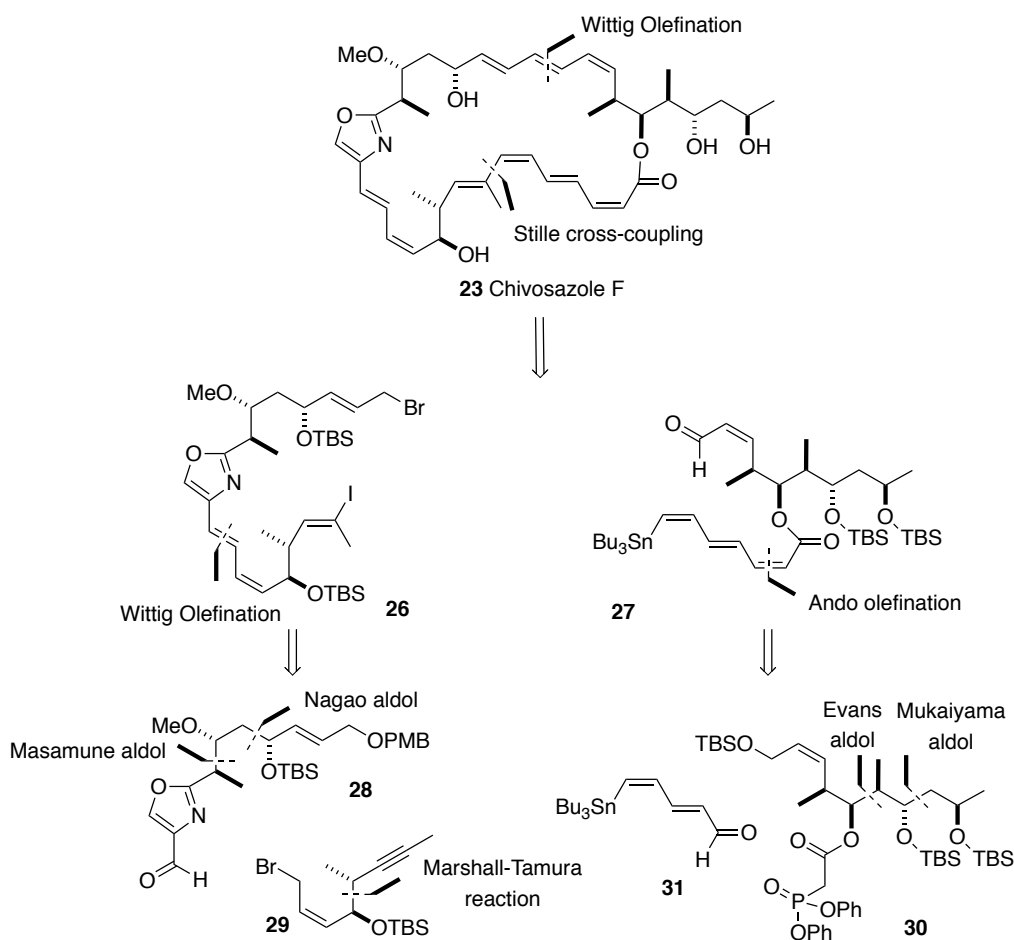
Due to the limited availability of chivosazole A, assignment of the remaining five stereocentres was achieved by a combination of computational modelling and genetic analysis.²² Molecular modelling of the chivosazole skeleton without all substituents provided a set of energy-minimised conformers first. The substituents were then superimposed onto the conformers, the configuration of which was manipulated to best fit the NMR coupling data, leading to an assignment of the absolute

configuration of chivosazole A. This assignment was subsequently supported by analysing chivosazole biosynthesis.²⁴

Confirmation of the proposed structure and the significant biological profile inspired efforts to investigate a total synthesis that led to the completion of chivosazole F by Kalesse in 2010,²⁵ which is discussed in detail in the next section.

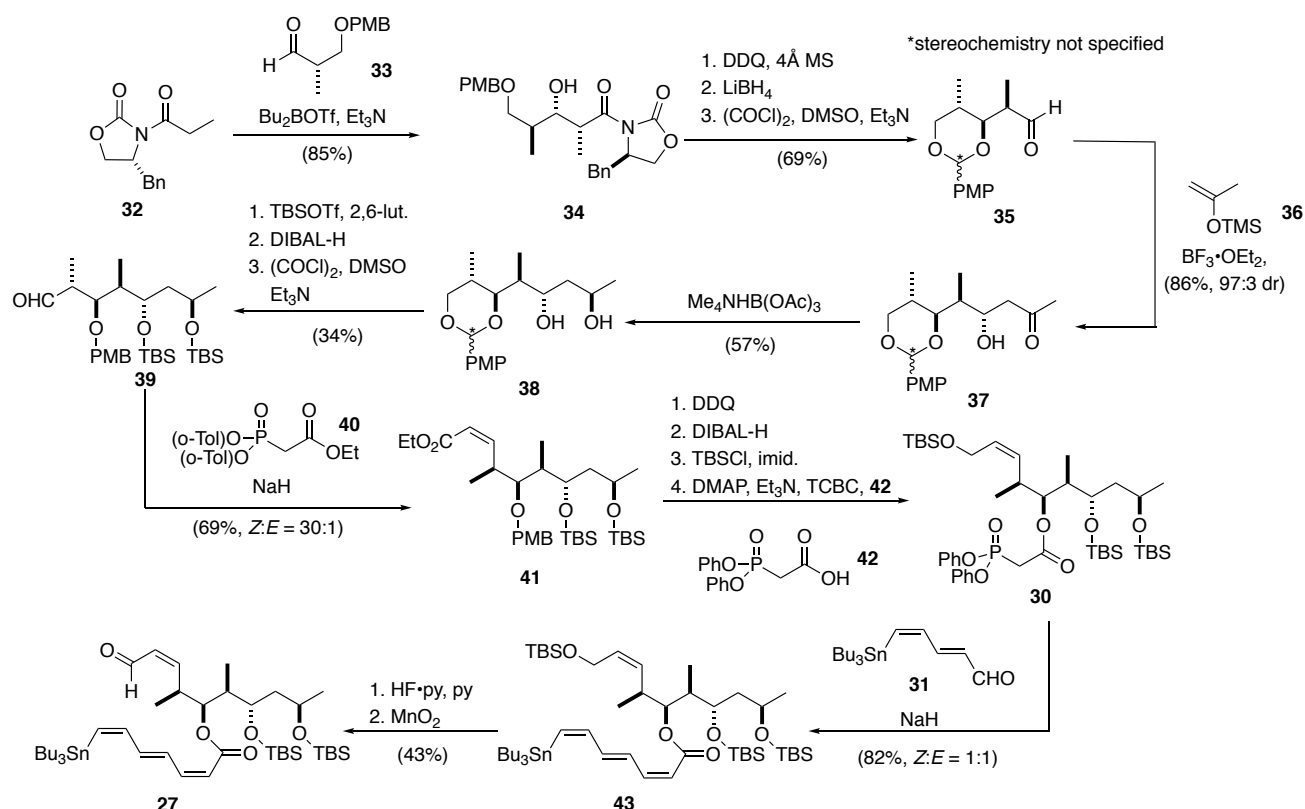
1.4 Kalesse's synthesis of chivosazole F

Considering the potential chemical instability of the polyenes, the triene region and tetraene region were installed last as part of the macrolactone formation. After retrosynthetic analysis, fragments **28-31** were proposed for the carbon backbone assembly (Scheme 1.2).



Scheme 1.2: Retrosynthetic analysis of chivosazole F (Kalesse)

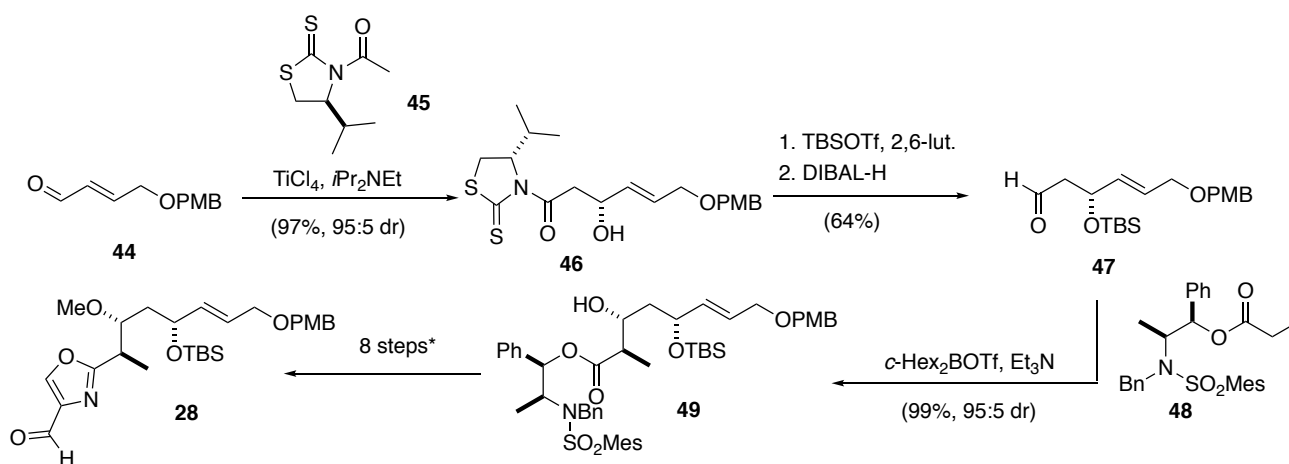
In the forward synthesis, preparation of fragment **27** was based on the synthetic route used to access fragment **25** for stereochemical verification (Scheme 1.3). Diastereoselective aldol methodology developed by Evans was first applied to install the 1,2-*syn* relationship in adduct **34**. Acyloxazolidinone **34** was transformed into aldehyde **35** in a sequence of three steps, followed by addition of silyl enol ether **36** via an 1,3-*anti*-selective Mukaiyama aldol reaction based on the Evans polar model²⁶ to give β -hydroxy ketone **37**. Reduction of ketone **37** under Evans-Saksena conditions ($\text{Me}_4\text{NBH}(\text{OAc})_3$, MeCN/AcOH)²⁷ constructed the 1,3-*anti* diol in **38**. Subsequent elaboration, including diol protection, PMP-acetal opening and alcohol oxidation, provided aldehyde **39**. The (*Z*)-double bond of enoate **40** was installed by Ando olefination²⁸ and the product was transformed into fragment **30** over four further steps. The coupling of phosphonate **30** and aldehyde **31** afforded the required olefin as a 1:1 mixture of geometrical isomers, which is a significant flaw in this route. Silyl deprotection and MnO_2 promoted oxidation provided eastern hemisphere **27**.



Scheme 1.3: Synthesis of eastern hemisphere **27** (Kalesse)

To commence the synthesis of the northeastern fragment **28**, a Nagao titanium-mediated acetate aldol reaction²⁹ was employed to afford adduct **46**. The newly formed hydroxyl group was protected

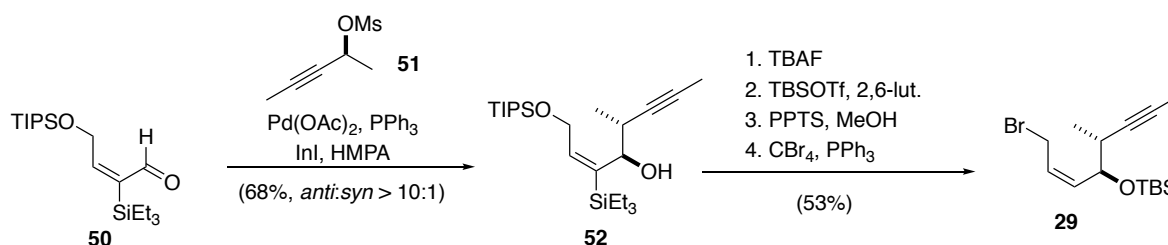
as a TBS ether and aldehyde **47** was provided by reduction with DIBAL-H. A boron-mediated aldol reaction³⁰ between aldehyde **47** and ester **48** under Masamune conditions gave *anti* adduct **49**. Aldehyde **28** was synthesised from **49** through a sequence of methylation, deprotection, oxidation, esterification, oxazole formation under Wipf conditions³¹ and DIBAL-H reduction.



* (1) MeI, Ag_2O , 3 Å MS; (2) LiAlH_4 ; (3) $(\text{COCl})_2$, DMSO, Et_3N ; (4) NaClO_2 , NaH_2PO_4 , $t\text{BuOH}$, H_2O ; (5) SerOMe, EDC, HOBT, $i\text{Pr}_2\text{NEt}$; (6) DAST; (7) DBU, BrCCl_3 ; (8) DIBAL-H

Scheme 1.4: Synthesis of northwestern fragment **28** (Kalesse)

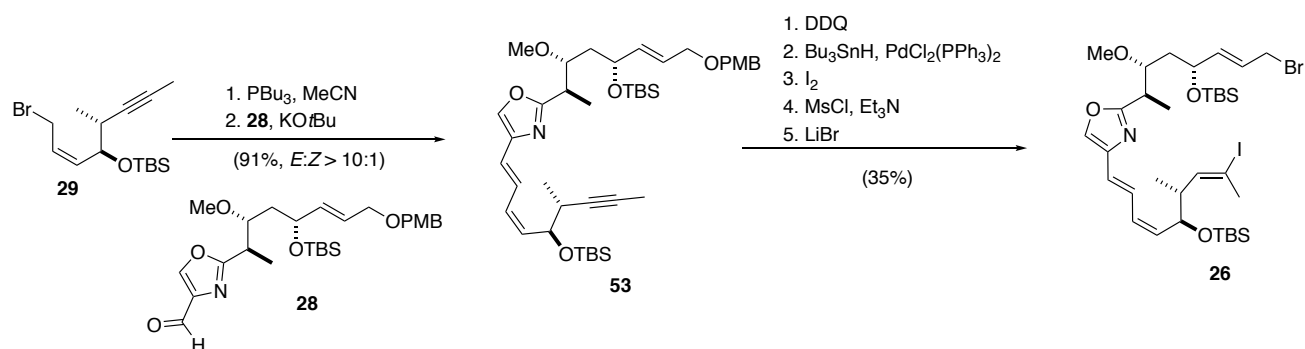
The *anti* relationship within fragment **29** was established by a Marshall-Tamura reaction with aldehyde **50** bearing a triethylsilyl ether in the α -position to increase the modest diastereoselectivity of the unsubstituted aldehyde (Scheme 1.5).³² Subsequent protecting group elaborations and bromination provided allyl bromide **29** in 53% yield over four steps.



Scheme 1.5: Synthesis of southwestern fragment **29** (Kalesse)

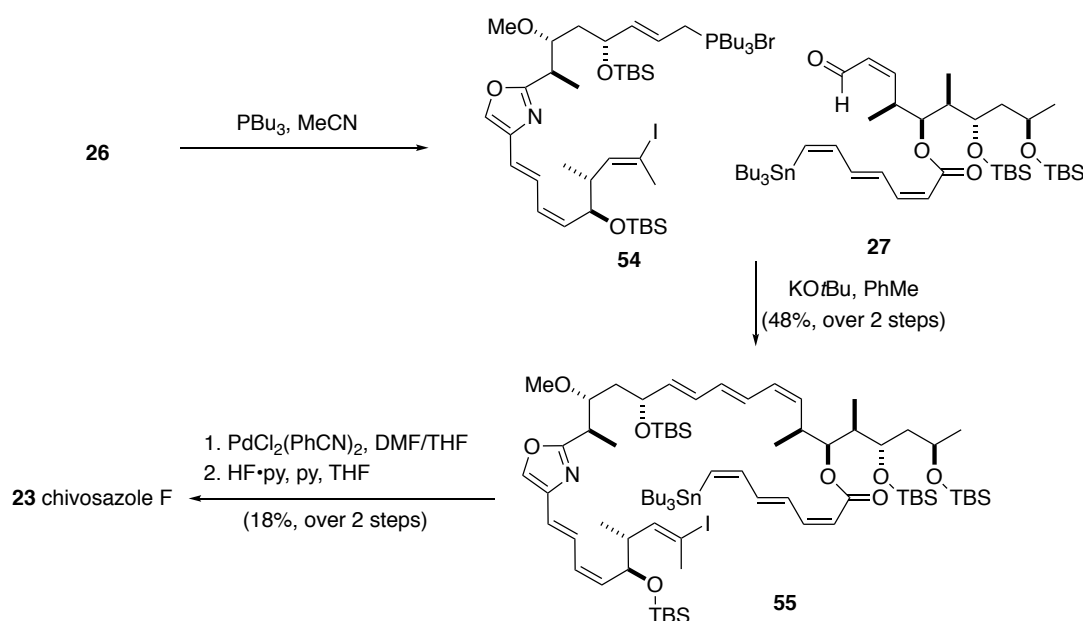
Wittig olefination³³ of aldehyde **28** with the phosphonium ylid derived from allyl bromide **29** was used to couple the fragments with good (*Z*)-selectivity. Intermediate **53** was then transformed into

western hemisphere **26** via a sequence of PMB deprotection, palladium-catalysed hydrostannylation, tin-iodine exchange and bromination.



Scheme 1.6: Synthesis of western hemisphere **26** (Kalesse)

With both hemispheres in hand, fragment union was achieved by conversion of bromide **26** into the phosphonium salt and subsequent Wittig reaction with **27** to construct the (*E,E,Z*)-triene configuration. Intramolecular Stille coupling was employed to achieve macrocyclisation to give the fully protected chivosazole. Finally, after global silyl deprotection, the total synthesis of chivosazole F was completed. The spectroscopic data were in accordance with the data originally reported for natural chivosazole F and confirmed the previously proposed configurational assignment.



Scheme 1.7: Completion of the first synthesis of chivosazole F by Kalesse et al.

Although the total synthesis was an impressive achievement in itself, the route suffers from several

deficiencies, such as poor selectivity in defining the olefinic geometry of the southern tetraenoate and low overall yield (<0.5%). Also, the protecting group strategy does not allow access to chivosazole A as the protecting group on C11 alcohol is not differentiated.

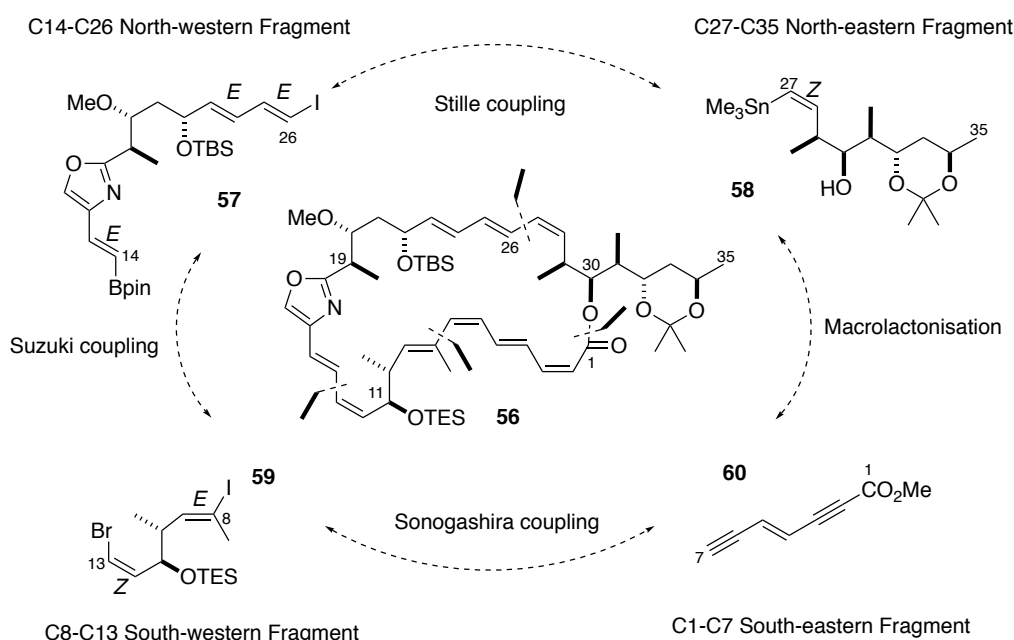
Studies towards the total synthesis of the chivosazoles in the Paterson group were intended to develop a more efficient synthetic strategy with better stereochemical control and higher overall yield. Furthermore, by differential protection of the C11 alcohol, selective glycosylation could be incorporated into the route, making chivosazole A accessible.

1.5 Synthetic strategy evolution

The chivosazoles have proved to be highly challenging synthetic targets, and considerable efforts have previously been pursued in our group, leading to a complex story as summarised here.

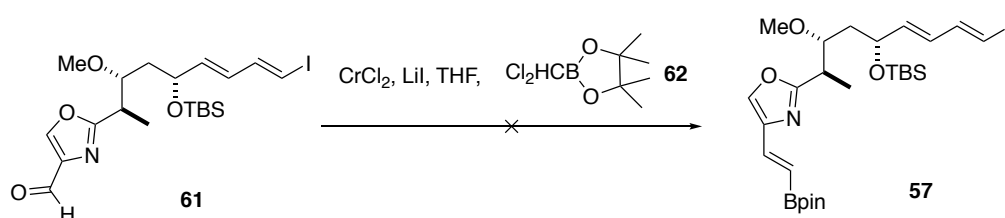
1.5.1 The first-generation endgame strategy

Through the exploration of the syntheses of initially selected chivosazole fragments and their proposed couplings, the endgame strategy has been through three iterations. These strategies are discussed in turn. In the first-generation endgame strategy proposed by Lisa Gibson and Jennifer Kan,^{34,59} the parent chivosazole structure was disconnected to reveal four fragments **57**, **58**, **59** and **60** of similar size and complexity, making the route highly convergent (Scheme 1.8). Sonogashira coupling of **59** and **60** would afford the southern hemisphere of chivosazole F. Due to the sensitivity of the tetraene, the (2*Z*)-alkene and the (6*Z*)-alkene were masked as alkynes in **60** so that the tetraene motif could be unveiled at a late stage. Stille coupling of **57** and **58** would generate the northern hemisphere, which could then be coupled with the southern hemisphere by Suzuki coupling. Ester hydrolysis followed by macrolactonisation was envisaged to close the ring. Alkyne reduction would then unveil the tetraene and afford macrolactone **56**.



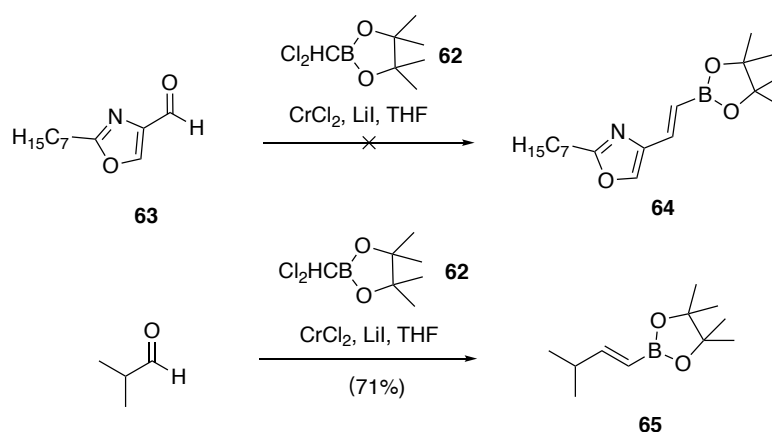
Scheme 1.8: First-generation endgame strategy

Investigation of the synthesis of the C14-C26 northwestern fragment **57** was carried out by Gibson.³⁴ It was found that installation of the pinacol boronate moiety onto a precursor oxazole aldehyde **61** via Takai olefination³⁵ was unsuccessful (Scheme 1.9).



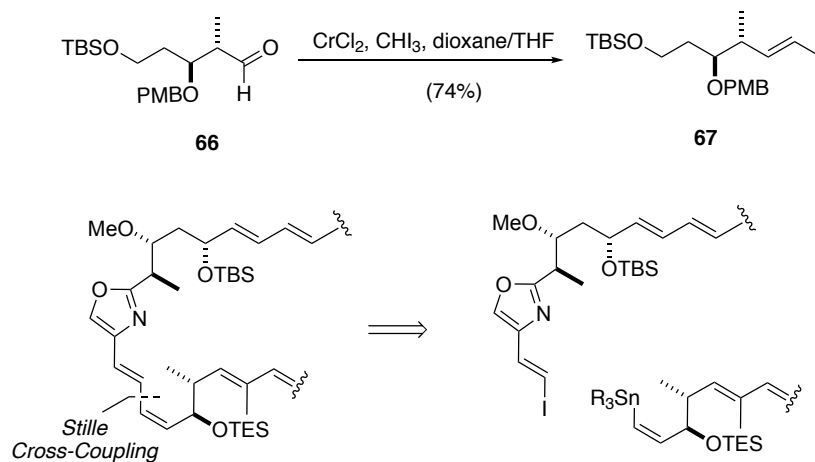
Scheme 1.9: Attempt to install pinacol boronate

The reason for the failure was deduced to be the incompatibility of the oxazole aldehyde moiety with the Takai olefination conditions used for this transformation. A test of this hypothesis was carried out by submitting oxazole aldehyde **63** and isobutyraldehyde to Takai olefination using reagent **62** (Scheme 1.10). Takai olefination of oxazole aldehyde **63** did not provide the expected product **64**. However, Takai olefination of isobutyraldehyde afforded the desired (*E*)-olefinic product **65** in 71% yield. Based on the test result, it appeared that installing pinacol boronate onto oxazole aldehyde **61** would prove challenging. A different coupling strategy was required to replace the Suzuki coupling.



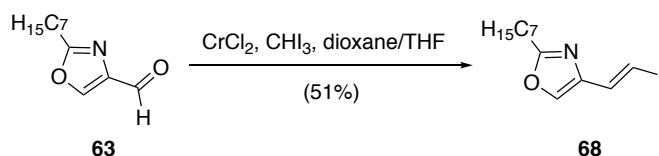
Scheme 1.10: Model systems for Takai olefination

With experience in our group of transforming aldehyde **66** into vinyl iodide **67** under more conventional Takai conditions using CHI_3 (Scheme 1.11),³⁶ it was proposed that the vinyl iodide might be an easier alternative functionality to install. This could then participate in a Stille cross-coupling to form the C14-C15 bond in our endgame strategy.



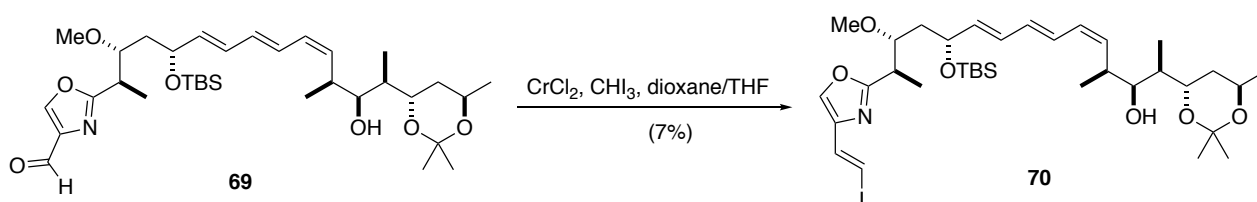
Scheme 1.11: Modified endgame strategy

Following this modification, an initial trial of the Takai olefination with the model oxazole aldehyde **63** afforded vinyl iodide **68** in 51% yield (Scheme 1.12).



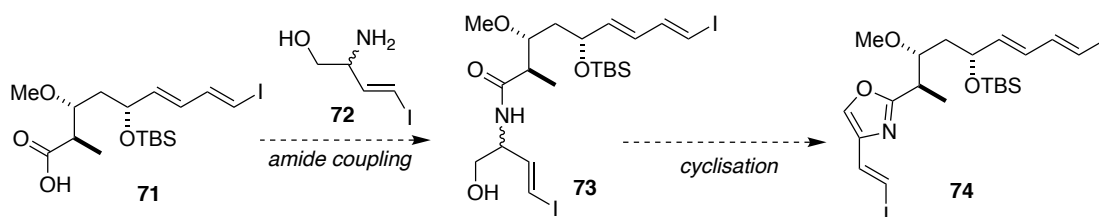
Scheme 1.12: Model system for testing the Takai olefination

When the same Takai reaction conditions were applied to the real system **69**, however, the desired vinyl iodide **70** was formed in a meagre 7% yield (Scheme 1.13).



Scheme 1.13: Takai olefination of **69**

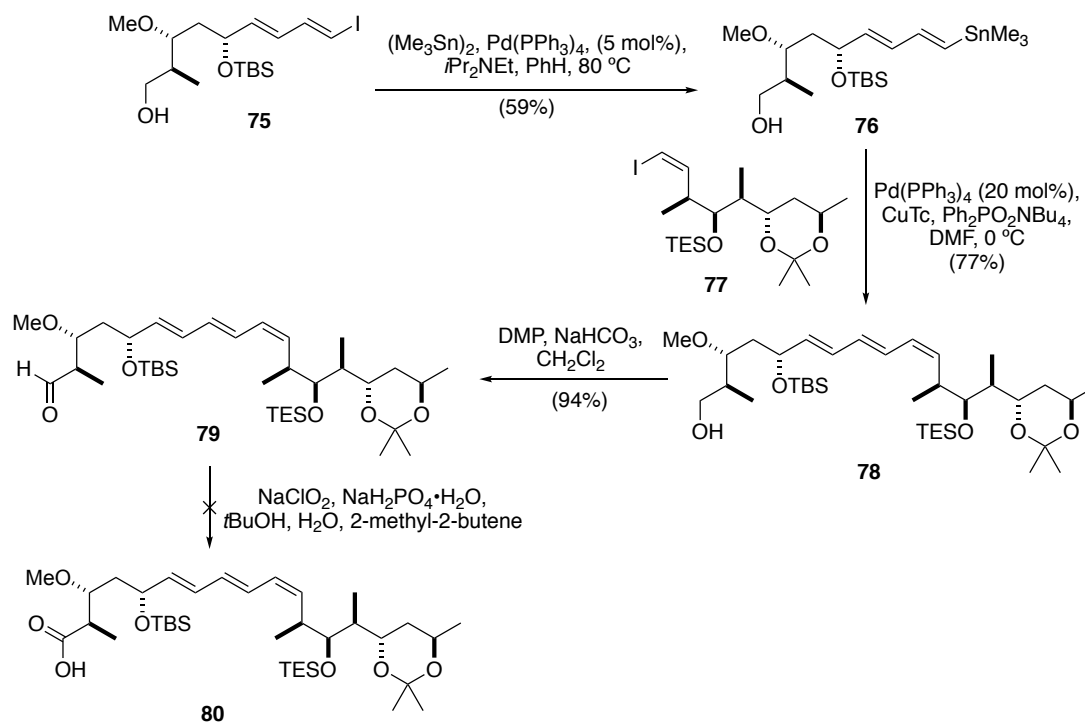
Given that neither of these two homologation approaches produced a synthetically useful result, pre-installing the vinyl iodide prior to formation of the oxazole was considered, as this could introduce the desired coupling handle with the additional benefit of greater convergency. Amide coupling of amino alcohol **72** with acid **71** followed by cyclisation was expected to yield the oxazole species **74** with the desired (*E*)-vinyl iodide moiety (Scheme 1.14).



Scheme 1.14: Envisioned pre-installation of the vinyl iodide and subsequent oxazole formation

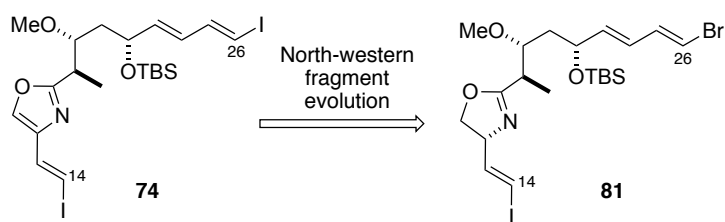
Having a vinyl iodide at both ends of the linchpin fragment **74** might cause a site-selectivity problem for the fragment coupling. To overcome this, construction of the northern hemisphere **78** was completed before installation of the oxazole vinyl iodide (Scheme 1.15). Iododiene **75** was transformed by Wulff-Stille stannylation³⁷ to stannane **76**, which was coupled with vinyl iodide **77**

to construct the northern hemisphere **78**. Alcohol **78** was then oxidised to aldehyde **79**. However, Pinnick oxidation of aldehyde **79** caused the triene to isomerise, yielding no desired product **80**. This result indicated that the vinyl iodide should be installed before the critical Stille fragment coupling.



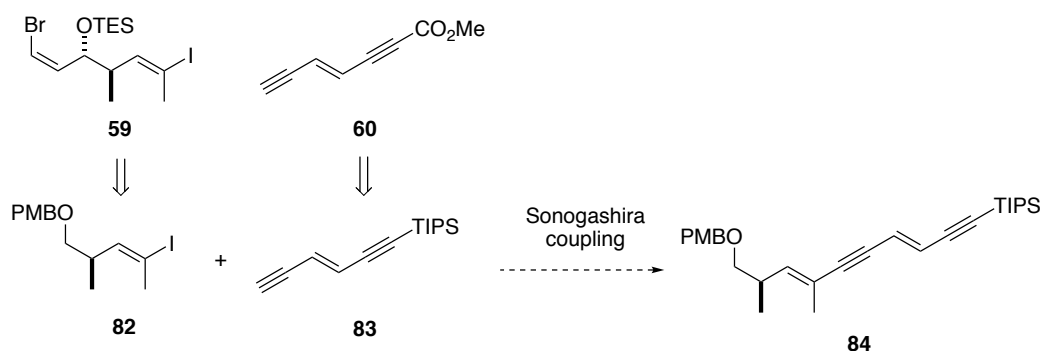
Scheme 1.15: Synthesis and modification of the northern hemisphere **78**

To tackle the site-selectivity issue for the fragment coupling, Mungyuen Li³⁸ prepared *bis*-halide **81** (Scheme 1.16), with a bromide at C26 in place of an iodide, as shown in Scheme 1.16. This approach was based on the premise that the reactivity of the vinyl iodide and the vinyl bromide should be sufficiently differentiated for the subsequent site-selective Stille cross-coupling at C14. The oxazole was masked as an oxazoline as de-iodination was observed during oxidation of the oxazoline to the required oxazole. It was concluded that this oxidation would best be carried out after cross-coupling to avoid this de-iodination side reaction.



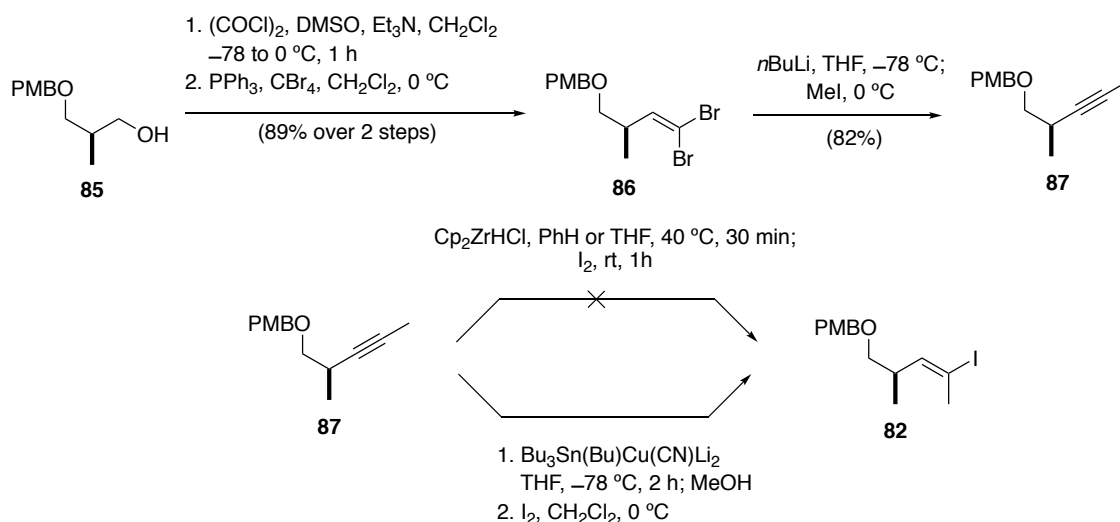
Scheme 1.16: Envisaged revision to fragment **74**

The focus was then turned to the Sonogashira coupling between the south-western fragment **59** and the south-eastern fragment **60**, which was studied by Jennifer Kan.⁵⁹ Two model compounds **82** and **83** were designed to test the Sonogashira coupling (Scheme 1.17).



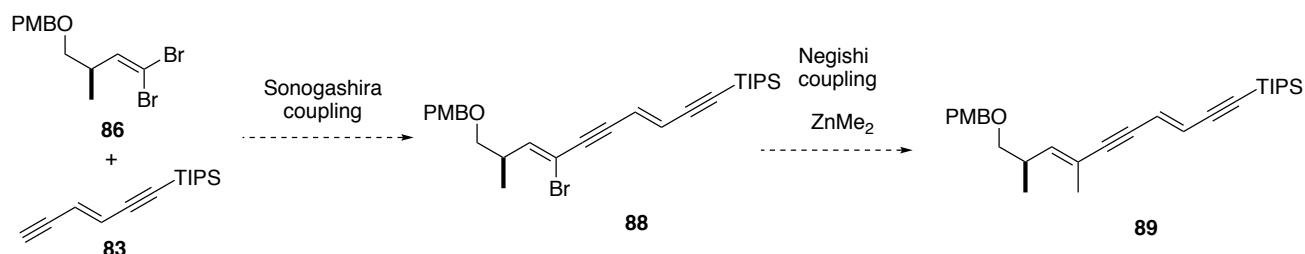
Scheme 1.17: The planned Sonogashira coupling

Preparation of iodide **82** started with Swern oxidation³⁹ and Corey-Fuchs olefination⁴⁰ of (*S*)-Roche ester-derived alcohol **85**. The resulting dibromide **86** was treated with *n*BuLi and quenched with methyl iodide, which gave alkyne **87**. Generating iodide **82** from alkyne **87** by Schwartz reagent-mediated hydrozirconation⁴¹ was undermined by isomerisation and PMB-deprotection. Stannylcupration and halogen-tin exchange proved more successful and provided vinyl iodide **82** as a single stereoisomer (Scheme 1.18).



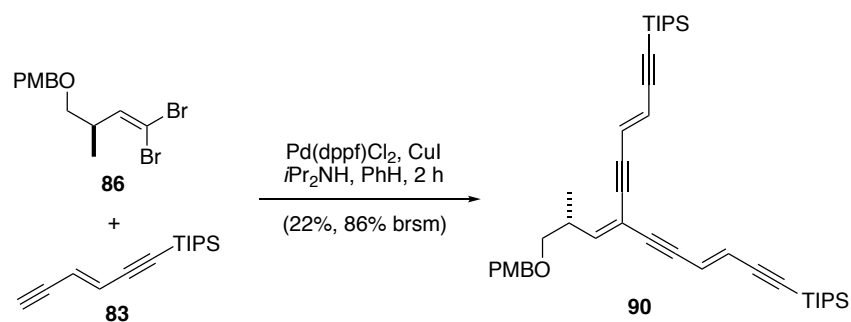
Scheme 1.18: Synthesis of (*E*)-vinyl iodide **82**

Though vinyl iodide **82** could be synthesised, it required an excess of n BuLi, Bu₃SnH and I₂. An alternative option would be to employ the intermediate dibromoolefin **86** for the coupling instead with control over the stereochemistry based on the steric effect of the vicinal (*Z*)-substituent,⁴² which could lead to a shorter, more economical and practical route (Scheme 1.19).



Scheme 1.19: An alternative way of constructing dienediynes **89**

However, after a screen of Sonogashira coupling conditions by Kan,⁵⁹ Uenishi conditions⁴³ were applied for the coupling between **86** and **83**, which yielded **90** as the sole product (Scheme 1.20).

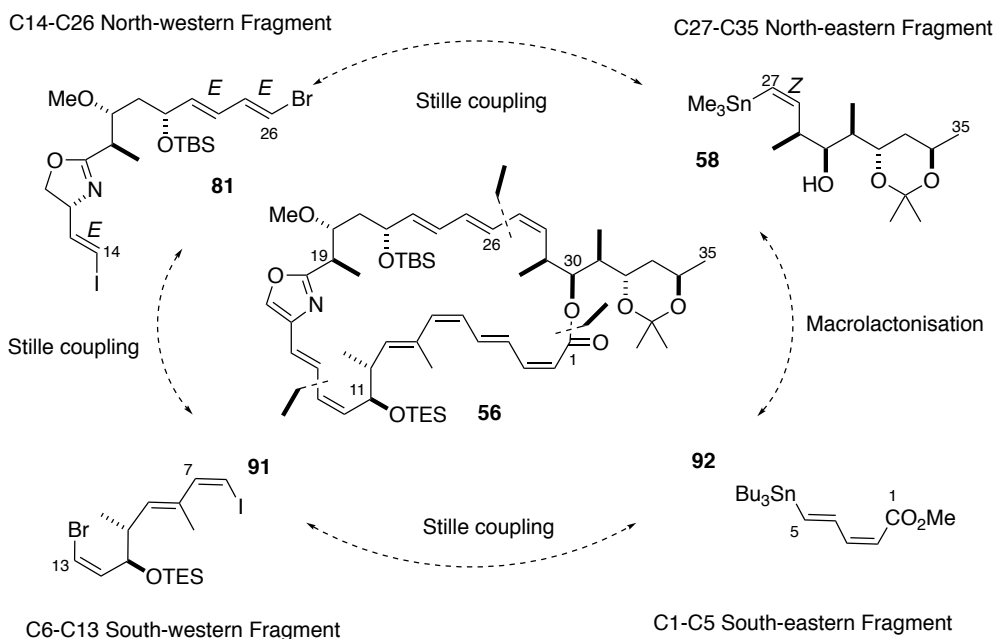


Scheme 1.20: Sonogashira coupling of dibromoolefin **86** with enediyne **83**

With the unsatisfying result of these trials and considering that the installation of conjugated (*Z,E*)-polyenes by late stage alkyne reduction seemed ambitious, a second endgame strategy was proposed.

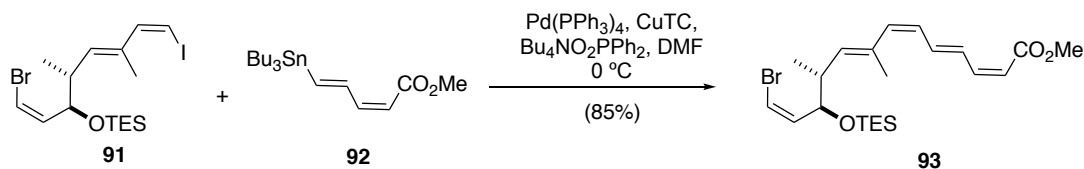
1.5.2 The second-generation endgame strategies

The second-generation endgame strategy features the modified linchpin fragment **81** and a different disconnection of the southern hemisphere, based on what had been learnt previously (Scheme 1.21). A Stille coupling utilising the stannane of **92** and the iodide terminus of **91** was proposed to construct the southern hemisphere. The C13 bromide would subsequently be transformed to a stannane. Fragment **81** incorporates an iodide and a bromide for the planned sequential Stille couplings with the new southern hemisphere and the north-eastern fragment **58**. Ester hydrolysis and macrolactonisation would then accomplish the ring closure and afford macrocycle **56**.



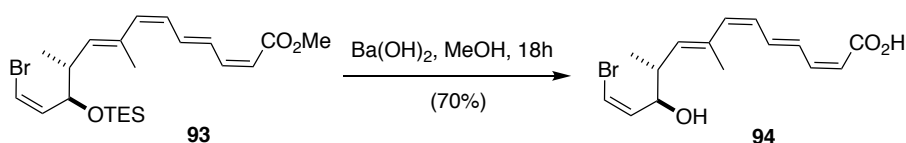
Scheme 1.21: Second-generation endgame strategy

Vinyl iodide **91** and stannane **92** were synthesised and conditions were found by Jennifer Kan⁵⁹ to effect the Stille coupling between **91** and **92** with no olefin isomerisation (Scheme 1.22).



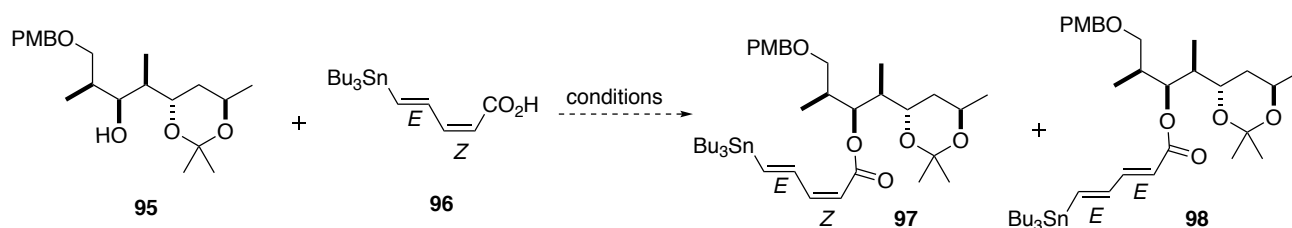
Scheme 1.22: Construction of the southern hemisphere **93**

One key premise of this endgame strategy is that the tetraenoate motif within the southern fragment **93** could undergo hydrolysis and esterification without compromising the sensitive olefin geometry. To test this hypothesis, hydrolysis of tetraenoate **93** to the corresponding carboxylic acid was first investigated. After a screen of conditions, Ba(OH)₂ in MeOH was chosen to facilitate the saponification, which afforded acid **94** as a single isomer in a satisfactory 70% yield. The TES ether was also cleaved under the reaction conditions (Scheme 1.23).



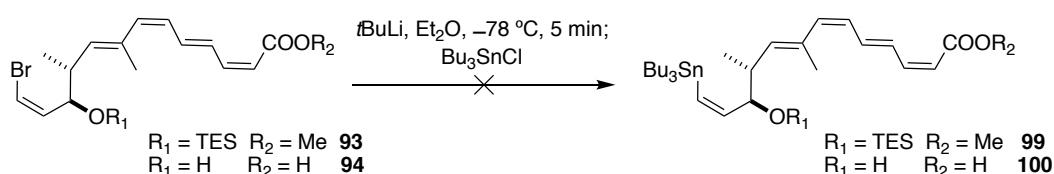
Scheme 1.23: Hydrolysis of tetraenoate **93**

Due to the tendency for alkene isomerisation of the activated tetraenoic acid **94**, a structurally simpler acid **96**, which is also a precursor to the southern fragment, was used to study the esterification with model alcohol **95** (Scheme 1.24). Nevertheless, after testing a series of conditions, either no desired product **97** was generated or the isomerised product **98** was obtained.



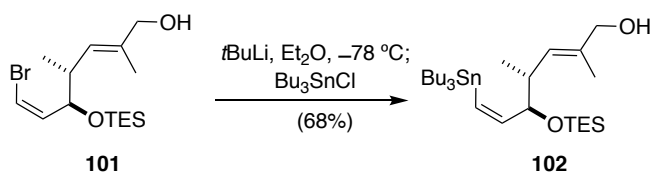
Scheme 1.24: Model system for testing esterification

Another key premise of the endgame strategy is the successful transformation of the C13 bromide to the stannane after the formation of **93**. Halogen-lithium exchange followed by stannylation with Bu_3SnCl was chosen for the transformation. Unfortunately, neither ester **93** nor acid **94** could be converted to the desired organostannanes under such conditions (Scheme 1.25). Instead, decomposition of the starting materials was observed.



Scheme 1.25: Attempted vinyl stannane synthesis through halogen-lithium-tin exchange

However, vinyl bromide **101**, a precursor to the southern fragment, was successfully transformed to the corresponding vinyl stannane **102** under the same conditions (Scheme 1.26). This indicated that the sensitive tetraenoate is incompatible with the halogen-tin exchange.

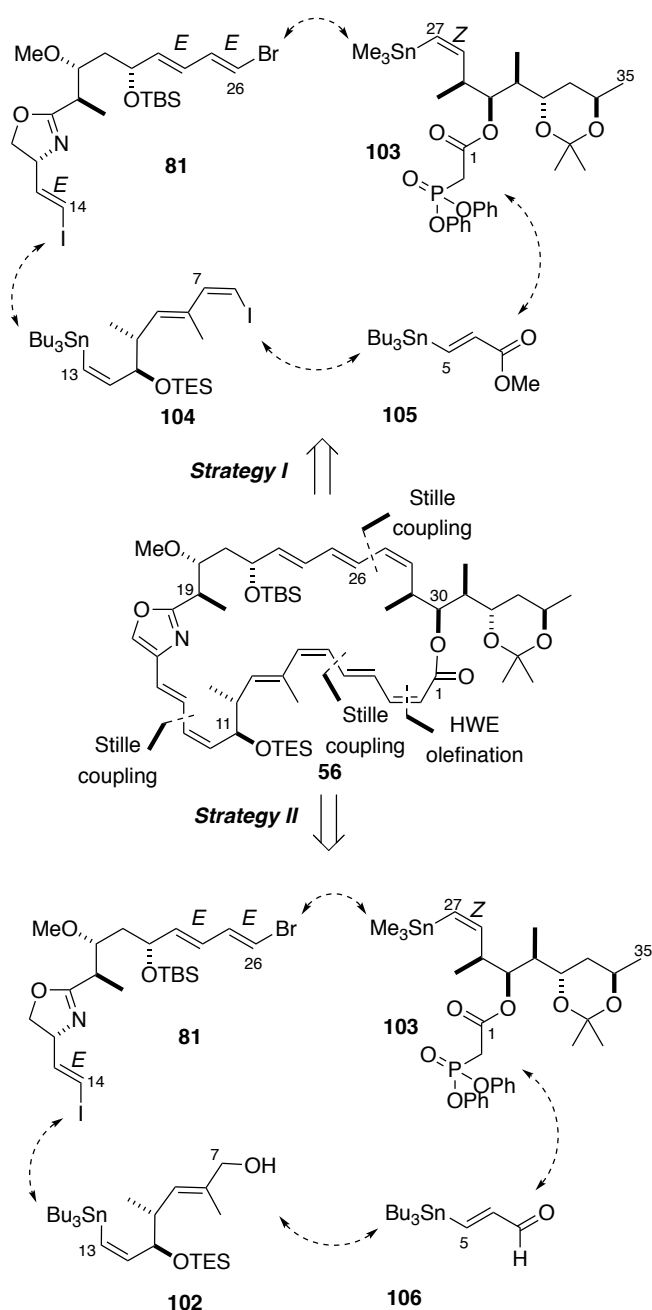


Scheme 1.26: halogen-lithium-tin exchange of vinyl bromide **101**

With the failure of the esterification and the stannylation, a third-generation endgame strategy was proposed.

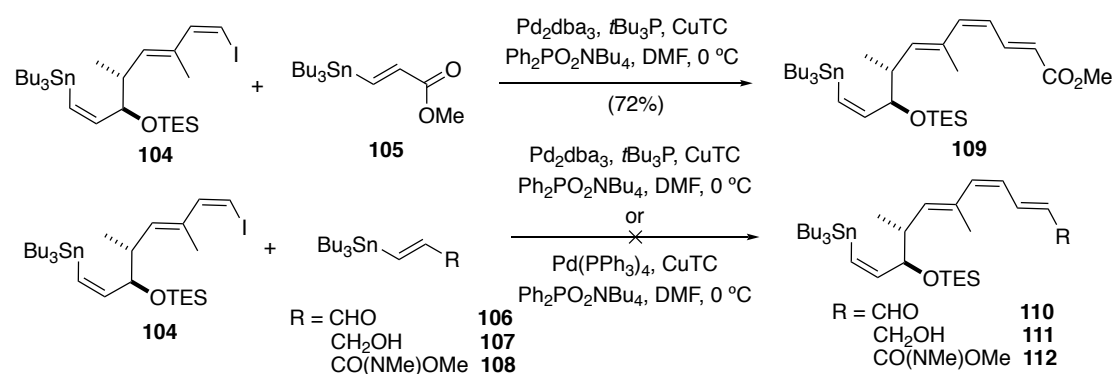
1.5.3 The third-generation endgame strategies

Due to the lability of the open-chain tetraenoate to alkene isomerisation, the crucial (2*Z*,4*E*,6*Z*,8*E*)-tetraenoate motif would be built up in conjunction with the macrocyclisation and two strategies were proposed to achieve this (Scheme 1.27). The north-eastern fragment **103** incorporates an Ando-type phosphonate at the hindered C30 alcohol, which would facilitate an HWE olefination to construct the (2*Z*)-alkene. The bond disconnections in both approaches are the same, but the ordering in the forward synthetic sense varies.



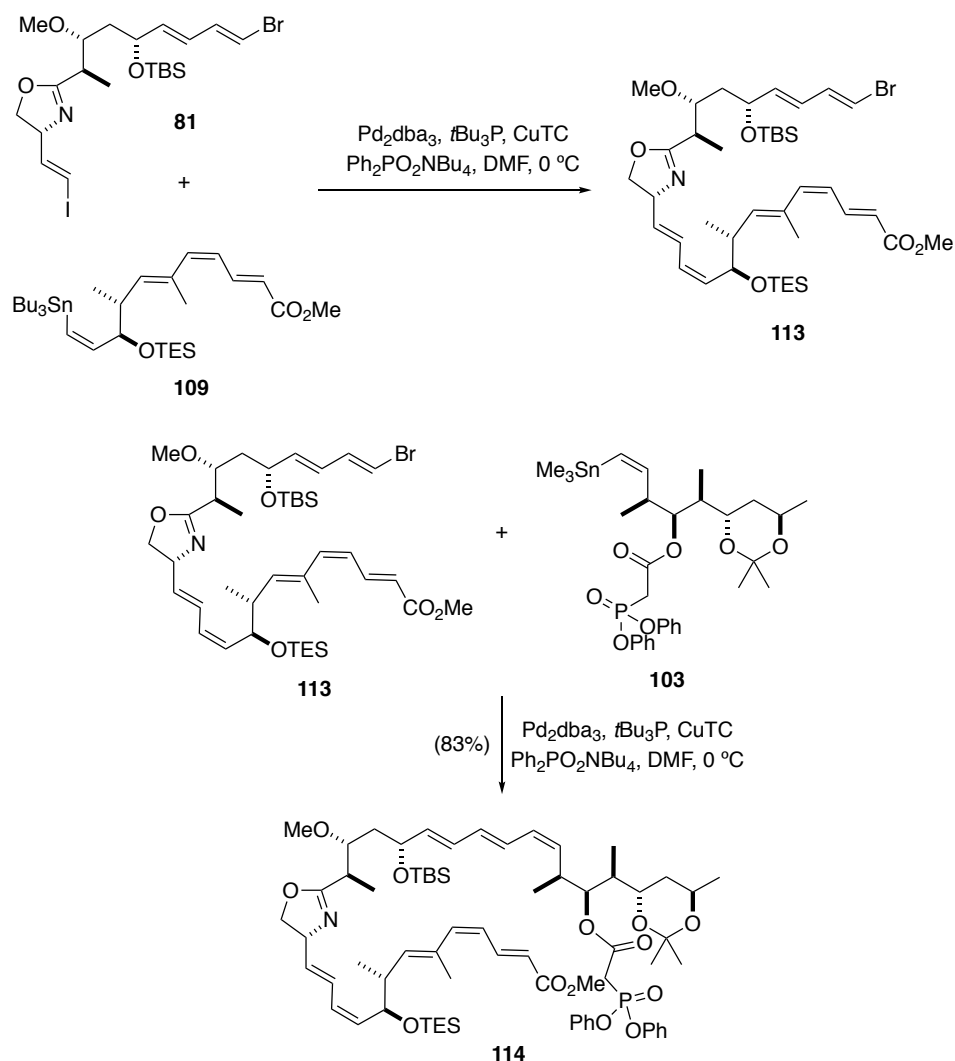
Scheme 1.27: Third-generation endgame strategy

Strategy I was studied by Jennifer Kan.⁵⁹ Stille coupling⁴⁴ between **104** and **105** was achieved to yield triene **109** with good configurational stability (Scheme 1.28). No homo-coupling product of iodostannane **104** was observed. The excellent site-selectivity could arise from a rate difference of Sn-Cu transmetalation between stannane **104** and stannane **105**. (*Z*)-vinyl stannane **104** is sterically more hindered compared to (*E*)-vinyl stannane **105** and so undergoes a slower transmetalation. Aldehyde **106**, alcohol **107** and Weinreb amide **108** were also tested in the Stille coupling with **104**. However, the corresponding triene products proved to be configurationally unstable.



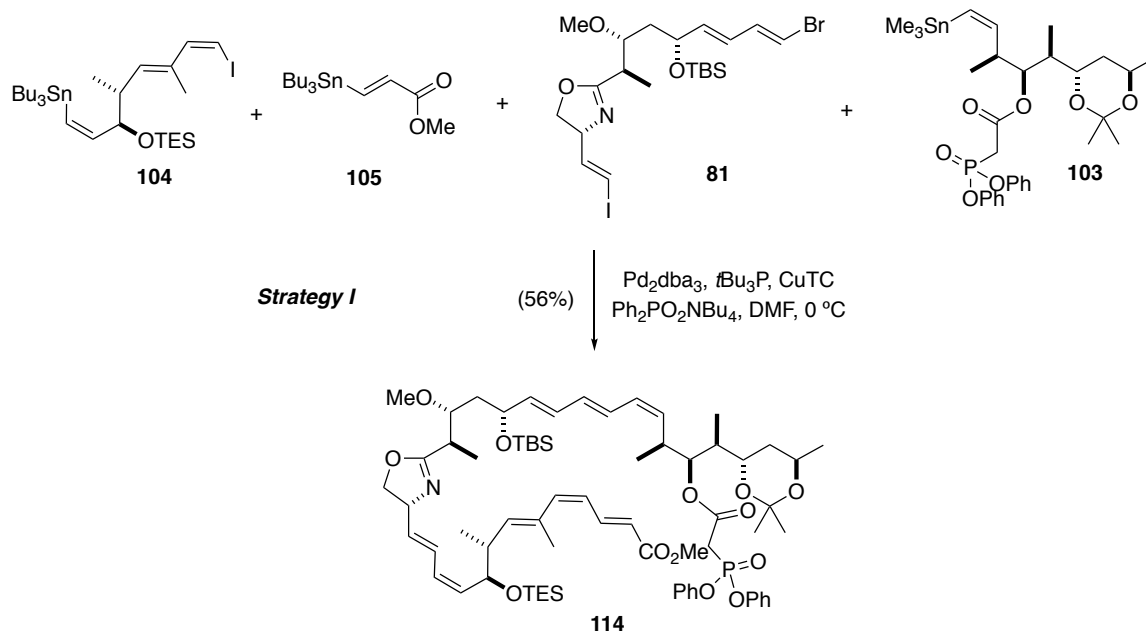
Scheme 1.28: Stille coupling to construct the triene motif

The same conditions were applied to the Stille coupling reaction between the north-western fragment **81** and the southern hemisphere **109**, and the Stille coupling reaction between the newly formed advanced fragment **113** and the north-eastern fragment **103**. Good yields and complete control over the desired alkene geometry were achieved in both Stille coupling reactions and the backbone of chivosazole F was constructed (Scheme 1.29).



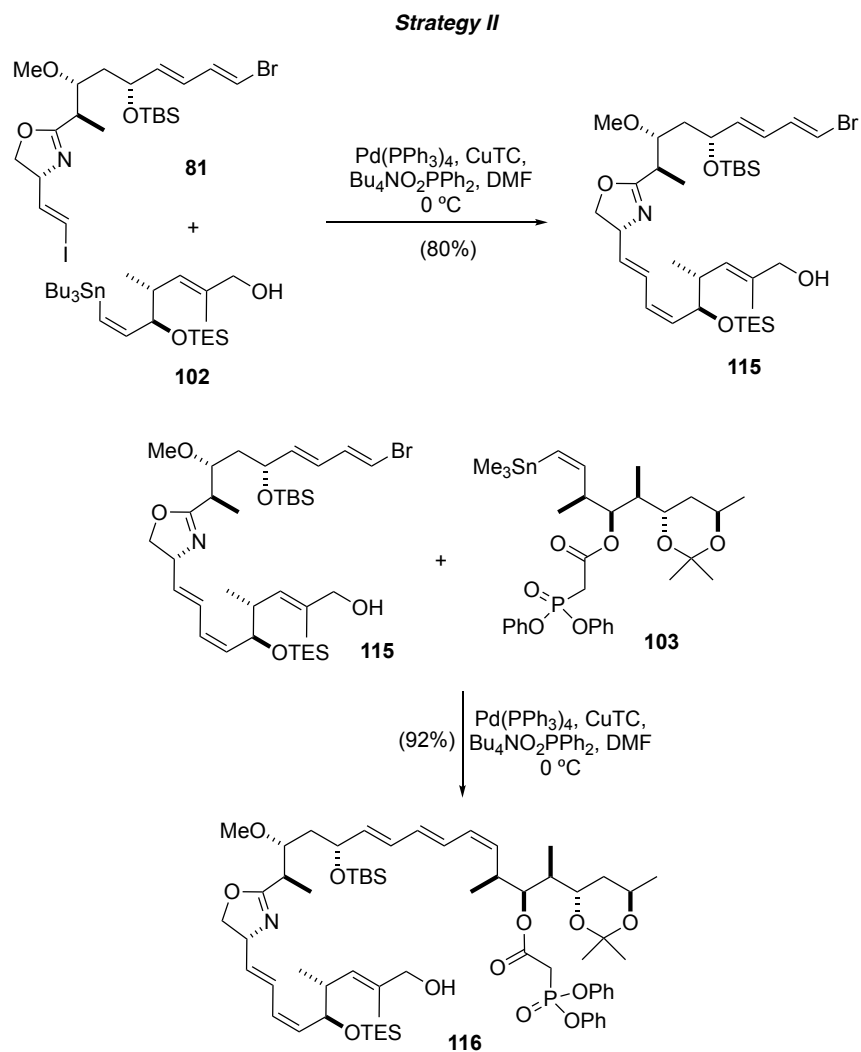
Scheme 1.29: Synthesis of **114** via two Stille coupling reactions

The universal Stille-coupling conditions led to an attempt to achieve the three sequential couplings in a one-pot process (Scheme 1.30). The reaction was carefully monitored to ensure the fragments were fully consumed before the addition of the next building block. The desired coupling product **114** was afforded in 56% yield with excellent site-selectivity and stereoselectivity. The efficient one-pot process both maximised step economy and minimised waste generation. However, transformation of the ester in **114** to aldehyde for the intramolecular HWE olefination was unsuccessful due to triene isomerisation, which diverted the focus onto the more conservative strategy II (Scheme 1.27).



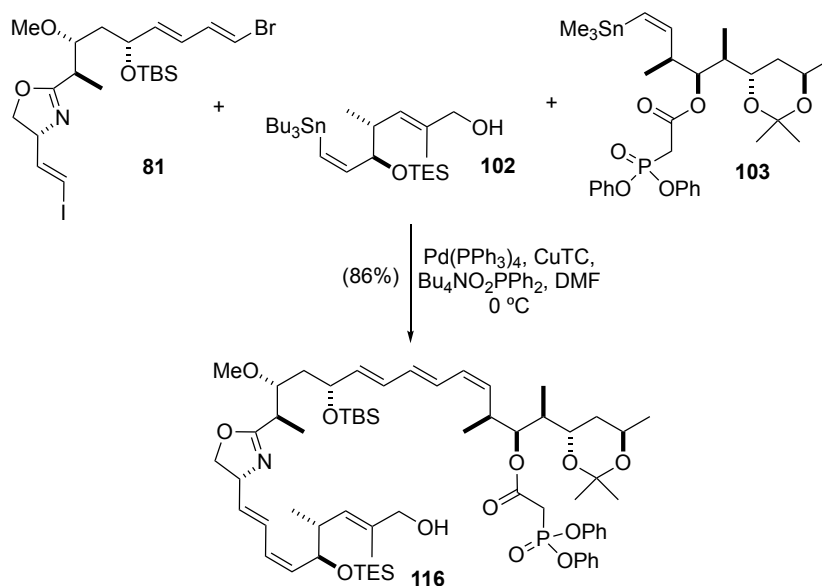
Scheme 1.30: Synthesis of **114** via a one-pot process

Strategy II was studied by Li.³⁸ Stille coupling between **81** and **102** was firstly effected under Fürstner-type conditions⁸³ to afford **115** in 80% yield. The same conditions were then applied to the Stille coupling between **115** and **103** to construct **116** in 92% yield (Scheme 1.31).



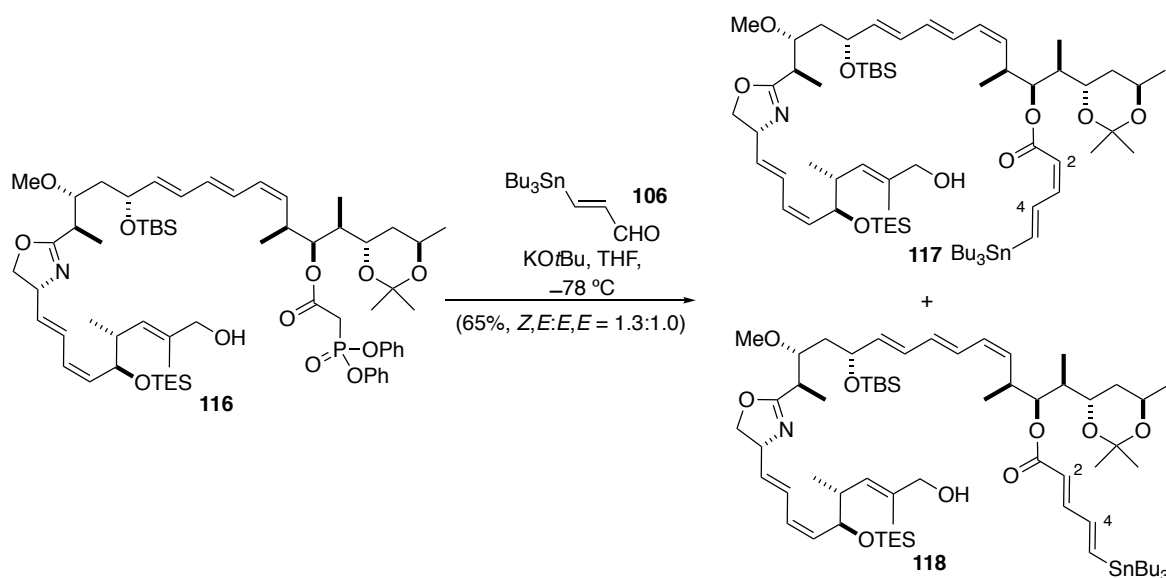
Scheme 1.31: Construction of **116** via two Stille couplings

With the same reaction conditions, these two Stille couplings could also be carried out in a one-pot process, leading to **116** in an overall 86% yield with complete control over the desired alkene geometry (Scheme 1.32).



Scheme 1.32: Site-selective Stille coupling reactions to form **116**

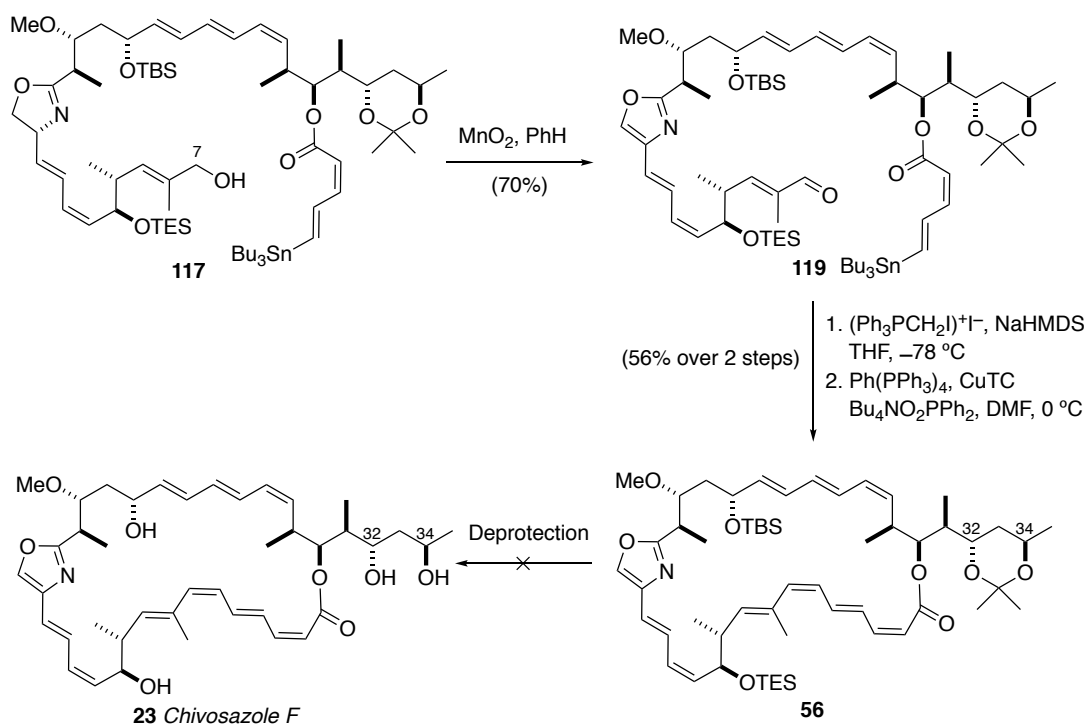
With the advanced fragment **116** in hand, an Ando-type HWE olefination of **116** was effected to afford a mixture of (2*Z*,4*E*)-dienoate **117** and (2*E*,4*E*)-dienoate **118** (Scheme 1.33). The best selectivity (**117**:**118** = 1.3:1) was achieved using KO^{*t*}Bu as the base at -78°C .



Scheme 1.33: Ando-type HWE olefination of **116**

MnO₂ was used to oxidise both the C7 alcohol and the oxazoline of the desired (2*Z*,4*E*)-dienoate **117** to afford **119** (Scheme 1.34). Stork-Zhao olefination⁷¹ of aldehyde **119** transformed the C7 aldehyde

into the (*Z*)-vinyl iodide. Due to its vulnerability to isomerisation, the resulting vinyl iodide was immediately submitted to intramolecular Stille reaction to construct macrocycle **56**. It is worth noting, however, that Li³⁸ reported problems with the global deprotection step with the acetonide on C32 and C34 appearing more stable than anticipated.



Scheme 1.34: Modifications towards the total synthesis of chivosazole F

As the southern (*4E,6Z,8E*)-triene motif of **114** was reported to be highly susceptible to alkene isomerisation, Strategy II was selected as the more promising strategy and is investigated in detail in this thesis. The more adventurous Strategy I may still be feasible with further refinement. The key issues that needed to be tackled in Strategy II were as follows:

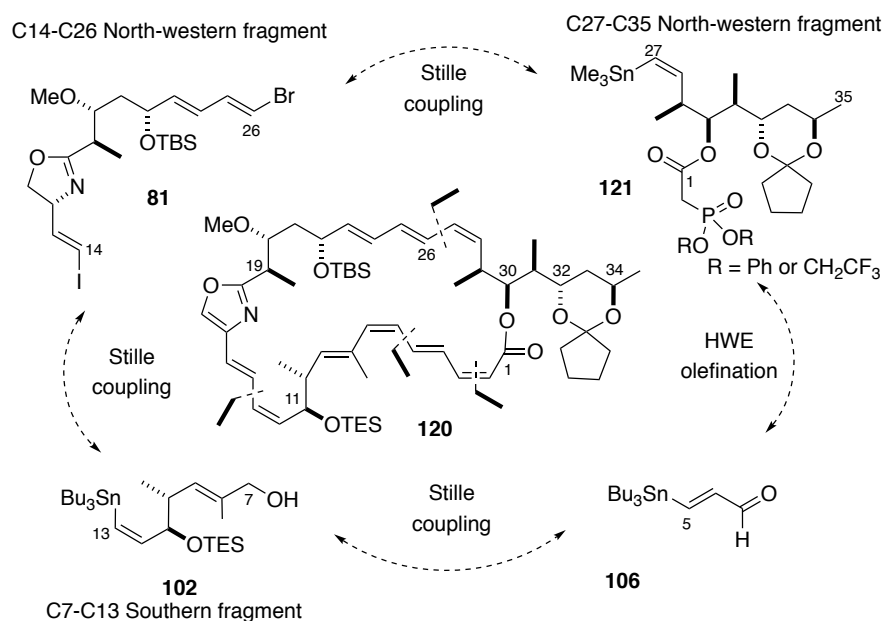
- The poor selectivity of the late stage Ando-type olefination (Scheme 1.33), which provided (*2Z,4E*)-dienoate **117** and (*2E,4E*)-dienoate **118** as a 1.3 : 1.0 mixture;
- The protecting group strategy to make the final global deprotection step as straightforward as possible.
- Several steps would benefit from improvement in the yield by further reaction optimisation.

To begin to overcome these shortcomings, the first objective was to replicate the synthesis of the key

chivosazole fragments and optimise the reaction conditions. These studies are discussed in the following chapter.

Chapter 2 Results and discussion on Chivosazole F

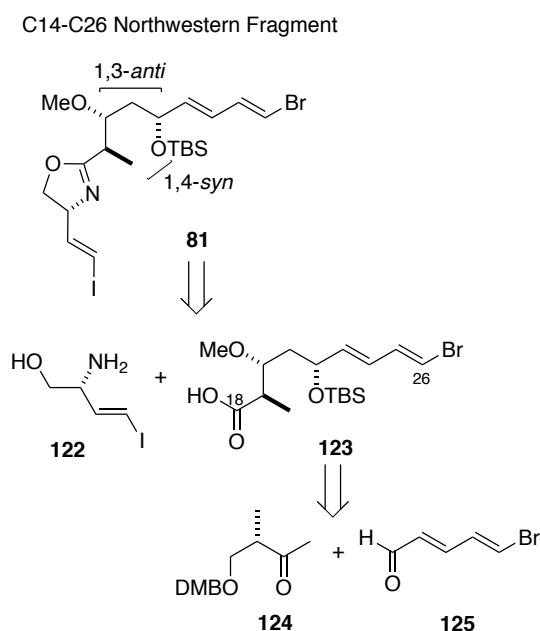
The retrosynthetic analysis of **120** (Scheme 2.1) is based on the third-generation endgame strategy with some modifications. North-western fragment **81** incorporates a C14 iodide and a C26 bromide for the planned sequential Stille cross-couplings with stannane **102** and stannane **121**. Aldehyde **106** is supposed to react with phosphonate **121** *via* an Ando-type/Still-Gennari-type HWE olefination to construct the (2*Z*)-alkene. The C7 alcohol of **102** would be transformed to a (*Z*)-vinyl iodide for a macro-Stille coupling with the stannane of **106** to afford the macrocycle **120**. The synthesis of fragment **81**, **121** and **102**, fragment couplings and subsequent modifications will be discussed in turn in this chapter.



Scheme 2.1: Retrosynthetic analysis

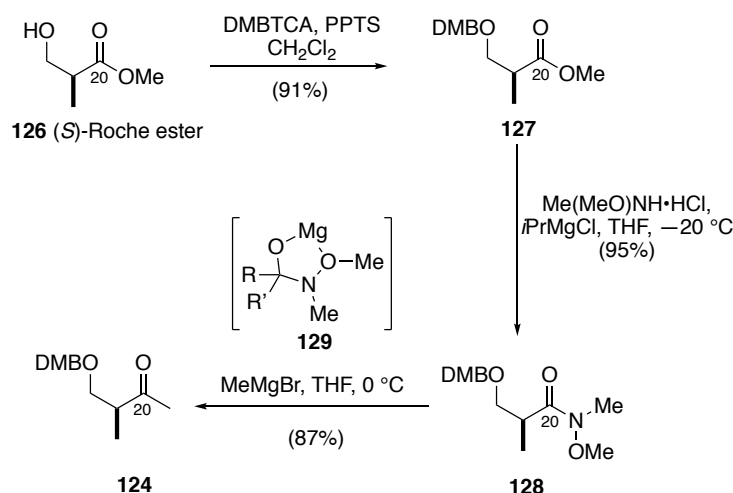
2.1 Synthesis of the C14-C26 north-western fragment

The north-western fragment **81** possesses a 1,3-*anti*, 1,4-*syn* stereochemical motif (Scheme 2.2). The 1,4-*syn* relationship could be constructed by an asymmetric aldol reaction between the Roche ester derived methyl ketone **124** and the corresponding aldehyde **125**. The 1,3-*anti* stereochemical relationship would be installed *via* a diastereoselective 1,3-*anti* reduction. As discussed before, owing to the low yield obtained in forming the vinyl iodide at C15 from precursor aldehyde **69** (Scheme 1.13), the vinyl iodide moiety was to be attached before the formation of the oxazoline.



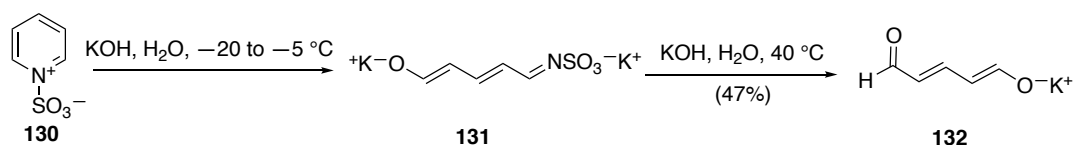
Scheme 2.2: Retrosynthetic analysis of the northwestern fragment **81**

In the forward synthetic sense, the (*S*)-Roche ester derived methyl ketone **124** was prepared *via* a three-step reaction sequence. Firstly, the alcohol group of (*S*)-Roche ester **126** was protected as the 3,4-dimethoxybenzyl ether **127** with DMBTCA and PPTS in 91% yield (Scheme 2.3). Ester **127** was transformed into Weinreb amide **128** with *N,O*-dimethylhydroxylamine and *iso*-propyl magnesium chloride in 95% yield.⁴⁵ Mono-addition of MeMgBr *via* chelated intermediate **129**⁴⁶ gave the methyl ketone **124** in 87% yield.



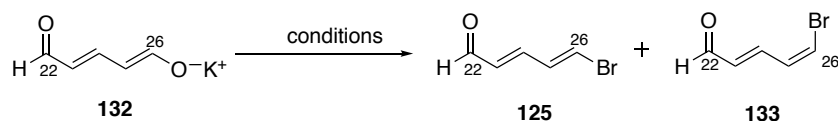
Scheme 2.3: Preparation of DMB-protected methyl ketone **124**

Bromodienal **125** was synthesised in two steps from sulphur trioxide pyridine complex **130** (Scheme 2.4).⁴⁷ Hydrolysis of pyridinium complex **130** with KOH gave potassium glutaconaldehyde salt **132** *via* the formation of the intermediate iminesulfonate dianion **131**.



Scheme 2.4: Hydrolysis of sulfur trioxide pyridine complex **130**

Bromination of the hydrolysis product **132** yielded the required bromodienyl aldehyde **125** and the *Z*-isomer **133** (Scheme 2.5). The bromination conditions with PPh₃ and Br₂⁴⁸ (Table 2.1, Entry 1) gave a disappointingly low yield of 3%. At the same time, numerous unidentified side products were observed when monitoring the reaction process. A screen of reaction conditions was then carried out to try and improve the yield.



Scheme 2.5: Bromination of potassium glutaconaldehyde salt **132**

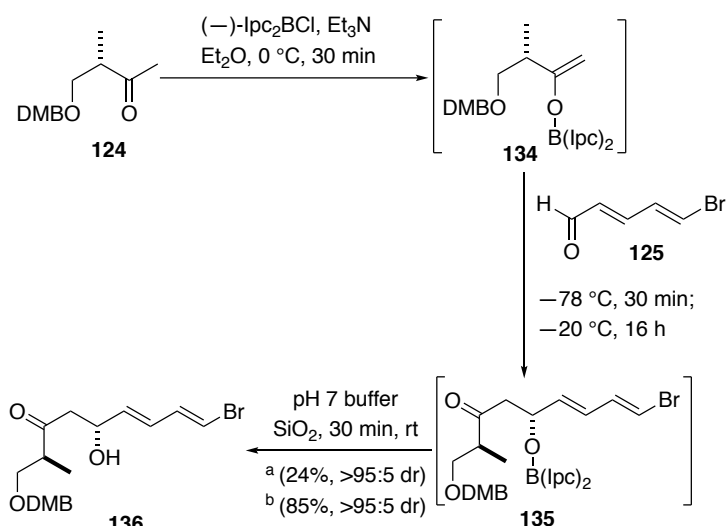
Table 2.1: Optimization of conditions for the bromination reaction

Entry	Scale	Reagent	Solvent	Temperature	Time	Yield
1	500 mg	Br ₂ (1.2 eq.), PPh ₃ (1.2 eq.)	CH ₂ Cl ₂	0 °C	3 h	3%
2	1 g	Br ₂ (1.2 eq.), PPh ₃ (1.2 eq.)	CH ₂ Cl ₂	0 °C to rt	16 h	9%
3	500 mg	Br ₂ (1.5 eq.), PPh ₃ (1.5 eq.)	CH ₂ Cl ₂	0 °C to rt	16 h	10%
4	500 mg	NBS (2.0 eq.), PPh ₃ (2.0 eq.)	CH ₂ Cl ₂	0 °C to rt	7 h	11%
5	500 mg	NBS (2.0 eq.), PPh ₃ (2.0 eq.)	CH ₂ Cl ₂	0 °C to rt	16 h	20%
6	100 mg	CBr ₄ (1.5 eq.), PPh ₃ (1.5 eq.)	CH ₂ Cl ₂	0 °C to rt	16 h	0
7	100 mg	PBr ₃ (1.5 eq.)	Et ₂ O	0 °C to rt	16 h	9%
8	100 mg	PBr ₃ (1.5 eq.)	THF	50 °C	5 h	3%
9	500 mg	NBS (2.0 eq.), PPh ₃ (2.0 eq.)	CH ₂ Cl ₂	40 °C	16 h	20%
10	6 g	NBS (2.0 eq.), PPh ₃ (2.0 eq.)	CH ₂ Cl ₂	0 °C to rt	16 h	20%
11	5 g	NBS (2.0 eq.), PPh ₃ (2.0 eq.)	CH ₂ Cl ₂	0 °C to rt	40 h	30%

No significant improvement in yield was observed when the temperature was raised and the reaction time was prolonged (Entry 2). Raising the number of equivalents of the reagents from 1.2 to 1.5 did not affect the yield significantly (Entry 3). Several common conditions for bromination were also tried. Potassium glutaconaldehyde stirred in dichloromethane with *N*-bromosuccinimide and triphenylphosphine⁴⁹ for 7 h (Entry 4) formed a black solution, and after workup and purification, an 11% yield of product **125** was obtained. As the starting material was not very soluble, it was difficult to monitor the reaction conversion. Therefore, an extended reaction time (16 h) was employed to maximise the conversion, which improved the yield from 11% to 20% (Entry 5). Carbon tetrabromide with triphenylphosphine⁵⁰ (Entry 6) was also tested but unfortunately no reaction was observed. Phosphorus tribromide⁵¹ gave an initial 9% yield at room temperature (Entry 7). However, warming up the reaction to 50 °C reduced the yield to 3% (Entry 8).

Having surveyed a number of different bromination conditions, the most promising result was produced by *N*-bromosuccinimide and triphenylphosphine, and so these conditions were selected for further optimisation experiments. Neither gentle warming of the reaction (Entry 9) nor increasing the reaction scale (Entry 10) improved the yield, but extending the reaction time to 40 h raised the yield from 20% to 30% (Entry 11) for the desired *E,E*-diene **85**.

With methyl ketone **124** and aldehyde **125** in hand, the asymmetric boron-mediated aldol reaction developed in the Paterson group,⁵² was employed to install the required stereochemistry (Scheme 2.6). Methyl ketone **124** was enolised with (–)-Ipc₂BCl and triethylamine in Et₂O at 0 °C to form boron enolate **134**, which reacted with aldehyde **125** to give the 1,4-*syn* aldol product **136** with excellent diastereoselectivity but in a disappointing yield (24%, >95:5 dr).



Scheme 2.6: Diastereoselective boron-mediated 1,4-*syn* aldol reaction
^a commercial (–)-Ipc₂BCl reagent; ^b Freshly prepared (–)-Ipc₂BCl reagent

Two possible transition states are compared in Figure 2.1. Aldol reactions of such unsubstituted enolborinates are proposed to proceed *via* a boat transition state,⁵³ stabilised by a formyl hydrogen bond between the aldehyde proton and the β-alkoxy group on the enolate.⁵⁴ For transition state **TS 138**, there is an unfavourable eclipsing interaction between the alkene and the methyl group on the enolate, which is absent in **TS 137**, the favoured transition state. This leads to the desired stereochemistry in the product **136**.

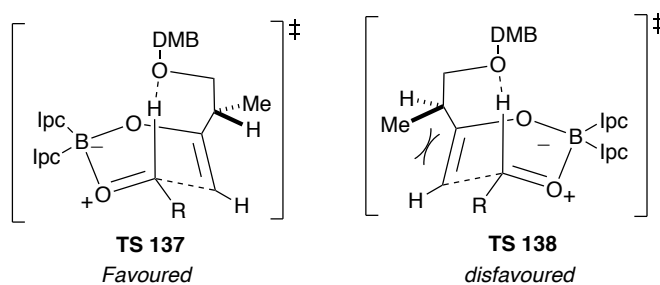
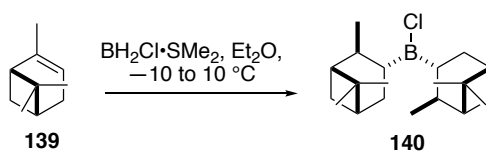


Figure 2.1: Comparison of the possible transition states

The oxidative workup with hydrogen peroxide usually employed for such reactions was not used for the cleavage of the resulting boron species **135** (Scheme 2.6) as the bromodiene was susceptible to isomerisation and oxidation. An alternative workup using pH 7 buffer and silica gel was applied. Despite the mild work up, the yield was unsatisfactory as the reaction did not go to completion, and this was attributed to the low quality of commercial (–)-Ipc₂BCl. Methods were therefore investigated for the preparation of fresh (–)-Ipc₂BCl.

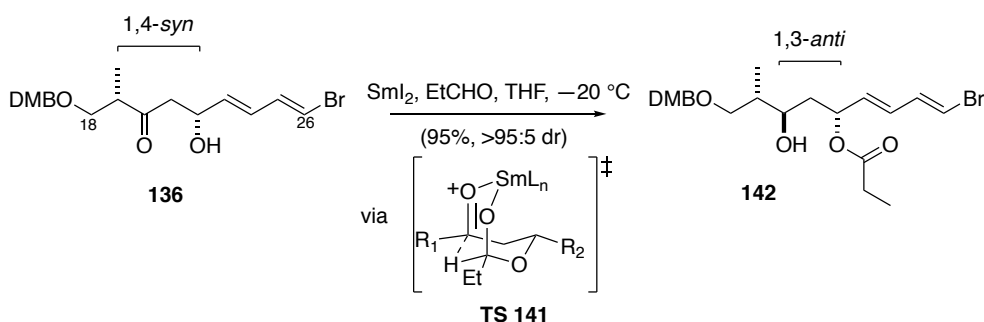
The most convenient preparation of (–)-Ipc₂BCl **140** was by double hydroboration of pinene **139** with monochloroborane which produced the reagent as a 1M solution in Et₂O (Scheme 2.7).⁵⁵ Using the freshly prepared reagent in the aldol reaction between methyl ketone **124** and aldehyde **125** improved the yield to 85% with excellent diastereoselectivity (>95:5 dr) for formation of the desired adduct **136** (Scheme 2.6).



Scheme 2.7: Preparation of (–)-Ipc₂BCl

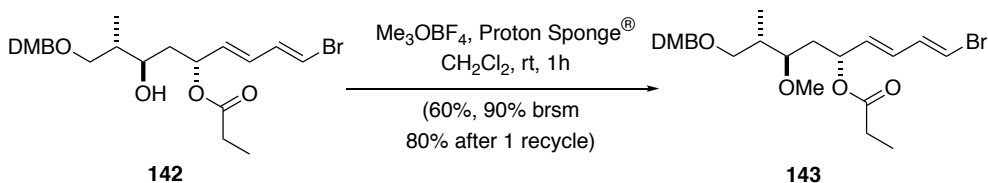
With the aldol adduct **136** in hand, reduction under Evans-Tishchenko conditions⁵⁶ was employed to install the 1,3-*anti* relationship between the hydroxyl stereocentres at C20 and C22 (Scheme 2.8). Samarium(III) acts as a Lewis acid catalyst to promote the formation of a hemiacetal from β-hydroxy ketone **136** and propionaldehyde. This intermediate can undergo intramolecular hydride transfer *via* the chelated, bicyclic transition state **TS 141** to afford the propionate modified 1,3-diol **142**. The

product **142** was obtained in excellent yield (95%) and diastereoselectivity (>95:5 dr) through this transformation. At this stage, all the required stereochemistry had been installed for the north-western fragment and attention was focused towards the installation of the oxazole.



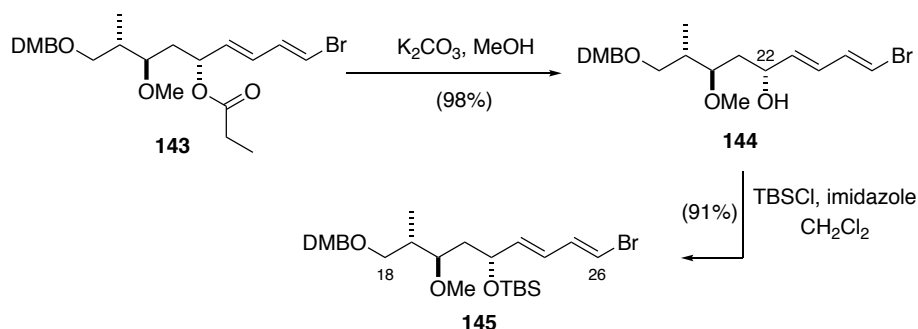
Scheme 2.8: Evans-Tishchenko selective 1,3-*anti* reduction of **136**

The newly-formed hydroxyl group was transformed into the corresponding methyl ether **143** by reaction of alcohol **142** with Meerwein's salt and Proton Sponge[®] in CH₂Cl₂ at room temperature (Scheme 2.9). Unfortunately, complete conversion could not be achieved even with a large excess of reagents. The starting material **142** could, however, be recovered and resubmitted to provide methyl ether **143** in 80% yield after one recycle.



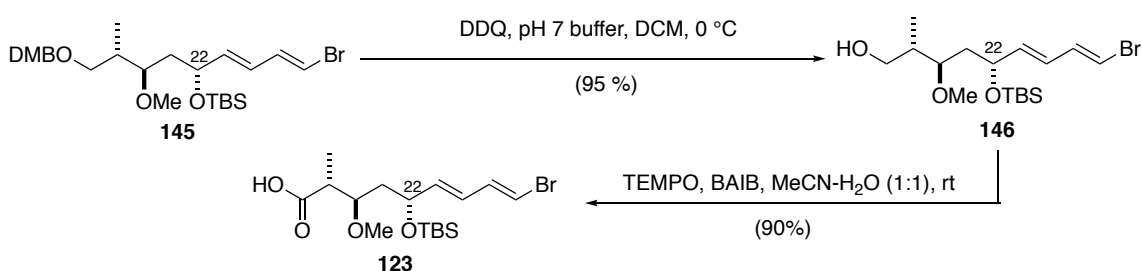
Scheme 2.9: Methylation of alcohol **142**

Methanolysis of the propionate ester **143** using K₂CO₃ in methanol generated alcohol **144** (Scheme 2.10), and the free hydroxyl group at C22 was protected as the TBS ether **145** (TBSCl, imidazole, CH₂Cl₂) in 89% yield over two steps.



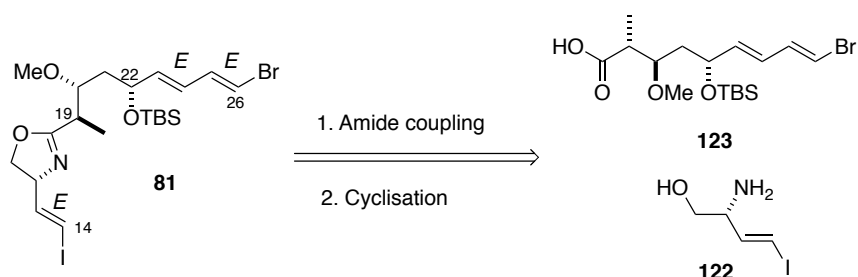
Scheme 2.10: Protecting group exchange at C22

The remaining steps to access the oxazole precursor involved DDQ-mediated oxidative cleavage of the DMB group to form alcohol **146** in 95% yield (Scheme 2.11). Due to the lower oxidation potential of the DMB ether, it was considered a superior choice to the PMB protecting group in order to avoid potential allylic oxidation at C22.^{57,58} Alcohol **146** was oxidised to carboxylic acid **123** in 90% yield by treatment with TEMPO and BAIB in MeCN and H₂O (1:1)⁵⁹ in readiness for the subsequent amide coupling.



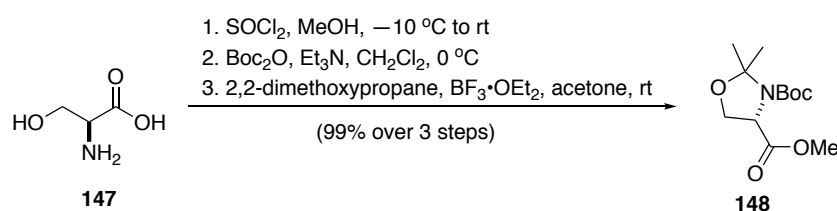
Scheme 2.11: DDQ-mediated oxidative cleavage and oxidation

Having prepared acid **123**, amino alcohol **122** containing the vinyl iodide terminus was needed as the fragment coupling partner (Scheme 2.12).



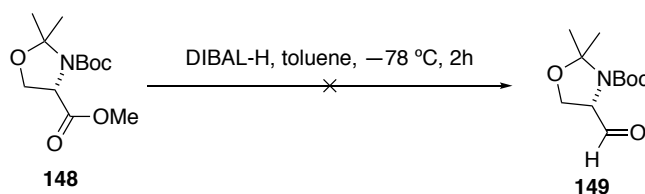
Scheme 2.12: Proposed method for oxazoline formation

The synthesis of vinyl iodide **122** commenced by transforming serine **147** into the corresponding methyl ester using thionyl chloride and methanol (Scheme 2.13). The amine group was selectively protected as the Boc carbamate with Boc_2O and Et_3N in CH_2Cl_2 . After protection of the amine and the alcohol as the acetal by treatment with 2,2-dimethoxypropane and $\text{BF}_3 \cdot \text{OEt}_2$, ester **148** was obtained in 99% yield over 3 steps.⁶⁰ Methods were then explored to reduce the ester of **148** to an aldehyde for a subsequent Takai olefination to install the (*E*)-vinyl iodide.



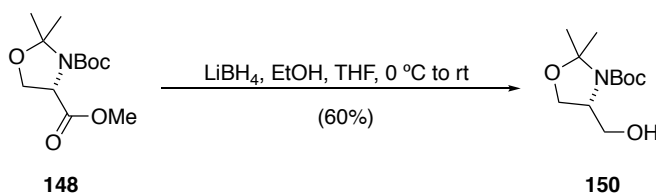
Scheme 2.13: Preparation of ester **148**

An attempt was made to reduce ester **148** directly to aldehyde **149** with DIBAL-H at $-78\text{ }^\circ\text{C}$ ⁶¹ (Scheme 2.14). However, this reaction failed to provide any product and the starting material **148** was recovered.



Scheme 2.14: Proposed DIBAL-H reduction of ester **148**

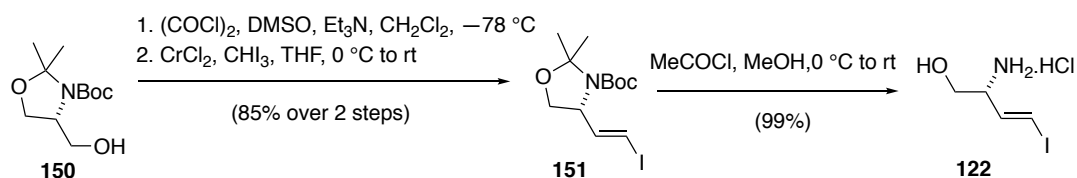
Ester **148** was reduced to alcohol **150** with lithium borohydride in 60% yield (Scheme 2.15). The newly formed alcohol would then be oxidised to the aldehyde.



Scheme 2.15: Proposed method for reduction of ester **148** into alcohol **150**

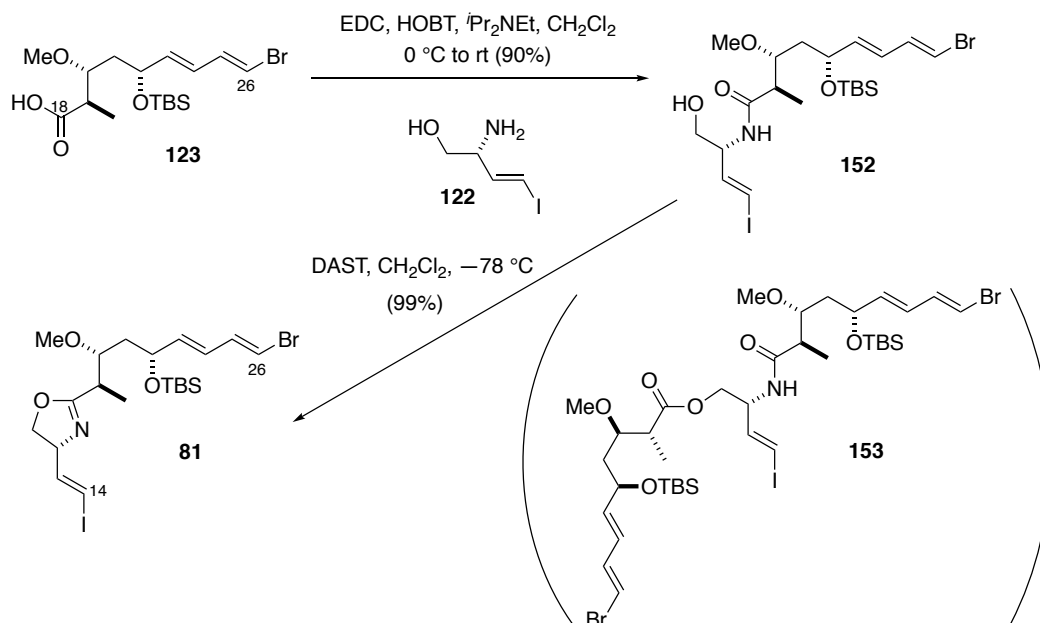
Alcohol **150** was oxidised under Swern conditions⁶² to give aldehyde **149**. Aldehyde **149** was

immediately subjected to a Takai olefination to afford vinyl iodide **151** with the desired *E*-geometry cleanly in 85% yield over two steps. Finally, deprotection of the acetonide and Boc group under acidic conditions supplied amino alcohol **122** as the HCl salt in 99% yield. No decomposition of amino alcohol **122** was observed when the product was stored in the dark at $-20\text{ }^{\circ}\text{C}$ (Scheme 2.16).



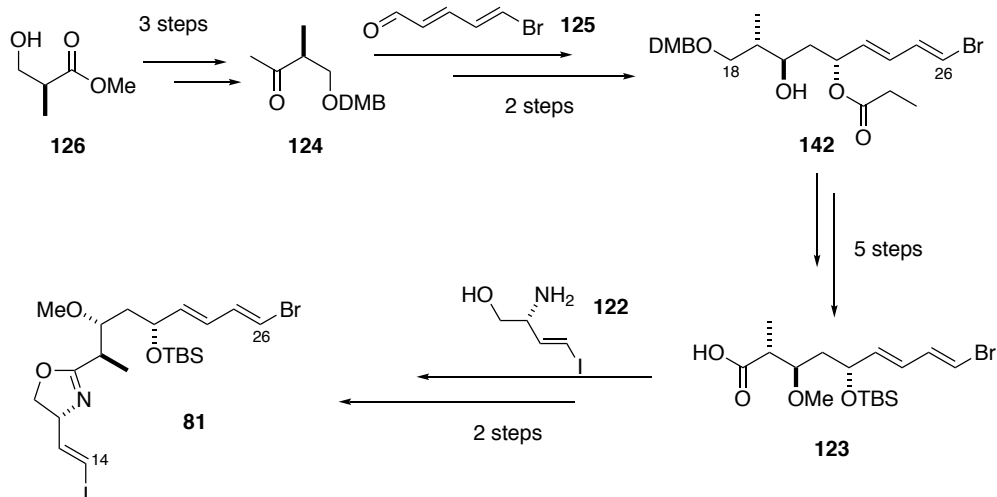
Scheme 2.16: Preparation of amino alcohol **122** from alcohol **150**

It now remained to couple the amino alcohol **122** to carboxylic acid **123** and subsequently cyclise to form an oxazoline ring. EDC-mediated amide coupling (EDC, HOBT, *i*Pr₂NEt, CH₂Cl₂) was employed in the coupling of the two components to form amide **152** in 90% yield (Scheme 2.17). Careful monitoring of this reaction by TLC avoided formation of the *bis*-coupled product **153**. Cyclisation of amide **152** to oxazoline **81** using DAST proceeded smoothly in 99% yield. Kan⁵⁹ demonstrated that oxidation of the oxazoline to the oxazole was possible using MnO₂; however, this reaction did not tolerate the vinyl iodide. Oxidation was thus delayed until after fragment coupling and oxazoline **81** was used as the northwestern fragment for the fragment coupling.



Scheme 2.17: Completion of C14-C26 northwestern fragment **81**

The whole north-western fragment **81** was synthesised in 33% yield over 12 steps, which compares well with the 17% yield reported by Li.³⁸



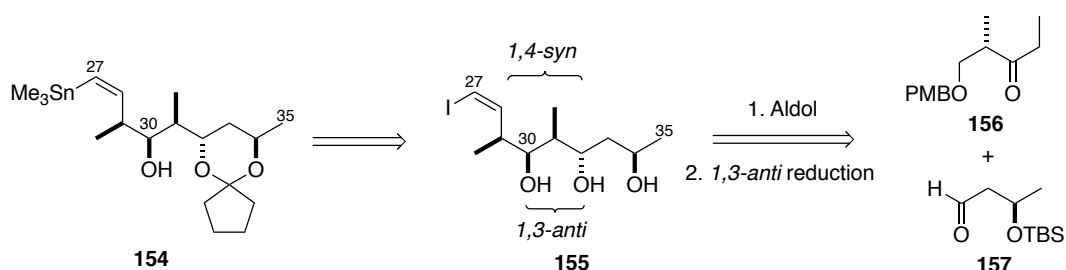
Scheme 2.18: Overview of the synthetic route for the northwestern fragment **81**

2.2 Synthesis of the C27-C35 north-eastern fragment

2.2.1 Modifications of the C27-C35 Fragment

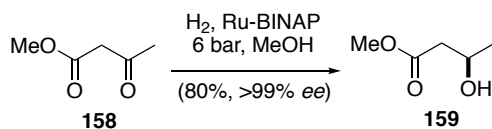
The synthetic strategy for the C27-C35 fragment is based on Gibson's work⁶³. Removal of the acetonide in the final steps of the synthesis was identified as a potentially difficult step due to the sensitivity of the natural product and so an alternative protecting group strategy was explored.

Cyclopentylidene ketals are more labile than acetonides, as cyclic ketals experience bond-angle strain introduced by the 1,3-dioxolane ring that could facilitate activation for hydrolysis.⁶⁴ Therefore, 2,2-dimethoxypropane was replaced by 1,1-dimethoxycyclopentane for the regioselective ketal formation with triol **155**. Triol **155** could be accessed from ketone **156** and aldehyde **157** via a boron aldol reaction (Scheme 2.19).



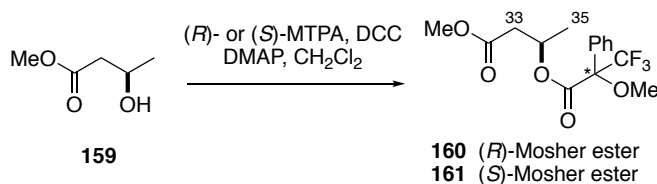
Scheme 2.19: Retrosynthetic analysis of C27-C35 fragment **154**

Ketone **156** was available as a starting material from other projects in this laboratory. Preparation of the β -hydroxy aldehyde **157** started with an asymmetric Noyori reduction^{65, 66} of methyl acetoacetate **158**. This was transformed into β -hydroxy ester **159** in 80% yield (Scheme 2.20) utilising the *in situ* formed (*R*)-BINAP-Ru(II) catalyst under a hydrogen atmosphere (6 bar).



Scheme 2.20: Preparation of β -hydroxy ester **159**

The absolute configuration of the newly formed alcohol was confirmed by application of the advanced Mosher method.^{67,68} Alcohol **159** was converted to the corresponding Mosher esters **160** and **161** (Scheme 2.21).



Scheme 2.21: Preparation of (*R*)- and (*S*)-Mosher ester derivatives

The α -proton, the ester carbonyl and the trifluoromethyl group of the ester lie in the same plane in both MTPA ester derivatives (Figure 2.2). The diamagnetic effect of the phenyl group shields protons H_a , H_b , H_c in the (*R*)-MTPA ester causing an upfield shift of their signals in the ^1H NMR when compared to the corresponding signals in the (*S*)-MTPA ester. Hence, when $\Delta\delta$ ($\delta_S - \delta_R$) is calculated, $\Delta\delta$ values should be positive for protons H_a , H_b , H_c , and $\Delta\delta$ values should be negative for protons H_x , H_y , H_z , thus allowing the assignment of the configuration of the stereocentre in question.

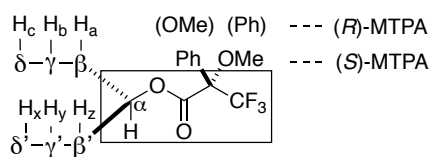


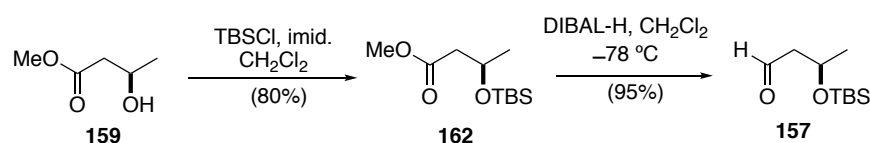
Figure 2.2: Configurational model for Mosher ester analysis

^1H NMR chemical shift analysis of the Mosher ester derivatives **160** and **161** is shown in Table 2.2. The $\Delta\delta$ value for H_{35} is positive and the $\Delta\delta$ values for H_{OMe} , H_{33a} and H_{33b} are negative, showing that the desired (*S*)-configuration was formed in alcohol **159**.

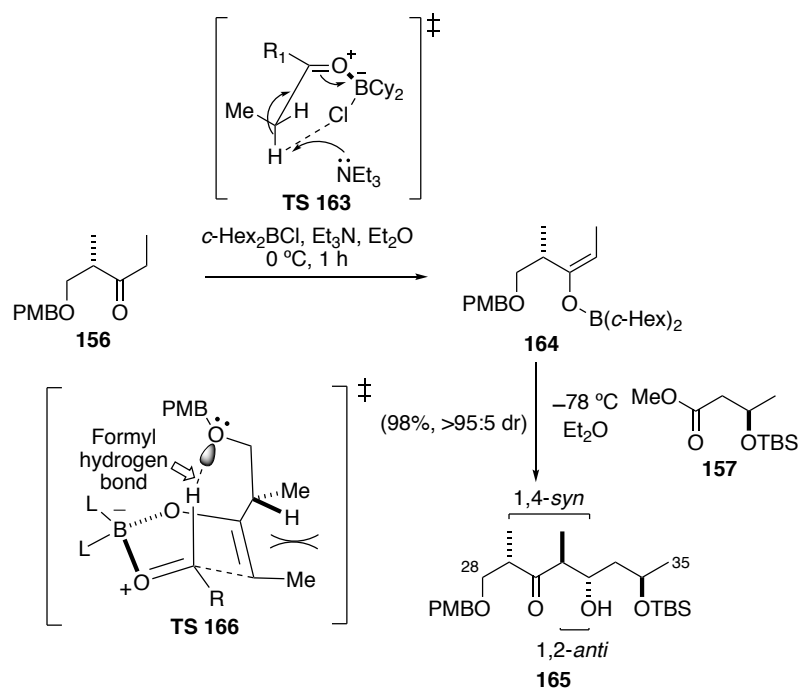
Table 2.2: Mosher ester ^1H NMR analysis of **159**

Position	$\delta_{\text{H}}(S)\text{-MTPA}$ / ppm	$\delta_{\text{H}}(R)\text{-MTPA}$ / ppm	$\Delta\delta$ ($\delta_S - \delta_R$) / ppm
OMe	3.58	3.65	-0.07
33a	2.69	2.71	-0.02
33b	2.54	2.56	-0.02
34	5.55	5.53	+0.02
35	1.43	1.32	+0.11

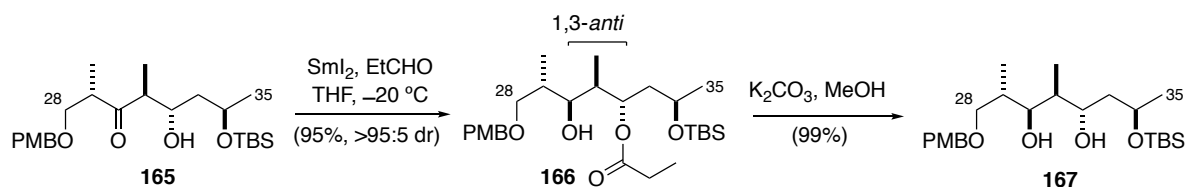
Completion of the β -hydroxy aldehyde **157** was achieved by TBS protection of the newly formed hydroxyl group and DIBAL-H reduction of the ester to the aldehyde (Scheme 2.22).

**Scheme 2.22:** Elaboration to β -hydroxy aldehyde **157**

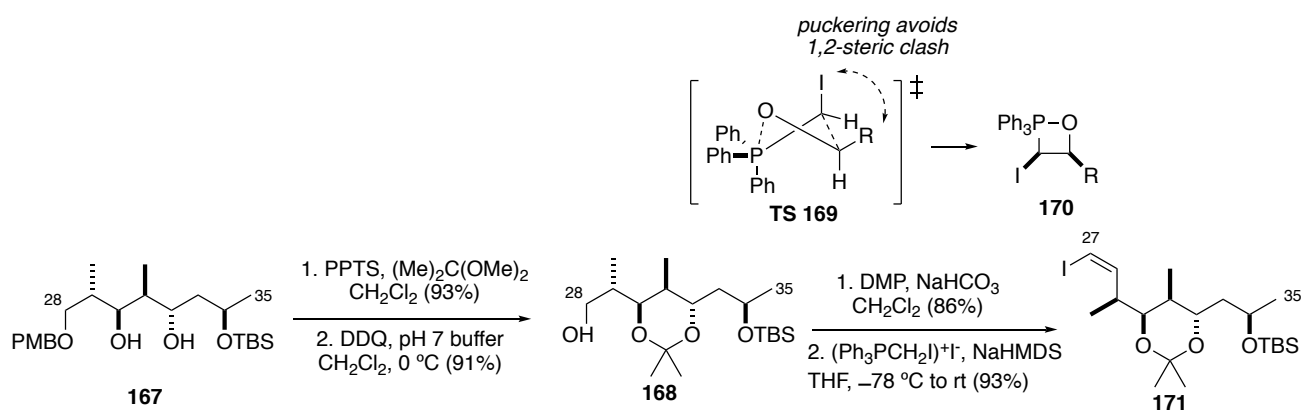
Ethyl ketone **156** was treated with *c*-Hex $_2\text{BCl}$ and Et_3N to form the (*E*)-boron enolate **164** via transition state **TS 163** (Scheme 2.23). As **TS 163** shows, chloride as a relatively poor leaving group adds bulk to the B centre, which sits on the opposite side of the carbonyl to R_1 in order to minimise steric interactions. This forces the methyl group away from the boron centre. Additionally, the chloride can activate the C-H bond further, favouring deprotonation through this conformation. The (*E*)-boron enolate **164** is thus formed through an E2 mechanism.⁶⁹ Addition of aldehyde **157** to the enolate **164** afforded the 1,2-*anti*, 1,4-*syn* adduct in 98% yield and high diastereoselectivity (>95:5). Computational studies have shown that the aldol reaction proceeds via a boat-like transition state⁵³ (**TS 166**), which minimises the 1,3-allylic strain within the enolate while a formyl hydrogen bond helps stabilise the transition state,⁵⁴ leading to the 1,4-*syn* product **165**.



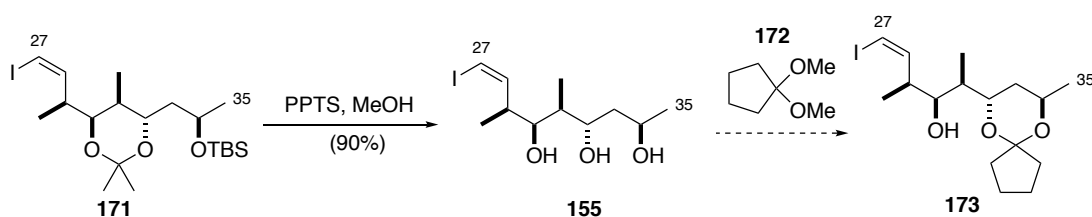
An Evans-Tishchenko reduction⁵⁶ was then effected to introduce the 1,3-*anti* relationship between C30 and C32 (For mechanism, see Chapter 2.1). The newly formed ester was cleaved to give diol **167**.



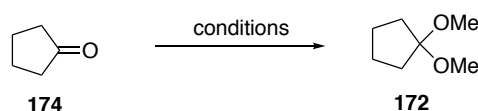
Acetonide protection of diol **167** followed by DDQ-mediated oxidative cleavage of the PMB ether provided alcohol **168** (Scheme 2.25). The released primary alcohol was transformed into the (*Z*)-vinyl iodide over 2 steps: Dess-Martin oxidation⁷⁰ and Stork-Zhao olefination⁷¹. The transition state and the intermediate for the Stork-Zhao olefination are shown. The ylid generated from (Ph₃PCH₂I)⁺I⁻ and NaHMDS is non-stabilised, which leads to the early transition state **TS 169**. **TS 169** is puckered to avoid steric clashes, yielding *cis*-oxaphosphetane **170**, which collapses to give the (*Z*)-vinyl iodide product **171**.



The acetonide and TBS groups were removed with catalytic PPTS in methanol (Scheme 2.26). Conditions were then screened for protection of the terminal diol with 1,1-dimethoxycyclopentane **172**.



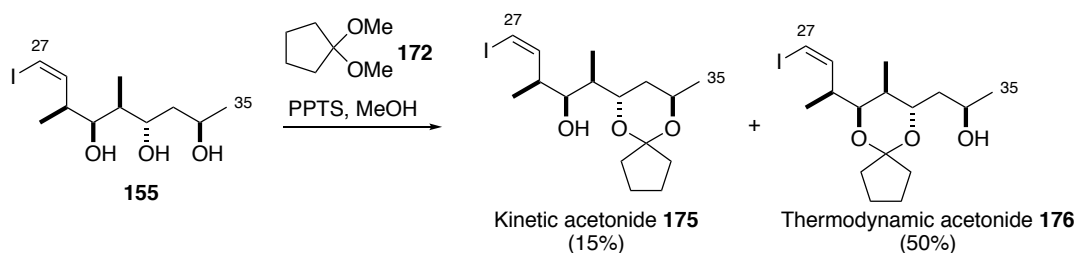
Cyclopentanone was chosen as the starting material for the preparation of 1,1-dimethoxycyclopentane **172**. Several sets of conditions to effect this transformation were investigated as shown in Table 2.3:

Table 2.3: Attempted acetal formation of cyclopentanone

Entry	Conditions (equiv.)	Result
1	(CH ₃ O) ₃ CH (3.0), TsOH (0.5%), MeOH, 16 h	Full conversion
2	(CH ₃ O) ₃ CH (2.0), TsOH (0.5%), MeOH, 16 h	50% conversion
3	TiCl ₄ (0.01), Et ₃ N (0.12), MeOH, 1 h	15% yield
4	TiCl ₄ (0.01), Et ₃ N (0.12), MeOH, 16 h	32% yield

Trimethyl orthoformate and *p*-toluenesulfonic acid in methanol⁷² were initially selected (Entry 1), which resulted in full conversion of cyclopentanone indicated by the NMR data of the crude product. However, the 1,1-dimethoxycyclopentane **172** yielded could not be separated from the unreacted trimethyl orthoformate *via* distillation. It was assumed that by adding less trimethyl orthoformate, the product could be purified more easily. Hence the number of equivalents of trimethyl orthoformate was reduced from 3 to 2 (Entry 2). However, under the modified conditions, only 50% of the cyclopentanone was transformed into 1,1-dimethoxycyclopentane **172**, and the product and the unreacted trimethyl orthoformate were still inseparable. It appeared that the yield was highly dependent on the equivalents of trimethyl orthoformate, thus using one equivalent of trimethyl orthoformate was expected to result in an even lower yield with some unreacted trimethyl orthoformate mixed with the product. At this point, alternative conditions utilising titanium tetrachloride and triethylamine⁷³ were investigated. After a reaction time of one hour, the product was purified by distillation in 15% yield (Entry 3). Keeping the reaction for a longer time (16 h) gave a better yield (32%) of the product.

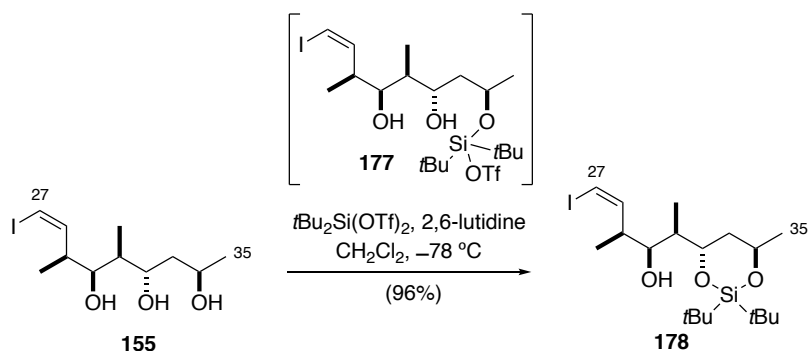
With 1,1-dimethoxycyclopentane **172** in hand, terminal acetonide formation from triol **155** was tested.



Scheme 2.27: Acetonide formation of triol **155**

The reaction proceeded significantly more slowly (full conversion in 3 h) than with 2,2-dimethoxypropane (full conversion in 5 min), presumably due to the bulkier cyclopentyl group. Unfortunately, the thermodynamic ketal **176** was formed as the major product (50%) rather than the desired kinetic ketal **175** (15%) (Scheme 2.27).

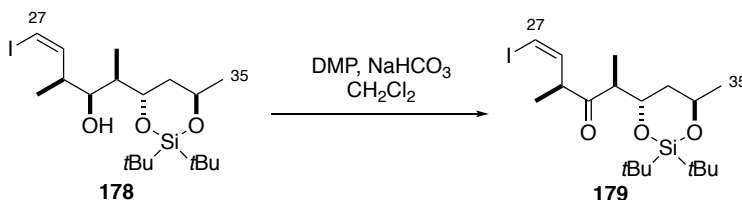
Following this disappointing result, we considered other protecting groups that might allow selective protection of the C32 and C34 alcohols and also facilitate straightforward deprotection in the endgame. A silylene acetal would match the silyl groups present in the other fragments and would hopefully fulfill this objective. Di-*tert*-butylsilyl bis(trifluoromethanesulfonate) was thus tried as an alternative reagent for the terminal diol protection. Considering the steric bulk of the reagent, it was expected to react with the terminal C34 alcohol first to form silyl ether **177** (Scheme 2.28), followed by a second reaction with the adjacent C32 alcohol, giving the protected product **178**. To our delight, the reaction went smoothly and afforded product **178** in 96% yield. No migration to the internal position was observed.



Scheme 2.28: Terminal diol protection of triol **155**

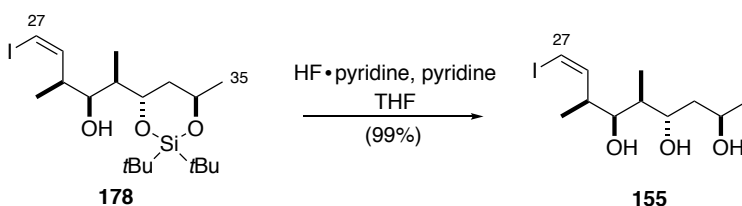
Alcohol **178** was oxidised⁷⁰ to ketone **179** to confirm the structure of the product (Scheme 2.29). The

proton signals for H30, H32 and H34 were identified by COSY correlations. After the oxidation, the H32 and H34 signals were identified but the H30 signal had disappeared, suggesting that the desired alcohol **178** was the product from the last step.



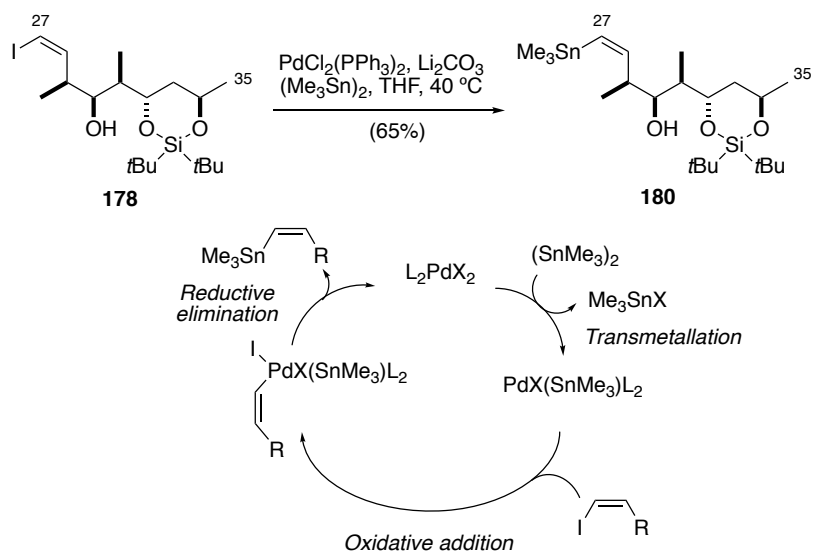
Scheme 2.29: Oxidation of alcohol **178**

Another concern was whether the silyl group could be removed during the final deprotection. This was tested by applying the anticipated global deprotection conditions to **178** (Scheme 2.30), which afforded the desired product **155** in excellent yield.



Scheme 2.30: Deprotection of the silyl group

To couple this fragment with the northwestern fragment **81** *via* a Stille-coupling reaction, vinyl iodide **178** needed to be transformed into vinyl stannane **180**. This was accomplished by a Wulff-Stille reaction³⁷ *via* a Pd-mediated catalytic cycle (Scheme 2.31).

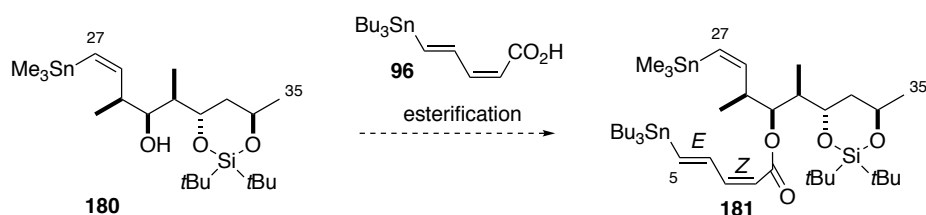


Scheme 2.31: Wulff-Stille reaction of vinyl iodide **178** and mechanism

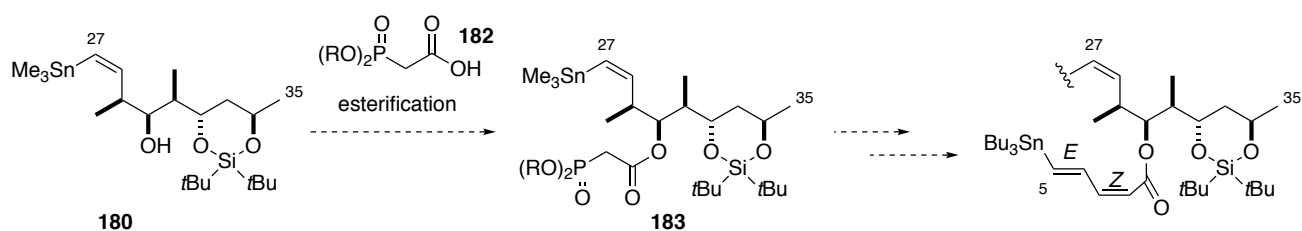
2.2.2 Installation of the dienyl stannane motif

The dienyl stannane motif at C30 needed to be incorporated into the fragment either at this point or at a later stage, to be used as a coupling handle for the macrocyclisation. Two approaches were considered and tested (Scheme 2.32). The first approach was to explore the coupling of alcohol **180** with carboxylic acid **96**. Based on Kan's unsuccessful trial⁵⁹ a further investigation of coupling conditions was proposed. In the second approach, esterification would be employed first to install a β -phosphono ester, which would be transformed to the $(2Z,4E)$ -diene *via* a stereoselective olefination after the fragment coupling stage.

Approach I

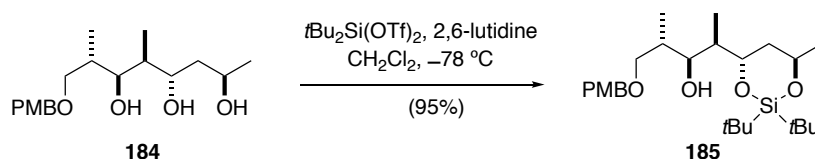


Approach II



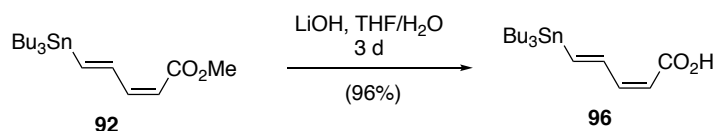
Scheme 2.32: Installation of $(2Z,4E)$ -dienyl stannane onto alcohol **180**

As vinyl stannane **180** was valuable and vulnerable, the alcohol **185** was prepared from intermediate **184** as a model substrate for the test reactions (Scheme 2.33).



Scheme 2.33: Preparation of the model alcohol **185**

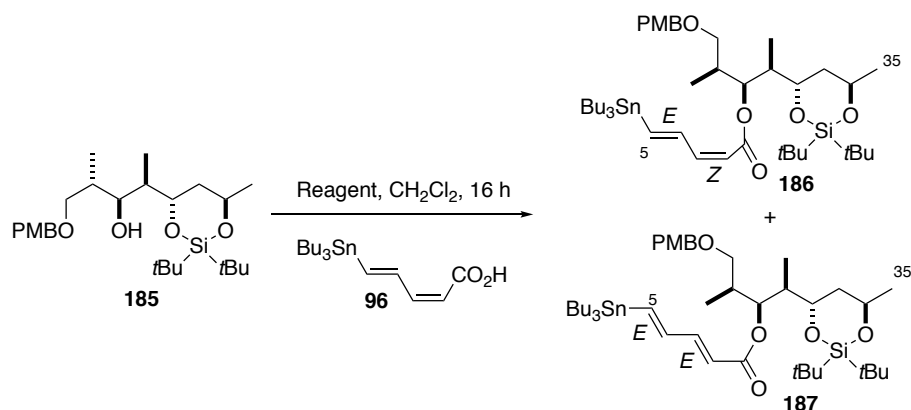
Acid **96** for approach I (Scheme 2.32) was prepared by the hydrolysis of ester **92** (from Jennifer Kan) with LiOH in 96% yield (Scheme 2.34).



Scheme 2.34: Preparation of acid **96**

A detailed screen of esterification conditions for approach I was previously carried out by Kan.⁵⁹ Unfortunately, none of the conditions tested could deliver the desired product **186**, either resulting in no reaction, or affording the undesired ester **187** with (E,E) -diene geometry. A new screen was undertaken as a further exploration of alternative conditions. The results are shown in Table 2.4:

Table 2.4: Screen of esterification conditions

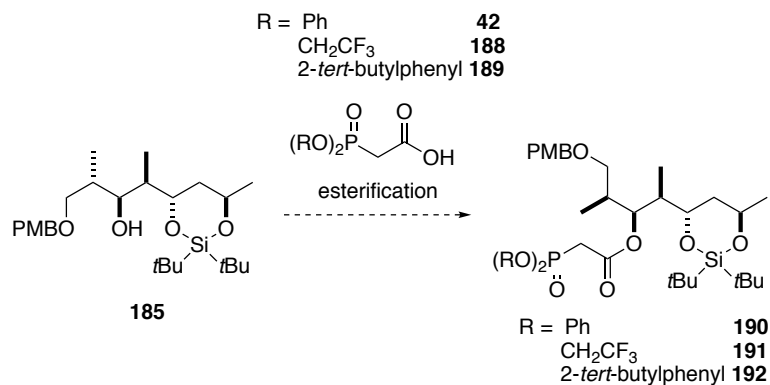


Entry	Reagent	<i>E,Z</i> : <i>E,E</i>
1	EDC + DMAP	0 : 1
2	EDC	No product
3	DCC + DMAP	0 : 1
4	DCC	No product
5	DCC + DIPEA	No product
6	DCC + DIPEA + HOBt	No product
7	DCC + LiHMDS	1 : 0 (15% yield)

Steglich esterification⁷⁴ (Entry 1) with EDC was tried first, yielding only the undesired (*E,E*)-diene ester **187**. Isomerisation was likely caused by reversible Michael addition of DMAP to the activated dienoic acid prior to ester bond formation. Removing DMAP from the conditions (Entry 2) resulted in no reaction. Steglich esterification with DCC (Entry 3) also gave the undesired (*E,E*)-diene ester **187** as the only product. Again, the reaction with only DCC (Entry 4) gave no product. DIPEA was used as a substitute for DMAP (Entry 5) to no avail. Addition of another activating agent, HOBt (Entry 6), still failed to deliver any product. Pleasingly, when alcohol **185** was premixed with LiHMDS for one hour at -78 °C before the mixture of DCC and acid **96** was added, the desired product **186** was formed as a single isomer. However, the yield (15%) was insufficient for practical purposes.

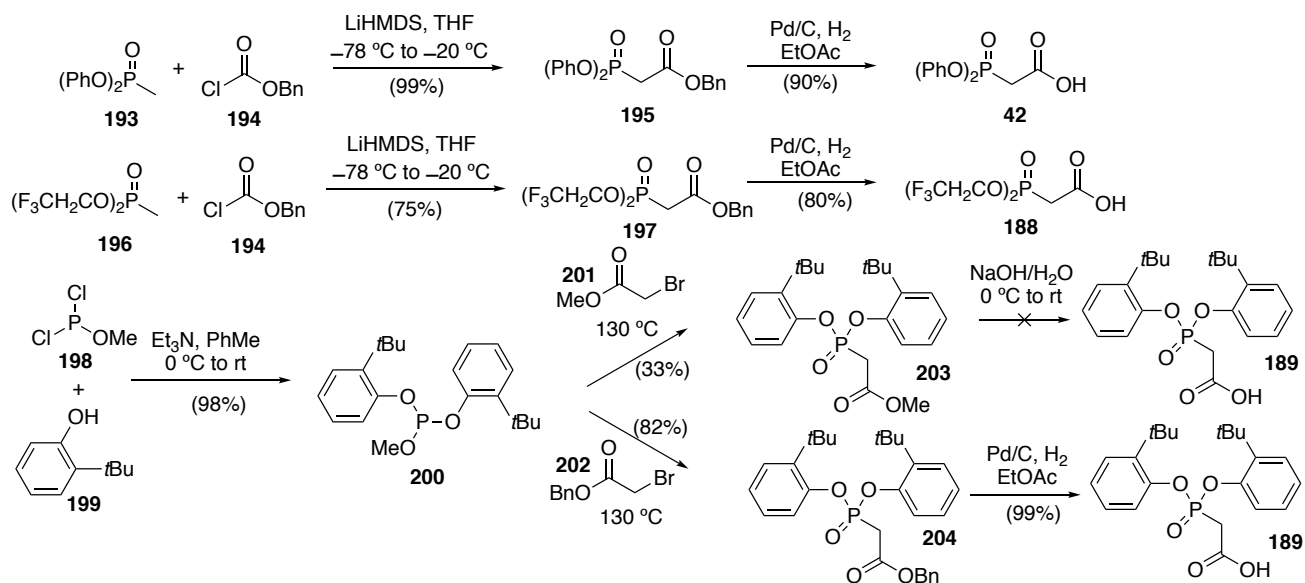
After the unsuccessful trial of approach I, approach II (Scheme 2.32) was investigated. Phosphonate

acids **42**, **188** and **189** were made in order to prepare phosphonate esters **190-192** from alcohol **185** by esterification (Scheme 2.35).

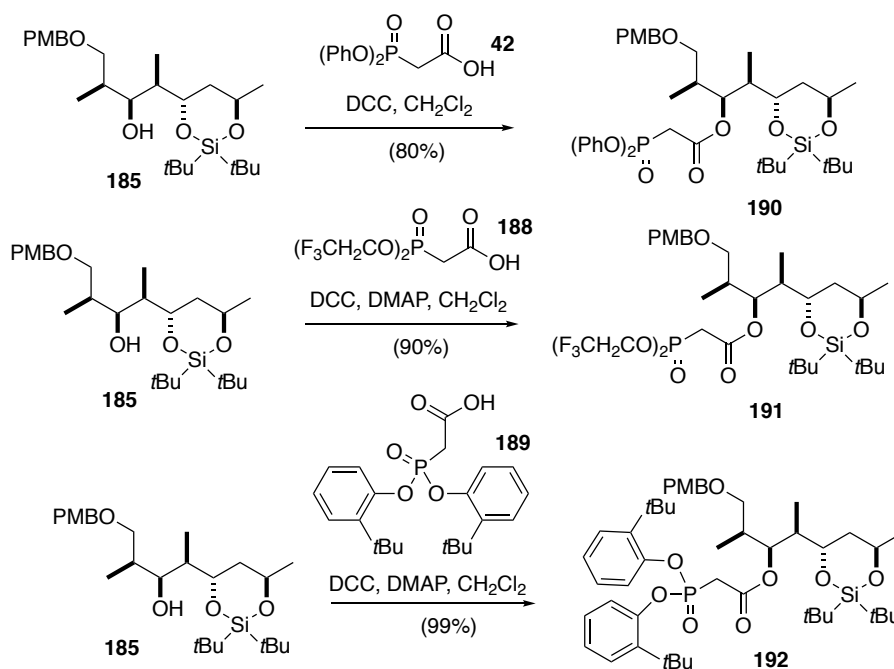


Scheme 2.35: Esterification of alcohol **185**

Phosphonate acids **42** and **188** were prepared by the addition of lithiated diphenyl methylphosphonate **193** or bis(2,2,2-trifluoroethyl) methylphosphonate **196** to benzyl chloroformate **194**, followed by the cleavage of the benzyl group using hydrogen and activated palladium (Scheme 2.36).⁷⁵ The synthesis of phosphonate acid **189** started with the reaction of methyl dichlorophosphite **198** and 2-*tert*-butylphenol **199**. An Arbuzov reaction with either methyl bromoacetate **201** or benzyl bromoacetate **202** afforded the corresponding phosphonates **203** and **204**.⁷⁶ Hydrolysis of methyl ester **203** did not yield the desired phosphonate acid **189**. Pleasingly, cleavage of the benzyl group from phosphonoester **204** under hydrogen atmosphere gave the target phosphonate acid **189** in 99% yield.

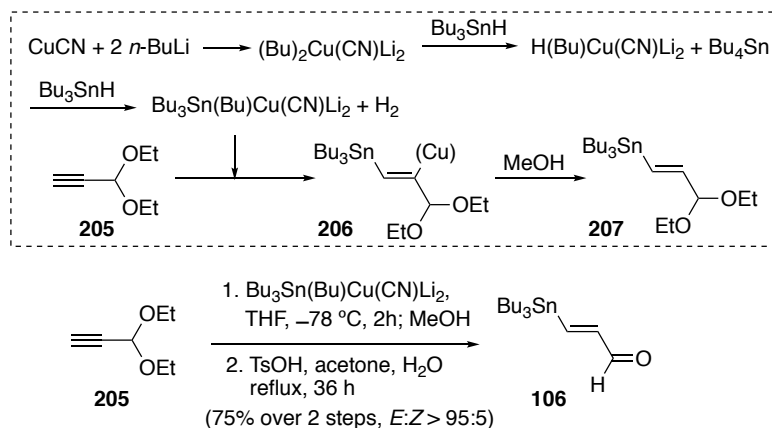


With the phosphonate acids in hand, alcohol **185** was transformed into phosphonate esters **190-192** *via* esterification under Steglich conditions⁷⁴ in good yields (Scheme 2.37).



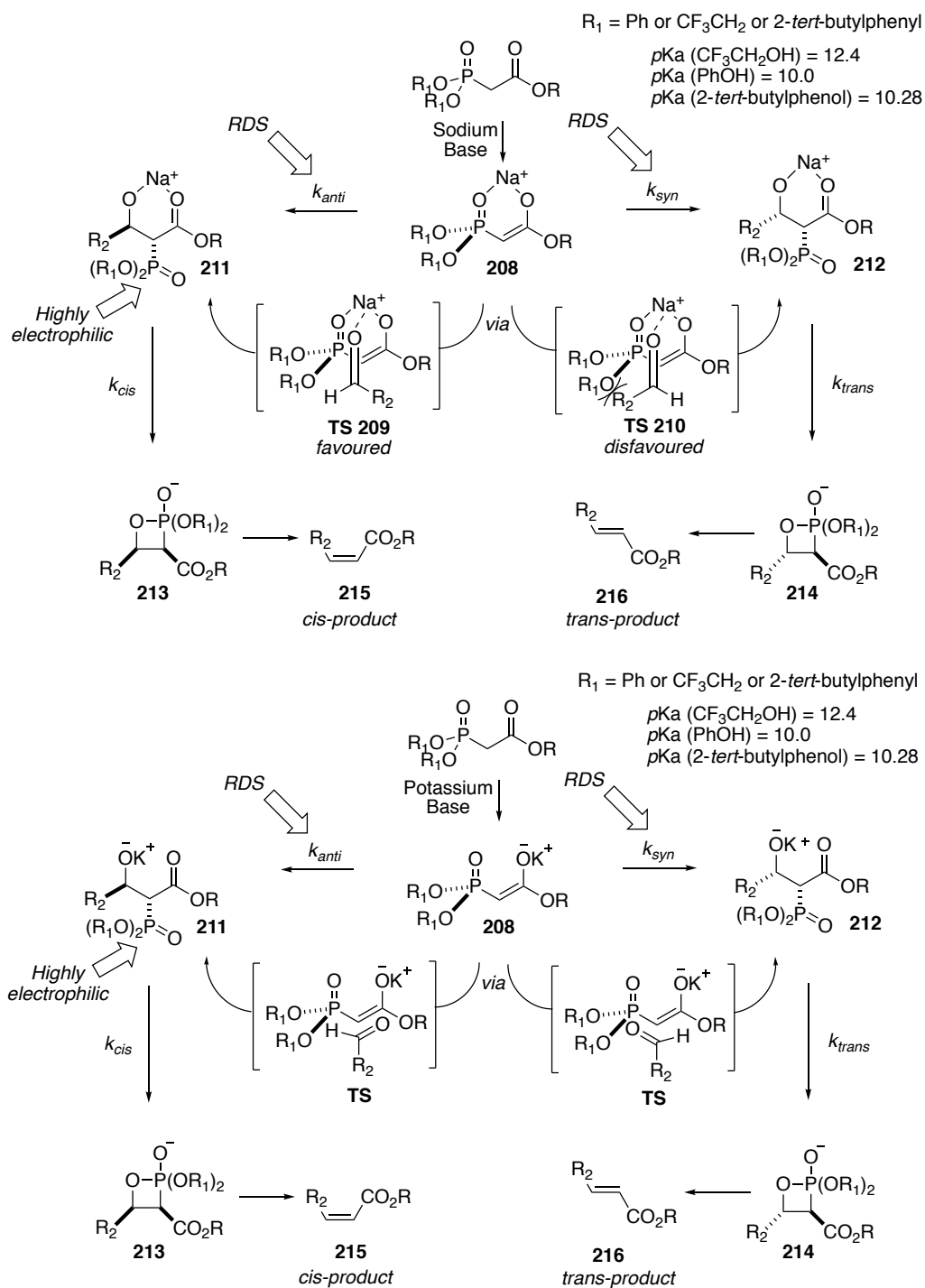
Preparation of stannylenal **106** started with *syn*-stannylcupration of diethoxypropyne **205** using Lipshutz reagent ($\text{Bu}_3\text{Sn}(\text{Bu})\text{Cu}(\text{CN})\text{Li}_2$),⁷⁷ followed by quenching the resulting organocuprate with

methanol.⁷⁸ The crude vinyl stannane was then submitted to acid-catalysed acetal hydrolysis to give stannylenal **106** in 75% yield and excellent stereoselectivity over 2 steps (Scheme 2.38).



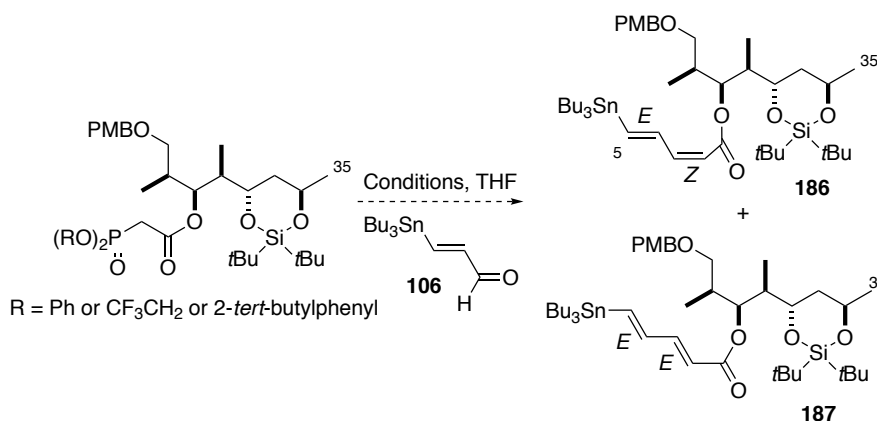
Scheme 2.38: Preparation of stannylenal **106**

With the phosphonate esters **190-192** and the stannylenal **106** in hand, the stereoselective olefination was attempted, as shown in Table 2.5. The mechanisms for all the three types of olefination are similar (Scheme 2.39). The first step is deprotonation of the β -phosphonoester, which would then attack the aldehyde that co-ordinates with the sodium cation to give intermediates **211** and **212**. The *anti*-intermediate **211** would cyclise to form the *cis*-oxaphosphetane **213** which collapses to yield the *cis*-product **215**. In contrast, the *syn*-intermediate **212** would generate the *trans*-product **216** via the *trans*-oxaphosphetane **214**. The electron withdrawing R_1 groups endow the electron-deficient phosphorous with high electrophilicity, leading to fast formation of oxaphosphetanes **213** and **214** from intermediates **211** and **212**. The slower generation of the intermediates **211** and **212** hence becomes the rate determining step ($k_{\text{cis}}/k_{\text{trans}} > k_{\text{syn}}/k_{\text{anti}}$). The *anti*-intermediate **211** is generated faster due to the favoured transition state **TS 209** with less steric hindrance ($k_{\text{anti}} > k_{\text{syn}}$), resulting in the *cis*-product **215** as the major product. However, due to the low chelation ability of potassium cation, the aldehyde is not co-ordinated with the potassium ion while being attacked by the enolate **208**, leading to the two transition states with similar energy. Therefore, the *cis*-product **215** and the *trans*-product **216** are generated in nearly 1:1 ratio when using potassium bases.



Scheme 2.39: Mechanism of the olefinations

Table 2.5: Tests of stereoselective olefination

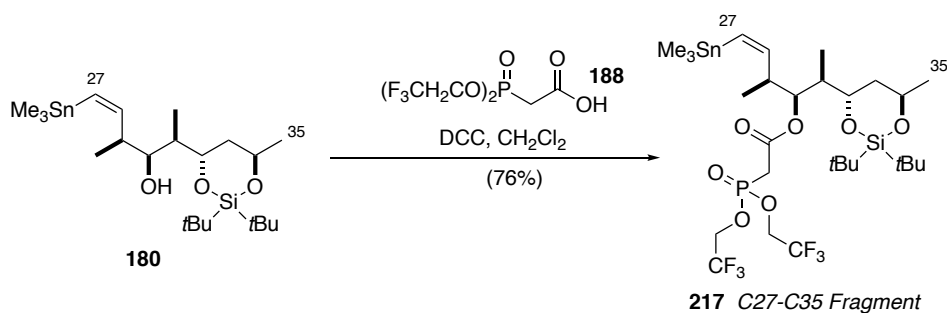


Entry	R	Base	Temperature	Time	<i>E,Z</i> : <i>E,E</i>
1	Ph	NaH	−78 to −10°C	6 h	1.4 : 1
2	Ph	KOtBu	−78 to −20°C	16 h	1.4 : 1
3	Ph	KOtBu	−78 to −40°C	16 h	1.4 : 1
4	Ph	KOtBu	−78°C	40 h	1.3 : 1
5	2- <i>tert</i> -butylphenyl	KOtBu	−78°C to rt	72 h	No product
6	2- <i>tert</i> -butylphenyl	NaH	−78 to 0°C	48 h	1.3 : 1
7	CF ₃ CH ₂	KHMDS, 18-crown-6	−78°C	40 h	No product
8	CF ₃ CH ₂	KOtBu	−78 to −30°C	20 h	1.8 : 1
9	CF ₃ CH ₂	KOtBu	−78°C	72 h	2.0 : 1
10	CF ₃ CH ₂	NaH	−78 to −30°C	20 h	2.0 : 1

All the test reactions gave full conversion of the phosphonate esters except Entries 5 and 7, the starting materials of which were recovered. Ando-type olefinations (R = Ph) were first tried. With NaH as the base (Entry 1), the reaction was complete in 6 hours with a moderate selectivity for the desired *E,Z*-product (**186:187** = 1.4:1). Changing the base from NaH to KOtBu and maintaining a colder temperature of −20°C instead of −10°C (Entry 2) resulted in a longer reaction time, but the same selectivity was observed. Keeping the reaction below −40°C (Entry 3) did not increase the reaction time, but the selectivity was not improved either. Keeping the reaction at −78°C (Entry 4) resulted in a longer reaction time, and the selectivity was slightly worse than before (**186:187** =

1.3:1). Replacing the phenyl group with 2-*tert*-butylphenyl (Entry 5 and 6) was proposed to improve the selectivity as a bulkier R₁ group might disfavour **TS 210** (Scheme 2.39), resulting in a better ratio of the *E,Z*-product **186**. KO*t*Bu was first used as the base (Entry 5) but the reaction yielded no product. NaH was then trialled at –78 to 0°C (Entry 6) and provided the product with a selectivity **186:187** = 1.3:1. Still-Gennari-type olefinations (R = CF₃CH₂) were last attempted. The most common conditions for Still-Gennari reactions (KHMDs, 18-crown-6, Entry 7) were tested first, but no product was detected. KO*t*Bu was then used as an alternative base (Entry 8). Pleasingly, after 20 hours, the products were isolated with improved selectivity (**186:187** = 1.8:1). With the assumption that keeping the reaction at a lower temperature would provide a better selectivity, the reaction was left at –78°C for 72 hours (Entry 9), and the selectivity did improve further (**186:187** = 2.0:1). Lastly, NaH was tested as the base (Entry 10). This condition required shorter reaction time (20 h) and the selectivity stayed the same.

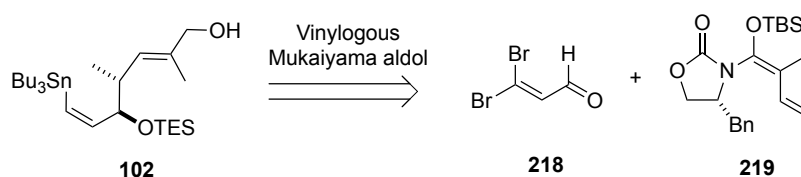
The best result from optimisation of the olefination conditions was using the Still-Gennari-type phosphonate and NaH at –78°C. The corresponding phosphonate acid **188** was thus installed onto alcohol **180** by esterification in 76% yield, finalising the synthesis of the north-eastern fragment **217** in an overall 23% yield over 14 steps LLS.



Scheme 2.40: Synthesis of the north-eastern fragment **217**

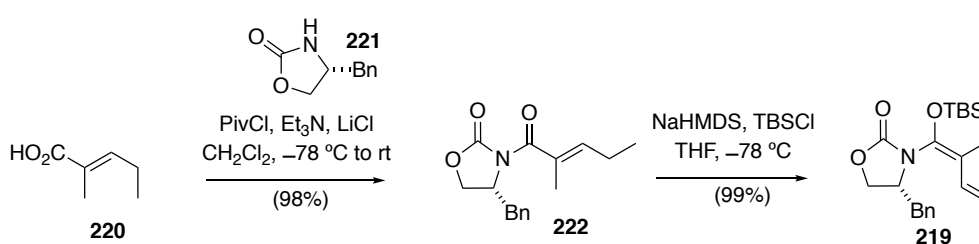
2.3 Synthesis of the C7-C13 Southern fragment

The C7-C13 southern fragment **102** was synthesised based on Kan's work⁷⁹. The C8-C9 trisubstituted olefin and the C10 and C11 stereogenic centres would be set up in a single operation using a chiral auxiliary-based vinylogous Mukaiyama aldol reaction⁸⁰ between dibromoacrolein **218** and silyl ketene aminal **219** (Scheme 2.41).



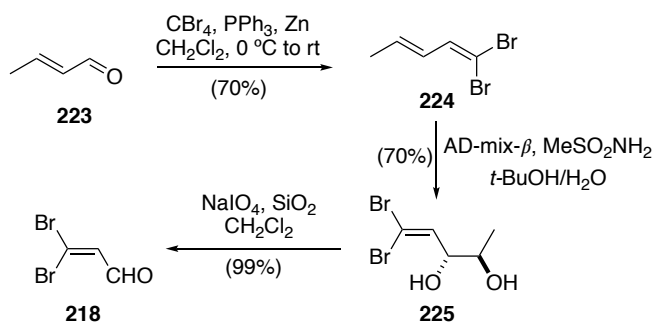
Scheme 2.41: Retrosynthetic analysis of C7-C13 southern fragment **102**

For the preparation of vinylogous silyl ketene aminal **219**, D-phenylalanine-derived oxazolidinone **221** was acylated with 2-methyl-2-pentenoic acid **220**, giving imide **222** in 98% yield. Imide **222** was then enolised using NaHMDS and the resulting dienolate was trapped with TBSCl to provide silyl ketene aminal **219** (Scheme 2.42). The (*E,E*)-geometry formation is presumed to be controlled by dicarbonyl chelation⁸¹ and minimisation of A^{1,3}-strain during deprotonation.



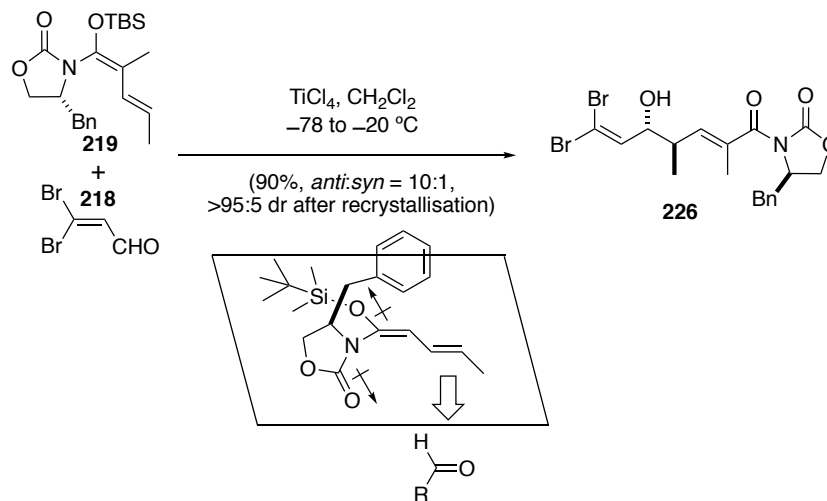
Scheme 2.42: Preparation of vinylogous silyl ketene aminal **219**

Dibromoacrolein **218** was synthesised in 3 steps from crotonaldehyde **223** (Scheme 2.43). Corey-Fuchs reaction of crotonaldehyde **223** provided dibromodiene **224**, which was submitted to Sharpless asymmetric dihydroxylation followed by oxidative cleavage to give dibromoacrolein **218**. Sharpless asymmetric dihydroxylation was applied due to its improved regioselectivity over other achiral methods rather than to provide good enantioselectivity.



Scheme 2.43: Synthesis of dibromoacrolein **218**

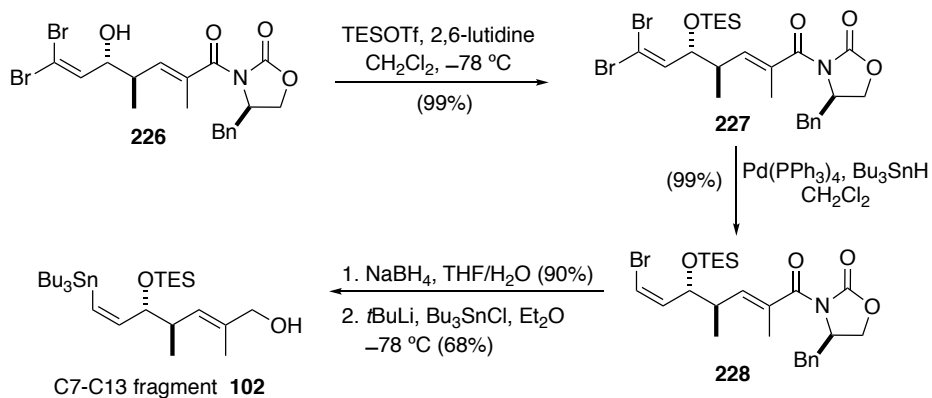
Aminal **219** and dibromoacrolein **218** were submitted to the vinylogous aldol reaction using freshly distilled TiCl_4 to generate the aldol adduct in 90% yield and 10:1 diastereoselectivity. The product was recrystallised to give the *anti*-adduct **226** as a single diastereomer. The high degree of diastereoselectivity can be attributed to the favoured conformation of silyl ketene aminal **219**. Opposing dipole moments place the benzyl group above the top face (as drawn in Scheme 2.44), providing a less hindered lower π -face, on which side the dibromoacrolein **218** approaches to minimise steric strain.



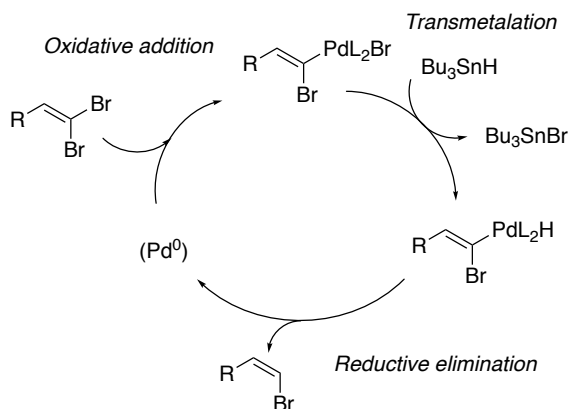
Scheme 2.44: Vinylogous Mukaiyama aldol reaction

The C11 hydroxyl group of aldol adduct **226** was then protected as a TES ether **227**. Stereoselective hydrogenolysis⁸² of the product **227** afforded (*Z*)-vinyl bromide **228** in 99% yield (Scheme 2.45). The mechanism is shown in Scheme 2.46. The high selectivity of this reaction is due to faster oxidative addition of $\text{Pd}(0)$ to the less hindered *trans* C-Br bond, followed by transmetalation with Bu_3SnH and reductive elimination. The chiral auxiliary of **228** was cleaved with NaBH_4 and the

vinyl bromide was transformed into a vinyl stannane by a halogen-lithium-tin exchange to yield C7-C13 fragment **102**. Overall, this C7-C13 southern fragment **102** was synthesised in 52% yield over 7 steps LLS.



Scheme 2.45: Synthesis of C7-C13 fragment **102**

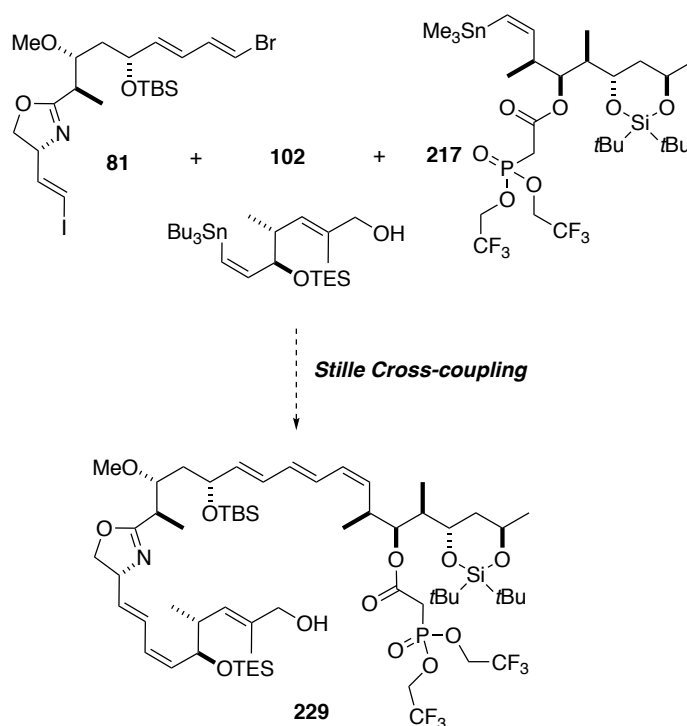


Scheme 2.46: Mechanism of stereoselective hydrogenolysis

2.4 Fragment coupling and endgame strategy

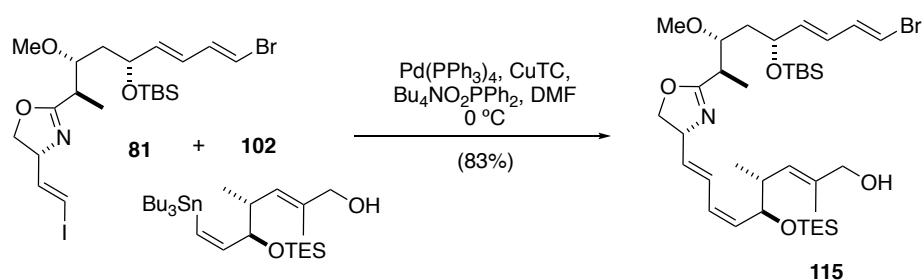
2.4.1 One-pot Stille cross-coupling

With all the three fragments in hand, the next step was to couple them *via* the previously established one-pot Stille cross-coupling method.



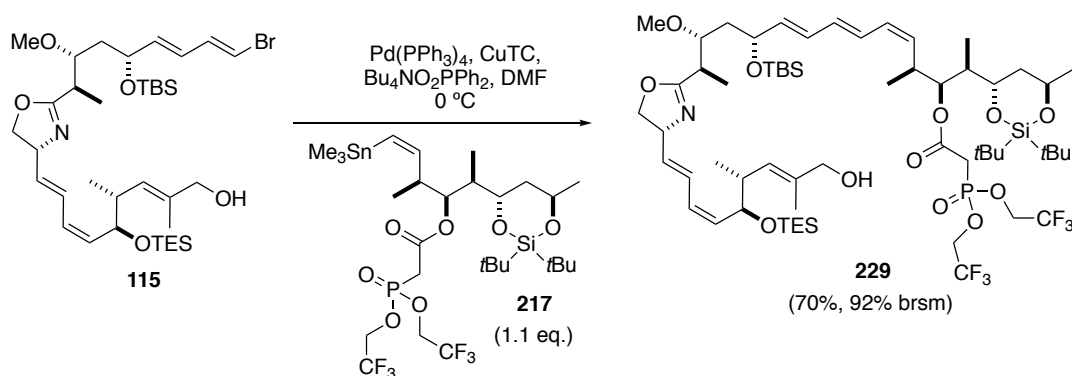
Scheme 2.47: One-pot Stille cross-coupling reaction of the three fragments

To gain a better understanding of how well the Stille coupling would work on our system, the coupling of the north-western fragment **81** and the southern fragment **102** was tried first. Pleasingly, the reaction was straightforward under Fürstner-type conditions,⁸³ yielding the product **115** in 83% yield after 1.5 hours (Scheme 2.48). No double bond isomerisation or reaction with the vinyl bromide was observed.



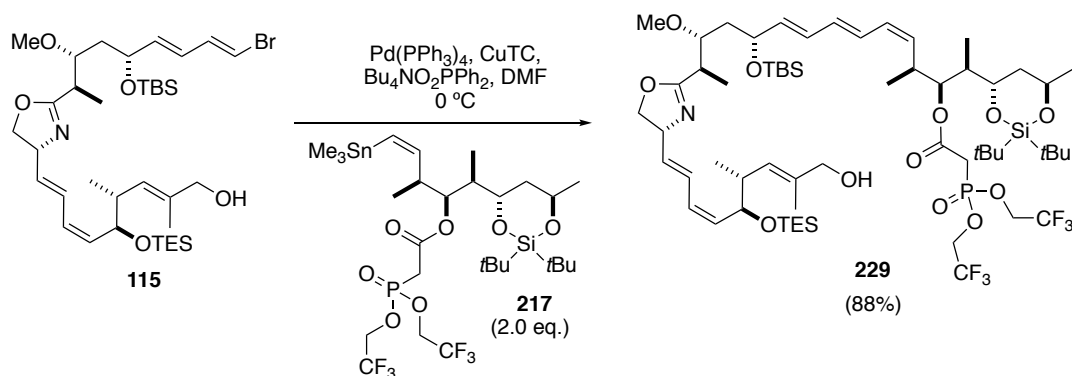
Scheme 2.48: Stille coupling of fragment **81** and fragment **102**

The second Stille coupling between fragment **115** and the north-eastern fragment **217** was carried out under the same conditions. The north-eastern fragment **217** was fully consumed in one hour, yielding the product **229** in 70% yield, and 22% of fragment **115** was recovered (Scheme 2.49). Although the north-eastern fragment **217** was used in excess (1.1 eq.), fragment **115** did not completely react. This was attributed to the slow destannylation of **217** during the reaction, which was supported by NMR data analysis.



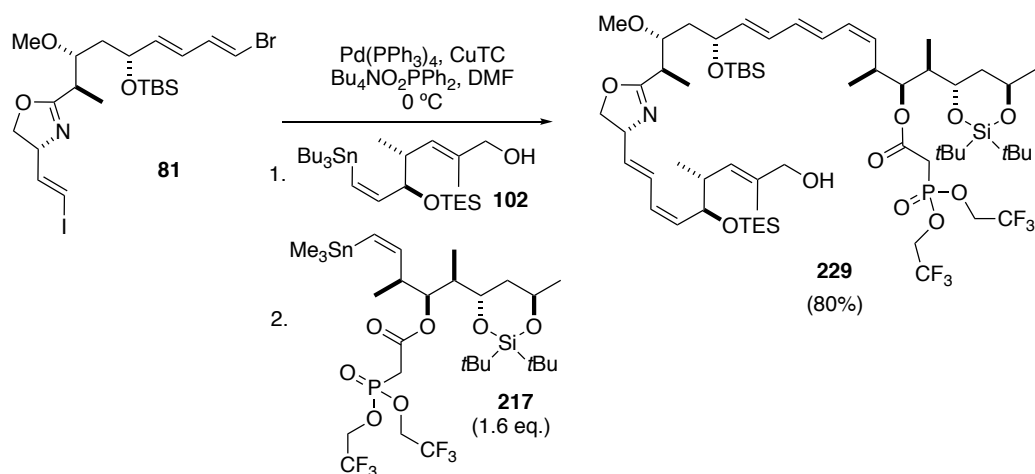
Scheme 2.49: Stille coupling of fragment **115** and fragment **217**

To improve the yield, the stoichiometry of the north-eastern fragment **217** was increased to 2.0 eq. In this trial, the fragment **115** was fully consumed after one hour, giving 88% yield of the desired product **229** (Scheme 2.50).



Scheme 2.50: Improved Stille coupling of fragment **115** and fragment **217**

With the conditions for two sequential Stille cross-couplings established, conducting them in a one-pot manner was next pursued. The reaction was carefully monitored to ensure the fragments were fully consumed before the addition of the next building block. The desired product **229** was formed in 80% yield with no observed side products (Scheme 2.51).

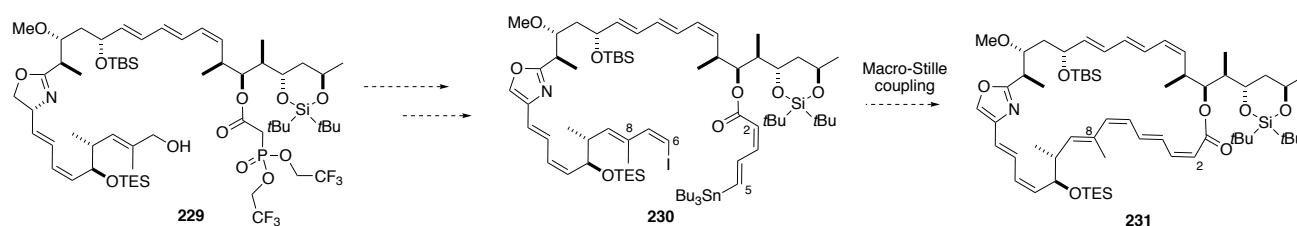


Scheme 2.51: One-pot Stille cross-coupling of the three fragments

The same Fürstner-type conditions⁸³ for the two sequential Stille coupling reactions made the efficient multi-component assembly in a single synthetic operation possible. This one-pot method reduced loss of the valuable intermediate **115** and minimised waste generation by avoiding work up and purification for the intermediate **115**.

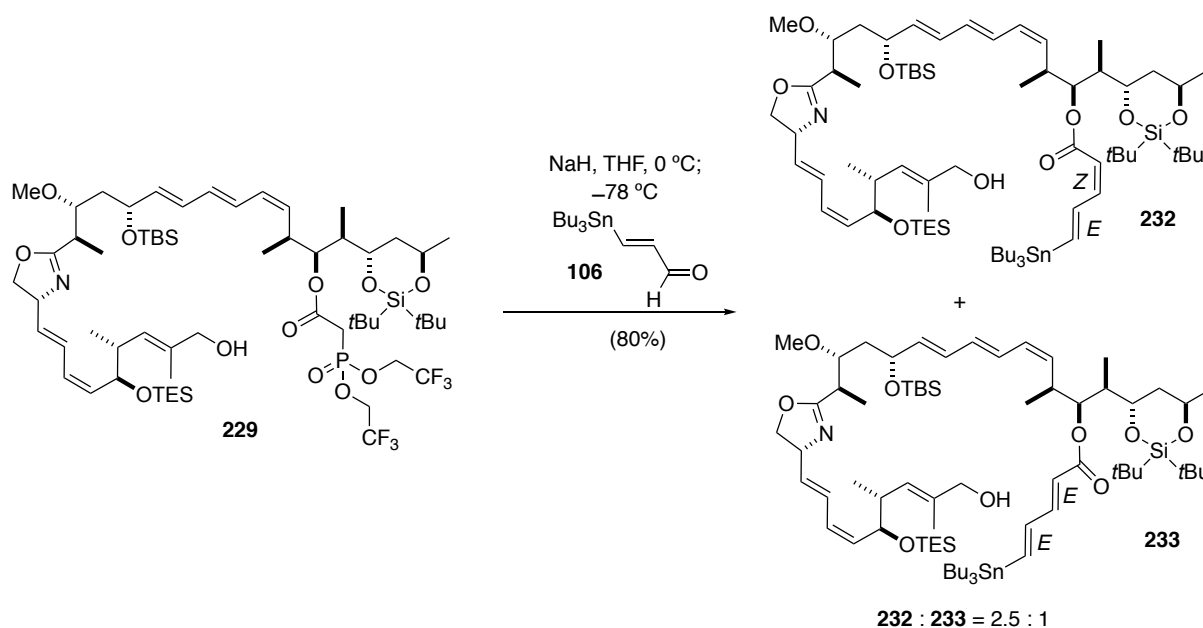
2.4.2 Construction of the macrocycle

Following the successful assembly of the three fragments, construction of the (2*Z*,4*E*)-diene and the (6*Z*,8*E*)-diene from the advanced intermediate **229** was next pursued. Intermediate **230** bearing a vinyl stannane at C5 and a vinyl iodide at C6 was targeted for the final macro-Stille coupling which would provide the tetraene motif and close the ring.



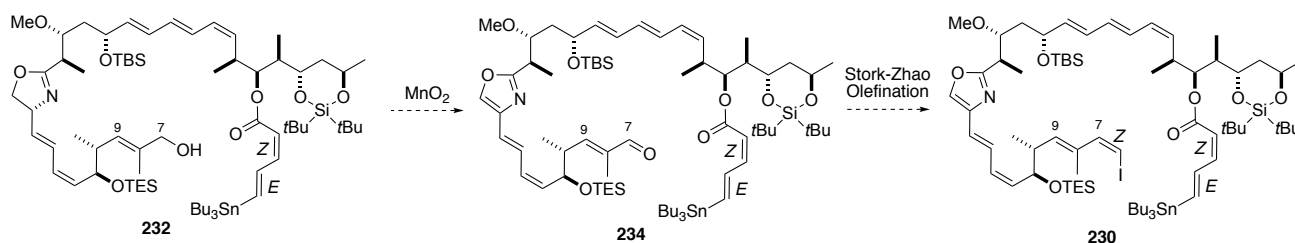
Scheme 2.52: The proposed approach for constructing the macrocycle **231**

The (2*Z*,4*E*)-diene was generated *via* the optimised Still-Gennari conditions⁸⁴ as previously discussed in Chapter 2.2.2. Phosphoryl ester **229** was deprotonated with NaH at 0 °C for one hour before the mixture was cooled down to -78 °C, at which point aldehyde **106** was added. After 20 hours, (Z,*E*)-isomer **232** and (E,*E*)-isomer **233** were isolated as a 2.5 : 1 mixture in 80% yield.



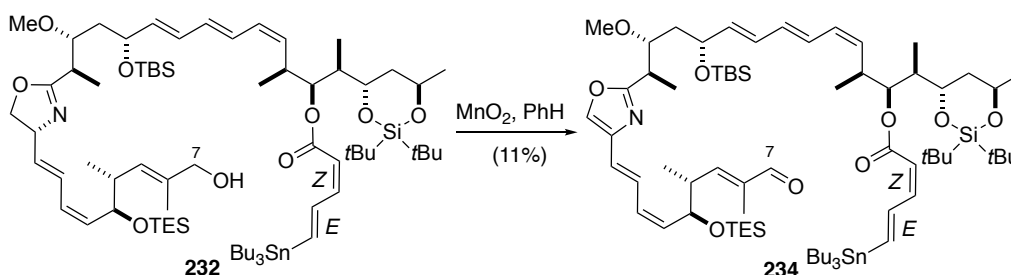
Scheme 2.53: Still-Gennari olefination of phosphoryl ester **229**

Construction of the (6*Z*,8*E*)-iodo-diene **230** was designed as a two-step sequence: (1) MnO₂ mediated double oxidation of the C7 alcohol and the oxazoline,⁸⁵ (2) Stork-Zhao olefination of the newly formed C7 aldehyde to give (*Z*)-vinyl iodide (Scheme 2.54).



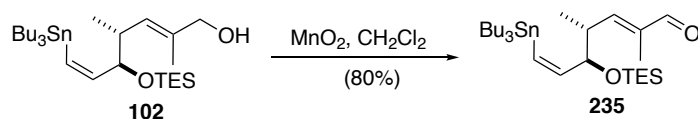
Scheme 2.54: The proposed approach for the construction of (6*Z*,8*E*)-iodo-diene **230**

For the double oxidation step, excess MnO₂ was added in one portion and the reaction was kept at room temperature for 16 hours. Although the desired product **234** was isolated cleanly, the yield was a disappointing 11% (Scheme 2.55).



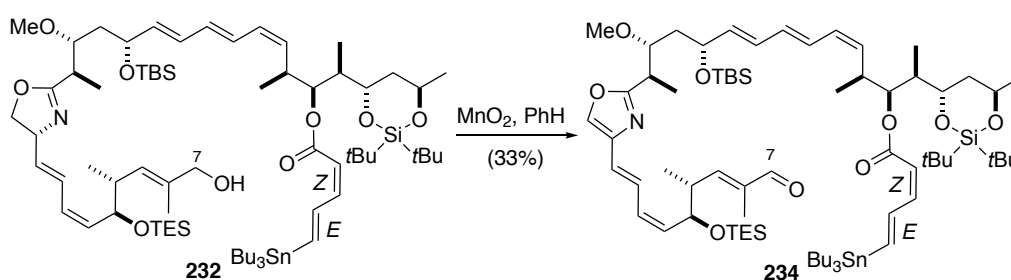
Scheme 2.55: First trial of the double oxidation reaction

The southern fragment **102** was used to investigate the oxidation conditions. Submitting the fragment **102** into the same oxidation conditions gave the desired aldehyde **235** in 80% yield after two hours (Scheme 2.56). This result possibly implies that although the oxidation conditions provided the product **234**, the sensitive polyene motifs made the product prone to decomposition under the reaction conditions if kept for too long.



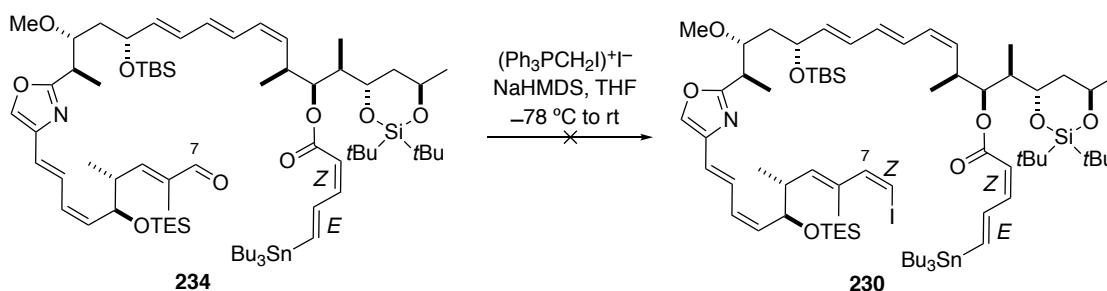
Scheme 2.56: Test of the oxidation conditions on fragment **102**

With this assumption, the oxidation conditions were modified: MnO_2 was added into the reaction in several small portions instead of in one portion. The reaction was carefully monitored and quenched immediately once the starting material **232** was consumed. With the new method, the yield increased to 33% (Scheme 2.57). Many efforts were made to further improve the yield but nothing helped. The problem was deduced to be with the oxazoline-oxazole oxidation, as oxidation of an unactivated oxazoline to an oxazole is quite challenging.



Scheme 2.57: The double oxidation reaction with the improved conditions

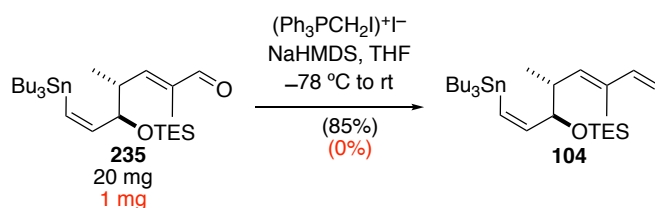
Stork-Zhao olefination was then applied to aldehyde **234** aiming to provide (*Z*)-vinyl iodide **230** (Scheme 2.58). NaHMDS and $(\text{Ph}_3\text{PCH}_2\text{I})^+\text{I}^-$ were mixed to generate the corresponding ylid, into which 5 mg of aldehyde **234** was added at -78°C . However, the NMR data of the crude showed only the starting material **234** with no desired product **230** found.



Scheme 2.58: Stork-Zhao olefination of aldehyde **234**

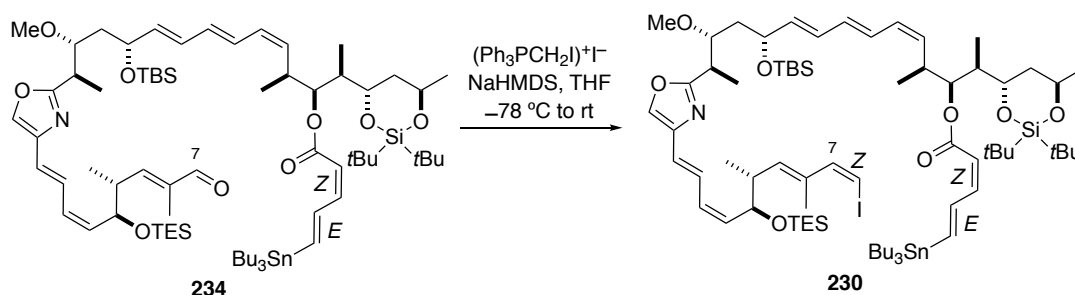
Aldehyde **235** generated from the southern fragment **102** (Scheme 2.56) was used to test the olefination conditions. Pleasingly, submitting 20 mg of aldehyde **235** into the same conditions gave (*Z*)-vinyl iodide **104** in 85% yield with full conversion (Scheme 2.59). The difference between the results of the two olefinations might arise from the difficulty in protecting the ylid from being quenched by adventitious moisture on small scales. This hypothesis was supported by repeating the

same reaction with 1 mg of aldehyde **235**, which yielded no desired product **104**.



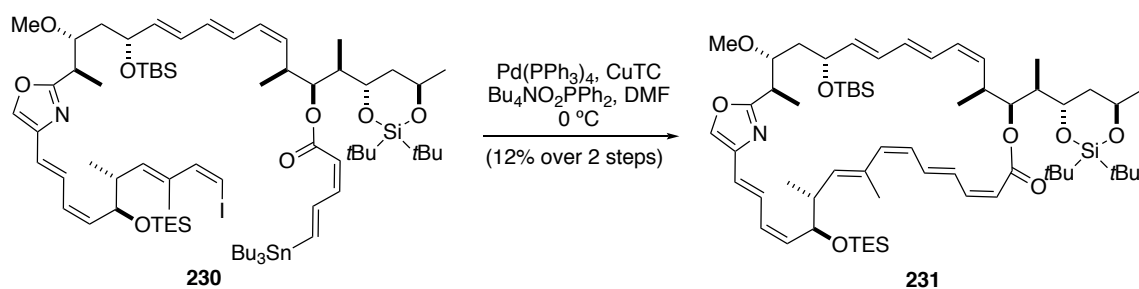
Scheme 2.59: Stork-Zhao olefination of aldehyde **235**

Following on from that discovery, it was proposed that a solution would be to prepare a stock solution of the ylid from NaHMDS and $(\text{Ph}_3\text{PCH}_2\text{I})^+\text{I}^-$ on a large scale, and add the desired amount of the pre-formed ylid to the reaction. This method proved effective on aldehyde **234**, giving the desired (Z)-vinyl iodide **230** (Scheme 2.60).



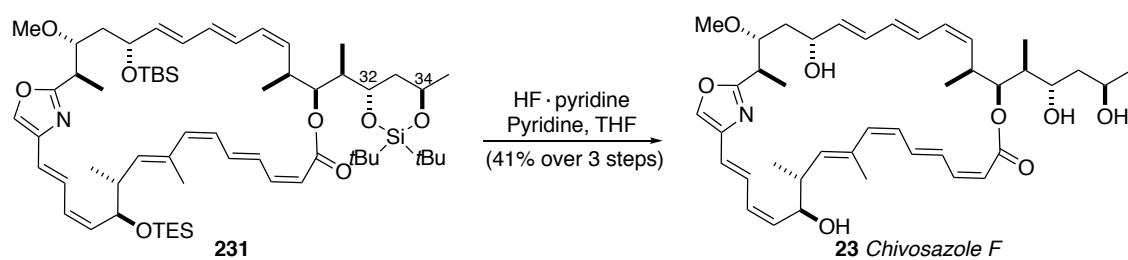
Scheme 2.60: Stork-Zhao olefination of aldehyde **234** with the new method

Due to the risk of isomerisation of the intermediate **230**, this compound was submitted into the macrocyclisation step as the crude material without further purification. Fürstner-type conditions were chosen for the macro-Stille reaction. Although the desired macrocycle **231** was obtained, the yield was only 12% over these two steps (Scheme 2.61). The low yield was attributed to the faster intermolecular Stille coupling reactions, which resulted in the side products from polymerisation. To minimise this problem, Simon Williams⁸⁶ proposed a way of adding the starting material **230** *via* syringe pump to ensure slow addition of **230** and high dilution of the reaction system, which improved the yield of the macrocyclisation.



Scheme 2.61: Macrocyclisation with a Stille reaction

The final deprotection step was completed by Williams⁸⁶. HF·pyridine-mediated removal of all the silicon-based protecting groups (including the silylene at C32/C34) afforded chivosazole F over 3 steps in 41% yield (Scheme 2.62). Gratifyingly, all ^1H and ^{13}C NMR spectroscopic data for this synthetic material correlated precisely with those reported for natural chivosazole F.²⁵



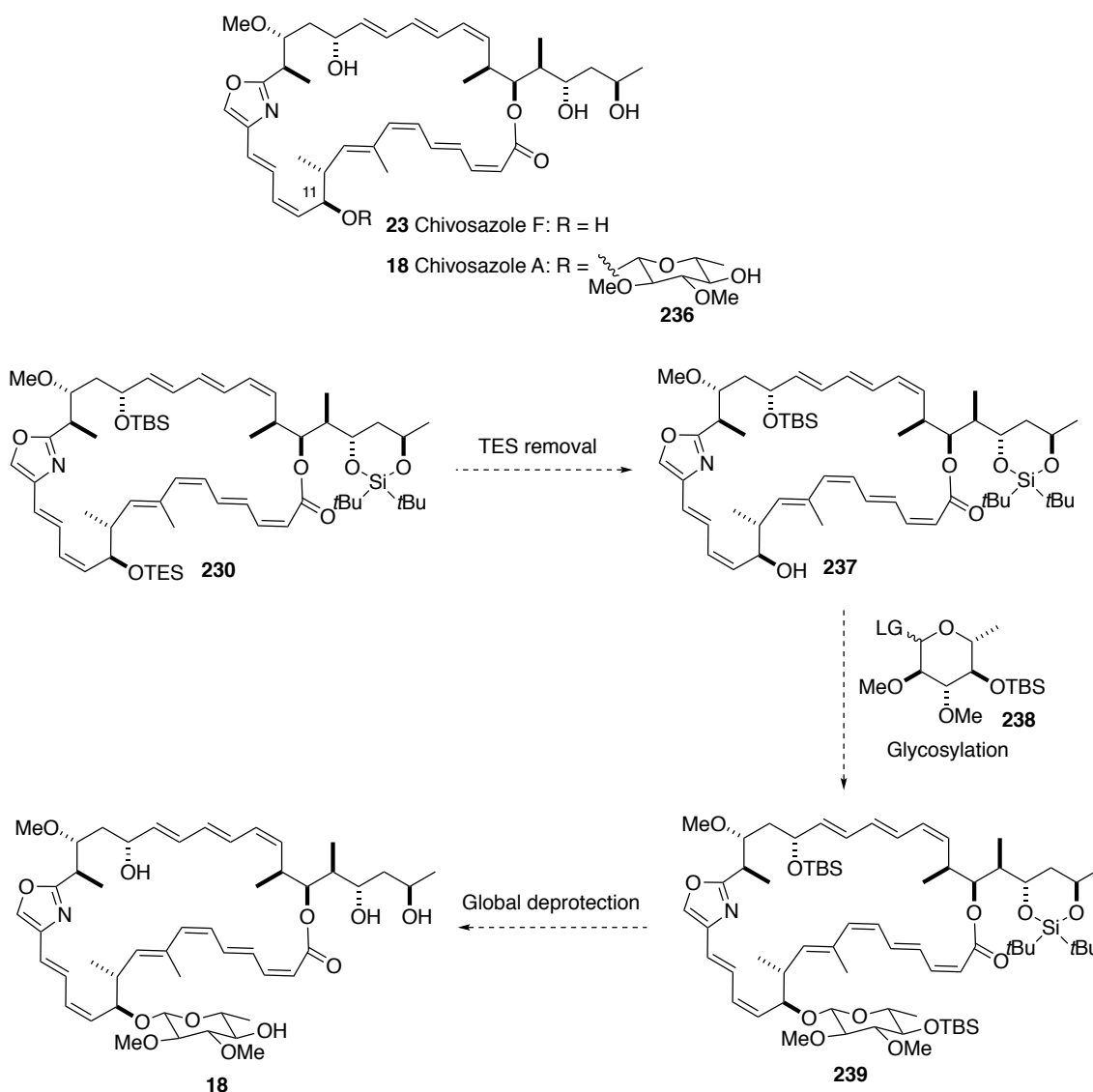
Scheme 2.62: Global deprotection (Williams)

2.5 Conclusions

The structurally complex macrocycle **231** was synthesised over 19 steps in an overall 0.73% yield. Synthesis of the three fragments **81**, **102** and **217** of similar size and complexity was first achieved. The macrocycle **231** was then assembled efficiently through the orchestration of the three Stille cross-coupling reactions, making the synthetic route highly convergent. Ten stereocentres and nine double bond geometries were installed with precise control. With improvement of the macrocyclisation step and completion of the global deprotection step (Williams), the total synthesis of chivosazole F has been achieved over 20 steps in an overall 2.5% yield.

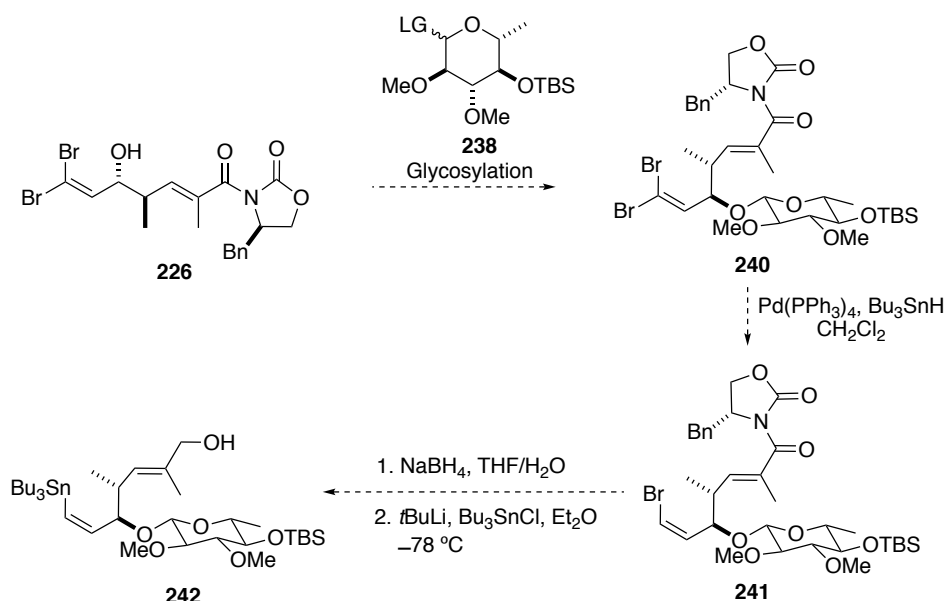
Chapter 3 Results and discussion on glycosylation

Chivosazole F and chivosazole A differ by a 6-deoxyglucopyranoside sugar side chain **236** at C11 of chivosazole A. The plan for the synthesis of the chivosazoles allowed for the synthesis of chivosazole A by selective removal of the TES group after the macrocyclisation step (Chapter 2.4.2) and glycosylation with the glycosyl donor **238**, followed by a global deprotection (Scheme 3.1).



Scheme 3.1: The initial plan for the synthesis of chivosazole A

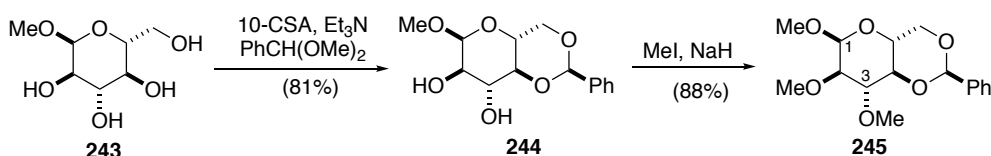
This strategy was based on the hypothesis that as the least bulky silyl protecting group on intermediate **230**, TES would be the easiest to remove. However, finding the optimal selective deprotection conditions by relying only on the minor difference among the three silyl protecting groups was eventually considered too risky and not enough material was available to test it. An alternative and more reliable plan was devised, to install the sugar side chain onto the southern fragment before the fragment coupling stage, which requires a new southern fragment **242** (Scheme 3.2). According to this strategy, having obtained the intermediate alcohol **226**, instead of the TES protection in Scheme 2.45, a glycosylation would be effected with the prepared glycosyl donor **238** to provide the glycoside **240**. Stereoselective reduction⁸² of the vinyl dibromide moiety of glycoside **240** would afford the (*Z*)-vinyl bromide **241**. Removal of the chiral auxiliary and the tin-lithium-halogen exchange would generate the new southern fragment **242**.



Scheme 3.2: The proposed synthetic route for the southern fragment **242**

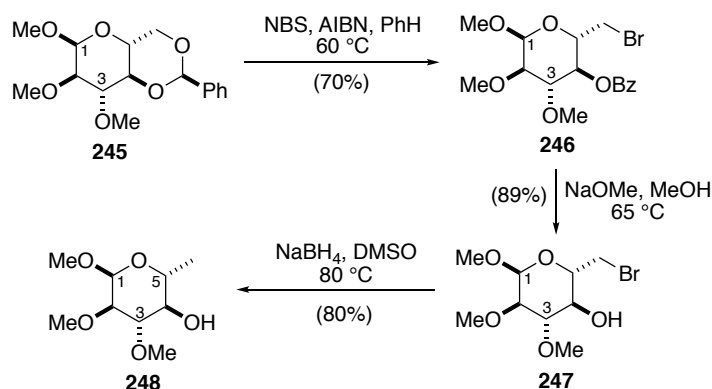
3.1 Glycosyl fluoride synthesis

Synthesis of the glycosyl donor **238** started with 1,2,3-trimethoxy sugar **245**, which was prepared by Rachel Elliott from methyl- α -D-glucopyranoside **243** over two steps: benzylidene acetal formation and methylation (Scheme 3.3).⁸⁷



Scheme 3.3: Preparation of 1,2,3-trimethoxy sugar **245** (Rachel Elliott)

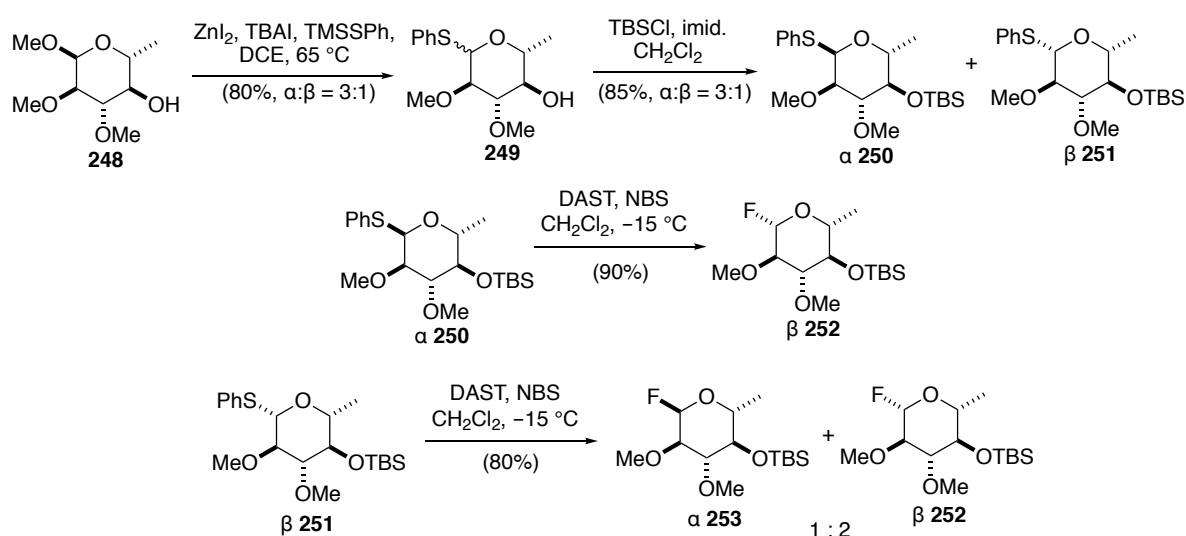
The regioselective bromination of the sugar **245** *via* a radical mechanism gave the 4-benzoyl-6-bromo sugar **246** as the single product.⁸⁸ The benzoate on **246** was then removed with NaOMe in methanol⁸⁹ to yield 6-bromo-4-hydroxy sugar **247**, which was submitted into the reductive debromination with NaBH_4 to afford the 4-hydroxy-5-methyl sugar **248**.⁹⁰



Scheme 3.4: Synthesis of the 4-hydroxy-5-methyl sugar **248**

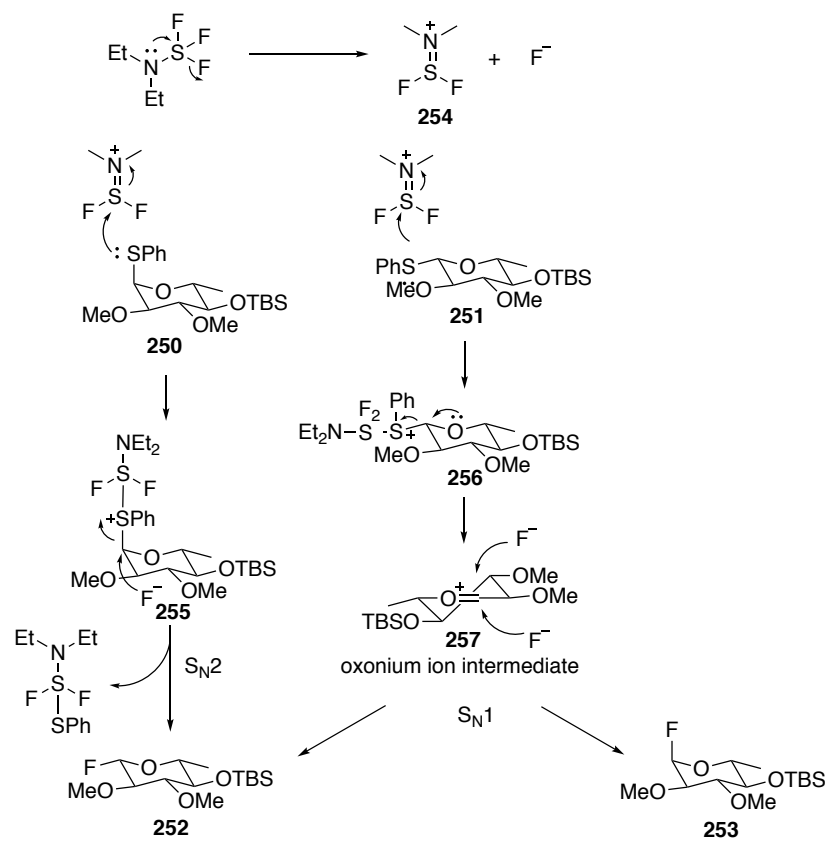
With the sugar **248** in hand, the next goal was to transform the C1-methoxy motif to a suitable leaving group for the planned β -glycosylation. According to studies conducted by Elliott,⁸⁷ the glycosyl fluorides **252** and **253** gave the best results. For this reason, the glycosyl fluorides **252** and **253** were prepared first. Installation of the thiophenyl moiety⁹¹ on the sugar **248** generated the thioglycoside **249** as an inseparable mixture of two anomers ($\alpha:\beta = 3:1$) in 80% yield (Scheme 3.5).

The secondary alcohol on the thioglycoside **249** was then protected with TBSCl to give the thioglycosides **250** and **251**. TBS instead of TES was used as the protecting group here as Rachel Elliott⁸⁷ reported that TES tended to be labile during the glycosylation process. The two anomers could be separated *via* careful column chromatography at this stage. The thiophenyl motif on the anomers **250** and **251** was then converted into the fluoride using DAST and NBS.⁹² The α -thioglycoside **250** gave the β -glycosyl fluoride **252** as the single anomer, the β -thioglycoside **251** gave the α -glycosyl fluoride **253** and the β -glycosyl fluoride **252**.



Scheme 3.5: Synthesis of the glycosyl fluorides **252** and **253**

The mechanism for the leaving group conversion is shown below (Scheme 3.6). DAST releases a fluoride anion first, and the remaining cation **254** coordinatively binds to the thiophenyl motif on the thioglycoside **250** or **251** to form the activated intermediates **255** and **256**. These intermediates can either react through an $\text{S}_{\text{N}}2$ mechanism with stereochemical inversion, or form an oxonium ion intermediate **257** facilitated by the lone pair electrons on the adjacent oxygen. For the α -thioglycoside **250**, the activated intermediate **255** is stable enough due to the anomeric effect, and can easily go through the $\text{S}_{\text{N}}2$ pathway, forming the β -glycosyl fluoride **252**. The activated intermediate **256** formed from the β -thioglycoside **251**, however, is relatively less stable and tends to form the oxonium ion intermediate **257**, which then goes through the $\text{S}_{\text{N}}1$ pathway, yielding both the α -glycosyl fluoride **253** and the β -glycosyl fluoride **252**.

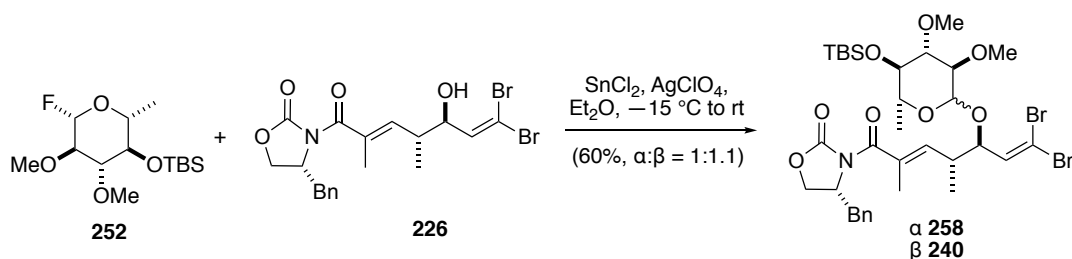


Scheme 3.6: Proposed mechanism for the leaving group conversion

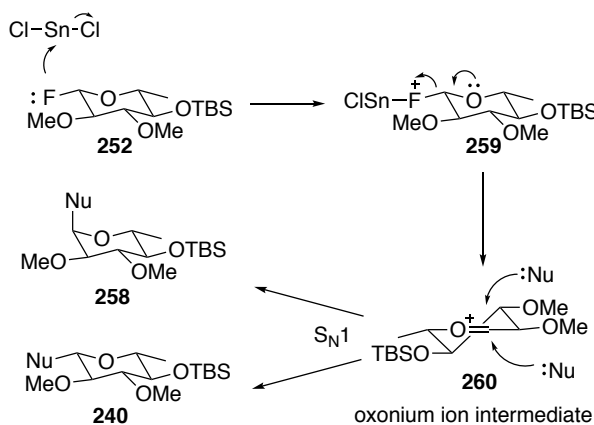
3.2 Glycosylation

3.2.1 Glycosylation with glycosyl fluoride

The optimal conditions for the glycosylation developed by Elliott⁸⁷ were applied to the reaction between intermediate **226** and glycosyl fluoride **252** (Scheme 3.7). The glycosylation adduct was provided as an inseparable 1:1.1 α : β mixture in 60% yield without the previously reported concomitant silyl group deprotection.⁸⁷ However, reproducing this result proved troublesome. Either no reaction was observed or a lower yield (35%) was obtained. At this point, we set out to explore a more reliable glycosylation procedure.



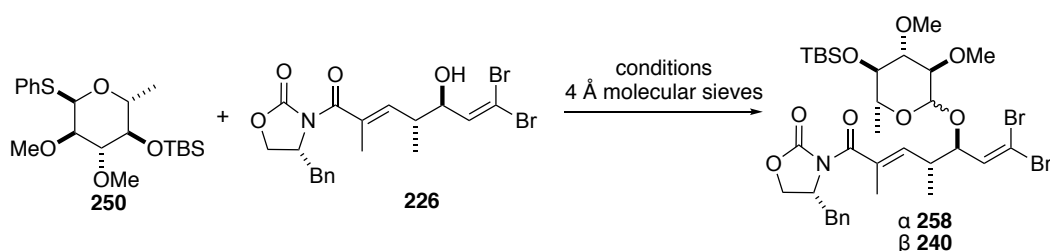
The proposed mechanism of the glycosylation is shown in Scheme 3.8.



3.2.2 Glycosylation with thioglycoside

Due to the poor yield (31%) of the β -glycoside product **240**, a new method of glycosylation⁹³ was tried using thioglycoside **250** (Table 3.1).

Table 3.1: Test of the conditions of glycosylation with thioglycoside **250**

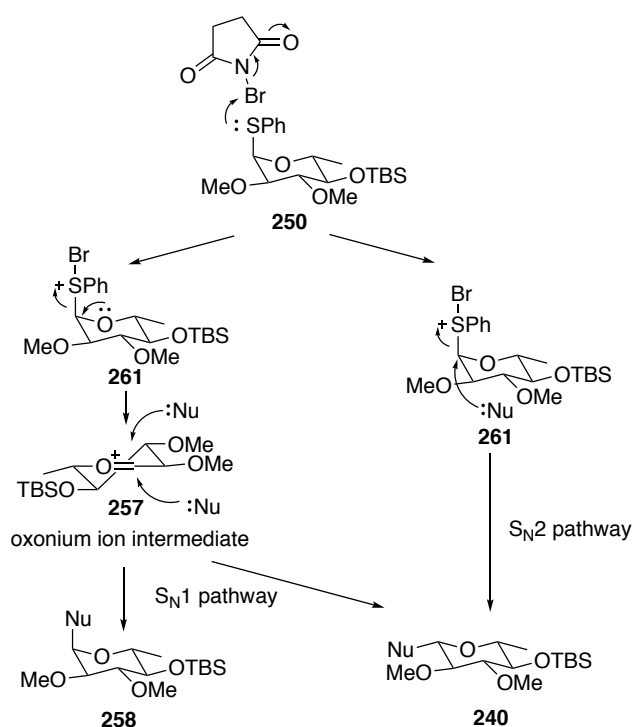


Entry	Reagent	Solvent	Temperature	Time	Yield	α : β
1	NBS	CH ₂ Cl ₂	−20°C to rt	16 h	99%	5:1
2	NBS	CH ₃ CN	rt	16 h	25%, 75% brsm	1.4:1
3	NBS	CH ₃ CN	−20°C	1 h	99%	1:1.3
4	NIS	CH ₃ CN	−20°C to rt	72 h	60%	1.4:1

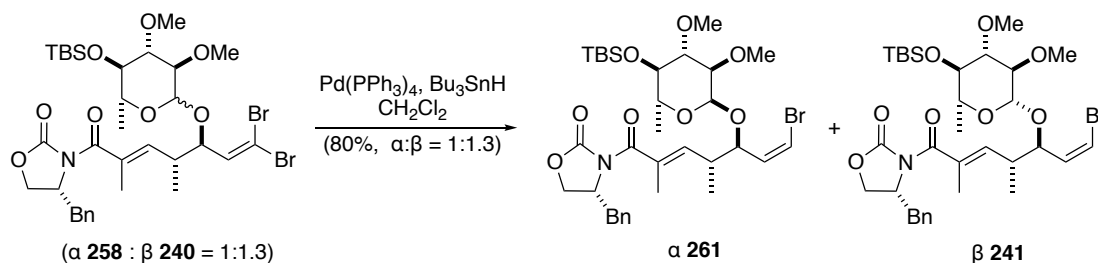
Entry 1 shows that the major product was the undesired α -glycoside product **258**, suggesting that oxonium ion intermediate formation followed by direct nucleophile attack was the dominant pathway. Replacing the solvent with CH₃CN and keeping the reaction at room temperature (Entry 2) improved the selectivity. Keeping the reaction at −20°C (Entry 3) further improved the selectivity. Replacing NBS with NIS resulted in longer reaction time, lower yield and worse selectivity.

According to the mechanism (Scheme 3.9), the reaction could either go *via* S_N1 or S_N2 mechanism. The S_N1 pathway affords either the α -glycoside product **258** or the β -glycoside product **240**. The S_N2 pathway could only generate the β -glycoside product **240**. Considering **258** was yielded under all the conditions discussed before, the reaction must not have proceeded *via* a S_N2 pathway purely. When CH₂Cl₂ was the solvent, the ratio of **258** in the product mixture was 83%, meaning the S_N1 pathway was absolutely dominant, or even possibly the only pathway. Changing the solvent to

CH₃CN increased the ratio of **240** in the product. The better selectivity is attributed to the co-ordination of CH₃CN to the oxonium ion from the axial position, leading to a larger proportion of the β -glycoside product **240**. The lower temperature would make the kinetic S_N2 pathway the dominant pathway, yielding the β -glycoside product **240** as the major product.



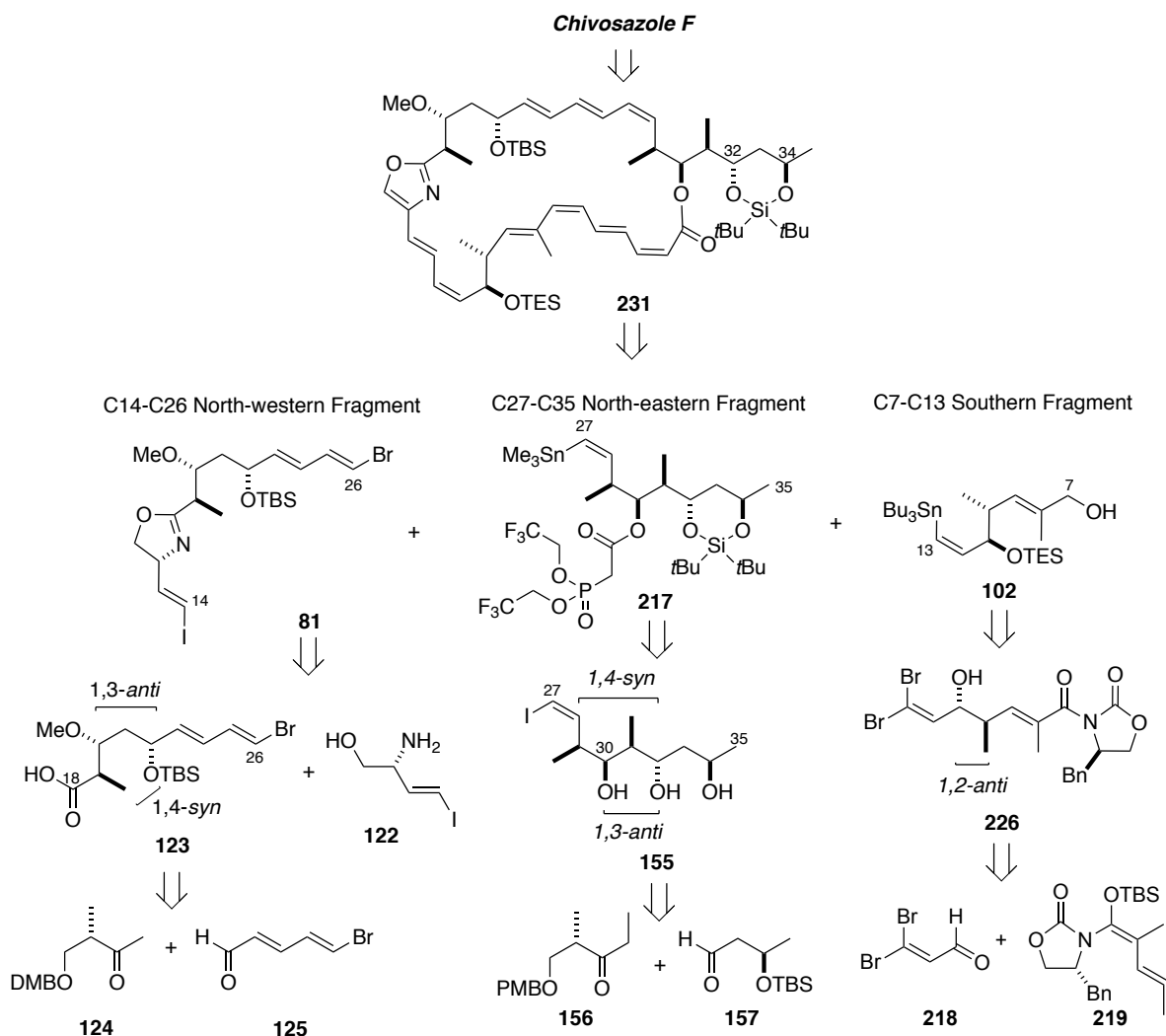
With a stereoselective hydrogenolysis⁸² transforming the dibromoolefins of **258** and **240** to the (*Z*)-vinyl bromides, the two diastereomers **261** and **241** could be separated and characterised respectively.



Chapter 4 Conclusions and future work

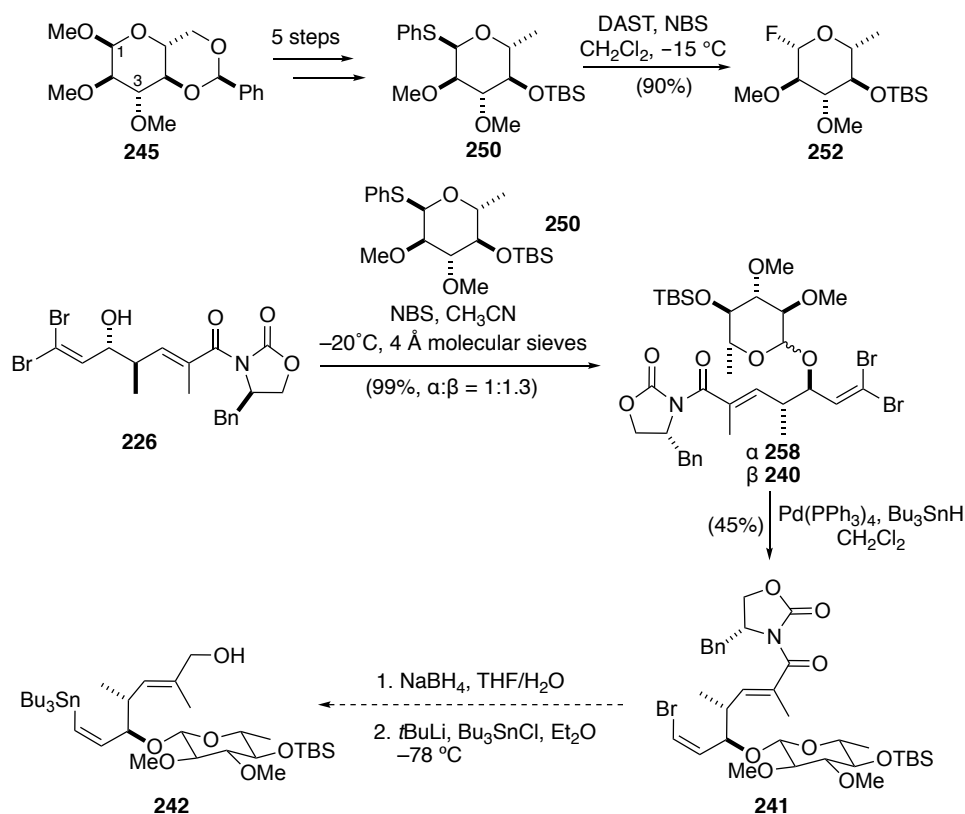
Synthesis of the macrocycle **231** of chivosazole F has been achieved over 19 steps with an overall 0.73% yield. Ten stereocentres and nine double bond geometries were installed with precise control. Construction of the backbone relied on an orchestrated sequence of Stille cross-couplings of the three advanced fragments **81**, **217** and **102** *via* an efficient one-pot process. The oxazole in chivosazole F was masked as an oxazoline in fragment **81**, which was installed by amide coupling of **123** and **122**, followed by DAST mediated cyclisation. The 1,4-*syn* and 1,3-*anti* stereochemical relationships within fragment **123** and fragment **155** were constructed *via* boron aldol reactions followed by Evans-Tishchenko reduction. The C32/C34 diol of **155** was selectively protected as a silylene, which could be successfully deprotected later. The key stereochemistry of fragment **226** was defined with a vinylogous Mukaiyama aldol reaction between **218** and **219** (Scheme 4.1).

Williams⁸⁶ managed to improve the yield of the macrocyclisation step and complete the global deprotection step, affording chivosazole F over 20 steps with an overall 2.5% yield (Kalesse's total synthesis of chivosazole F: 25 steps with an overall 0.48% yield).



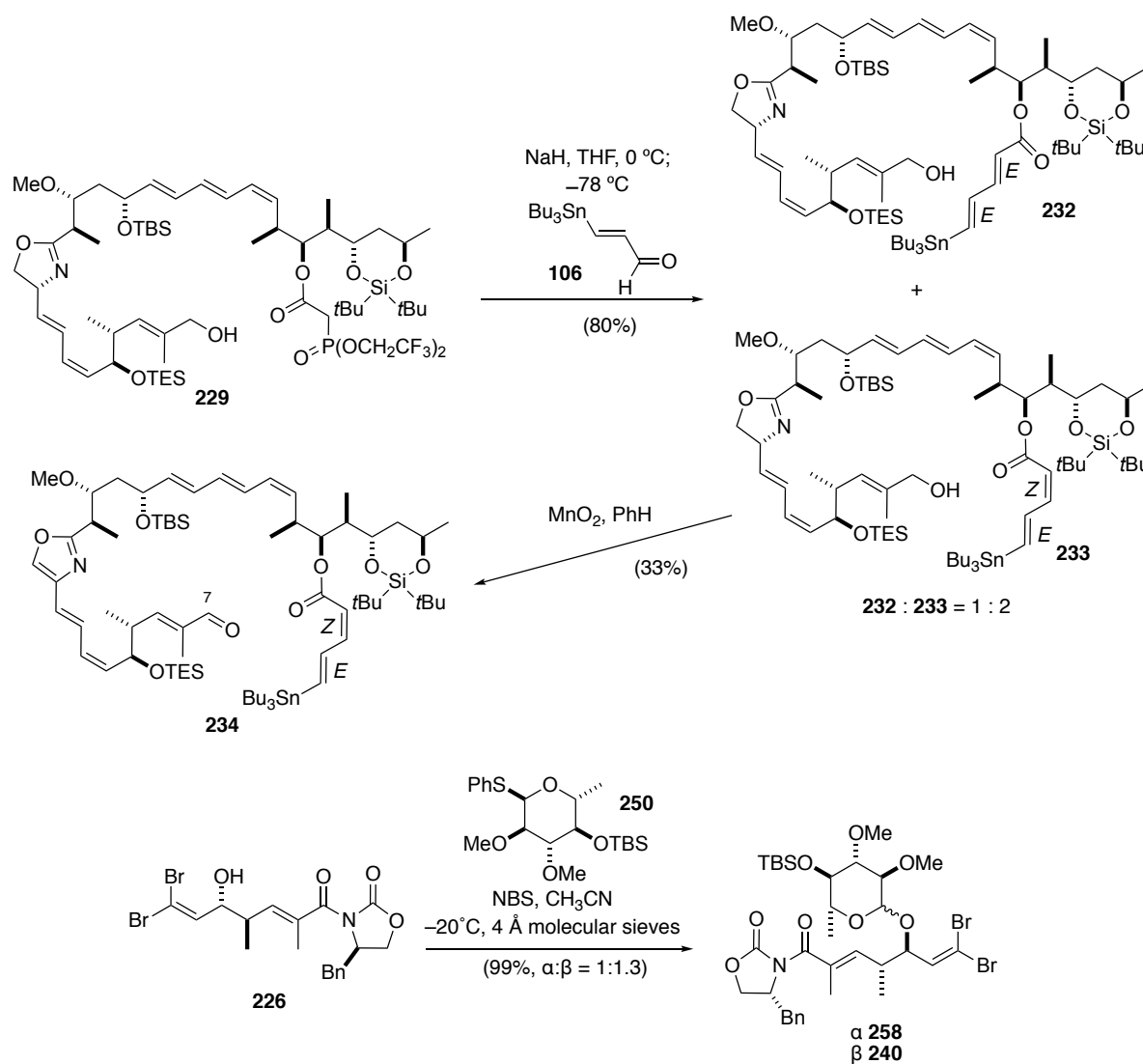
The highly convergent and versatile route was also utilised to explore the total synthesis of chivosazole A by introducing the 6-deoxyglucopyranoside sugar side chain during the synthesis of the southern fragment **242** (Scheme 4.2). Thioglycoside **250** was synthesised from **245** over 5 steps and used in the glycosylation reaction. It was shown that thioglycoside **250** performed better than glycosyl fluoride **252** in the glycosylation reaction, providing **258** and **240** as a 1:1.3 mixture. The desired diastereomer **241** could be isolated after the stereoselective reduction. The two-step sequence of chiral auxiliary cleavage and bromide-lithium-stannane exchange will afford the southern fragment **242**. This will be submitted to the fragment coupling step and the subsequent steps that were applied in the total synthesis of chivosazole F to generate chivosazole A. It is expected that the sugar should not interfere with the fragment coupling step and the subsequent steps, and the TBS group on the sugar can be removed under the global deprotection conditions. Thus, applying the

same synthetic route from the total synthesis of chivosazole F to the total synthesis of chivosazole A is promising, highlighting the flexibility of our synthetic route.



Scheme 4.2: The proposed synthetic route for the southern fragment **242**

The yields and selectivity of some reactions can still be optimised further (Scheme 4.3). The selectivity of the HWE olefination of **229** might be improved by exploring other types of HWE olefinations considering many conditions have been tested for the Ando-type and Still-Gennari-type HWE olefinations of **229**. Better oxidation conditions for unactivated oxazolines will hopefully increase the yield of the double oxidation reaction of **233**. Changing the conditions (solvent, temperature) of the glycosylation could be a way of improving the selectivity. Glycosyl donors besides thioglycosides and glycosyl fluorides are also worth trying.



Scheme 4.3: Reactions which require further optimisation

Overall, the total synthesis of the structurally complex, biologically active chivosazole F has been completed by our group in an expedient way. This synthetic route is adventurous and highly convergent, and could potentially be applicable to the synthesis of useful quantities of chivosazole F. This established route was also modified and utilised for studies towards the total synthesis of chivosazole A, which has provided promising results already.

Chapter 5 Experimental

5.1 General and analytical procedures

Reactions were carried out under an atmosphere of argon using oven dried glassware and standard techniques for handling air sensitive chemicals, unless the reaction contained aqueous reagents or unless otherwise stated.

Reagents were purified using standard laboratory procedures. Benzene, toluene, dichloromethane, and acetonitrile were distilled from CaH_2 and stored under an atmosphere of argon. Tetrahydrofuran and diethyl ether were distilled from potassium or sodium wire/benzophenone and stored under argon. Methanol was distilled from magnesium methoxide and stored under argon. 2,6-lutidine, triethylamine and HMPA were distilled from CaH_2 and stored over CaH_2 under an atmosphere of argon. DMF and DMSO were distilled from and stored over 4Å molecular sieves. Propionaldehyde was distilled from CaCl_2 and used immediately. TiCl_4 was distilled under argon and reduced pressure. DDQ was recrystallised from CHCl_3 . Proton Sponge[®] was recrystallised from ethanol. All other chemicals were used as received from the manufacturer unless otherwise stated.

Aqueous solutions of ammonium chloride (NH_4Cl), sodium bicarbonate (NaHCO_3), sodium thiosulfate ($\text{Na}_2\text{S}_2\text{O}_3$), brine (NaCl) and sodium/potassium (Na/K) tartrate were saturated. Buffer solutions were prepared as directed from stock tablets.

Purification by flash column chromatography was carried out using Kieselgel 60 (230-400 mesh), Merck aluminium oxide 90 or Sigma-Aldrich Florisil[®] (<200 mesh) under a positive pressure. Preparative thin layer chromatography used Merck Kieselgel 60 F₂₅₄ plates.

TLC was carried out using Merck Kieselgel 60 F₂₅₄ plates which were visualised using UV light (254

nm) and stained using potassium permanganate or phosphomolybdic acid/cerium(III) sulfate dips. Petroleum ether, boiling point 40-60 °C is abbreviated to PE.

NMR spectra were recorded using the following machines: Bruker Avance TXO cryoprobe (700 MHz), Avance DCH cryoprobe (500 MHz), Avance 500 BB (500 MHz), Avance TCI cryoprobe (500 MHz) and Avance 400 DRX (400 MHz). ^1H NMR spectra were recorded at 298 K using an internal deuterium lock for CDCl_3 ($\delta_{\text{H}} = 7.26$) or MeOD ($\delta_{\text{H}} = 3.31$ ppm). ^1H NMR data are presented as: chemical shift δ (in ppm, relative to TMS ($\delta_{\text{TMS}} = 0$), integration, multiplicity (s = singlet, d = doublet, t = triplet, q = quartet, qn = quintet, m = multiplet, br = broad, *app* = apparent), coupling constants (J in Hz) and interpretation. Substituents are denoted by the backbone carbon they are attached to. Assignments have been made based on the 1D data presented along with a range of 2D spectra, and comparison with fully assigned spectra for similar compounds. Data is regarded in agreement with literature values or that reported by other people if the difference of δ is within 0.01 ppm and the difference of J is within 0.5 Hz. ^{13}C NMR spectra were recorded at 298 K with proton decoupling and an internal deuterium lock for CDCl_3 ($\delta_{\text{C}} = 77.0$ ppm) or MeOD ($\delta_{\text{C}} = 49.0$ ppm). Data are listed by chemical shift (δ/ppm) relative to TMS ($\delta_{\text{TMS}} = 0$). Multiplicity and coupling constants are listed where coupling to a heteroatom is observed.

Fourier transform IR spectroscopy (FT-IR) was carried out using a Perkin-Elmer Spectrum-One spectrometer, and spectra were recorded as a thin film. Wavelengths of maximum absorption (ν_{max}) are reported in wavenumbers (cm^{-1}).

Optical rotations were measured using a Perkin-Elmer 241 polarimeter at the sodium D line (589 nm) and are reported as $[\alpha]_{\text{D}}^{20}$, concentration (c in g/100 mL) and solvent.

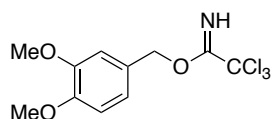
High resolution mass spectroscopy (HRMS) was carried out by the EPSRC National Mass Spectrometry facility (Swansea, UK). The parent ion $[\text{M}+\text{NH}_4]^+$, $[\text{M}+\text{Na}]^+$ or $[\text{M}+\text{H}]^+$ is quoted.

5.2 Preparation of Reagents

Samarium (II) diiodide (0.1 M in THF)

To samarium metal (643 mg, 4.28 mmol) and 1,2-diiodoethane (603 mg, 2.14 mmol) under argon was added THF (20 mL). The mixture was sonicated for 30 min and the resulting dark blue solution (approx. 0.1 M) was used immediately.

3,4-dimethoxybenzyl 2,2,2-trichloroacetimidate (DMBTCA)



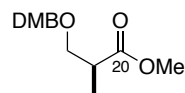
To a solution of potassium hydroxide (50% aqueous, 75 mL) and tetrabutylammonium hydrogen sulphate (211 mg, 0.620 mmol) in CH_2Cl_2 (75 mL) at $-10\text{ }^\circ\text{C}$ was added 3,4-dimethoxybenzyl alcohol (9.00 mL, 61.9 mmol) and trichloroacetonitrile (7.14 mL, 71.2 mmol) dropwise. The resulting solution was stirred for 3 h before being extracted with Et_2O ($3 \times 40\text{ mL}$). The combined organic extracts were dried (Na_2SO_4) and concentrated *in vacuo*. Purification by flash column chromatography over alumina (EtOAc/PE 1:9) yielded the acetimidate (16.1 g, 51.5 mmol, 83%) as a colourless oil.

^1H NMR (500 MHz, CDCl_3) δ_{H} 8.35 (1H, s, NH), 6.99-6.95 (2H, m, ArH), 6.86-6.84 (1H, m, ArH), 5.26 (2H, s, OCH_2Ar), 3.86 (6H, s, ArOMe).

5.3 Detailed experimental procedures

a. North-western fragment

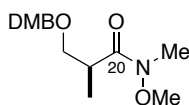
(*S*)-methyl 3-(3,4-dimethoxybenzyloxy)-2-methylpropanoate (**127**)



PPTS (2.35 g, 9.40 mmol) was added to a solution of DMBTCA (30.6 g, 97.6 mmol) and methyl-(*S*)-3-hydroxy-2-methylpropanoate (**126**) (9.72 mL, 87.1 mmol) in CH₂Cl₂ (200 mL) and the mixture was stirred at rt for 2 h. The reaction mixture was quenched with saturated NaHCO₃ solution (70 mL) and the phases were separated. The aqueous layer was extracted with CH₂Cl₂ (3 × 50 mL) and the combined organic extracts were dried (MgSO₄) and concentrated *in vacuo*. The residue was triturated with cold hexanes (ca. 1 L), filtered through a plug of Celite[®] and concentrated *in vacuo*. The residue was purified by flash column chromatography (EtOAc/PE 1:9) to give the ester **127** (21.2 g, 79.3 mmol, 91%) as a colourless oil.

R_f 0.45 (EtOAc/PE 1:1); ¹H NMR (500 MHz, CDCl₃) δ_H 6.87-6.81 (3H, m, ArH), 4.46 (2H, s, OCH₂Ar), 3.89 (3H, s, ArOMe), 3.87 (3H, s, ArOMe), 3.68 (3H, s, OMe), 3.63 (1H, dd, *J* = 9.2, 7.4 Hz, H_{18a}), 3.45 (1H, dd, *J* = 9.2, 5.9 Hz, H_{18b}), 2.80-2.73 (1H, m, H₁₉), 1.16 (3H, d, *J* = 7.1 Hz, Me₁₉). Data in agreement with literature values.⁵⁸

(*S*)-3-(3,4-dimethoxybenzyloxy)-*N*-methoxy-*N*,2-dimethylpropanamide (**128**)

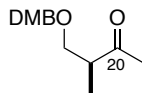


N,*O*-Dimethylhydroxylamine hydrochloride (5.34 g, 82.5 mmol) was dried by stirring *in vacuo* for 4

h. A solution of ester **127** (14.8 g, 55.0 mmol) in THF (100 mL) was added and the reaction mixture was cooled to $-20\text{ }^{\circ}\text{C}$. Isopropylmagnesium chloride (181 mL, 0.913 M in Et₂O, 164 mmol) was added dropwise. After stirring for 2 h, the reaction mixture was quenched with NH₄Cl solution (100 mL) and the phases were separated. The aqueous phase was extracted with Et₂O ($2 \times 100\text{ mL}$) and the combined organic phases were dried (MgSO₄) and concentrated *in vacuo*. The crude product was purified by flash column chromatography (EtOAc/PE 1:4) to yield the amide **128** (16.2 g, 60.9 mmol, 95%) as a colourless oil.

R_f 0.19 (EtOAc/PE 1:1); **¹H NMR** (400 MHz, CDCl₃) δ_{H} 6.88-6.81 (3H, m, ArH), 4.45 (2H, ABq, $J = 12.0\text{ Hz}$, OCH₂Ar), 3.87 (3H, s, ArOMe), 3.86 (3H, s, ArOMe), 3.70-3.66 (1H, m, H_{18a}), 3.68 (3H, s, NOME), 3.40 (1H, dd, $J = 8.7, 5.8\text{ Hz}$, H_{18b}), 3.30-3.23 (1H, m, H₁₉), 3.20 (3H, s, NMe), 1.11 (3H, d, $J = 7.1\text{ Hz}$, Me₁₉). Data in agreement with literature values.⁵⁷

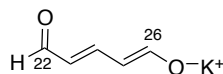
(S)-4-(3,4-dimethoxybenzyloxy)-3-methylbutan-2-one (124)



Methylmagnesium bromide (60.8 mL, 3.0 M in Et₂O, 182 mmol) was added dropwise to a solution of Weinreb amide **128** (16.2 g, 60.8 mmol) in THF (300 mL) at $0\text{ }^{\circ}\text{C}$. The reaction mixture was stirred for 2.5 h, quenched with NH₄Cl solution (150 mL) and warmed to rt. The layers were separated and the aqueous phase was extracted with Et₂O ($3 \times 100\text{ mL}$). The combined organic layers were dried (MgSO₄) and concentrated *in vacuo*. The crude product was purified by flash column chromatography (EtOAc/PE 1:4) to yield methyl ketone **124** (11.6 g, 52.9 mmol, 87%) as a colourless oil.

R_f 0.38 (EtOAc/PE 3:7); **¹H NMR** (400 MHz, CDCl₃) δ_{H} 6.86-6.80 (3H, m, ArH), 4.43 (2H, ABq, $J = 12.0\text{ Hz}$, OCH₂Ar), 3.88 (3H, s, ArOMe), 3.87 (3H, s, ArOMe), 3.60 (1H, dd, $J = 9.2, 7.6\text{ Hz}$, H_{18a}), 3.46 (1H, dd, $J = 9.2, 5.5\text{ Hz}$, H_{18b}), 2.90-2.81 (1H, m, H₁₉), 2.18 (3H, s, H₂₁), 1.09 (3H, d, $J = 7.1\text{ Hz}$, Me₁₉). Data in agreement with that reported by Findlay.⁹⁴

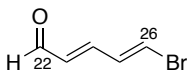
Potassium (1*E*,3*E*)-5-oxopenta-1,3-dien-1-olate (**132**)



Pyridinium-1-sulfonate **130** (100 g, 628 mmol) was added portionwise to a stirred solution of potassium hydroxide (146 g, 2.60 mol) in H₂O at –20 °C. The resulting solution was stirred for 1 h, warmed to rt over 4 h and heated at 40 °C for 30 min. After cooling to –20 °C, the precipitate was filtered through a pad of Celite[®], washed with cold acetone (2 × 100 mL) and air-dried overnight. Activated charcoal (5 g) was added to a solution of the residue in MeOH (1 L) and heated at reflux for 20 min before filtering immediately. The solution was concentrated *in vacuo* to a volume of *ca.* 50 mL. The precipitated product was filtered and washed with cold acetone (2 × 50 mL) to yield potassium glutaconaldehyde **132** (40.0 g, 294 mmol, 47%) as a yellow crystalline salt.

¹H NMR (500 MHz, DMSO) δ_H 8.65 (2H, d, *J* = 9.2 Hz, H₂₂+H₂₆), 7.04 (1H, t, *J* = 13.1 Hz, H₂₄), 5.09 (2H, dd, *J* = 13.1, 9.2 Hz, H₂₃+H₂₅). Data in agreement with literature values.⁴⁷

(2*E*, 4*E*)-5-Bromo-2,4-pentadienal (**125**)

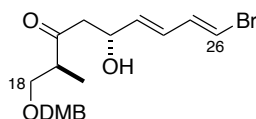


A solution of *N*-bromosuccinimide (14.4 g, 80.7 mmol) in CH₂Cl₂ (300 mL) was added *via* cannula to a stirred solution of triphenylphosphine (21.2 g, 80.7 mmol) in CH₂Cl₂ (200 mL) at 0 °C. The mixture was warmed to rt and stirred for 45 min before potassium glutaconaldehyde salt **132** (5.00 g, 36.7 mmol) was added in one portion. After stirring for 40 h, the reaction mixture was quenched with pH 7 buffer solution (200 mL). The phases were separated and the aqueous phase was extracted with CH₂Cl₂ (3 × 200 mL). The combined organic extracts were dried (MgSO₄) and concentrated *in vacuo*. The resultant crude was triturated with cold 30-40 petroleum ether and filtered through a pad of Celite[®]. The resulting solution was concentrated *in vacuo*. The crude product was purified by flash column chromatography (Et₂O/PE 30-40 1:19) to yield the product **125** (1.70 g, 11.0 mmol, 30%) as

a yellow crystalline solid.

R_f 0.20 (EtOAc/PE 1:9); **¹H NMR** (500MHz, CDCl₃) δ_H 9.58 (1H, d, *J* = 7.8 Hz, CHO), 7.04-6.92 (3H, m, H₂₄+H₂₅+H₂₆), 6.22-6.14 (1H, m, H₂₃). Data in agreement with that reported by Findlay.⁹⁴

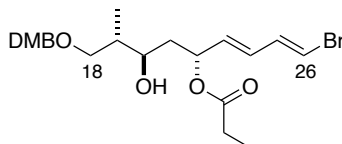
(2*S*,5*R*,6*E*,8*E*)-9-bromo-1-((3,4-dimethylbenzyl)oxy)-5-hydroxy-2-methylnona-6,8-dien-3-one (136)



Et₃N (3.00 mL, 21.5 mmol) was added to a 1 M solution of (–)-Ipc₂BCl in Et₂O (17.5 mL, 17.5 mmol) at 0 °C. A solution of ketone **124** (3.20 g, 12.7 mmol) in Et₂O (15 mL) was added and the reaction mixture was stirred for 30 min. The mixture was cooled to –78 °C and aldehyde **125** (1.40 g, 8.50 mmol) in Et₂O/CH₂Cl₂ (1:1, 10 mL) was added dropwise. The reaction mixture was stirred for 30 min and warmed to –20 °C for 16 h. The reaction was quenched with pH 7 buffer solution (30 mL) at 0 °C and stirred for 1 h. The layers were separated and the aqueous phase was extracted with Et₂O (3 × 30 mL). The combined organic extracts were washed with brine (50 mL) and stirred over silica (30 g) for 1 hour. The resulting slurry was filtered and the filtrate was concentrated *in vacuo* and purified by flash column chromatography (EtOAc/PE 1:4) to afford product **136** (3.05 g, 7.21 mmol, 85%, >95:5 dr) as a yellow oil.

R_f 0.20 (EtOAc/PE 3:7); **¹H NMR** (500 MHz, CDCl₃) δ_H 6.81 (3H, s, ArH), 6.65 (1H, dd, *J* = 13.5, 11.0 Hz, H₂₅), 6.29 (1H, d, *J* = 13.5 Hz, H₂₆), 6.16 (1H, dd, *J* = 15.3, 10.8 Hz, H₂₄), 5.67 (1H, dd, *J* = 15.4, 5.5 Hz, H₂₃), 4.63-4.56 (1H, m, H₂₂), 4.40 (2H, s, OCH₂Ar), 3.87 (6H, s, ArOMe), 3.57 (1H, t, *J* = 8.5 Hz, H_{18a}), 3.47 (1H, dd, *J* = 9.2, 5.0 Hz, H_{18b}), 3.24 (1H, d, *J* = 3.8 Hz, OH), 2.91-2.83 (1H, m, H₁₉), 2.72 (1H, dd, *J* = 17.5, 3.3 Hz, H_{21a}), 2.64 (1H, dd, *J* = 17.4, 8.8 Hz, H_{21b}), 1.05 (3H, d, *J* = 7.2 Hz, Me₁₉). Data in agreement with that reported by Li.³⁸

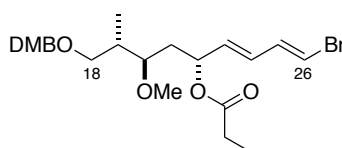
(1*E*,3*E*,5*R*,7*R*,8*S*)-1-bromo-9-((3,4-dimethylbenzyl)oxy)-7-hydroxy-8-methylnona-1,3-dien-5-yl propionate (142)



A 0.1 M solution of samarium diiodide in THF (3.20 mL, 0.320 mmol) was added to a solution of propionaldehyde (1.45 mL, 20.1 mmol) in THF (20 mL) at -20°C . To the resultant yellow mixture was added a solution of aldol product **136** (1.34 g, 3.24 mmol) in THF (50 mL). The reaction mixture was stirred for 3 h before being quenched with NaHCO_3 solution (50 mL). The layers were separated and the aqueous phase was extracted with Et_2O (3×50 mL). The combined organic extracts were dried (Na_2SO_4) and concentrated *in vacuo*. The residue was purified by flash chromatography (EtOAc/PE 1:4) to afford alcohol **142** (1.45 g, 3.08 mmol, 95%, >95:5 dr) as a colourless oil.

R_f 0.20 (EtOAc/PE 3:7); $^1\text{H NMR}$ (500 MHz, CDCl_3) δ_{H} 6.86-6.79 (3H, m, ArH), 6.64 (1H, dd, $J = 13.5, 10.9$ Hz, H_{25}), 6.32 (1H, d, $J = 13.5$ Hz, H_{26}), 6.15 (1H, dd, $J = 15.4, 10.9$ Hz, H_{24}), 5.68 (1H, dd, $J = 15.3, 6.7$ Hz, H_{23}), 5.56-5.50 (1H, m, H_{22}), 4.45-4.39 (2H, m, OCH_2Ar), 3.87 (3H, s, ArOMe), 3.86 (3H, s, ArOMe), 3.52 (1H, dd, $J = 9.3, 4.8$ Hz, H_{18a}), 3.51-3.46 (1H, m, H_{20}), 3.43 (1H, dd, $J = 9.3, 6.7$ Hz, H_{18b}), 3.37 (1H, d, $J = 4.0$ Hz, OH), 2.32 (2H, q, $J = 7.6$ Hz, $\text{CO}_2\text{CH}_2\text{CH}_3$), 1.85-1.75 (2H, m, $\text{H}_{19}+\text{H}_{21a}$), 1.60 (1H, ddd, $J = 13.8, 10.5, 3.0$ Hz, H_{21b}), 1.12 (3H, t, $J = 7.6$ Hz, $\text{CO}_2\text{CH}_2\text{CH}_3$), 0.90 (3H, d, $J = 7.0$ Hz, Me_{19}). Data in agreement with that reported by Li.³⁸

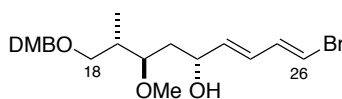
(1*E*,3*E*,5*R*,7*R*,8*S*)-1-bromo-9-((3,4-dimethylbenzyl)oxy)-7-methoxy-8-methylnona-1,3-dien-5-yl propionate (143)



Proton Sponge[®] (7.60 g, 35.5 mmol) and trimethyloxonium tetrafluoroborate (7.02 g, 47.3 mmol) were added to a solution of alcohol **142** (1.41 g, 2.97 mmol) in CH₂Cl₂ (30 mL) at 0 °C. The reaction mixture was stirred for 2 h, quenched with NaHCO₃ solution (50 mL) and filtered through a pad of Celite[®]. The layers were separated and the aqueous phase was extracted with CH₂Cl₂ (2 × 50 mL). The combined organic extracts were washed with aqueous citric acid solution (100 mL, 1.0 M), dried (MgSO₄) and concentrated *in vacuo*. After purification by flash chromatography (EtOAc/PE 1:4), alcohol **143** was recovered and resubmitted to the reaction conditions. Methyl ether **107** (1.15 g, 2.38 mmol, 80%) was obtained as a colourless oil.

R_f 0.41 (EtOAc/PE 3:7); **¹H NMR** (500 MHz, CDCl₃) δ_H 6.88-6.81 (3H, m, ArH), 6.65 (1H, dd, *J* = 13.6, 10.9 Hz, H₂₅), 6.32 (1H, d, *J* = 13.5 Hz, H₂₆), 6.14 (1H, dd, *J* = 15.4, 11.0 Hz, H₂₄), 5.65 (1H, dd, *J* = 15.3, 6.9 Hz, H₂₃), 5.48-5.43 (1H, m, H₂₂), 4.43 (2H, s, OCH₂Ar), 3.88 (3H, s, ArOMe), 3.87 (3H, s, ArOMe), 3.33 (1H, d, *J* = 6.5 Hz, H₁₈), 3.29 (3H, s, OMe), 3.29-3.25 (1H, m, H₂₀) 2.31 (2H, q, *J* = 7.6 Hz, CO₂CH₂CH₃), 2.18-2.11 (1H, m, H₁₉), 1.70 (1H, ddd, *J* = 14.1, 9.9, 2.2 Hz, H_{21a}), 1.59 (1H, ddd, *J* = 14.1, 9.9, 3.1 Hz, H_{21b}), 1.12 (3H, t, *J* = 7.5 Hz, CO₂CH₂CH₃), 0.88 (3H, d, *J* = 7.0 Hz, Me₁₉). Data in agreement with that reported by Li.³⁸

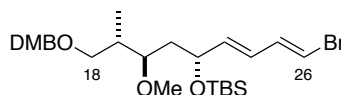
(1*E*,3*E*,5*R*,7*R*,8*S*)-1-bromo-9-((3,4-dimethylbenzyl)oxy)-7-methoxy-8-methylnona-1,3-dien-5-ol (144)



K₂CO₃ (421 mg, 3.05 mmol) was added to a solution of ester **143** (740 mg, 1.53 mmol) in MeOH (20 mL). The reaction mixture was stirred for 16 h and subsequently diluted with water (20 mL). The mixture was extracted with CH₂Cl₂ (3 × 20 mL). The combined organic extracts were dried (Na₂SO₄) and concentrated *in vacuo*. The crude residue was purified by flash chromatography (EtOAc/PE 3:7) to yield alcohol **144** (644 mg, 1.50 mmol, 98%) as a colourless oil.

R_f 0.30 (EtOAc/PE 3:7); **¹H NMR** (500 MHz, CDCl₃) δ 6.86-6.79 (3H, m, ArH), 6.68 (1H, dd, *J* = 13.4, 10.9 Hz, H₂₅), 6.27 (1H, d, *J* = 13.4 Hz, H₂₆), 6.18 (1H, ddd, *J* = 15.2, 10.9, 1.5 Hz, H₂₄), 5.72 (1H, dd, *J* = 15.3, 5.2 Hz, H₂₃), 4.40 (2H, s, OCH₂Ar), 4.39-4.32 (1H, m, H₂₂), 3.86 (3H, s, ArOMe), 3.85 (3H, s, ArOMe), 3.57-3.51 (1H, m, H₂₀), 3.36-3.32 (2H, m, H₁₈), 3.32 (3H, s, OMe), 3.21 (1H, d, *J* = 5.2 Hz, OH), 2.24-2.15 (1H, m, H₁₉), 1.68 (1H, ddd, *J* = 14.7, 8.9, 3.2 Hz, H_{21a}), 1.55 (1H, ddd, *J* = 14.7, 8.0, 3.1 Hz, H_{21b}), 0.87 (3H, d, *J* = 7.0 Hz, Me₁₉). Data in agreement with that reported by Li.³⁸

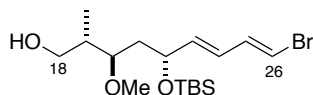
(((1*E*,3*E*,5*R*,7*R*,8*S*)-1-bromo-9-((3,4-dimethylbenzyl)oxy)-7-methoxy-8-methylnona-1,3-dien-5-yl)oxy)(*tert*-butyl)dimethylsilane (145)



Imidazole (146 mg, 2.15 mmol) was added to a solution of alcohol **144** (836 mg, 1.95 mmol) in CH₂Cl₂ (40 mL) at 0 °C. After stirring for 10 min, TBSCl (324 mg, 2.15 mmol) was added. The reaction mixture was warmed to rt and stirred for 16 h and, when complete by TLC, was quenched with NaHCO₃ solution (10 mL). The layers were separated and the aqueous phase was extracted with CH₂Cl₂ (3 × 20 mL). The combined organic extracts were dried (MgSO₄) and concentrated *in vacuo*. The crude product was purified by flash chromatography (EtOAc/PE 1:4) to yield TBS ether **145** (965 mg, 1.77 mmol, 91%) as a colourless oil.

R_f 0.70 (EtOAc/PE 1:4); **¹H NMR** (500 MHz, CDCl₃) δ_H 6.89-6.80 (3H, m, ArH), 6.66 (1H, dd, *J* = 13.6, 11.0 Hz, H₂₅), 6.25 (1H, d, *J* = 13.6 Hz, H₂₆), 6.06 (1H, dd, *J* = 15.4, 11.0 Hz, H₂₄), 5.69 (1H, dd, *J* = 15.3, 6.8 Hz, H₂₃), 4.42 (2H, ABq, *J* = 11.8 Hz, OCH₂Ar), 4.34-4.28 (1H, m, H₂₂), 3.88 (3H, s, ArOMe), 3.87 (3H, s, ArOMe), 3.53-3.47 (1H, m, H₂₀), 3.31 (3H, s, OMe), 3.31 (1H, dd, *J* = 9.5, 6.7 Hz, H_{18a}), 3.24 (1H, dd, *J* = 9.0, 6.7 Hz, H_{18b}), 2.29-2.21 (1H, m, H₁₉), 1.45-1.39 (2H, m, H₂₁), 0.89 (9H, s, SiC(CH₃)₃), 0.86 (3H, d, *J* = 6.9 Hz, Me₁₉), 0.05 (3H, s, SiCH₃), 0.01 (3H, s, SiCH₃). Data in agreement with that reported by Li.³⁸

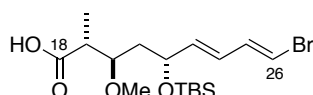
(2*S*,3*R*,5*R*,6*E*,8*E*)-9-bromo-5-((*tert*-butyldimethylsilyl)oxy)-3-methoxy-2-methylnona-6,8-dien-1-ol (146)



A solution of DDQ (250 mg, 1.10 mmol) and pH 7 buffer solution (8 mL) in CH₂Cl₂ (10 mL) were added to a solution of DMB ether **145** (400 mg, 0.920 mmol) in CH₂Cl₂ (30 mL) at 0 °C. The reaction mixture was stirred for 3 h before being quenched with NaHCO₃ solution (30 mL). The layers were separated and the aqueous phase was extracted with CH₂Cl₂ (3 × 20 mL). The combined organic extracts were dried (Na₂SO₄) and concentrated *in vacuo*. The residue was purified by flash chromatography (EtOAc/PE 1:9) to yield alcohol **146** (348 mg, 0.880 mmol, 95%) as a yellow oil.

R_f 0.50 (EtOAc/PE 3:7); **¹H NMR** (500 MHz, CDCl₃) δ_H 6.69 (1H, dd, *J* = 13.5, 11.0 Hz, H₂₅), 6.29 (1H, d, *J* = 13.5 Hz, H₂₆), 6.09 (1H, dd, *J* = 15.2, 10.8 Hz, H₂₄), 5.71 (1H, dd, *J* = 15.2, 7.0 Hz, H₂₃), 4.31 (1H, *app* q, *J* = 6.5 Hz, H₂₂), 3.62 (1H, dd, *J* = 10.7, 5.0 Hz, H_{18a}), 3.54 (1H, dd, *J* = 10.9, 6.4 Hz, H_{18b}), 3.47-3.42 (1H, m, H₂₀), 3.38 (3H, s, OMe), 2.24 (1H, br s, OH), 2.00-1.95 (1H, m, H₁₉), 1.58 (2H, *app* t, *J* = 6.1 Hz, H₂₁), 0.90 (3H, d, *J* = 7.0 Hz, Me₁₉), 0.89 (9H, s, SiC(CH₃)₃), 0.08 (3H, s, SiCH₃), 0.02 (3H, s, SiCH₃). Data in agreement with that reported by Li.³⁸

(2*R*,3*R*,5*R*,6*E*,8*E*)-9-bromo-5-((*tert*-butyldimethylsilyl)oxy)-3-methoxy-2-methylnona-6,8-dienoic acid (123)

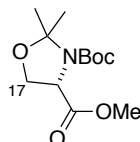


TEMPO (128 mg, 0.820 mmol) and PhI(OAc)₂ (708 mg, 2.20 mmol) were added to a solution of alcohol **146** (247 mg, 0.632 mmol) in MeCN/H₂O (1:1, 10 mL). The reaction mixture was stirred for 2 h and subsequently diluted with EtOAc/H₂O (1:1, 20 mL). The layers were separated, and the aqueous phase was extracted with EtOAc (3 × 10 mL). The combined organic extracts were dried

(Na₂SO₄) and concentrated *in vacuo*. The residue was purified by flash chromatography (EtOAc/PE 1:4) to give acid **123** (231 mg, 0.570 mmol, 90%) as a yellow oil.

R_f 0.30 (EtOAc/PE 3:7); **¹H NMR** (500 MHz, CDCl₃) δ_H 6.67 (1H, dd, *J* = 13.4, 10.8 Hz, H₂₅), 6.27 (1H, d, *J* = 13.4 Hz, H₂₆), 6.08 (1H, dd, *J* = 15.2, 10.8 Hz, H₂₄), 5.69 (1H, dd, *J* = 15.2, 6.8 Hz, H₂₃), 4.34-4.27 (1H, m, H₂₂), 3.80-3.74 (1H, m, H₂₀), 3.37 (3H, s, OMe), 2.95-2.86 (1H, m, H₁₉), 1.63-1.48 (2H, m, H₂₁), 1.09 (3H, d, *J* = 7.0 Hz, Me₁₉), 0.89 (9H, s, SiC(CH₃)₃), 0.07 (3H, s, SiCH₃), 0.01 (3H, s, SiCH₃). Data in agreement with that reported by Li.³⁸

(S)-3-Tert-butyl 4-methyl 2,2-dimethyloxazolidine-3,4-dicarboxylate (**148**)



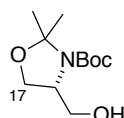
Thionyl chloride (8.32 mL, 114 mmol) was added dropwise to a solution of L-serine (2.00 g, 19.0 mmol) in MeOH (40 mL) at -10 °C. The reaction mixture was warmed to rt, stirred for 20 h and then concentrated *in vacuo*. Et₃N (6.64 mL, 47.6 mmol) and Boc₂O (4.60 g, 21.1 mmol) were added to a solution of the crude residue in CH₂Cl₂ (40 mL) at 0 °C. The layers were separated upon complete consumption of the starting material by TLC. The aqueous phase was extracted with CH₂Cl₂ (3 × 5 mL), and the combined organic extracts were washed with brine (20 mL), dried (MgSO₄), and concentrated *in vacuo*. 2,2-dimethoxypropane (17.4 mL, 142 mmol) and BF₃•OEt₂ (0.240 mL, 1.90 mmol) were added to a solution of the crude material in acetone (24 mL) at rt. The reaction mixture was stirred for 2.5 h and subsequently Et₃N (0.240 mL, 1.72 mmol) was added. The mixture was concentrated *in vacuo* and partitioned between Et₂O (10 mL) and NaHCO₃ solution (10 mL). The aqueous phase was extracted with Et₂O (3 × 5 mL). The combined organic extracts were washed with brine (20 mL), dried (MgSO₄), and concentrated *in vacuo* to provide methyl ester **148** (4.90 g, 18.9 mmol, 99%) as a colourless oil as a 1.5:1 mixture of rotamers.

R_f 0.35 (EtOAc/PE 3:7); **¹H NMR** (400 MHz, CDCl₃) δ_H 4.44 (1H, dd, *J* = 6.8, 2.5 Hz, H₁₆^{*}), 4.34

(1H, dd, $J = 7.0, 3.0$ Hz, H₁₆), 4.14-4.06 (2H, m, H₁₇), 4.03-3.96 (2H, m, H₁₇^{*}), 3.73 (3H, s, OMe^{*}), 3.71 (3H, s, OMe), 1.66-1.64 (6H, m, CMe₂^{*}), 1.54-1.52 (6H, m, CMe₂), 1.49 (9H, br s, *t*Bu^{*}), 1.41 (9H, br s, *t*Bu). Data in agreement with literature values.⁶⁰

* Minor rotamer

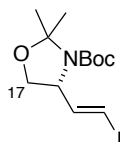
(*R*)-Tert-butyl 4-(hydroxymethyl)-2,2-dimethyloxazolidine-3-carboxylate (150**)**



A solution of methyl ester **148** (2.00 g, 7.72 mmol) in THF (8 mL) was added dropwise to a stirred solution of LiBH₄ (336 mg, 15.4 mmol) in EtOH (10 mL) at -20 °C. The reaction mixture was warmed to rt and stirred for 16 h before being quenched with NH₄Cl solution (2 mL). The layers were separated and the aqueous phase was extracted with EtOAc (3×2 mL). The combined organic extracts were washed with brine, dried (MgSO₄), and concentrated *in vacuo*. The residue was purified by flash chromatography (EtOAc/PE 3:7) to yield primary alcohol **150** (1.07 g, 4.63 mmol, 60%) as a colourless oil.

R_f 0.50 (Et₂O/PE 3:7); **¹H NMR** (400 MHz, CDCl₃) δ 4.92-4.83 (1H, m, OH), 3.93-3.83 (2H, m, H₁₇), 3.81-3.68 (1H, m, H₁₆), 3.54-3.47 (1H, m, H_{15a}), 3.21-3.13 (1H, m, H_{15b}), 1.45 (3H, s, CMe₂), 1.41 (9H, s, *t*Bu), 1.39 (3H, s, CMe₂). Data in agreement with literature values.⁶⁰

(*R,E*)-tert-butyl 4-(2-iodovinyl)-2,2-dimethyloxazolidine-3-carboxylate (151**)**

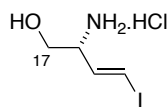


A solution of oxalyl chloride (280 μ L, 3.24 mmol) in CH₂Cl₂ (5 mL) was added to a solution of DMSO (460 μ L, 6.48 mmol) in CH₂Cl₂ (3 mL) at -78 °C. After stirring for 15 min, alcohol **150** (500

mg, 2.16 mmol) in CH₂Cl₂ (5 mL) was added and the reaction mixture was stirred for a further 1 h at -78 °C. Et₃N (1.80 mL, 13.0 mmol) was added and the reaction mixture was stirred at 0 °C for 30 min. The reaction was quenched with NH₄Cl solution (10 mL) and the layers were separated. The aqueous phase was extracted with CH₂Cl₂ (3 × 5 mL). The combined organic extracts were dried (MgSO₄), concentrated *in vacuo* and the crude aldehyde was used immediately in the subsequent reaction. The crude aldehyde was dissolved in THF (15 mL) and added to a vigorously stirred solution of CrCl₂ (4.29 g, 34.9 mmol) in THF (30 mL) at 0 °C. The mixture was stirred for 5 min before CHI₃ (4.29 g, 10.9 mmol) was added. The reaction mixture was warmed to rt and stirred in the dark for 18 h. The reaction was diluted with H₂O (30 mL) and the layers were separated. The aqueous phase was extracted with Et₂O (3 × 20 mL). The organic extracts were washed with brine (20 mL), filtered through a pad of silica, dried (MgSO₄) and concentrated *in vacuo*. The crude product was purified by flash chromatography (EtOAc/PE 1:9) to give vinyl iodide **151** (648 mg, 1.84 mmol, 85%) as a yellow oil.

R_f 0.40 (EtOAc/PE 1:9); **¹H NMR** (500 MHz, CDCl₃, 323 K) δ_H 6.50 (1H, dd, *J* = 14.3, 7.6 Hz, H₁₅), 6.33 (1H, br d, *J* = 14.3 Hz, H₁₄), 4.29 (1H, br s, H₁₆), 3.99 (1H, dd, *J* = 9.0, 6.3 Hz, H_{17a}), 3.76 (1H, dd, *J* = 9.0, 2.0 Hz, H_{17b}), 1.59 (3H, s, CMe₂), 1.50 (3H, s, CMe₂), 1.46 (9H, s, *t*Bu). Data in agreement with that reported by Kan.⁵⁹

(*R,E*)-2-amino-4-iodobut-3-en-1-ol (**122**)

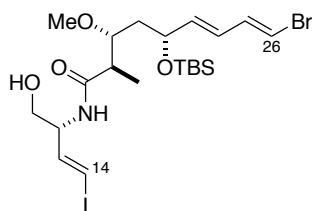


Acetyl chloride (3.03 mL, 42.5 mmol) was added dropwise to MeOH (30 mL) at 0 °C. A solution of protected amino alcohol **151** (200 mg, 0.566 mmol) in MeOH (10 mL) was added dropwise to the solution. The reaction mixture was warmed to rt and stirred for 1 h. Removal of all volatiles *in vacuo* gave amino alcohol **122** (141 mg, 0.560 mmol, 99%) as a yellow hydrochloride salt.

¹H NMR (500 MHz, MeOD) δ_H 6.91 (1H, d, *J* = 15.0 Hz, H₁₄), 6.62 (1H, dd, *J* = 15.0, 8.1 Hz, H₁₅),

3.89-3.80 (1H, m, H₁₆), 3.73 (1H, dd, $J = 11.6, 4.3$ Hz, H_{17a}), 3.61 (1H, dd, $J = 11.6, 6.7$ Hz, H_{17b}). Data in agreement with that reported by Kan.⁵⁹

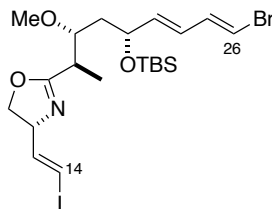
(2*R*,3*R*,5*R*,6*E*,8*E*)-9-bromo-5-((*tert*-butyldimethylsilyl)oxy)-*N*-((*R*,*E*)-1-hydroxy-4-iodobut-3-en-2-yl)-3-methoxy-2-methylnona-6,8-dienamide (152)



A solution of HOBt (33.1 mg, 0.245 mmol) in CH₂Cl₂ (3 mL), *i*Pr₂NEt (113 μ L, 0.615 mmol) and EDC (26.0 μ L, 0.148 mmol) were added successively to a solution of acid **123** (50.0 mg, 0.123 mmol) at 0 °C. The resulting mixture was stirred for 10 min, and amino alcohol **122** (61.1 mg, 0.245 mmol) was added. The reaction mixture was warmed to rt and stirred for 1h. The reaction was quenched with water (2 mL) and the layers were separated. The aqueous phase was extracted with CH₂Cl₂ (3 \times 2 mL). The combined organic extracts were washed with NaHCO₃ solution (5 mL) and brine (5 mL), dried (Na₂SO₄) and concentrated *in vacuo*. The residue was purified by flash column chromatography (EtOAc/PE 4:6) to yield amide **152** (66.8 mg, 0.111 mmol, 90%) as a white solid.

R_f 0.20 (EtOAc/PE 1:4); **¹H NMR** (500 MHz, CDCl₃) δ _H 6.67 (1H, dd, $J = 13.5, 11.0$ Hz, H₂₅), 6.56 (1H, dd, $J = 14.7, 6.2$ Hz, H₁₅), 6.41 (1H, d, $J = 14.7$ Hz, H₁₄), 6.40 (1H, d, $J = 8.2$ Hz, NH), 6.30 (1H, d, $J = 13.5$ Hz, H₂₆), 6.08 (1H, dd, $J = 15.2, 11.0$ Hz, H₂₄), 5.67 (1H, dd, $J = 15.2, 7.0$ Hz, H₂₃), 4.55-4.49 (1H, m, H₁₆), 4.32-4.26 (1H, m, H₂₂), 3.71-3.63 (2H, m, H₁₇), 3.48-3.43 (1H, m, H₂₀), 3.40 (3H, s, OMe), 2.47 (1H, dt, $J = 6.9, 6.6$ Hz, H₁₉), 1.69-1.55 (2H, m, H₂₁), 1.16 (3H, d, $J = 7.0$ Hz, Me₁₉), 0.89 (9H, s, SiC(CH₃)₃), 0.06 (3H, s, SiCH₃), 0.02 (3H, s, SiCH₃). Data in agreement with that reported by Li.³⁸

(R)-2-((2R,3R,5R,6E,8E)-9-bromo-5-((tert-butyldimethylsilyl)oxy)-3-methoxynona-6,8-dien-2-yl)-4-((E)-2-iodovinyl)-4,5-dihydrooxazole (81)

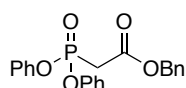


DAST (109 μ L, 0.831 mmol) was added dropwise to a solution of amide **152** (50.0 mg, 83.1 μ mol) in CH_2Cl_2 (1 mL) at -78°C . After stirring for 20 min, the reaction mixture was quenched with K_2CO_3 (171 mg, 1.24 mmol), warmed to rt and diluted with NaHCO_3 solution (2 mL). The phases were separated and the aqueous phase was extracted with CH_2Cl_2 (3×2 mL). The combined organic extracts were washed with brine (2 mL), dried (Na_2SO_4) and concentrated *in vacuo*. The crude residue was purified by flash column chromatography (EtOAc/PE 1:4) to afford oxazoline **81** (48.2 mg, 82.3 μ mol, 99%) as a pale yellow oil.

R_f 0.70 (EtOAc/PE 1:4); **¹H NMR** (500 MHz, CDCl_3) δ_{H} 6.66 (1H, dd, $J = 13.5, 11.0$ Hz, H_{25}), 6.50 (1H, dd, $J = 14.5, 6.6$ Hz, H_{15}), 6.41 (1H, d, $J = 14.5$ Hz, H_{14}), 6.27 (1H, d, $J = 13.5$ Hz, H_{26}), 6.07 (1H, dd, $J = 15.4, 11.0$ Hz, H_{24}), 5.69 (1H, dd, $J = 15.4, 6.8$ Hz, H_{23}), 4.60 (1H, dt, $J = 8.3, 6.5$ Hz, H_{16}), 4.34-4.26 (2H, m, $\text{H}_{17a}+\text{H}_{22}$), 3.97 (1H, *app* t, $J = 8.0$ Hz, H_{17b}), 3.74-3.68 (1H, m, H_{20}), 3.36 (3H, s, OMe), 3.00-2.93 (1H, m, H_{19}), 1.55-1.43 (2H, m, H_{21}), 1.12 (3H, d, $J = 7.1$ Hz, Me_{19}), 0.89 (9H, s, $\text{SiC}(\text{CH}_3)_3$), 0.06 (3H, s, SiCH_3), 0.00 (3H, s, SiCH_3). Data in agreement with that reported by Li.³⁸

b. North-eastern fragment

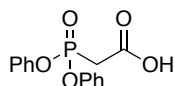
Benzyl 2-(diphenoxyphosphoryl)acetate (195)



To a solution of diphenylmethylphosphonate (4.10 mL, 20.0 mmol) and benzyl chloroformate (2.55 mL, 17.9 mmol) in THF (10 mL) at $-78\text{ }^{\circ}\text{C}$ was added LiHMDS (1 M in THF, 35.0 mL, 35.0 mmol) dropwise. The reaction mixture was stirred at $-20\text{ }^{\circ}\text{C}$ for 16 h before being quenched with NH_4Cl (20 mL) and extracted with CH_2Cl_2 ($3 \times 20\text{ mL}$). The combined organic extracts were dried (MgSO_4) and concentrated *in vacuo*. Purification by flash chromatography ($\text{Et}_2\text{O}/\text{PE}$ 1:4) yielded ester **195** (6.85 g, 17.9 mmol, 99%) as a colourless oil.

R_f 0.22 (EtOAc/PE 3:7); **¹H NMR** (400 MHz, CDCl_3) δ_{H} 7.39-7.28 (10H, m, OPh), 7.21-7.14 (5H, m, OCH_2Ph), 5.22 (2H, s, OCH_2Ph), 3.31 (2H, d, $J = 21.6\text{ Hz}$, PCH_2). Data in agreement with literature values.⁹⁵

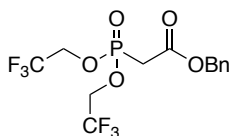
2-(diphenoxyphosphoryl)acetic acid (**42**)



To a solution of phosphonate **195** (6.85 g, 17.9 mmol) in EtOAc (50 mL) was added Pd/C (5%, 623 mg). The reaction was stirred under H_2 for 16 h before being filtered through Celite® and concentrated *in vacuo* to yield acid **42** (4.71 g, 16.1 mmol, 90%) as a white solid.

R_f 0.05 (EtOAc/PE 3:7); **¹H NMR** (400 MHz, CDCl_3) δ_{H} 7.34-7.28 (4H, m, OPh), 7.23-7.15 (6H, m, OCH_2Ph), 3.28 (2H, d, $J = 21.6\text{ Hz}$, PCH_2). Data in agreement with literature values.⁹⁵

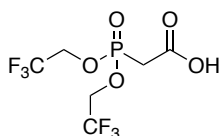
Benzyl 2-(bis(2,2,2-trifluoroethoxy)phosphoryl)acetate (**197**)



To a solution of bis(2,2,2-trifluoroethyl) methylphosphonate (3.61 mL, 20.0 mmol) and benzyl chloroformate (2.70 mL, 17.9 mmol) in THF (10 mL) at $-78\text{ }^{\circ}\text{C}$ was added LiHMDS (1 M in THF, 35.0 mL, 35.0 mmol) dropwise. The reaction mixture was stirred at $-20\text{ }^{\circ}\text{C}$ for 16 h before being quenched with NH_4Cl (20 mL) and extracted with CH_2Cl_2 ($3 \times 20\text{ mL}$). The combined organic extracts were dried (MgSO_4) and concentrated *in vacuo*. Purification by flash chromatography ($\text{Et}_2\text{O}/\text{PE}$ 1:4) yielded ester **197** (5.34 g, 13.5 mmol, 75%) as a colourless oil.

R_f 0.18 (EtOAc/PE 3:7); **¹H NMR** (400 MHz, CDCl_3) δ_{H} 7.33-7.28 (5H, OCH_2Ph), 5.13 (2H, s, OCH_2Ph), 4.39-4.20 (4H, m, OCH_2CF_3), 3.14 (2H, d, $J = 21.4\text{ Hz}$, PCH_2). Data in agreement with literature values.⁹⁵

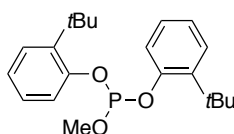
2-(bis(2,2,2-trifluoroethoxy)phosphoryl)acetic acid (**188**)



To a solution of phosphonate **197** (5.34 g, 13.5 mmol) in EtOAc (50 mL) was added Pd/C (5%, 931 mg). The reaction was stirred under H_2 for 16 h before being filtered through Celite[®] and concentrated *in vacuo* to yield acid **188** (3.28 g, 10.8 mmol, 80%) as a white solid.

R_f 0.04 (EtOAc/PE 3:7); **¹H NMR** (400 MHz, CDCl_3) δ_{H} 4.55-4.35 (4H, m, OCH_2CF_3), 3.18 (2H, d, $J = 21.4\text{ Hz}$, PCH_2). Data in agreement with literature values.⁹⁵

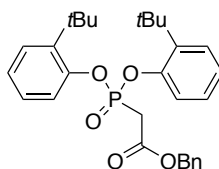
Bis(2-(*tert*-butyl)phenyl) methyl phosphite (**200**)



To a solution of 2-*tert*-butylphenol (1.00 mL, 6.50 mmol) in toluene (20 mL) at 0 °C was added trimethylamine (0.950 mL, 6.87 mmol) and a solution of methyl dichlorophosphite (0.320 mL, 3.33 mmol) in Et₂O (3 mL). The reaction mixture was stirred at rt for 3 h, before being filtered through a pad of alumina. The filtrate was concentrated *in vacuo* to yield phosphite **200** (1.15 g, 3.18 mmol, 98%) as a colourless oil.

¹H NMR (400 MHz, CDCl₃) δ_H 7.39-7.35 (2H, m, ArH), 7.23-7.19 (2H, m, ArH), 7.16-7.10 (2H, m, ArH), 7.06-7.00 (2H, m, ArH), 3.79 (3H, d, *J* = 8.4 Hz, OMe), 1.43 (18H, s, *t*Bu).

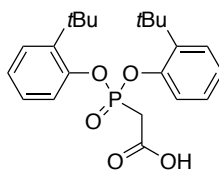
Benzyl 2-(bis(2-(*tert*-butyl)phenoxy)phosphoryl)acetate (**204**)



To phosphite **200** (1.00 g, 2.78 mmol) was added benzyl bromoacetate (0.660 mL, 4.16 mmol). The reaction mixture was stirred at 130 °C for 16 h. The excess of benzyl bromoacetate was removed under reduced pressure to yield acetate **204** (1.13 g, 2.28 mmol, 82%) as a colourless oil.

¹H NMR (400 MHz, CDCl₃) δ_H 7.68-7.65 (2H, m, ArH), 7.39-7.28 (5H, m, ArH), 7.24-7.21 (2H, m, ArH), 7.14-7.06 (4H, m, ArH), 5.08 (2H, s, OCH₂Ph), 3.40 (3H, d, *J* = 21.8 Hz, PCH₂), 1.34 (18H, s, *t*Bu).

2-(bis(2-(*tert*-butyl)phenoxy)phosphoryl)acetic acid (**189**)

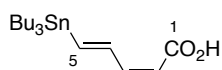


To a solution of phosphonate **204** (1.13 g, 1.14 mmol) in EtOAc (20 mL) was added Pd/C (5%, 157

mg). The reaction was stirred under H₂ for 16 h before being filtered through Celite® and concentrated *in vacuo* to yield acid **189** (461 mg, 1.14 mmol, 99%) as a white solid.

¹H NMR (400 MHz, CDCl₃) δ_H 7.65-7.61 (2H, m, ArH), 7.39-7.35 (2H, m, ArH), 7.17-7.08 (4H, m, ArH), 3.36 (3H, d, *J* = 21.7 Hz, PCH₂), 1.36 (18H, s, *t*Bu).

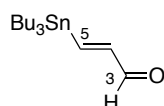
(2*Z*,4*E*)-5-(tributylstannyl)penta-2,4-dienoic acid (96)



To dienoate **92** (100 mg, 0.25 mmol) in THF (45 mL) was added LiOH (1M in H₂O, 25 mL) and H₂O (15 mL). The reaction mixture was stirred for 48 h before being acidified with NaHSO₄, extracted with EtOAc (3 × 30 mL), dried (Na₂SO₄) and concentrated *in vacuo* to yield acid **96** (92.3 mg, 0.239 mmol, 96%) as a yellow oil.

R_f 0.41 (EtOAc/PE 1:2); ¹H NMR (500 MHz, CDCl₃) δ_H 7.82 (1H, *app* dd, *J* = 18.8, 10.7 Hz, H₄), 6.83 (1H, *app* d, *J* = 18.8 Hz, H₅), 6.60 (1H, *app* t, *J* = 11.1 Hz, H₃), 5.61 (1H, br d, *J* = 11.2 Hz, H₂), 1.57-1.48 (6H, m, SnBu₃), 1.37-1.26 (6H, m, SnBu₃), 1.00-0.87 (15H, m, SnBu₃). Data in agreement with that reported by Kan.⁵⁹

(*E*)-3-(tributylstannyl)acrylaldehyde (106)

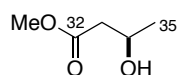


To a slurry of CuCN (2.1 g, 23.6 mmol) in THF at −78 °C was added *n*BuLi (1.6 M in hexanes, 29.6 mL, 47.3 mmol) dropwise. The reaction mixture was stirred at −40 °C until a clear, yellow solution was obtained. Bu₃SnH (12.7 mL, 47.3 mmol) was then added dropwise at −78 °C. The mixture was stirred at −40 °C for 15 min, to which 3,3-diethoxy-1-propyne (2.8 mL, 19.7 mmol) was added at −78 °C. After stirring for 2 h, MeOH (3 mL) was added to give a deep red solution, which was

stirred for 30 min before being quenched with NH_4Cl (100 mL) at 0 °C. The mixture was filtered and extracted with Et_2O (3×50 mL). The combined organic extracts were dried (MgSO_4) and concentrated *in vacuo*. The crude was redissolved in acetone (75 mL) and water (8 mL), to which *p*-toluenesulfonic acid (187 mg, 0.985 mmol) was added, and the solution was stirred at 60 °C for 36 h. The acetone was evaporated and the residue was dissolved in Et_2O (100 mL) and the layers were separated. The organic layer was washed with NaHCO_3 (50 mL), dried (MgSO_4) and concentrated *in vacuo*. Purification by flash chromatography ($\text{Et}_2\text{O}/\text{PE}/\text{Et}_3\text{N}$ 1:19:0.2) afforded aldehyde **106** (5.11 g, 14.8 mmol, 75%, *E:Z* > 95:5) as a yellow oil.

R_f 0.42 ($\text{Et}_2\text{O}/\text{PE}$ 1:20); $^1\text{H NMR}$ (500 MHz, CDCl_3) δ_H 9.41 (1H, d, $J = 7.6$ Hz, CHO), 7.79 (1H, *app* d, $J = 19.2$ Hz, H_5), 6.62 (1H, *app* dd, $J = 19.2, 7.6$ Hz, H_4), 1.55-1.47 (6H, m, SnBu_3), 1.35-1.27 (6H, m, SnBu_3), 1.04-0.98 (6H, m, SnBu_3), 0.93-0.86 (9H, m, SnBu_3). Data in agreement with literature values.⁹⁶

Methyl (*R*)-3-hydroxybutanoate (**159**)

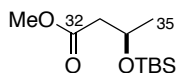


To $[\text{RuCl}_2(\text{C}_6\text{H}_5)]_2$ (86.8 mg, 0.172 mmol) and (*R*)-BINAP (227 mg, 0.364 mmol) in a Schlenk tube was added dry DMF (6.0 mL). The reaction mixture was stirred at 100 °C for 10 min, before being cooled and concentrated (50 °C, 1 mm/Hg). The mixture was further concentrated (50 °C, 0.1 mm/Hg) for 1 h to afford Ru-BINAP as a reddish brown solid. Methylacetoacetate (20.0 mL, 185 mmol) was lyophilised three times before dry methanol (40.0 mL) was added. The mixture was lyophilised 3 more times before Ru-BINAP was added. The mixture was lyophilised twice before being transferred to an autoclave and placed under 6 bar H_2 and left for 48 h. The reaction mixture was then concentrated *in vacuo* and distilled (76-78 °C, 15 mm/Hg) to yield alcohol **159** (17.5 g, 148 mmol, 80%, >99% *ee*) as a colourless oil.

$^1\text{H NMR}$ (500 MHz, CDCl_3) δ_H 4.24-4.17 (1H, m, H_{34}), 3.72 (3H, s, OMe), 2.85 (1H, br s, OH),

2.51 (1H, dd, $J = 16.4, 3.6$ Hz, H_{33a}), 2.44 (1H, dd, $J = 16.7, 8.6$ Hz, H_{33b}), 1.24 (3H, d, $J = 6.4$ Hz, H₃₅). Data in agreement with literature values.⁶⁶

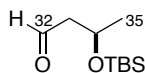
Methyl (*R*)-3-((*tert*-butyldimethylsilyl)oxy)butanoate (**162**)



To a solution of alcohol **159** (10.0 g, 84.6 mmol) in CH₂Cl₂ (250 mL) was added imidazole (17.3 g, 254 mmol) and TBSCl (25.5 g, 169 mmol). The reaction mixture was stirred at rt for 16 h before being quenched with NaHCO₃ (100 mL) and extracted with CH₂Cl₂ (3 × 100 mL). The combined organic extracts were dried (MgSO₄) and concentrated *in vacuo*. Purification by flash chromatography (EtOAc/PE 1:9) yielded ester **162** (15.7 g, 67.7 mmol, 80%) as a colourless oil.

R_f 0.60 (EtOAc/PE 1:4); **¹H NMR** (500 MHz, CDCl₃) δ_H 4.32–4.23 (1H, m, H₃₄), 3.66 (3H, s, OMe), 2.48 (1H, dd, $J = 14.5, 7.7$ Hz, H_{33a}), 2.37 (1H, dd, $J = 14.5, 5.3$ Hz, H_{33b}), 1.19 (3H, d, $J = 6.1$ Hz, H₃₅), 0.86 (9H, s, SiC(CH₃)₃), 0.06 (3H, s, SiCH₃), 0.04 (3H, s, SiCH₃). Data in agreement with literature values.⁹⁷

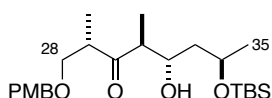
(*R*)-3-((*tert*-butyldimethylsilyl)oxy)butanal (**157**)



To a solution of ester **162** (15.2 g, 65.4 mmol) in CH₂Cl₂ (200 mL) at −78 °C was added DIBAL-H (1M in hexane, 71.9 mL, 71.9 mmol) dropwise. The reaction mixture was stirred for 3 h, before being quenched with Na⁺/K⁺ tartrate (200 mL) at 0 °C. The mixture was stirred for 2 h before being extracted with CH₂Cl₂ (3 × 100 mL). The combined organic extracts were dried (MgSO₄) and concentrated *in vacuo*. Purification by flash chromatography (Et₂O/PE 1:9) yielded ester **157** (12.6 g, 62.1 mmol, 95%) as a colourless oil.

R_f 0.12 (Et₂O/PE 1:19); **¹H NMR** (500 MHz, CDCl₃) δ_H 9.80 (1H, t, *J* = 2.4 Hz, H₃₂), 4.39-4.32 (1H, m, H₃₄), 2.55 (1H, ddd, *J* = 15.6, 7.0, 2.9 Hz, H_{33a}), 2.46 (1H, dd, *J* = 15.7, 5.0, 2.0 Hz, H_{33b}), 1.24 (3H, d, *J* = 6.2 Hz, H₃₅), 0.87 (9H, s, SiC(CH₃)₃), 0.08 (3H, s, SiCH₃), 0.06 (3H, s, SiCH₃). Data in agreement with literature values.⁹⁷

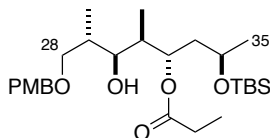
(2*S*,4*S*,5*S*,7*R*)-7-((*tert*-butyldimethylsilyl)oxy)-5-hydroxy-1-((4-methoxybenzyl)oxy)-2,4-dimethyl octan-3-one (165)



To a solution of dicyclohexylboron chloride (8.41 mL, 38.4 mmol) in Et₂O (100 mL) at 0 °C was added Et₃N (6.24 mL, 44.8 mmol), followed by a solution of ketone **156** (7.56 g, 32.0 mmol) in Et₂O (100 mL). The reaction mixture was stirred at 0 °C for 1 h, before aldehyde **157** (9.71 g, 48.0 mmol) in Et₂O was added at –78 °C. The reaction mixture was stirred at –78 °C for 1 h, then –20 °C for 16 h, before being quenched at 0 °C with MeOH (130 mL), pH 7 buffer (130 mL), and H₂O₂ (100 mL). The solution was stirred for 1 h, poured into H₂O (200 mL) and extracted with Et₂O (3 × 100 mL). The combined organic extracts were washed with NaHCO₃ (200 mL), dried (MgSO₄) and concentrated *in vacuo*. Purification by flash chromatography (EtOAc/PE 1:9) yielded aldol adduct **165** (13.8 g, 31.4 mmol, 98%, >95:5 dr) as a colourless oil.

R_f 0.45 (EtOAc/PE 3:7); **¹H NMR** (500 MHz, CDCl₃) δ_H 7.20 (2H, d, *J* = 8.6 Hz, ArH), 6.86 (2H, d, *J* = 8.6 Hz, ArH), 4.40 (2H, ABq, *J* = 11.7, OCH₂Ar), 4.16-4.09 (1H, m, H₃₂), 4.04-3.98 (1H, m, H₃₄), 3.79 (3H, s, ArOMe), 3.64 (1H, *app* t, *J* = 8.7 Hz, H_{28a}), 3.49 (1H, d, *J* = 4.4 Hz, OH), 3.41 (1H, dd, *J* = 8.8, 4.9 Hz, H_{28b}), 3.11-3.04 (1H, m, H₂₉), 2.69 (1H, *app* qn, *J* = 7.2 Hz, H₃₁), 1.54 (1H, ddd, *J* = 14.1, 7.2, 2.2 Hz, H_{33a}), 1.47 (1H, ddd, *J* = 14.1, 10.1, 3.1 Hz, H_{33b}), 1.17 (3H, d, *J* = 6.3 Hz, H₃₅), 1.06 (3H, d, *J* = 7.2 Hz, Me₃₁), 1.04 (3H, d, *J* = 7.0 Hz, Me₂₉), 0.89 (9H, s, SiC(CH₃)₃), 0.07 (3H, s, SiCH₃), 0.06 (3H, s, SiCH₃). Data in agreement with that reported by Gibson.³⁴

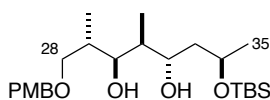
(2*R*,4*S*,5*R*,6*S*,7*S*)-2-((*tert*-butyldimethylsilyl)oxy)-6-hydroxy-8-((4-methoxybenzyl)oxy)-5,7-dimethyloctan-4-yl propionate (166)



To a solution of propionaldehyde (9.0 mL, 126 mmol) in THF (100 mL) at $-20\text{ }^{\circ}\text{C}$ was added samarium diiodide (20.5 mL, 0.1 M in THF, 2.05 mmol), followed by a solution of aldol adduct **165** (9.0 g, 20.5 mmol) in THF (200 mL) dropwise. The reaction mixture was warmed to $-10\text{ }^{\circ}\text{C}$ over 2 h, before being quenched with NaHCO_3 (200 mL) and extracted with Et_2O ($3 \times 100\text{ mL}$). The combined organic extracts were dried (Na_2SO_4) and concentrated *in vacuo*. Purification by flash chromatography (EtOAc/PE 1:9) yielded alcohol **166** (9.63 g, 19.5 mmol, 95%, >95:5 dr) as a colourless oil.

R_f 0.62 (EtOAc/PE 3:7); **¹H NMR** (500 MHz, CDCl_3) δ_{H} 7.23 (2H, d, $J = 8.6\text{ Hz}$, ArH), 6.86 (2H, d, $J = 8.6\text{ Hz}$, ArH), 4.98 (1H, ddd, $J = 9.9, 6.5, 1.8\text{ Hz}$, H₃₂), 4.43 (2H, s, OCH_2Ar), 3.85-3.80 (1H, m, H₃₄), 3.79 (3H, s, ArOMe), 3.66 (1H, dd, $J = 9.0, 5.0\text{ Hz}$, H_{28a}), 3.55 (1H, dd, $J = 9.0, 4.5\text{ Hz}$, H_{28b}), 3.37-3.31 (1H, m, H₃₀), 3.26 (1H, s, OH), 2.33 (2H, q, $J = 7.6\text{ Hz}$, $\text{CO}_2\text{CH}_2\text{CH}_3$), 1.92-1.85 (1H, m, H₂₉), 1.85-1.78 (1H, m, H₃₁), 1.73 (1H, ddd, $J = 14.5, 9.4, 1.9\text{ Hz}$, H_{33a}), 1.58 (1H, ddd, $J = 14.5, 9.8, 2.6\text{ Hz}$, H_{33b}), 1.14 (3H, d, $J = 6.1\text{ Hz}$, H₃₅), 1.14 (3H, t, $J = 7.6\text{ Hz}$, $\text{CO}_2\text{CH}_2\text{CH}_3$), 0.93 (3H, d, $J = 7.0\text{ Hz}$, Me₂₉), 0.91 (3H, d, $J = 7.0\text{ Hz}$, Me₃₁), 0.87 (9H, s, $\text{SiC}(\text{CH}_3)_3$), 0.03 (3H, s, SiCH_3), 0.00 (3H, s, SiCH_3). Data in agreement with that reported by Gibson.³⁴

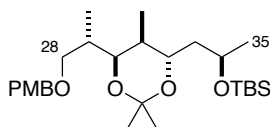
(2*S*,3*S*,4*S*,5*S*,7*R*)-7-((*tert*-butyldimethylsilyl)oxy)-1-((4-methoxybenzyl)oxy)-2,4-dimethyloctane-3,5-diol (167)



To a solution of alcohol **166** (6.26 g, 12.6 mmol) in MeOH/H₂O (10:1, 330 mL) was added K₂CO₃ (10.5 g, 75.6 mmol). The reaction mixture was stirred for 16 h, before being quenched with H₂O (200 mL) and extracted with CH₂Cl₂ (3 × 100 mL). The combined organic extracts were dried (Na₂SO₄) and concentrated *in vacuo*. Purification by flash chromatography (EtOAc/PE 1:9) yielded diol **167** (5.50 g, 12.5 mmol, 99%) as a colourless oil.

R_f 0.49 (EtOAc/PE 3:7); **¹H NMR** (500 MHz, CDCl₃) δ_H 7.23 (2H, d, *J* = 8.6 Hz, ArH), 6.86 (2H, d, *J* = 8.6 Hz, ArH), 4.45 (2H, ABq, *J* = 11.4 Hz, OCH₂Ar), 4.26-4.18 (1H, m, H₃₄), 3.95 (1H, ddd, *J* = 10.3, 5.4, 1.7, H₃₂), 3.89-3.85 (1H, m, H₃₀), 3.79 (3H, s, ArOMe), 3.57-3.50 (2H, m, H₂₈), 2.00-1.90 (1H, m, H₂₉), 1.77 (1H, ddd, *J* = 14.0, 10.3, 3.6 Hz, H_{33a}), 1.56-1.48 (2H, m, H₃₁+H_{33b}), 1.23 (3H, d, *J* = 6.3 Hz, H₃₅), 0.96 (3H, d, *J* = 7.0 Hz, Me₃₁), 0.89 (9H, s, SiC(CH₃)₃), 0.78 (3H, d, *J* = 6.9 Hz, Me₂₉), 0.09 (3H, s, SiCH₃), 0.08 (3H, s, SiCH₃). Data in agreement with that reported by Gibson.³⁴

***tert*-butyl(((*R*)-1-((4*S*,5*S*,6*S*)-6-((*S*)-1-((4-methoxybenzyl)oxy)propan-2-yl)-2,2,5-trimethyl-1,3-dioxan-4-yl)propan-2-yl)oxy)dimethylsilane (262)**

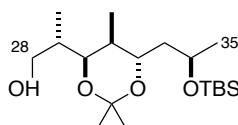


To a solution of diol **167** (6.20 g, 14.1 mmol) in CH₂Cl₂ (200 mL) was added 2,2-dimethoxypropane (85.5 mL, 697 mmol) and pyridinium *p*-toluenesulfonate (360 mg, 1.41 mmol). The reaction mixture was stirred for 16 h, quenched with NaHCO₃ (200 mL), and extracted with CH₂Cl₂ (3 × 100 mL). The combined organic extracts were dried (MgSO₄) and concentrated *in vacuo*. Purification by flash chromatography (EtOAc/PE 1:9) yielded acetone **262** (6.30 g, 13.1 mmol, 93%) as a colourless oil.

R_f 0.80 (EtOAc/PE 3:7); **¹H NMR** (500 MHz, CDCl₃) δ_H 7.24 (2H, d, *J* = 8.6 Hz, ArH), 6.86 (2H, d, *J* = 8.6 Hz, ArH), 4.40 (2H, s, OCH₂Ar), 3.95-3.87 (1H, m, H₃₄), 3.79 (3H, s, ArOMe), 3.63 (1H, dd, *J* = 10.9, 4.5 Hz, H₃₀), 3.54 (1H, dd, *J* = 8.8, 3.0 Hz, H_{28a}), 3.42-3.34 (2H, m, H₃₂+H_{28b}), 1.88-1.78 (1H, m, H₂₉), 1.60-1.50 (3H, m, H₃₁+H₃₃), 1.32 (3H, s, OC(CH₃)₂), 1.27 (3H, s, OC(CH₃)₂), 1.13 (3H,

d, $J = 6.1$ Hz, H_{35}), 0.92 (3H, d, $J = 6.7$ Hz, Me_{29}), 0.88 (9H, s, $SiC(CH_3)_3$), 0.84 (3H, d, $J = 6.7$ Hz, Me_{31}), 0.05 (3H, s, $SiCH_3$), 0.04 (3H, s, $SiCH_3$). Data in agreement with that reported by Gibson.³⁴

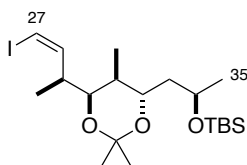
(*S*)-2-(((4*S*,5*S*,6*S*)-6-((*R*)-2-((*tert*-butyldimethylsilyl)oxy)propyl)-2,2,5-trimethyl-1,3-dioxan-4-yl)propan-1-ol (168)



To a solution of acetone **262** (6.20 g, 12.9 mmol) in CH_2Cl_2 (200 mL) and pH 7 buffer (40 mL) at 0 °C was added DDQ (3.22 g, 14.2 mmol). The reaction mixture was stirred at 0 °C for 1 h, before being quenched by $NaHCO_3$ (100 mL) and extracted with CH_2Cl_2 (3×100 mL). The combined organic extracts were dried (Na_2SO_4) and concentrated *in vacuo*. Purification by flash chromatography (EtOAc/PE 1:9) yielded alcohol **168** (4.20 g, 11.7 mmol, 91%) as a colourless oil.

R_f 0.30 (EtOAc/PE 1:4); 1H NMR (500 MHz, $CDCl_3$) δ_H 3.96-3.87 (1H, m, H_{34}), 3.67 (1H, dd, $J = 10.5, 4.5$ Hz, H_{30}), 3.62-3.55 (1H, m, H_{32}), 3.55-3.48 (1H, m, H_{28a}), 3.46-3.40 (1H, m, H_{28b}), 3.21 (1H, dd, $J = 9.7, 1.8$ Hz, OH), 1.97-1.83 (1H, m, H_{29}), 1.63-1.52 (3H, m, $H_{31}+H_{33}$), 1.38 (3H, s, $OC(CH_3)_2$), 1.34 (3H, s, $OC(CH_3)_2$), 1.14 (3H, d, $J = 6.1$ Hz, H_{35}), 0.89 (9H, s, $SiC(CH_3)_3$), 0.87 (3H, d, $J = 6.7$ Hz, Me_{29}), 0.75 (3H, d, $J = 6.8$ Hz, Me_{31}), 0.06 (3H, s, $SiCH_3$), 0.05 (3H, s, $SiCH_3$). Data in agreement with that reported by Gibson.³⁴

***tert*-butyl(((*R*)-1-((4*S*,5*S*,6*S*)-6-((*S*,*Z*)-4-iodobut-3-en-2-yl)-2,2,5-trimethyl-1,3-dioxan-4-yl)propan-2-yl)oxy)dimethylsilane (171)**

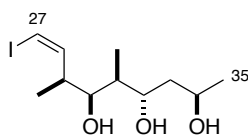


To a solution of alcohol **168** (4.20 g, 11.7 mmol) in CH₂Cl₂ (300 mL) was added NaHCO₃ (5.83 g, 70.0 mmol) and Dess-Martin periodinane (14.8 g, 35.0 mmol). The reaction mixture was stirred for 1 h, before being concentrated *in vacuo*. Purification by flash chromatography (EtOAc/PE 1:19) yielded the aldehyde (3.64 g, 10.1 mmol, 86%) as a colourless oil, which was immediately used in the subsequent step.

To a suspension of (Ph₃PCH₂I)⁺I⁻ (13.4 g, 25.2 mmol) in THF (150 mL) was added NaHMDS (1.0 M in THF, 25.2 mL, 25.2 mmol). The solution was stirred until a deep orange solution was obtained. The reaction mixture was then cooled to -78 °C, before a solution of the aldehyde (3.64 g, 10.1 mmol) in THF (100 mL) was added. The reaction mixture was warmed to rt over 2 h, before being diluted with hexane. The mixture was filtered through a short pad of Celite® and concentrated *in vacuo*. Purification by flash chromatography (EtOAc/PE 1:19) afforded vinyl iodide **171** (4.53 g, 9.39 mmol, 93%) as a colourless oil.

R_f 0.90 (EtOAc/PE 1:4); **¹H NMR** (500 MHz, CDCl₃) δ_H 6.15 (1H, d, *J* = 7.5 Hz, H₂₇), 6.12 (1H, *app* t, *J* = 7.4 Hz, H₂₈), 3.96-3.87 (1H, m, H₃₄), 3.70 (1H, dd, *J* = 9.1, 4.7 Hz, H₃₀), 3.43-3.36 (1H, m, H₃₂), 2.64-2.53 (1H, m, H₂₉), 1.65-1.57 (1H, m, H₃₁), 1.57-1.51 (2H, m, H₃₃), 1.31 (3H, s, OC(CH₃)₂), 1.29 (3H, s, OC(CH₃)₂), 1.14 (3H, d, *J* = 6.2 Hz, H₃₅), 0.93 (3H, d, *J* = 6.8 Hz, Me₂₉), 0.89 (9H, s, SiC(CH₃)₃), 0.87 (3H, d, *J* = 6.8 Hz, Me₃₁), 0.06 (3H, s, SiCH₃), 0.04 (3H, s, SiCH₃). Data in agreement with that reported by Gibson.³⁴

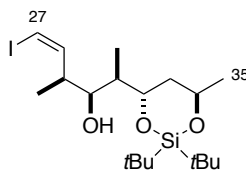
(2*R*,4*S*,5*S*,6*S*,7*S*,*Z*)-9-iodo-5,7-dimethylnon-8-ene-2,4,6-triol (155**)**



To a solution of TBS ether **171** (3.55 g, 7.36 mmol) in MeOH (50 mL) was added PPTS (555 mg, 2.21 mmol). The mixture was stirred for 16 h, the volatiles were removed *in vacuo* and the crude product purified by flash column chromatography (EtOAc/PE 1:4) to yield triol **155** (2.17 g, 6.62 mmol, 90%) as an off-white solid.

R_f 0.29 (EtOAc/PE 1:4); $[\alpha]_D^{20} = +30.0$ (c 0.20, CHCl₃); **IR** ν_{\max} = 3347, 2966, 2930, 2348, 2326, 1456, 1376, 1260, 1066, 972, 804, 699; **¹H NMR** (500 MHz, CDCl₃) δ_H 6.33 (1H, d, J = 7.4 Hz, H₂₇), 6.18 (1H, dd, J = 8.8, 7.4 Hz, H₂₈), 4.24-4.15 (1H, m, H₃₄), 4.05-3.97 (1H, m, H₃₂), 3.92-3.87 (1H, m, H₃₀), 3.12 (3H, d, J = 5.2 Hz, OH), 2.78-2.69 (1H, m, H₂₉), 1.82 (1H, ddd, J = 14.5, 9.6, 3.1 Hz, H_{33a}), 1.77-1.70 (1H, m, H₃₁), 1.56 (1H, ddd, J = 14.5, 7.4, 2.4 Hz, H_{33b}), 1.28 (3H, d, J = 6.3 Hz, H₃₅), 1.03 (3H, d, J = 7.1 Hz, Me₃₁), 0.96 (3H, d, J = 6.8 Hz, Me₂₉); **¹³C NMR** (125 MHz, CDCl₃) δ_C 144.0, 83.3, 75.0, 72.6, 65.9, 43.1, 42.2, 39.3, 23.4, 16.0, 10.7; **HRMS** (ES⁺) calc for C₁₁H₂₂IO₃ [M+H]⁺ 329.0608, found 329.0611.

(2*R*,3*S*,4*S*,*Z*)-2-((4*S*,6*R*)-2,2-di-*tert*-butyl-6-methyl-1,3,2-dioxasilinan-4-yl)-6-iodo-4-methylhex-5-en-3-ol (178)

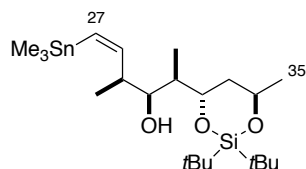


To a solution of triol **155** (500 mg, 1.52 mmol) in CH₂Cl₂ (20 mL) at −78 °C was added 2,6-lutidine (0.88 mL, 7.60 mmol) and *t*Bu₂Si(OTf)₂ (0.59 mL, 1.82 mmol) dropwise. The mixture was stirred at −78 °C for 1h, before being quenched with MeOH (5 mL) followed by NaHCO₃ solution (20 mL). The residue was extracted with CH₂Cl₂ (3 × 20 mL), and the combined organic extracts were dried (MgSO₄) and concentrated in *vacuo*. Purification by flash chromatography (EtOAc/PE 1:20) afforded alcohol **178** (684 mg, 1.46 mmol, 96%) as a colourless oil.

R_f 0.25 (Et₂O/PE 9:1); $[\alpha]_D^{20} = +59.5$ (c 1.0, CHCl₃); **IR** ν_{\max} = 3481, 2964, 2932, 2892, 2858, 1474, 1385, 1259, 1134, 978, 896, 865, 825, 797, 730, 648; **¹H NMR** (500 MHz, CDCl₃) δ_H 6.29-6.23 (2H, m, H₂₇+H₂₈), 4.47-4.40 (1H, m, H₃₄), 4.24 (1H, ddd, J = 10.1, 5.4, 1.9 Hz, H₃₂), 3.96 (1H, dd, J = 8.0, 1.7 Hz, H₃₀), 3.00 (1H, br s, OH), 2.74-2.64 (1H, m, H₂₉), 2.19 (1H, ddd, J = 14.3, 10.1, 5.9 Hz, H_{33a}), 1.72-1.65 (1H, m, H₃₁), 1.52-1.47 (1H, m, H_{33b}), 1.30 (3H, d, J = 6.6 Hz, H₃₅), 1.03 (3H, d, J = 7.0 Hz, Me₃₁), 1.00 (18H, s, Si*t*Bu₂), 0.95 (3H, d, J = 6.9 Hz, Me₂₉); **¹³C NMR** (125 MHz, CDCl₃) δ_C

144.8, 82.2, 74.6, 73.2, 67.8, 43.0, 40.7, 38.8, 27.5, 27.4, 23.8, 21.5, 20.8, 16.5, 10.9; **HRMS** (ES^+) calc for $\text{C}_{19}\text{H}_{38}\text{IO}_3\text{Si}$ $[\text{M}+\text{H}]^+$ 469.1629, found 469.1619.

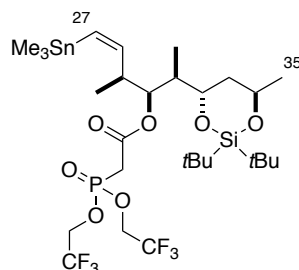
(2*R*,3*S*,4*S*,*Z*)-2-((4*S*,6*R*)-2,2-di-*tert*-butyl-6-methyl-1,3,2-dioxasilinan-4-yl)-4-methyl-6-(trimethylstannyl)hex-5-en-3-ol (180)



To a stirred solution of vinyl iodide **178** (916 mg, 1.96 mmol) in THF (20 mL) was added $\text{PdCl}_2(\text{PPh}_3)_2$ (138 mg, 0.20 mmol), Li_2CO_3 (723 mg, 9.78 mmol) and $(\text{Me}_3\text{Sn})_2$ (2.03 mL, 9.78 mmol). The reaction was stirred at 40 °C for 3h, cooled to rt and concentrated *in vacuo*. Purification by flash chromatography (EtOAc/PE 1:20) afforded stannane **180** (644 mg, 1.27 mmol, 65%) as a colourless oil.

R_f 0.58 (Et₂O/PE 1:9); $[\alpha]_D^{20} = +65.0$ (c 0.1, CHCl_3); **IR** ν_{max} = 2962, 2930, 2857, 2360, 1726, 1598, 1474, 1376, 1258, 1133, 1101, 981, 899, 864, 825, 799, 769, 730; **¹H NMR** (500 MHz, CDCl_3) δ_{H} 6.38 (1H, dd, $J = 12.3, 9.5$ Hz, H_{28}), 5.94 (1H, d, $J = 12.4$ Hz, H_{27}), 4.39 (1H, ddq, $J = 12.5, 6.1, 2.6$ Hz, H_{34}), 4.24 (1H, ddd, $J = 9.4, 6.4, 2.4$ Hz, H_{32}), 3.96 (1H, br d, $J = 8.0$ Hz, H_{30}), 2.51 (1H, d, $J = 1.8$ Hz, OH), 2.15 (1H, ddq, $J = 9.5, 6.5, 3.1$ Hz, H_{29}), 2.11 (1H, ddd, $J = 14.3, 9.8, 5.7$ Hz, H_{33a}), 1.64 (1H, ddq, $J = 7.1, 7.1, 1.5$ Hz, H_{31}), 1.56 (1H, ddd, $J = 14.2, 2.4, 2.4$ Hz, H_{33b}), 1.29 (3H, d, $J = 6.7$ Hz, H_{35}), 1.01 (9H, s, $\text{Si}t\text{Bu}_2$), 0.99 (9H, s, $\text{Si}t\text{Bu}_2$), 0.92 (3H, d, $J = 7.1$ Hz, Me_{31}), 0.91 (3H, d, $J = 6.7$ Hz, Me_{29}), 0.18 (9H, s, SnMe_3); **¹³C NMR** (125 MHz, CDCl_3) δ_{C} 152.5, 130.4, 73.0, 72.4, 67.6, 44.6, 39.9, 38.7, 27.3, 27.3, 23.7, 21.4, 20.7, 17.4, 9.7, -8.3; **HRMS** (ES^+) calc for $\text{C}_{22}\text{H}_{47}\text{O}_3\text{Si}^{112}\text{Sn}$ $[\text{M}+\text{H}]^+$ 499.2337, found 499.2337.

(2*R*,3*S*,4*S*,*Z*)-2-((4*S*,6*R*)-2,2-di-*tert*-butyl-6-methyl-1,3,2-dioxasilinan-4-yl)-4-methyl-6-(trimethylstannyl)hex-5-en-3-yl 2-(bis(2,2,2-trifluoroethoxy)phosphoryl)acetate (217)

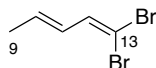


To a solution of alcohol **180** (410 mg, 811 μmol) and acid **188** (370 mg, 1.22 mmol) in CH_2Cl_2 (20 mL) was added DCC (1 M, 0.89 mL, 890 μmol) and the mixture was stirred for 10 min before being concentrated *in vacuo*. Purification by flash chromatography (EtOAc/PE 1:20) afforded phosphonate **217** (488 mg, 616 μmol , 76%) as a yellow oil.

R_f 0.21 (Et₂O/PE 1:9); $[\alpha]_D^{20} = +62.4$ (c 1.0, CHCl_3); **IR** ν_{max} = 2971, 2860, 1736, 1474, 1386, 1298, 1267, 1174, 1143, 1097, 1071, 963, 900, 826, 769, 648; **¹H NMR** (500 MHz, CDCl_3) δ_{H} 6.30 (1H, dd, $J = 12.3, 9.8$ Hz, H₂₈), 5.81 (1H, d, $J = 12.2$ Hz, H₂₇), 5.54 (1H, dd, $J = 9.6, 1.3$ Hz, H₃₀), 4.51-4.38 (4H, m, OCH_2CF_3), 4.39-4.32 (1H, m, H₃₄), 3.82 (1H, ddd, $J = 9.8, 8.9, 3.1$ Hz, H₃₂), 3.13-2.96 (2H, m, H₂), 2.36-2.26 (1H, m, H₂₉), 1.87-1.76 (2H, m, H₃₁+H_{33a}), 1.67 (1H, ddd, $J = 14.4, 4.2, 3.6$ Hz, H_{33b}), 1.28 (3H, d, $J = 6.4$ Hz, Me₃₅), 1.00 (9H, s, Si*t*Bu), 0.99 (3H, d, $J = 6.5$ Hz, Me₂₉), 0.98 (9H, s, Si*t*Bu), 0.84 (3H, d, $J = 7.0$ Hz, Me₃₁), 0.18 (9H, s, SnMe₃); **¹³C NMR** (125 MHz, CDCl_3) δ_{C} 164.1 (d, $J = 2.8$ Hz), 151.0, 129.9, 122.3 (qd, $J = 278, 6.5$ Hz), 122.2 (qd, $J = 278, 6.0$ Hz), 76.9, 69.9, 67.3, 63.0-62.2 (2C, m), 44.3, 40.9, 38.2, 34.1, 27.5, 27.2, 23.8, 20.6 (d, $J = 33.5$ Hz), 17.7, 9.5, -8.3; **HRMS** (ES⁺) calc for C₂₈H₅₅F₆O₇PSi¹¹²SnN [M+NH₄]⁺ 802.2434, found 802.2439.

c. Southern Fragment

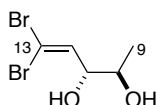
(*E*)-1,1-dibromopenta-1,3-diene (**224**)



To a solution of triphenylphosphine (25.2 g, 96.4 mmol) in CH_2Cl_2 (150 mL) at 0 °C was added CBr_4 (32.0 g, 96.4 mmol). After stirring for 10 minutes, zinc (6.30 g, 96.4 mmol) was added. The reaction mixture was warmed to rt and stirred for 24 h. Crotonaldehyde **223** (4.0 mL, 48.2 mmol) was added at 0 °C. After stirring for 2 h at rt, the reaction mixture was poured into ice-cold pentane. The suspension was filtered, and the residue was washed with ice-cold pentane. The filtrate was concentrated *in vacuo*. Purification by flash chromatography (PE) afforded diene **224** (7.62 g, 33.7 mmol, 70%) as a yellow oil.

R_f 0.81 ($\text{Et}_2\text{O}/\text{PE}$ 1:4); $^1\text{H NMR}$ (500 MHz, CDCl_3) δ_{H} 6.89 (1H, d, $J = 10.0$ Hz, H_{12}), 6.10 (1H, ddq, $J = 15.4, 10.0, 1.6$ Hz, H_{11}), 5.92 (1H, ddq, $J = 15.4, 6.8, 0.73$ Hz, H_{10}), 1.77 (3H, ddd, $J = 6.8, 1.6, 0.39$ Hz, Me_{10}). Data in agreement with literature values.⁹⁸

(2*R*,3*R*)-5,5-dibromopent-4-ene-2,3-diol (**225**)

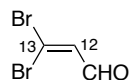


To a solution of potassium osmate dihydrate (42.4 mg, 115 μmol) and $(\text{DHQD})_2\text{PHAL}$ (111 g, 142 μmol) in *t*BuOH (150 mL) and water (150 mL) was added $\text{CH}_3\text{SO}_2\text{NH}_2$ (2.81 g, 28.6 mmol). The reaction mixture was stirred for 30 min, before K_2CO_3 (11.8 g, 85.7 mmol), NaHCO_3 (7.21 g, 85.7 mmol) and $\text{K}_3[\text{Fe}(\text{CN})_6]$ (28.3 g, 85.7 mmol) were added. The mixture was stirred for a further 30 min and cooled to 0 °C. Diene **224** (6.44 g, 28.6 mmol) was added dropwise and the slurry was warmed to rt and stirred for 16 h. Na_2SO_3 (350 mg) was added at 0 °C and the mixture was stirred at

rt for 1 h. The resulting mixture was extracted with EtOAc, and the combined organic extracts were washed with 1M NaOH (100 mL), dried (Na₂SO₄) and concentrated *in vacuo*. Purification by flash chromatography (Et₂O/PE 1:1), followed by recrystallisation (EtOH) yielded diol **225** (5.20 g, 20.0 mmol, 70%) as a white crystalline solid.

R_f 0.25 (Et₂O/PE 1:1); **¹H NMR** (500 MHz, CDCl₃) δ_H 6.48 (1H, d, *J* = 8.6 Hz, H₁₂), 4.11 (1H, dd, *J* = 8.6, 6.6 Hz, H₁₁), 3.74 (1H, dq, *J* = 6.6, 6.4 Hz, H₁₀), 2.79-2.58 (2H, m, OH), 1.23 (3H, d, *J* = 6.4 Hz, Me₁₀). Data in agreement with literature values.⁹⁹

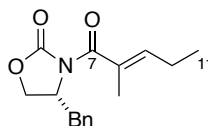
3,3-dibromoacrylaldehyde (**218**)



To a stirred solution of silica gel (60 g) in CH₂Cl₂ (500 mL) was added a solution of NaIO₄ (6.39 g, 30.0 mmol) in H₂O (50 mL) dropwise. After 15 min, a solution of diol **225** (6.0 g, 23.1 mmol) in CH₂Cl₂ (50 mL) was added. After a further 15 min, the mixture was dried (Na₂SO₄) and filtered. The filtrate was concentrated *in vacuo* to yield aldehyde **218** (4.93 g, 22.9 mmol, 99%) as a yellow oil.

R_f 0.75 (Et₂O/PE 1:1); **¹H NMR** (500 MHz, CDCl₃) δ_H 9.67 (1H, d, *J* = 6.4 Hz, CHO), 6.96 (1H, dd, *J* = 6.4 Hz, H₁₂). Data in agreement with that reported by Kan.⁵⁹

(*R,E*)-4-benzyl-3-(2-methylpent-2-enoyl)oxazolidin-2-one (**222**)

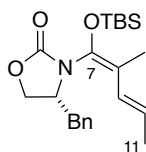


To a solution of trans-2-methyl-2-pentenoic acid **220** (1.19 g, 10.4 mmol) in CH₂Cl₂ (30 mL) at −78 °C was added Et₃N (3.53 mL, 25.3 mmol), followed by trimethylacetyl chloride (1.25 mL, 10.1 mmol) dropwise. The reaction mixture was warmed to rt and stirred for 1 h, before being cooled to −78 °C. Oxazolidinone **221** (1.80 g, 10.1 mmol) in CH₂Cl₂ (5 mL) was added dropwise, followed by

LiCl (648 mg, 15.3 mmol). The reaction mixture was warmed to rt and stirred for 18 h, before being quenched with water (20 mL), extracted with CH₂Cl₂ (3 × 10 mL), and the combined organic extracts were washed with brine (20 mL), dried (Na₂SO₄) and concentrated *in vacuo*. Purification by flash chromatography (Et₂O/PE 1:4) yielded imide **222** (2.73 g, 10.0 mmol, 98%) as a yellow oil.

R_f 0.24 (EtOAc/PE 1:4); **¹H NMR** (500 MHz, CDCl₃) δ_H 7.35-7.30 (2H, m, ArH), 7.29-7.24 (1H, m, ArH), 7.22-7.17 (2H, m, ArH), 6.08 (1H, tq, *J* = 7.3, 1.4 Hz, H₉), 4.74-4.68 (1H, m, NCH), 4.23 (1H, *app* t, *J* = 8.6 Hz, CH_{2a}Ar), 4.14 (1H, dd, *J* = 9.0, 5.6 Hz, CH_{2b}Ar), 3.33 (1H, dd, *J* = 13.5, 3.5 Hz, OCH_{2a}CH), 2.84 (1H, dd, *J* = 13.5, 9.2 Hz, OCH_{2b}CH), 2.21 (2H, *app* qn, *J* = 7.5 Hz, H₁₀), 1.91 (3H, s, Me₈), 1.06 (3H, t, *J* = 7.5 Hz, Me₁₀). Data in agreement with literature values.¹⁰⁰

(*R*)-4-benzyl-3-((1*E*,3*E*)-1-((*tert*-butyldimethylsilyl)oxy)-2-methylpenta-1,3-dien-1-yl)oxazolidin-2-one (219**)**

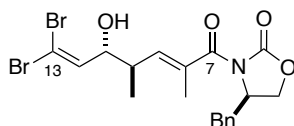


To a solution of imide **222** (4.0 g, 14.6 mmol) in THF (300 mL) at −78 °C was added NaHMDS (1 M in THF, 22.0 mL, 22.0 mmol) dropwise. After stirring for 1.5 h, TBSCl (4.4 g, 29.3 mmol) in THF (100 mL) was added dropwise. The reaction mixture was stirred for a further 1 h, before being quenched with NH₄Cl (100 mL). The solvent was removed *in vacuo* and the residue was extracted with EtOAc (3 × 50 mL). The combined organic extracts were dried (Na₂SO₄) and concentrated *in vacuo*. Purification by flash chromatography (EtOAc/PE 1:9 to 1:4) yielded silyl ketene aminal **219** (5.6 g, 14.5 mmol, 99%) as a colourless oil.

R_f 0.15 (EtOAc/PE 1:4); **¹H NMR** (500 MHz, CDCl₃) δ_H 7.34-7.27 (2H, m, ArH), 7.27-7.22 (1H, m, ArH), 7.17-7.10 (2H, m, ArH), 6.17 (1H, d, *J* = 15.6 Hz, H₉), 5.68 (1H, dq, *J* = 15.6, 6.7 Hz, H₁₀), 4.31-4.21 (2H, m, NCH+CH_{2a}Ar), 4.17-4.09 (1H, m, CH_{2b}Ar), 3.12 (1H, br d, *J* = 13.0 Hz, OCH_{2a}CH), 2.69-2.55 (1h, m, OCH_{2b}CH), 1.82 (6H, s, Me₈+Me₁₀), 0.99 (9H, s, Si*t*BuMe₂), 0.21 (3H,

s, Si*t*BuMe₂), 0.14 (3H, s, Si*t*BuMe₂). Data in agreement with literature values.¹⁰¹

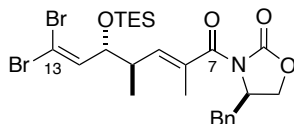
(*R*)-4-benzyl-3-((4*R*,5*R*,*E*)-7,7-dibromo-5-hydroxy-2,4-dimethylhepta-2,6-dienoyl)oxazolidin-2-one (226)



To a solution of aldehyde **218** (4.9 g, 23.1 mmol) in CH₂Cl₂ (80 mL) at –78 °C was added TiCl₄ (1.64 mL, 15.0 mmol) dropwise, followed by a solution of silyl ketene aminal **219** (5.8 g, 15.0 mmol) in CH₂Cl₂ (80 mL). The reaction mixture was warmed to –20 °C and stirred for 18 h, before being quenched with pyridine (5 mL), Na⁺/K⁺ tartrate (50 mL) and NaHCO₃ (50 mL). The mixture was stirred at rt until a homogeneous solution was formed. The solution was extracted with EtOAc (3 × 50 mL), and the combined organic extracts were dried (Na₂SO₄) and concentrated *in vacuo*. Purification by flash chromatography (EtOAc/PE 1:4) yielded aldol adduct **226** (6.0 g, 12.3 mmol, 82%) as a white solid.

R_f 0.30 (EtOAc/PE 1:2); **¹H NMR** (500 MHz, CDCl₃) δ_H 7.36-7.31 (2H, m, ArH), 7.31-7.27 (1H, m, ArH), 7.21-7.17 (2H, m, ArH), 6.51 (1H, d, *J* = 8.6 Hz, H₁₂), 5.75 (1H, dq, *J* = 10.4, 1.5 Hz, H₉), 4.85-4.78 (1H, m, NCH), 4.31 (1H, *app* t, *J* = 8.8 Hz, OCH_{2a}CH), 4.19 (1H, dd, *J* = 9.0, 6.4 Hz, OCH_{2b}CH), 4.10 (1H, *app* t, *J* = 8.4 Hz, H₁₁), 3.31 (1H, dd, *J* = 13.5, 3.4 Hz, CH_{2a}Ar), 3.26 (1H, br s, OH), 2.88 (1H, dd, *J* = 13.5, 9.0 Hz, CH_{2b}Ar), 2.75-2.66 (1H, m, H₁₀), 1.97 (3H, d, *J* = 1.5 Hz, Me₈), 1.06 (3H, d, *J* = 6.8 Hz, Me₁₀). Data in agreement with that reported by Kan.⁵⁹

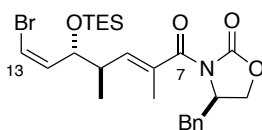
(R)-4-benzyl-3-((4R,5R,E)-7,7-dibromo-2,4-dimethyl-5-(triethylsilyl)hepta-2,6-dienoyl)oxazolidin-2-one (227)



To a solution of alcohol **226** (1.95 g, 4.00 mmol) in CH₂Cl₂ (160 mL) at -78 °C was added 2,6-lutidine (1.4 mL, 12.32 mmol), followed by TESOTf (2.2 mL, 9.84 mmol) dropwise. The reaction mixture was warmed to -65 °C over 30 min, before being quenched with NaHCO₃ (50 mL) and extracted with CH₂Cl₂ (3 × 50 mL). The combined organic extracts were dried (MgSO₄) and concentrated *in vacuo*. Purification by flash chromatography (Et₂O/PE 1:4) yielded TES ether **227** (2.38 g, 3.96 mmol, 99%) as a white solid.

R_f 0.60 (EtOAc/PE 1:2); ¹H NMR (500 MHz, CDCl₃) δ_H 7.35-7.29 (2H, m, ArH), 7.29-7.25 (1H, m, ArH), 7.22-7.18 (2H, m, ArH), 6.55 (1H, d, *J* = 8.4 Hz, H₁₂), 5.95 (1H, dq, *J* = 10.1, 1.5 Hz, H₉), 4.73-4.65 (1H, m, NCH), 4.27 (1H, dd, *J* = 8.4, 4.1 Hz, H₁₁), 4.24 (1H, *app* t, *J* = 8.4 Hz, OCH_{2a}CH), 4.15 (1H, dd, *J* = 9.0, 5.2 Hz, OCH_{2b}CH), 3.34 (1H, dd, *J* = 13.5, 3.4 Hz, CH_{2a}Ar), 2.85 (1H, dd, *J* = 13.5, 9.0 Hz, CH_{2b}Ar), 2.73-2.63 (1H, m, H₁₀), 1.91 (3H, d, *J* = 1.5 Hz, Me₈), 1.08 (3H, d, *J* = 6.8 Hz, Me₁₀), 0.95 (9H, t, *J* = 8.0 Hz, Si(CH₂CH₃)₃), 0.61 (6H, q, *J* = 8.0 Hz, Si(CH₂CH₃)₃). Data in agreement with that reported by Kan.⁵⁹

(R)-4-benzyl-3-((2E,4R,5R,6Z)-7-bromo-2,4-dimethyl-5-(triethylsilyl)hepta-2,6-dienoyl)oxazolidin-2-one (228)

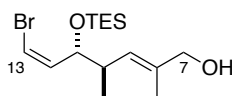


To Pd(PPh₃)₄ (922 mg, 0.798 mmol) was added a solution of dibromoolefin **227** (2.40 g, 3.99 mmol)

in CH₂Cl₂ (120 mL) and Bu₃SnH (1.61 mL, 5.99 mmol). The solution was stirred for 1 h and concentrated *in vacuo*. Purification by flash chromatography (Et₂O/PE 1:4) yielded (*Z*)-vinyl bromide **228** (2.07 g, 3.96 mmol, 99%) as a colourless oil.

R_f 0.60 (EtOAc/PE 1:2); **¹H NMR** (500 MHz, CDCl₃) δ_H 7.35-7.29 (2H, m, ArH), 7.29-7.25 (1H, m, ArH), 7.22-7.18 (2H, m, ArH), 6.24 (1H, *app* t, *J* = 7.5 Hz, H₁₂), 6.17 (1H, d, *J* = 7.3 Hz, H₁₃), 6.06 (1H, br d, *J* = 10.0 Hz, H₉), 4.73-4.64 (1H, m, NCH), 4.55 (1H, dd, *J* = 8.2, 3.9 Hz, H₁₁), 4.23 (1H, *app* t, *J* = 8.4 Hz, OCH_{2a}CH), 4.14 (1H, dd, *J* = 9.0, 5.2 Hz, OCH_{2b}CH), 3.34 (1H, dd, *J* = 13.5, 3.4 Hz, CH_{2a}Ar), 2.85 (1H, dd, *J* = 13.5, 9.2 Hz, CH_{2b}Ar), 2.75-2.65 (1H, m, H₁₀), 1.89 (3H, s, Me₈), 1.09 (3H, d, *J* = 6.8 Hz, Me₁₀), 0.95 (9H, t, *J* = 8.0 Hz, Si(CH₂CH₃)₃), 0.61 (6H, q, *J* = 8.0 Hz, Si(CH₂CH₃)₃). Data in agreement with that reported by Kan.⁵⁹

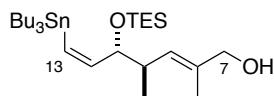
(2*E*,4*R*,5*R*,6*Z*)-7-bromo-5-(diethyl(methyl)silyl)-2,4-dimethylhepta-2,6-dien-1-ol (263)



To a solution of imide **228** (2.00 g, 3.83 mmol) in THF/H₂O (5:1, 90 mL) was added NaBH₄ (725 mg, 19.1 mmol). The reaction mixture was stirred in the dark for 3 h, before being quenched with NH₄Cl (20 mL) at 0 °C. THF was evaporated *in vacuo* and the residue was extracted with Et₂O (3 × 30 mL). The combined organic extracts were dried (Na₂SO₄) and concentrated *in vacuo*. Purification by flash chromatography (EtOAc/PE 1:4) yielded alcohol **263** (1.20 g, 3.45 mmol, 90%) as a colourless oil.

R_f 0.52 (EtOAc/PE 1:2); **¹H NMR** (500 MHz, CDCl₃) δ_H 6.17 (1H, d, *J* = 7.3 Hz, H₁₃), 6.09 (1H, *app* t, *J* = 7.7 Hz, H₁₂), 5.32 (1H, d, *J* = 9.7 Hz, H₉), 4.45 (1H, dd, *J* = 8.2, 5.2 Hz, H₁₁), 4.00 (2H, d, *J* = 5.8 Hz, H₇), 2.65-2.55 (1H, m, H₁₀), 1.68 (3H, s, Me₈), 0.99 (3H, d, *J* = 6.8 Hz, Me₁₀), 0.94 (9H, t, *J* = 8.0 Hz, Si(CH₂CH₃)₃), 0.59 (6H, q, *J* = 8.0 Hz, Si(CH₂CH₃)₃). Data in agreement with that reported by Kan.⁵⁹

(2*E*,4*R*,5*R*,6*Z*)-5-(diethyl(methyl)silyl)-2,4-dimethyl-7-(tributylstannyl)hepta-2,6-dien-1-ol (102)

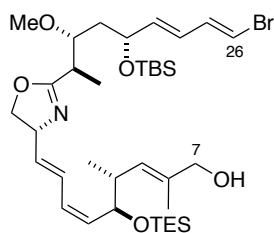


To a solution of vinyl bromide **263** (200 mg, 0.572 mmol) in Et₂O (10 mL) at –78 °C was added *t*BuLi (1.7 M in pentane, 1.35 mL, 2.29 mmol) dropwise. After stirring for 5 min, Bu₃SnCl (0.93 mL, 3.43 mmol) was added and the reaction mixture was warmed to rt, quenched with H₂O (10 mL) and extracted with EtOAc (3 × 10 mL). The organic extracts were washed with H₂O (10 mL), dried (Na₂SO₄) and concentrated *in vacuo*. Purification by flash chromatography (Et₂O/PE/Et₃N 1:9:0.02) afforded stannane **102** (218 mg, 0.389 mmol, 68%) as a colourless oil.

R_f 0.50 (EtOAc/PE 1:5); **¹H NMR** (500 MHz, CDCl₃) δ_H 6.42 (1H, dd, *J* = 13.1, 8.4 Hz, H₁₂), 5.83 (1H, d, *J* = 13.1 Hz, H₁₃), 5.40 (1H, *app* d, *J* = 9.8 Hz, H₉), 4.00 (2H, br s, H₇), 3.77 (1H, dd, *J* = 8.4, 4.1 Hz, H₁₁), 2.46 (1H, ddq, *J* = 9.8, 6.9, 4.2 Hz, H₁₀), 1.64 (3H, s, Me₈), 1.53-1.45 (6H, m, SnBu₃), 1.36-1.28 (6H, m, SnBu₃), 0.97 (3H, d, *J* = 6.9 Hz, Me₁₀), 0.97-0.87 (15H, m, SnBu₃), 0.93 (9H, t, *J* = 8.0 Hz, Si(CH₂CH₃)₃), 0.56 (6H, q, *J* = 8.0 Hz, SiCH₂CH₃). Data in agreement with that reported by Kan.⁵⁹

d. Fragment coupling

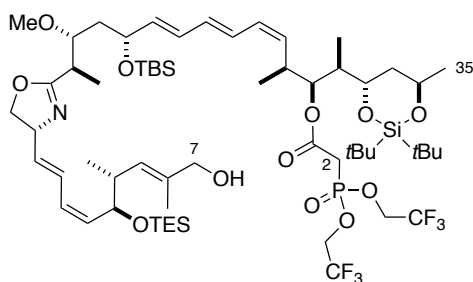
(2*E*,4*R*,5*S*,6*Z*,8*E*)-9-((*R*)-2-((2*R*,3*R*,5*R*,6*E*,8*E*)-9-bromo-5-((*tert*-butyldimethylsilyl)oxy)-3-methoxynona-6,8-dien-2-yl)-4,5-dihydrooxazol-4-yl)-2,4-dimethyl-5-(triethylsilyl)nona-2,6,8-trien-1-ol (115)



To a solution of Pd(PPh₃)₄ (25.8 mg, 22.4 μmol), CuTC (34.1 mg, 179 μmol) and [Ph₂PO₂][NBu₄] (82.2 mg, 179 μmol) in DMF (3 mL) at 0 °C, was added a solution of *bis*-halide **81** (52.2 mg, 89.4 μmol) and stannane **102** (50.0 mg, 89.4 μmol) in DMF (3 mL). After stirring at 0 °C in the dark for 3 h, the reaction was quenched with water (5 mL) and extracted with Et₂O (2 × 3 mL) and EtOAc (2 × 3 mL). The organic extracts were dried (Na₂SO₄) and concentrated *in vacuo*. Purification by flash chromatography (EtOAc/PE 1:4) gave diene **115** (53.9 mg, 74.2 μmol, 83%) as a pale yellow oil.

R_f 0.24 (EtOAc/PE 1:4); ¹H NMR (500 MHz, CDCl₃) δ_H 6.66 (1H, dd, *J* = 13.5, 10.9 Hz, H₂₅), 6.36 (1H, dd, *J* = 15.1, 11.4 Hz, H₁₄), 6.26 (1H, d, *J* = 13.5 Hz, H₂₆), 6.06 (1H, dd, *J* = 15.3, 10.8 Hz, H₂₄), 5.98 (1H, t, *J* = 11.2 Hz, H₁₃), 5.69 (1H, dd, *J* = 15.3, 6.8 Hz, H₂₃), 5.64 (1H, dd, *J* = 15.0, 5.7 Hz, H₁₅), 5.39 (1H, dd, *J* = 11.2, 8.6 Hz, H₁₂), 5.06 (1H, d, *J* = 9.9 Hz, H₉), 4.69-4.63 (1H, m, H₁₆), 4.45 (1H, dd, *J* = 8.2, 4.5 Hz, H₁₁), 4.32 (1H, dd, *J* = 10.1, 8.2 Hz, H_{17a}), 4.29-4.26 (1H, m, H₂₂), 3.95 (2H, br d, *J* = 6.6 Hz, H₇), 3.91 (1H, t, *J* = 7.9 Hz, H_{17b}), 3.69 (1H, ddd, *J* = 9.3, 5.1, 2.5 Hz, H₂₀), 3.35 (3H, s, OMe), 2.95-2.88 (1H, m, H₁₉), 2.67-2.59 (1H, m, H₁₀), 1.72 (3H, d, *J* = 1.1 Hz, Me₈), 1.54-1.45 (2H, m, H₂₁), 1.15 (3H, d, *J* = 7.1 Hz, Me₁₉), 0.94 (9H, t, *J* = 8.0 Hz, Si(CH₂CH₃)₃), 0.93 (3H, d, *J* = 6.3 Hz, Me₁₀), 0.89 (9H, s, Si*t*BuMe₂), 0.56 (6H, q, *J* = 8.0 Hz, Si(CH₂CH₃)₃), 0.06 (3H, s, Si*t*BuMe₂), 0.00 (3H, s, Si*t*BuMe₂). Data in agreement with that reported by Li.³⁸

(2*R*,3*S*,4*S*,5*Z*,7*E*,9*E*,11*R*,13*R*,14*R*)-11-((*tert*-butyldimethylsilyl)oxy)-2-((4*S*,6*R*)-2,2-di-*tert*-butyl-6-methyl-1,3,2-dioxasilinan-4-yl)-14-((*R*)-4-((1*E*,3*Z*,5*S*,6*R*,7*E*)-9-hydroxy-6,8-dimethyl-5-(triethylsilyl)nona-1,3,7-trien-1-yl)-4,5-dihydrooxazol-2-yl)-13-methoxy-4-methylpentadeca-5,7,9-trien-3-yl 2-(bis(2,2,2-trifluoroethoxy)phosphoryl)acetate (229**)**



To a solution of Pd(PPh₃)₄ (10.5 mg, 9.05 μmol), CuTC (17.2 mg, 90.5 μmol) and [Ph₂PO₂][NBu₄]

(100 mg, 218 μmol) in DMF (3.0 mL) at 0 °C was added a solution of vinyl bromide **115** (31.0 mg, 42.5 μmol) and stannane **217** (71.6 mg, 90.5 μmol) in DMF (3.0 mL). After stirring for 2 hours in the dark, the reaction was quenched with water (5 mL) and extracted with Et₂O (2 \times 5 mL) and EtOAc (2 \times 5 mL). The extracts were dried (Na₂SO₄) and concentrated *in vacuo*. Purification by flash chromatography (EtOAc/PE 1:4) gave phosphonate **229** (47.5 mg, 37.3 μmol , 88%) as a yellow oil.

One Pot Procedure

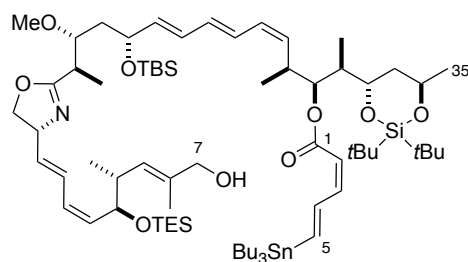
To a solution of Pd(PPh₃)₄ (9.9 mg, 8.57 μmol), CuTC (13.7 mg, 71.8 μmol) and [Ph₂PO₂][NBu₄] (33.0 mg, 71.8 μmol) in DMF (1.0 mL) at 0 °C as added a solution of *bis*-halide **81** (20.0 mg, 34.2 μmol) and stannane **102** (19.1 mg, 34.2 μmol) in DMF (1.0 mL). After stirring at 0 °C in the dark for 2 hours in the dark, a solution of stannane **217** (43.4 mg, 54.8 μmol) in DMF (1.0 mL) was added. The reaction was stirred for another 2 hours before being quenched with water (3 mL) and extracted with Et₂O (2 \times 2 mL) and EtOAc (2 \times 2 mL). The extracts were dried (Na₂SO₄) and concentrated *in vacuo*. Purification by flash chromatography (EtOAc/PE 1:2) gave triene **229** (35.0 mg, 27.5 μmol , 80%) as a yellow oil.

R_f 0.4 (EtOAc/PE 4:6); $[\alpha]_D^{20}$ +4.50 (*c* 1.0, CHCl₃); **IR** ν_{max} 2930, 1738, 1664, 1462, 1262, 1173, 1072, 964, 838, 805, 777, 744; **¹H NMR** (500 MHz, CDCl₃) δ_{H} 6.41-6.31 (2H, m, H₁₄+H₂₆), 6.23-6.13 (2H, m, H₂₄+H₂₅), 6.03 (1H, *app* t, *J* = 11.0 Hz, H₂₇), 5.98 (1H, *app* t, *J* = 11.2 Hz, H₁₃), 5.67 (1H, dd, *J* = 14.0, 7.4 Hz, H₂₃), 5.64 (1H, dd, *J* = 15.3, 5.4, H₁₅), 5.42-5.36 (2H, m, H₁₂+H₃₀), 5.31 (1H, *app* t, *J* = 10.3 Hz, H₂₈), 5.06 (1H, d, *J* = 10.0, H₉), 4.69-4.62 (1H, m, H₁₆), 4.51-4.29 (8H, m, H₁₁+H_{17a}+H₂₂+H₃₄+(OCH₂CF₃)₂), 3.95 (2H, s, H₇), 3.91 (1H, *app* t, *J* = 7.9 Hz, H_{17b}), 3.86 (1H, ddd, *J* = 8.8, 8.8, 2.8, H₃₂), 3.76-3.68 (2H, m, H₂₀+OH), 3.36 (3H, s, OMe), 3.05 (2H, d, *J* = 20.6 Hz, H₂), 2.99-2.87 (2H, m, H₁₉+H₂₉), 2.67-2.59 (1H, m, H₁₀), 1.90-1.80 (2H, m, H₃₁+H_{33a}), 1.72 (3H, s, Me₈), 1.66-1.60 (1H, m, H_{33b}), 1.54-1.49 (2H, m, H₂₁), 1.29 (3H, d, *J* = 6.5 Hz, H₃₅), 1.15 (3H, d, *J* = 6.8 Hz, Me₁₉), 1.02-0.85 (45H, m, Me₁₀+Me₂₉+Me₃₁+Si(*t*Bu)₂+Si(*t*Bu)Me₂+Si(CH₂CH₃)₃), 0.56 (6H, q, *J* = 7.9 Hz, Si(CH₂CH₃)₃), 0.06 (3H, s, Si(*t*Bu)Me₂), 0.00 (3H, s, Si(*t*Bu)Me₂); **¹³C NMR** (125 MHz, CDCl₃) 170.5, 164.1 (d, *J* = 3.8 Hz), 138.2, 135.7, 133.8, 133.7, 133.3, 132.8, 129.3, 129.3, 128.9, 127.2, 27.2, 126.9, 122.5 (dq, *J* = 277, 8.6 Hz), 122.5 (dq, *J* = 278, 8.3 Hz), 78.1, 78.1, 72.7, 71.7, 70.0, 69.6, 69.1, 67.3, 66.0, 62.5 (m), 57.1, 40.9, 40.1, 37.7, 35.7, 35.0, 33.8 (d, *J* = 145 Hz), 27.4,

27.1, 25.9, 23.6, 21.1, 20.7, 18.1, 17.5, 14.3, 13.9, 11.2, 9.5, 6.9, 4.9, -3.8, -4.9; ^{19}F NMR (470 MHz, CDCl_3) δ_{F} -75.42 (3F, t, J = 8.0 Hz), -75.48 (3F, t, J = 8.0 Hz); ^{31}P NMR (202 MHz, CDCl_3) δ_{P} 23.81; HRMS ESI calc. for $\text{C}_{61}\text{H}_{107}\text{F}_6\text{NO}_{12}\text{PSi}_3$ $[\text{M}+\text{H}]^+$ 1274.6737, found 1274.6739.

e. Endgame

(2*R*,3*S*,4*S*,5*Z*,7*E*,9*E*,11*R*,13*R*,14*R*)-11-((*tert*-butyldimethylsilyl)oxy)-2-((4*S*,6*R*)-2,2-di-*tert*-butyl-6-methyl-1,3,2-dioxasilinan-4-yl)-14-((*R*)-4-((1*E*,3*Z*,5*S*,6*R*,7*E*)-9-hydroxy-6,8-dimethyl-5-(triethylsilyl)nona-1,3,7-trien-1-yl)-4,5-dihydrooxazol-2-yl)-13-methoxy-4-methylpentadeca-5,7,9-trien-3-yl (2*Z*,4*E*)-5-(tributylstannyl)penta-2,4-dienoate (232)



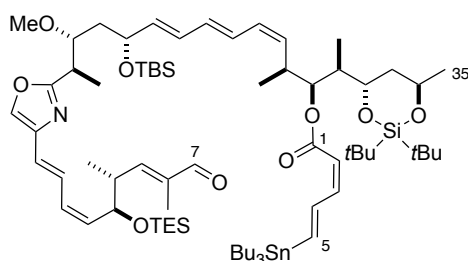
To a solution of phosphonate **229** (20.0 mg, 15.7 μmol) in THF (4.0 mL) at 0 °C was added sodium hydride (6.0 mg, 250 μmol). After 30 min, the reaction mixture was cooled to -78 °C and aldehyde **106** (20.0 mg, 58.8 μmol) in THF (1 mL) was added. After stirring for 48 hours, the reaction mixture was quenched with water (5 mL) and extracted with EtOAc (3 \times 10 mL). The organic layers were dried (Na_2SO_4) and concentrated *in vacuo*. Purification by flash chromatography ($\text{Et}_2\text{O}/\text{PE}$ 1:9) gave stannane **232** and **233** (17.1 mg, 12.6 μmol , 80%) as a colourless oil as a 2.5:1 mixture of *Z/E* isomers.

R_f 0.8 (EtOAc/PE 4:6); $[\alpha]_D^{20}$ +9.97 (c 1.1, CHCl_3); IR ν_{max} 2929, 1716, 1663, 1619, 1461, 1376, 1250, 1191, 1143, 1088, 1007, 837, 806, 776; ^1H NMR (500 MHz, CDCl_3) δ_{H} 7.79 (0.66H, ddd, J = 18.8, 10.6, 1.0 Hz, H_4), 7.14 (0.33H, dd, J = 15.3, 10.3 Hz, H_3^*), 6.79 (0.33H, d, J = 18.7 Hz, H_5^*), 6.69 (0.66H, d, J = 18.7 Hz, H_5), 6.63 (0.33H, dd, J = 18.5, 10.3 Hz, H_4^*), 6.45-6.33 (2.66H, m, $\text{H}_3+\text{H}_{14}+\text{H}_{26}$), 6.20-6.08 (2H, m, $\text{H}_{24}+\text{H}_{25}$), 6.05-5.94 (2H, m, $\text{H}_{13}+\text{H}_{27}$), 5.79 (0.33H, d, J = 15.4 Hz,

H₂*), 5.67-5.59 (2H, m, H₁₅+H₂₃), 5.51 (0.66H, d, *J* = 11.4 Hz, H₂), 5.46 (0.33H, *app* t, *J* = 10.5 Hz, H₂₈*), 5.42 (0.66H, dd, *J* = 10.5 Hz, H₂₈), 5.39 (1H, dd, *J* = 11.1, 8.5 Hz, H₁₂), 5.29-5.24 (1H, m, H₃₀), 5.06 (1H, dd, *J* = 10.0, 1.1 Hz, H₉), 4.66 (1H, m, H₁₆), 4.45 (1H, ddd, *J* = 8.3, 4.4, 1.1 Hz, H₁₁), 4.39 (1H, ddq, *J* = 6.4, 6.4, 2.3 Hz, H₃₄), 4.35-4.29 (1H, m, H₂₂), 4.32 (1H, dd, *J* = 10.2, 8.4 Hz, H_{17a}), 4.00-3.90 (1H, m, H₃₂), 3.95 (2H, s, H₇), 3.91 (1H, *app* t, *J* = 7.8 Hz, H_{17b}), 3.79-3.67 (2H, m, H₂₀+OH), 3.36 (3H, s, OMe), 2.98-2.90 (1H, m, H₂₉), 2.90 (1H, dq, *J* = 6.9, 5.5 Hz, H₁₉), 2.63 (1H, ddq, *J* = 9.6, 6.8, 3.8 Hz, H₁₀), 1.96-1.83 (2H, m, H₃₁+H_{33a}), 1.72 (3H, d, *J* = 1.1 Hz, Me₈), 1.56-1.46 (9H, m, H₂₁+H_{33b}+SnBu₃), 1.36-1.23 (9H, m, H₃₅+ SnBu₃), 1.15 (3H, d, *J* = 7.1 Hz, Me₁₉), 1.02-0.86 (60H, m, Me₁₀+Me₂₉+Me₃₁+ SnBu₃+Si(*t*Bu)₂+Si(*t*Bu)Me₂+Si(CH₂CH₃)₃), 0.56 (6H, q, *J* = 7.9 Hz, Si(CH₂CH₃)₃), 0.07 (3H, s, Si(*t*Bu)Me₂), 0.01 (3H, s, Si(*t*Bu)Me₂); ¹³C NMR (125 MHz, CDCl₃) 178.6, 167.0*, 165.5, 147.3, 146.8*, 146.4, 146.2*, 144.4*, 142.8, 137.2*, 137.4, 135.7, 134.0, 133. 132.8, 132.7, 129.8, 129.0, 128.9, 127.8, 127.6*, 127.2, 126.9, 120.2*, 116.2, 78.2, 76.0, 75.4, 72.7, 71.7, 70.2, 69.6*, 69.4, 69.1, 67.6, 66.0, 57.2, 41.6*, 41.4, 40.1, 40.1, 37.3, 35.8, 35.5*, 35.2, 29.1, 29.0*, 27.4, 27.3, 27.1, 25.9, 23.6, 21.3, 20.7, 18.1, 18.0*, 17.8, 14.3, 14.1, 13.9, 13.7, 11.4, 9.7, 9.6*, 6.9, 4.9, -3.6, -4.8; HRMS ESI calc. for C₇₂H₁₃₂NO₉Si₃¹¹²Sn [M+H]⁺ 1350.8253, found 1350.8276.

*Identifiable resonances for the minor *2E*-isomer.

(2*R*,3*S*,4*S*,5*Z*,7*E*,9*E*,11*R*,13*R*,14*R*)-11-((*tert*-butyldimethylsilyl)oxy)-2-((4*S*,6*R*)-2,2-di-*tert*-butyl-6-methyl-1,3,2-dioxasilinan-4-yl)-14-(4-((1*E*,3*Z*,5*S*,6*R*,7*E*)-6,8-dimethyl-9-oxo-5-(triethylsilyl)nona-1,3,7-trien-1-yl)oxazol-2-yl)-13-methoxy-4-methylpentadeca-5,7,9-trien-3-yl (2*Z*,4*E*)-5-(tributylstannyl)penta-2,4-dienoate (234)

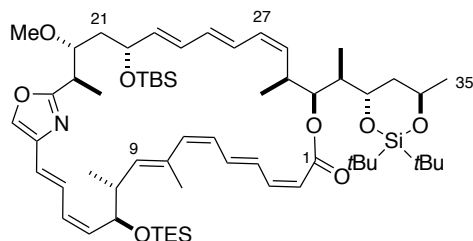


Oxazolines **232** and **233** (8.0 mg, 5.9 μmol) was dissolved in benzene (1.0 mL). Activated manganese dioxide (5 x 30 mg portions) was added every 30 min until the reaction was judged to be

complete by TLC analysis (2.5 h total). The reaction mixture was filtered through a short pad of Celite® and concentrated *in vacuo*. Purification by preparative thin layer chromatography (EtOAc/PE 1:10) afforded the pure *Z*-isomer **234** (1.6 mg, 1.2 μmol, 20%) along with a 1:1 mixture of *E* and *Z* isomers (1.0 mg, 0.75 μmol, 13%).

R_f 0.70 (EtOAc/PE 1:4); $[\alpha]_D^{20} +5.90$ (*c* 0.16, CHCl₃); **IR** ν_{max} 2927, 1716, 1691, 1457, 1377, 1246, 1093, 1038, 1006, 826, 742; **¹H NMR** (500 MHz, CDCl₃) δ_{H} 9.42 (1H, s, H₇), 7.81 (1H, dd, *J* = 18.8, 10.6 Hz, H₄), 7.52 (1H, s, H₁₇), 7.12 (1H, dd, *J* = 15.0, 11.8 Hz, H₁₄), 6.71 (1H, d, *J* = 19.0 Hz, H₅), 6.51 (1H, d, *J* = 10.0 Hz, H₉), 6.47-6.38 (2H, m, H₃+H₂₆), 6.38 (1H, d, *J* = 15.2 Hz, H₁₅), 6.21-6.09 (3H, m, H₁₃+H₂₄+H₂₅), 6.01 (1H, *app t*, *J* = 11.1 Hz, H₂₇), 5.61 (1H, dd, *J* = 14.3, 7.4 Hz, H₂₃), 5.52 (1H, d, *J* = 11.5 Hz, H₂), 5.48-5.38 (2H, m, H₁₂+H₂₈), 5.29 (1H, dd, *J* = 7.1, 4.1 Hz, H₃₀), 4.66 (1H, dd, *J* = 8.9, 4.5 Hz, H₁₁), 4.41 (1H, ddq, *J* = 6.6, 6.6, 1.5 Hz, H₃₄), 4.33 (1H, ddd, *J* = 9.5, 9.5, 2.5 Hz, H₂₂), 3.97 (1H, ddd, *J* = 8.2, 8.2, 1.5 Hz, H₃₂), 3.86-3.76 (1H, m, H₂₀), 3.42-3.35 (1H, m, H₁₉), 3.40 (3H, s, OMe), 2.94 (1H, dd, *J* = 9.8, 6.8 Hz, H₂₉), 2.89-2.80 (1H, m, H₁₀), 1.97-1.84 (2H, m, H₃₁+H_{33a}), 1.76 (3H, s, Me₈), 1.57-1.48 (9H, m, H₂₁+H_{33b}+SnBu₃), 1.376-1.28 (12H, m, H₃₅+Me₁₀+SnBu₃), 1.10 (3H, d, *J* = 7.1 Hz, Me₁₉), 1.04-0.86 (57H, m, Me₂₉+Me₃₁+SnBu₃+Si(*t*Bu)₂+Si(BuMe₂+Si(CH₂CH₃)₃), 0.59 (6H, q, *J* = 8.0 Hz, Si(CH₂CH₃)₃), 0.08 (3H, s, Si(*t*Bu)Me₂), 0.02 (3H, s, Si(*t*Bu)Me₂); **¹³C NMR** (125 MHz, CDCl₃) 195.6, 166.0, 165.5, 156.8, 147.4, 146.4, 142.8, 139.3, 138.7, 137.3, 135.4, 134.1, 133.8, 132.6, 129.8, 129.1, 128.9, 127.9, 124.9, 122.5, 116.2, 79.1, 75.3, 71.8, 70.3, 69.4, 67.6, 57.4, 41.4, 41.1, 40.2, 37.3, 36.0, 35.2, 29.1, 27.4, 27.3, 27.1, 25.9, 23.5, 21.3, 20.7, 18.1, 17.8, 16.1, 13.7, 11.5, 9.8, 9.7, 9.5, 6.8, 5.0, -3.7, -4.8; **HRMS** ESI calc. for C₇₂H₁₂₈NO₉Si¹²²Sn [M+H]⁺ 1346.7940 found 1346.7935.

(1²Z,2*R*,3*R*,5*R*,6*E*,8*E*,10*Z*,12*S*,13*S*,16*Z*,18*E*,20*Z*,22*E*,24*R*,25*S*,26*Z*,28*E*)-5-((*tert*-butyldimethylsilyl)oxy)-13-((*R*)-1-((4*S*,6*R*)-2,2-di-*tert*-butyl-6-methyl-1,3,2-dioxasilinan-4-yl)ethyl)-3-methoxy-2,12,22,24-tetramethyl-25-((triethylsilyl)oxy)-14-oxa-1(2,4)-oxazolacyclononacosaphane-6,8,10,16,18,20,22,26,28-nonaen-15-one (**231**)



To a suspension of $(\text{PPh}_3\text{CH}_2\text{I})^+\text{I}^-$ (100.0 mg, 189 μmol) in THF (3.0 mL) was added NaHMDS (0.63 M in THF, 300 μL , 189 μmol) to form a clear, orange solution. 300 μL of the solution was transferred to a dry flask and cooled to -78°C , to which a solution of aldehyde **234** (2.0 mg, 1.5 μmol) in THF (300+100 μL) was added *via* cannula. The reaction was stirred at -78°C for 1 h before being diluted with hexane (1 mL) and warmed to rt. The reaction mixture was filtered through a short plug of silica gel and concentrated *in vacuo* to yield vinyl iodide **230** which was used directly without further purification.

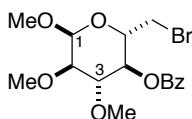
To a solution of $\text{Pd}(\text{PPh}_3)_4$ (5.0 mg, 4.2 μmol), CuTC (7.0 mg, 36.7 μmol) and $[\text{Ph}_2\text{PO}_2][\text{NBu}_4]$ (40.0 mg, 87.0 μmol) in DMF (0.5 mL) at 0°C was added a solution of the crude vinyl iodide **230** in DMF (1.5 mL). The reaction mixture stirred for 30 min before being filtered through a plug of silica, concentrated *in vacuo*. Purification by flash chromatography (EtOAc/PE 1:10) yielded macrocycle **231** (0.19 mg, 0.18 μmol , 12%) as a colourless oil.

R_f 0.46 (EtOAc/PE 1:9); ¹H NMR (500 MHz, CDCl₃) δ 7.72 (1H, dd, $J = 13.5, 7.8$ Hz, H₁₇), 7.09 (1H, dd, $J = 15.0, 11.7$ Hz, H₁₄), 6.86 (1H, dd, $J = 15.0, 11.3$ Hz, H₄), 6.76 (1H, dd, $J = 15.0, 10.6$ Hz, H₅), 6.43-6.35 (1H, m, H₂₆), 6.37 (1H, *app* t, $J = 11.5$ Hz, H₃), 6.28-6.20 (2H, m, H₁₅+H₂₄), 6.13 (1H, dd, $J = 14.5, 10.7$ Hz, H₂₅), 6.06 (1H, *app* t, $J = 11.5$ Hz, H₁₃), 5.92 (1H, *app* t, $J = 11.2$ Hz, H₂₇), 5.82 (1H, *app* t, $J = 11.0$ Hz, H₆), 5.77 (1H, d, $J = 11.3$ Hz, H₇), 5.71 (1H, dd, $J = 14.7, 3.8$ Hz, H₂₃), 5.50-5.44 (3H, m, H₁₂+H₂+H₃₀), 5.29 (1H, *app* t, $J = 10.7$ Hz, H₂₈), 4.95 (1H, br d, $J = 8.8$ Hz, H₉), 4.80-4.75 (1H, m, H₁₁), 4.42-4.37 (1H, m, H₂₂), 4.37-4.34 (1H, m, H₃₄), 3.90 (1H, dd, $J = 10.3, 3.6$

Hz, H₂₀), 3.87-3.82 (1H, m, H₃₂), 3.49-3.46 (1H, m, H₁₉), 3.46 (3H, s, OMe), 3.06-3.00 (1H, m, H₂₉), 2.83-2.77 (1H, m, H₁₀), 1.92 (3H, s, Me₈), 1.87-1.81 (1H, m, H₃₁), 1.65-1.57 (2H, m, H_{33a}+H_{21a}), 1.35-1.18 (7H, m, Me₁₉+H_{33b}+H₃₅), 1.04-0.81 (46H, Me₁₀+Me₂₉+Me₃₁+H_{21b}+Si(*t*Bu)₂+Si(*t*Bu)Me₂+Si(CH₂CH₃)₃), 0.59 (6H, q, *J* = 8.0 Hz, Si(CH₂CH₃)₃), 0.09 (3H, s, Si(*t*Bu)Me₂), 0.02 (3H, s, Si(*t*Bu)Me₂). Data in agreement with that reported by Williams.⁸⁶

f. **Sugar**

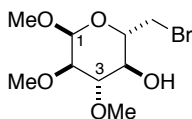
(2*S*,3*S*,4*S*,5*R*,6*S*)-2-(bromomethyl)-4,5,6-trimethoxytetrahydro-2*H*-pyran-3-yl benzoate (246**)**



To a solution of 1,2,3-trimethoxy sugar **245** (2.0 g, 6.44 mmol) in benzene (60 mL) was added NBS (1.15 g, 6.44 mmol) and AIBN (105.8 mg, 0.644 mmol). The reaction mixture was stirred at 60 °C for 1 h, before being quenched by NaHCO₃ (30 mL) and extracted with EtOAc (3 x 20 mL). The combined organic extracts were dried (Na₂SO₄) and concentrated *in vacuo*. Purification by flash chromatography (EtOAc/PE 1:4) yielded 4-benzoyl-6-bromo sugar **246** (1.75 g, 4.51 mmol, 70%) as a yellow oil.

R_f 0.40 (EtOAc/PE 1:1); **¹H NMR** (500 MHz, CDCl₃) δ_H 8.07 (2H, dd, *J* = 8.0, 1.3 Hz, ArH), 7.61 (1H, *app* t, *J* = 7.4 Hz, ArH), 7.48 (2H, *app* t, *J* = 7.8 Hz, ArH), 5.07 (1H, *app* t, *J* = 9.6 Hz, H₄), 4.93 (1H, d, *J* = 3.6 Hz, H₁), 4.02 (1H, ddd, *J* = 10.4, 8.3, 2.3 Hz, H₅), 3.74 (1H, t, *J* = 9.4 Hz, H₃), 3.56 (3H, s, OMe), 3.54 (3H, s, OMe), 3.50-3.46 (1H, m, H_{6a}), 3.48 (3H, s, OMe), 3.40 (1H, dd, *J* = 11.2, 8.2 Hz, H_{6b}), 3.38 (1H, dd, *J* = 9.6, 3.6 Hz, H₂). Data in agreement with literature values.¹⁰²

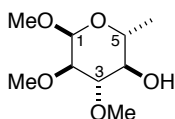
(2*S*,3*S*,4*S*,5*R*,6*S*)-2-(bromomethyl)-4,5,6-trimethoxytetrahydro-2*H*-pyran-3-ol (247**)**



To a solution of 4-benzoyl-6-bromo sugar **246** (886 mg, 2.28 mmol) in methanol (50 mL) was added NaOMe (6.2 mg, 0.114 mmol). The reaction mixture was stirred at 65 °C for 16 h, before being quenched by NH₄Cl (10 mL) and extracted with CH₂Cl₂ (3 x 20 mL). The combined organic extracts were dried (Na₂SO₄) and concentrated *in vacuo*. Purification by flash chromatography (EtOAc/PE 1:1) yielded 6-bromo-4-hydroxy sugar **247** (579 mg, 2.03 mmol, 89%) as a yellow oil.

R_f 0.22 (EtOAc/PE 1:1); **¹H NMR** (500 MHz, CDCl₃) δ_H 4.89 (1H, d, *J* = 3.6 Hz, H₁), 3.79-3.71 (2H, m, H₅+H_{6a}), 3.64 (3H, s, OMe), 3.57 (1H, dd, *J* = 11.1, 6.3 Hz, H_{6b}), 3.50 (3H, s, OMe), 3.47 (3H, s, OMe), 3.47 (1H, *app t*, *J* = 8.9 Hz, H₃), 3.42 (1H, dt, *J* = 8.9, 2.7 Hz, H₄), 3.26 (1H, dd, *J* = 9.3, 3.6 Hz, H₂), 2.44 (1H, d, *J* = 2.6 Hz, OH). Data in agreement with literature values.⁸⁹

(2*R*,3*R*,4*S*,5*R*,6*S*)-4,5,6-trimethoxy-2-methyltetrahydro-2*H*-pyran-3-ol (248**)**

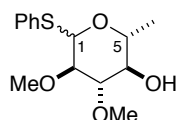


To a solution of 6-bromo-4-hydroxy sugar **247** (486 mg, 1.71 mmol) in DMSO (5 mL) was added NaBH₄ (323 mg, 8.55 mmol). The reaction mixture was stirred at 80 °C for 3 h, before being quenched by water (5 mL) and extracted with Et₂O (3 x 5 mL). The combined organic extracts were washed with brine (10 mL), dried (Na₂SO₄) and concentrated *in vacuo*. Purification by flash chromatography (EtOAc/PE 1:1) yielded 4-hydroxy-6-methyl sugar **248** (282 mg, 1.37 mmol, 80%) as a colourless oil.

R_f 0.13 (EtOAc/PE 1:1); **¹H NMR** (500 MHz, CDCl₃) δ_H 4.78 (1H, d, *J* = 3.6 Hz, H₁), 3.66 (1H, dq, *J* = 9.5, 6.2 Hz, H₅), 3.62 (3H, s, OMe), 3.58 (3H, s, OMe), 3.41 (3H, s, OMe), 3.40 (1H, *app t*, *J* =

9.2 Hz, H₃), 3.22 (1H, dd, $J = 9.6, 3.6$ Hz, H₂), 3.12 (1H, dt, $J = 9.2, 2.4$ Hz, H₄), 2.49 (1H, d, $J = 2.5$ Hz, OH), 1.27 (3H, d, $J = 6.3$ Hz, H₆). Data in agreement with literature values.¹⁰³

(2*R*,3*R*,4*S*,5*R*)-4,5-dimethoxy-2-methyl-6-(phenylthio)tetrahydro-2*H*-pyran-3-ol (249)

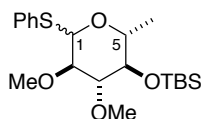


To a solution of 4-hydroxy-6-methyl sugar **248** (181 mg, 0.878 mmol) in DCE (8 mL) was added ZnI₂ (841 mg, 2.63 mmol), Bu₄NI (486 mg, 1.32 mmol) and TMSSPh (0.830 mL, 4.39 mmol). The reaction mixture was stirred at 65 °C for 2 h, before being cooled to rt and filtered through a pad of Celite®. The filtrate was dried (Na₂SO₄) and concentrated *in vacuo*. Purification by flash chromatography (EtOAc/PE 1:4) yielded thioglycoside **249** (197 mg, 0.693 mmol, 80%, $\alpha:\beta = 3:1$) as a colourless oil.

α -anomer: **R_f** 0.50 (EtOAc/PE 1:1); **¹H NMR** (500 MHz, CDCl₃) δ_{H} 7.55-7.50 (2H, m, ArH), 7.36-7.25 (3H, m, ArH), 5.69 (1H, d, $J = 5.3$ Hz, H₁), 4.24 (1H, dq, $J = 9.4, 6.2$ Hz, H₅), 3.68 (3H, s, OMe), 3.59 (1H, dd, $J = 9.5, 5.3$ Hz, H₂), 3.52 (3H, s, OMe), 3.35 (1H, *app t*, $J = 9.4$ Hz, H₃), 3.21 (1H, *app t*, $J = 9.3$ Hz, H₄), 2.43 (1H, d, $J = 2.6$ Hz, OH), 1.31 (3H, d, $J = 6.3$ Hz, H₆).

β : **R_f** 0.50 (EtOAc/PE 1:1); **¹H NMR** (500 MHz, CDCl₃) δ_{H} 7.57-7.52 (2H, m, ArH), 7.36-7.25 (3H, m, ArH), 4.57 (1H, d, $J = 9.3$ Hz, H₁), 3.68 (3H, s, OMe), 3.63 (3H, s, OMe), 3.41-3.33 (1H, m, H₅), 3.21 (1H, *app t*, $J = 9.0$ Hz, H₄), 3.15 (1H, *app t*, $J = 8.4$ Hz, H₃), 3.11 (1H, *app t*, $J = 8.4$ Hz, H₂), 2.35 (1H, d, $J = 2.4$ Hz, OH), 1.37 (3H, d, $J = 6.1$ Hz, H₆). Data in agreement with that reported by Elliott.⁸⁷

***tert*-butyl(((2*R*,3*R*,4*R*,5*R*)-4,5-dimethoxy-2-methyl-6-(phenylthio)tetrahydro-2*H*-pyran-3-yl)oxy)
dimethylsilane (250,251)**

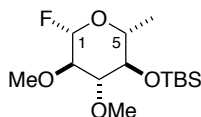


To a solution of thioglycoside **249** (187 mg, 0.658 mmol, $\alpha:\beta = 3:1$) in CH_2Cl_2 (10 mL) was added TBSCl (992 mg, 6.58 mmol), imidazole (896 mg, 13.2 mmol) and DMAP (161 mg, 1.32 mmol). The reaction mixture was stirred for 16 h, before being quenched with NH_4Cl (10 mL) and extracted with Et_2O (3 x 10 mL). The combined organic extracts were dried (Na_2SO_4) and concentrated *in vacuo*. Purification by flash chromatography ($\text{Et}_2\text{O}/\text{PE}$ 1:19) yielded α -TBS ether **250** (167 mg, 0.419 mmol, 64%) and β -TBS ether **251** (55.8 mg, 0.140 mmol, 21%) as colourless oil.

α -anomer: **R_f** 0.29 ($\text{Et}_2\text{O}/\text{PE}$ 1:9); $[\alpha]_D^{20} +174.4$ (c 1.0, CHCl_3); **IR** ν_{max} 3670, 2980, 2908, 1407, 1395, 1379, 1250, 1240, 1230, 1101, 1076, 1068, 1054, 893; **¹H NMR** (500 MHz, CDCl_3) δ_{H} 7.52-7.48 (2H, m, ArH), 7.33-7.22 (3H, m, ArH), 5.65 (1H, d, $J = 5.5$ Hz, H_1), 4.14 (1H, dq, $J = 8.8, 6.2$ Hz, H_5), 3.57 (3H, s, OMe), 3.53 (1H, dd, $J = 9.3, 5.5$ Hz, H_2), 3.50 (3H, s, OMe), 3.22 (1H, *app* t, $J = 8.8$ Hz, H_3), 3.17 (1H, *app* t, $J = 8.6$ Hz, H_4), 1.22 (3H, d, $J = 6.3$ Hz, H_6), 0.91 (9H, s, $\text{SiC}(\text{CH}_3)_3$), 0.13 (3H, s, SiCH_3), 0.08 (3H, s, SiCH_3); **¹³C NMR** (125 MHz, CDCl_3) 134.5, 131.1, 128.6, 126.7, 86.0, 83.4, 82.4, 75.9, 68.7, 61.0, 57.4, 25.6, 17.8, 17.7, -4.2, -5.0; **HRMS** ESI calc. for $\text{C}_{20}\text{H}_{38}\text{NO}_4\text{SSi}$ $[\text{M}+\text{NH}_4]^+$ 416.2291, found 416.2290.

β -anomer: **R_f** 0.29 ($\text{Et}_2\text{O}/\text{PE}$ 1:9); $[\alpha]_D^{20} -30.0$ (c 1.0, CHCl_3); **IR** ν_{max} 3672, 2952, 2930, 2892, 2858, 1473, 1382, 1250, 1169, 1145, 1097, 1072, 964, 860, 836, 777, 744, 691; **¹H NMR** (500 MHz, CDCl_3) δ_{H} 7.53-7.48 (2H, m, ArH), 7.31-7.21 (3H, m, ArH), 4.52 (1H, d, $J = 9.1$ Hz, H_1), 3.60 (3H, s, OMe), 3.56 (3H, s, OMe), 3.31-3.23 (1H, m, H_5), 3.16 (1H, *app* t, $J = 8.8$ Hz, H_4), 3.09-3.01 (2H, m, H_3+H_2), 1.26 (3H, d, $J = 6.2$ Hz, H_6), 0.89 (9H, s, $\text{SiC}(\text{CH}_3)_3$), 0.11 (3H, s, SiCH_3), 0.07 (3H, s, SiCH_3); **¹³C NMR** (125 MHz, CDCl_3) 133.7, 131.2, 128.5, 126.9, 88.1, 86.9, 83.3, 76.4, 75.4, 60.9, 60.2, 25.6, 18.2, 17.7, -4.3, -4.9; **HRMS** ESI calc. for $\text{C}_{20}\text{H}_{35}\text{O}_4\text{SSi}$ $[\text{M}+\text{H}]^+$ 399.2020, found 399.2022.

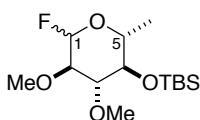
***tert*-butyl(((2*R*,3*R*,4*R*,5*R*,6*S*)-6-fluoro-4,5-dimethoxy-2-methyltetrahydro-2*H*-pyran-3-yl)oxy)dimethylsilane (**252**)**



To a solution of α -thioglycoside **250** (45.0 mg, 0.113 mmol) in CH_2Cl_2 (2 mL) at -15°C was added DAST (22.3 μL , 0.169 mmol). The reaction mixture was stirred for 2 min, before NBS (26.2 mg, 0.147 mmol) was added. The solution was stirred at -15°C for a further 30 min before being quenched with NaHCO_3 (1 mL) and extracted with CH_2Cl_2 (3 x 1 mL). The combined organic extracts were dried (Na_2SO_4) and concentrated *in vacuo*. Purification by flash chromatography ($\text{Et}_2\text{O}/\text{PE}$ 1:19) yielded β -glycosyl fluoride **252** (31.2 mg, 0.101 mmol, 90%) as a colourless oil.

R_f 0.52 ($\text{Et}_2\text{O}/\text{PE}$ 1:9); $[\alpha]_D^{20} +12.3$ (c 1.0, CHCl_3); **IR** ν_{max} 3674, 2984, 2900, 2357, 1389, 1256, 1161, 1105, 1048, 953, 858, 840, 780; **¹H NMR** (500 MHz, CDCl_3) δ_{H} 5.10 (1H, dd, $J = 53.4, 6.9$ Hz, H_1), 3.56 (3H, s, OMe), 3.54 (3H, s, OMe), 3.38 (1H, dq, $J = 9.2, 6.2$ Hz, H_5), 3.23 (1H, *app* t, $J = 9.0$ Hz, H_4), 3.14 (1H, ddd, $J = 12.7, 8.6, 7.0$ Hz, H_2), 3.02 (1H, *app* t, $J = 8.6$ Hz, H_3), 1.29 (3H, d, $J = 6.2$ Hz, H_6), 0.89 (9H, s, $\text{SiC}(\text{CH}_3)_3$), 0.11 (3H, s, SiCH_3), 0.08 (3H, s, SiCH_3); **¹³C NMR** (125 MHz, CDCl_3) 109.7 (d, $J = 214$ Hz), 85.2 (d, $J = 11.5$ Hz), 84.2 (d, $J = 21.0$ Hz), 75.2, 72.5, 60.9, 59.9, 25.9, 18.2, 18.1, -4.0 , -4.6 ; **HRMS** ESI calc. for $\text{C}_{14}\text{H}_{30}\text{FO}_4\text{Si}$ $[\text{M}+\text{H}]^+$ 309.1897, found 309.1898.

***tert*-butyl(((2*R*,3*R*,4*R*,5*R*)-6-fluoro-4,5-dimethoxy-2-methyltetrahydro-2*H*-pyran-3-yl)oxy)dime
thylsilane (**252,253**)**



To a solution of β -thioglycoside **251** (22.0 mg, 55.2 μmol) in CH_2Cl_2 (1 mL) at -15°C was added

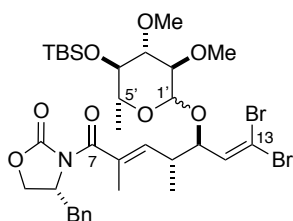
DAST (11.1 μ L, 84.1 μ mol). The reaction mixture was stirred for 2 min, before NBS (13.1 mg, 73.5 μ mol) was added. The solution was stirred at -15°C for a further 30 min before being quenched with NaHCO_3 (1 mL) and extracted with CH_2Cl_2 (3 x 1 mL). The combined organic extracts were dried (Na_2SO_4) and concentrated *in vacuo*. Purification by flash chromatography ($\text{Et}_2\text{O}/\text{PE}$ 1:19) yielded α -glycosyl fluoride **253** (2.3 mg, 7.37 μ mol, 13%) and β -glycosyl fluoride **252** (11.3 mg, 36.8 μ mol, 67%) as colourless oil.

α -anomer: **R_f** 0.50 ($\text{Et}_2\text{O}/\text{PE}$ 1:9); $[\alpha]_D^{20} +38.6$ (*c* 1.0, CHCl_3); **IR** ν_{max} 2929, 1463, 1256, 1160, 1094, 1024, 894, 861, 837, 777, 743; **¹H NMR** (500 MHz, CDCl_3) δ_{H} 5.61 (1H, dd, *J* = 53.7, 2.8 Hz, H₁), 3.81 (1H, dq, *J* = 9.3, 6.2 Hz, H₅), 3.56 (3H, s, OMe), 3.54 (3H, s, OMe), 3.31 (1H, *app* t, *J* = 9.1 Hz, H₄), 3.18 (1H, *app* t, *J* = 9.1 Hz, H₃), 3.17 (1H, ddd, *J* = 25.7, 9.5, 2.7 Hz, H₂), 1.24 (3H, d, *J* = 6.3 Hz, H₆), 0.90 (9H, s, $\text{SiC}(\text{CH}_3)_3$), 0.13 (3H, s, SiCH_3), 0.08 (3H, s, SiCH_3); **¹³C NMR** (125 MHz, CDCl_3) 104.5 (d, *J* = 226 Hz), 82.6 (d, *J* = 10.5 Hz), 82.5 (d, *J* = 14.5 Hz), 75.5, 70.6, 61.3, 58.8, 25.9, 18.2, 18.1, -3.9 , -4.6 ; **HRMS** ESI calc. for $\text{C}_{14}\text{H}_{30}^{19}\text{FO}_4\text{Si}$ [$\text{M}+\text{H}$]⁺ 309.1897, found 309.1897.

β -anomer: **R_f** 0.52 ($\text{Et}_2\text{O}/\text{PE}$ 1:9); **¹H NMR** (500 MHz, CDCl_3) δ_{H} 5.11 (1H, dd, *J* = 53.1, 6.8 Hz, H₁), 3.57 (3H, s, OMe), 3.55 (3H, s, OMe), 3.38 (1H, dq, *J* = 9.3, 6.2 Hz, H₅), 3.23 (1H, *app* t, *J* = 9.0 Hz, H₄), 3.14 (1H, ddd, *J* = 12.7, 8.5, 7.0 Hz, H₂), 3.01 (1H, *app* t, *J* = 8.6 Hz, H₃), 1.29 (3H, d, *J* = 6.1 Hz, H₆), 0.89 (9H, s, $\text{SiC}(\text{CH}_3)_3$), 0.11 (3H, s, SiCH_3), 0.08 (3H, s, SiCH_3).

g. Glycosylation

(4*R*)-4-benzyl-3-((4*R*,5*R*,*E*)-7,7-dibromo-5-(((3*R*,4*R*,5*R*,6*R*)-5-((*tert*-butyldimethylsilyl)oxy)-3,4-dimethoxy-6-methyltetrahydro-2*H*-pyran-2-yl)oxy)-2,4-dimethylhepta-2,6-dienoyl)oxazolidin-2-one (240,258)



With β -glycosyl fluoride **252**

To SnCl₂ (21.5 mg, 114 μ mol), AgClO₄ (23.5 mg, 114 μ mol) and 4Å molecular sieves (10 mg) in Et₂O (0.5 mL) at –15 °C was added a solution of alcohol **226** (11.1 mg, 22.7 μ mol) in Et₂O (0.2 mL). The reaction mixture was stirred for 2 min, before a solution of β -glycosyl fluoride **252** (14.0 mg, 45.4 μ mol) in Et₂O (0.2 mL) was added. The solution was stirred at –15 °C for 2 h before being warmed to rt and stirred for a further 16 h. The reaction mixture was diluted with Et₂O (2 mL) and filtered through a pad of Celite®. The filtrate was washed consecutively with NaHCO₃ (1 mL) and brine (1 mL), dried (Na₂SO₄) and concentrated *in vacuo*. Purification by flash chromatography (EtOAc/PE 1:4) yielded glycosylation adduct **258** and **240** (10.5 mg, 13.6 μ mol, 60%, α : β = 1:1.1) as a colourless oil.

With α -thioglycoside **250**

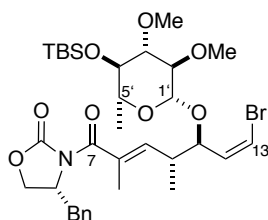
To α -thioglycoside **250** (200 mg, 0.502 mmol), alcohol **226** (163 mg, 0.334 mmol) and 4Å molecular sieves (200 mg) in CH₃CN (20 mL) at –20 °C was added *N*-bromosuccinimide (179 mg, 1.00 mmol). The reaction mixture was stirred at –20 °C for 2 h before being quenched with NaHSO₃ (20 mL) and extracted with EtOAc (3 x 10 mL). The combined organic extracts were dried (Na₂SO₄) and concentrated *in vacuo*. Purification by flash chromatography (EtOAc/PE 1:4) yielded glycosylation adduct **258** and **240** (256 mg, 0.332 mmol, 99%, α : β = 1:1.3) as a colourless oil.

α -diastereomer: **R_f** 0.70 (EtOAc/PE 3:7); **¹H NMR** (500 MHz, CDCl₃) δ _H 7.36-7.31 (2H, m, ArH), 7.30-7.27 (1H, m, ArH), 7.23-7.19 (2H, m, ArH), 6.55 (1H, d, *J* = 9.0 Hz, H₁₂), 5.94-5.90 (1H, m, H₉), 4.87 (1H, d, *J* = 3.4 Hz, H_{1'}), 4.64-4.58 (1H, m, NCH), 4.30 (1H, dd, *J* = 9.0, 5.9 Hz, H₁₁), 4.26-4.21 (1H, OCH_{2a}CH), 4.15 (1H, dd, *J* = 8.9, 4.6 Hz, OCH_{2b}CH), 3.69 (1H, dd, *J* = 9.3, 6.3 Hz, H_{5'}), 3.53 (3H, s, OMe), 3.42 (3H, s, OMe), 3.37 (1H, dd, *J* = 13.4, 3.2 Hz, PhCH_{2a}), 3.20 (2H, m, H_{2'+H3'}), 3.10 (1H, m, H_{4'}), 2.85 (1H, m, H₁₀), 2.81 (1H, dd, *J* = 13.4, 9.5, PhCH_{2b}), 1.95 (3H, d, *J* = 1.4 Hz, Me₈), 1.21 (3H, d, *J* = 7.0 Hz, H_{6'}), 1.14 (3H, d, *J* = 7.0 Hz, Me₁₀), 0.89 (9H, s, SiC(CH₃)₃), 0.11 (3H, s, SiCH₃), 0.07 (3H, s, SiCH₃); **¹³C NMR** (125 MHz, CDCl₃) 172.0, 153.2, 138.5, 138.1, 132.2, 130.1, 129.7, 128.9, 127.1, 93.9, 91.1, 86.7, 85.1, 80.2, 76.7, 68.9, 66.4, 61.1, 58.3, 55.7, 37.9, 37.0, 26.2, 18.3, 18.1, 15.8, 14.1, –4.7, –3.8.

β -diastereomer: **R_f** 0.70 (EtOAc/PE 3:7); **¹H NMR** (500 MHz, CDCl₃) δ _H 7.36-7.31 (2H, m, ArH), 7.30-7.27 (1H, m, ArH), 7.23-7.19 (2H, m, ArH), 6.59 (1H, d, *J* = 9.0 Hz, H₁₂), 5.94-5.90 (1H, m,

H₉), 4.70-4.63 (1H, m, NCH), 4.32 (1H, d, $J = 7.3$ Hz, H_{1'}), 4.26-4.21 (2H, H₁₁+OCH_{2a}CH), 4.16 (1H, dd, $J = 8.8, 4.1$ Hz, OCH_{2b}CH), 3.56 (3H, s, OMe), 3.54 (3H, s, OMe), 3.37 (1H, dd, $J = 13.4, 3.2$ Hz, PhCH_{2a}), 3.20 (1H, m, H_{5'}), 3.13 (1H, m, H_{4'}), 2.98 (2H, m, H_{2'}+H_{3'}), 2.81 (1H, dd, $J = 13.4, 9.5$, PhCH_{2b}), 2.80 (1H, m, H₁₀), 1.92 (3H, d, $J = 1.4$ Hz, Me₈), 1.20 (3H, d, $J = 7.0$ Hz, H_{6'}), 1.12 (3H, d, $J = 6.9$ Hz, Me₁₀), 0.89 (9H, s, SiC(CH₃)₃), 0.11 (3H, s, SiCH₃), 0.07 (3H, s, SiCH₃); ¹³C NMR (125 MHz, CDCl₃) 172.0, 153.2, 139.0, 138.1, 132.2, 130.1, 129.7, 128.9, 127.1, 104.7, 91.1, 86.7, 85.1, 84.8, 76.2, 73.3, 66.4, 60.8, 60.3, 55.5, 37.9, 37.2, 25.9, 18.3, 18.1, 16.0, 14.1, -4.7, -3.8. IR ν_{\max} 2957, 2927, 2856, 1789, 1684, 1455, 1383, 1350, 1303, 1258, 1213, 1156, 1087, 1039, 969, 861, 836, 796, 776, 703; HRMS ESI calc. for C₃₃H₅₃⁷⁹Br₂N₂O₈Si [M+NH₄]⁺ 791.1937, found 791.1938.

(R)-4-benzyl-3-((2E,4R,5R,6Z)-7-bromo-5-(((2R,3R,4R,5R,6R)-5-((tert-butyldimethylsilyl)oxy)-3,4-dimethoxy-6-methyltetrahydro-2H-pyran-2-yl)oxy)-2,4-dimethylhepta-2,6-dienoyl)oxazolidin-2-one (241)



To Pd(PPh₃)₄ (113 mg, 97.8 μ mol) was added a solution of dibromoolefin (760 mg, 0.980 mmol) in CH₂Cl₂ (20 mL) and Bu₃SnH (0.310 mL, 1.15 mmol). The solution was stirred for 2 h and concentrated *in vacuo*. Purification by flash chromatography (Et₂O/PE 1:4) yielded (Z)-vinyl bromide **241** (307 mg, 0.441 mmol, 45%) and the 1'-diastereomer **261** (239 mg, 0.343 mmol, 35%) as colourless oils.

R_f 0.70 (EtOAc/PE 3:7); $[\alpha]_D^{20} -19.9$ (c 1.0, CHCl₃); IR ν_{\max} 2930, 2857, 1788, 1682, 1455, 1385, 1349, 1303, 1250, 1212, 1156, 1086, 1006, 966, 859, 836, 776, 741, 702, 674; ¹H NMR (500 MHz, CDCl₃) δ_H 7.36-7.31 (2H, m, ArH), 7.30-7.27 (1H, m, ArH), 7.23-7.19 (2H, m, ArH), 6.31 (1H, dd, J

= 8.4, 7.3 Hz, H₁₂), 6.26 (1H, d, J = 7.3 Hz, H₁₃), 6.01 (1H, d, J = 10.0 Hz, H₉), 4.66-4.60 (1H, m, NCH), 4.52 (1H, dd, J = 8.5, 4.5 Hz, H₁₁), 4.32 (1H, d, J = 7.6 Hz, H₁'), 4.23 (1H, t, J = 9.0 Hz, OCH_{2a}CH), 4.15 (1H, dd, J = 9.0, 4.3 Hz, OCH_{2b}CH), 3.58 (3H, s, OMe), 3.55 (3H, s, OMe), 3.38 (1H, dd, J = 13.4, 3.2 Hz, PhCH_{2a}), 3.23-3.19 (1H, m, H₅'), 3.15-3.11 (1H, m, H₄'), 3.00-2.96 (2H, m, H₂' + H₃'), 2.83-2.78 (2H, m, H₁₀ + PhCH_{2b}), 1.90 (3H, d, J = 1.4 Hz, Me₈), 1.20 (3H, d, J = 6.1 Hz, H₆'), 1.16 (3H, d, J = 7.0 Hz, Me₁₀), 0.89 (9H, s, SiC(CH₃)₃), 0.10 (3H, s, SiCH₃), 0.05 (3H, s, SiCH₃); ¹³C NMR (125 MHz, CDCl₃) 171.6, 152.8, 138.1, 135.3, 135.2, 131.5, 129.5, 129.0, 127.4, 108.4, 104.3, 86.6, 85.0, 82.4, 76.0, 72.5, 66.4, 61.1, 60.6, 55.7, 37.5, 37.4, 26.0, 18.2, 18.1, 15.9, 13.9, -4.6, -3.9; HRMS ESI calc. for C₃₃H₅₃⁷⁹BrN₂O₈Si [M+NH₄]⁺ 713.2827, found 713.2828.

References

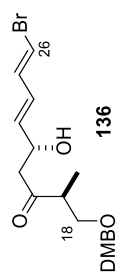
- ¹ D. J. Newman, G. M. Cragg, K. M. Snader, *Nat. Prod. Rep.* **2000**, *17*, 215.
- ² G. M. Cragg, D. J. Newman, *Annals of The New York Academy of Sciences* **2001**, 953, 3.
- ³ D. J. Newman, G. M. Cragg, *In Comprehensive Natural Products II Chemistry and Biology* **2010**, *2*, 623.
- ⁴ D. J. Newman, G. M. Cragg, *Future Med. Chem.* **2009**, *1*, 1415.
- ⁵ P. G. Grothaus, G. M. Cragg, D. J. Newman, *Curr. Org. Chem.* **2010**, *14*, 1781.
- ⁶ G. M. Cragg, D. G. I. Kingston, D. J. Newman, *Comprehensive Natural Products II Chemistry and Biology* **2010**, *2*, 5.
- ⁷ T. F. Molinski, *Nat Rev Drug Discov*, **2009**, *8*, 69.
- ⁸ G. M. Cragg, P. G. Grothaus, D. J. Newman, *J. Nat. Prod.* **2014**, *77*, 703.
- ⁹ D. Whitworth, *Myxobacteria: Multicellularity and Differentiation*; ASM Press: Washington, DC, 2007.
- ¹⁰ A. Demain, *Appl. Microbiol. Biotechnol.* **1999**, *52*, 455.
- ¹¹ K. Gerth, S. Pradella, O. Perlova, S. Beyer, R. Müller, *J. Biotechnol.* **2003**, *106*, 233.
- ¹² H. B. Bode, R. Müller, *Secondary Metabolism in Myxobacteria*; ASM Press: Washington, DC, 2008.
- ¹³ R. Jansen, H. Irschik, H. Reichenbach, V. Wray, G. Höfle, *Liebigs Ann.* **1994**, 759.
- ¹⁴ H. Irschik, R. Jansen, K. Gerth, G. Höfle, H. Reichenbach, *J. Antibiot.* **1987**, *40*, 7.
- ¹⁵ H. Irschik, R. Jansen, K. Gerth, G. Höfle, H. Reichenbach, *J. Antibiot.* **1995**, *48*, 886.
- ¹⁶ R. Jansen, H. Irschik, H. Reichenbach, G. Höfle, *Liebigs Ann.* **1997**, 1725.
- ¹⁷ T. Kiuchi, T. Nagai, K. Ohashi, K. Mizuno, *J. Cell Biol.* **2011**, *193*, 365.
- ¹⁸ B. Alberts, A. Johnson, J. Lewis, M. Raff, K. Roberts, P. Walter, *Molecular biology of the cell*; Garland Science: New York, NY, 2002.
- ¹⁹ (a) H. Irschik, R. Jansen, K. Gerth, G. Höfle, H. Reichenbach, *J. Antibiot.* **1995**, *48*, 962; (b) O. Perlova, K. Gerth, O. Kaiser, A. Hans, R. Müller, *J. Biotechnol.* **2006**, *121*, 174; (c) R. Dieste, H. Irschik, R. Jansen, M. W. Khalil, H. Reichenbach, F. Sasse, *ChemBioChem* **2009**, *10*, 2900.
- ²⁰ E. G. Yarmola, T. Somasundaram, T. A. Boring, I. Spector, M. R. Bubb, *J. Biol. Chem.* **2000**, *275*, 28120.
- ²¹ J. S. Allingham, V. A. Klenchin, I. Rayment, *Cell. Mol. Life Sci.* **2006**, *63*, 2119.
- ²² D. Janssen, D. Albert, R. Jansen, R. Müller, M. Kalesse, *Angew. Chem. Int. Ed.* **2007**, *46*, 4898.
- ²³ (a) S. D. Rychnovsky, B. N. Rogers, T. I. Richardson, *Acc. Chem. Res.* **1998**, *31*, 9; (b) D. A. Evans, D. L. Rieger, J. R. Gage, *Tetrahedron Lett.* **1990**, *31*, 7099.
- ²⁴ (a) R. Reid, M. Piagentini, E. Rodriguez, G. Ashley, N. Viswanathan, J. Carney, D. V. Santi, C. R. Hutchinson, R. McDaniel, *Biochemistry* **2003**, *42*, 72; (b) P. Caffrey, *ChemBioChem* **2003**, *4*, 654.
- ²⁵ T. Brodmann, D. Janssen, M. Kalesse, *J. Am. Chem. Soc.* **2010**, *132*, 13610.
- ²⁶ D. A. Evans, M. J. Dart, J. L. Duffy, M. G. Yang, *J. Am. Chem. Soc.* **1996**, *118*, 4322.
- ²⁷ (a) A. K. Saksena, P. Mangiaracina, *Tetrahedron Lett.* **1983**, *24*, 273; (b) D. A. Evans, K. T. Chapman, *Tetrahedron Lett.* **1986**, *27*, 5939.
- ²⁸ K. Ando, T. Oishi, M. Hirama, H. Ohno, T. Ibuka, *J. Org. Chem.* **2000**, *65*, 4745.
- ²⁹ (a) Y. Nagao, S. Yamada, T. Kumagi, M. Ochiai, E. Fujita, *Chem. Commun.* **1985**, 1418; (b) Y. Nagao, Y. Hagiwara, T. Kumagi, M. Ochiai, T. Inoue, K. Hashimoto, E. Fujita, *J. Org. Chem.* **1986**, *51*, 2391.
- ³⁰ A. Abiko, J. Liu, S. Masamune, *J. Am. Chem. Soc.* **1997**, *119*, 2586.
- ³¹ A. J. Phillips, Y. Uto, P. Wipf, M. J. Reno, D. R. Williams, *Org. Lett.*, **2000**, *2*, 1165.
- ³² (a) J. A. Marshall, P. Eidam, E. H. Schenk, *J. Org. Chem.* **2006**, *71*, 4840; (b) J. A. Marshall, *Chem. Rev.* **2000**, *100*, 3163.

- ³³ (a) R. Tamura, M. Kato, K. Saegusa, M. Kakihana, D. Oda, *J. Org. Chem.* **1987**, 52, 4121; (b) R. Tamura, K. Saegusa, M. Kakihana, D. Oda, *J. Org. Chem.* **1988**, 53, 2723.
- ³⁴ L. Gibson, *PhD Thesis*, University of Cambridge, **2011**.
- ³⁵ S. Nakatsukasa, K. Takai, K. Utimoto, *J. Org. Chem.* **1986**, 51, 5045.
- ³⁶ I. Paterson, G. J. Naylor, A. E. Wright, *Chem. Commun.* **2008**, 6248.
- ³⁷ (a) W. D. Wulff, G. A. Peterson, W. E. Bauta, K. Chan, K. L. Faron, S. R. Gilbertson, R. W. Kaesler, D. C. Yang, C. K. Murray, *J. Org. Chem.* **1986**, 51, 277; (b) W. J. Scott, J. K. Stille, *J. Am. Chem. Soc.* **1986**, 108, 3033.
- ³⁸ M. Li, *PhD Thesis*, University of Cambridge, **2013**.
- ³⁹ (a) S. L. Huang, D. Swern, *J. Org. Chem.* **1978**, 43, 4537; (b) K. Omura, D. Swern, *Tetrahedron* **1978**, 34, 1651.
- ⁴⁰ E. J. Corey, P. L. Fuchs, *Tetrahedron Lett.* **1972**, 3769.
- ⁴¹ F. E. Hart, T. F. Blackburn, J. Schwartz, *J. Am. Chem. Soc.* **1975**, 97, 679.
- ⁴² A. Minato, K. Suzuki, K. Tamao, *J. Am. Chem. Soc.* **1987**, 109, 1257.
- ⁴³ (a) J. Uenishi, K. Matsui, *Tetrahedron Lett.* **2001**, 42, 4353; (b) J. Uenishi, K. Matsui, H. Ohmaya, *J. Organomet. Chem.* **2002**, 653, 141.
- ⁴⁴ A. F. Littke, L. Schwarz, G. C. Fu, *J. Am. Chem. Soc.* **2002**, 124, 6343.
- ⁴⁵ J. M. Williams, R. B. Johnson, N. Yasuda, G. Marchesini, U. Dolling, E. J. J. Grabowski, *Tetrahedron Lett.* **1995**, 36, 461.
- ⁴⁶ S. Nahm, S. M. Weinreb, *Tetrahedron Lett.* **1981**, 22, 3815.
- ⁴⁷ J. Becher, *Org. Synth.* **1980**, 59, 79.
- ⁴⁸ I. Paterson, G. J. Florence, A. C. Heimann, A. C. Mackay, *Angew. Chem. Int. Ed.* **2005**, 44, 1130.
- ⁴⁹ B. H. Lipshutz, B. Ullman, C. Lindsley, S. Pecchi, D. J. Buzard, D. Dickson, *J. Org. Chem.* **1998**, 63, 6092.
- ⁵⁰ K. J. Frankowski, J. E. Golden, Y. Zeng, Y. Lei, J. Aubé, *J. Am. Chem. Soc.* **2008**, 130, 6018.
- ⁵¹ S. L. Drew, A. L. Lawrence, M. S. Sherburn, *Angew. Chem. Int. Ed.* **2013**, 52, 4221.
- ⁵² I. Paterson, R. D. Norcross, R. A. Ward, P. Romea, M. A. Lister, *J. Am. Chem. Soc.* **1994**, 116, 11287.
- ⁵³ J. M. Goodman, R. S. Paton, *Chem. Commun.* **2007**, 2124.
- ⁵⁴ R. S. Paton, J. M. Goodman, *J. Org. Chem.* **2008**, 73, 1253.
- ⁵⁵ C. W. Moeder, J. R. Sowa, *J. Phys. Org. Chem.* **2004**, 17, 317.
- ⁵⁶ D. A. Evans, A. H. Hoveyda, *J. Am. Chem. Soc.* **1990**, 112, 6447.
- ⁵⁷ I. Paterson, R. D. M. Davies, R. Marquez, *Angew. Chem. Int. Ed.* **2001**, 40, 603.
- ⁵⁸ I. Paterson, R. D. M. Davies, A. C. Heimann, R. Marquez, A. Meyer, *Org. Lett.* **2003**, 5, 4477.
- ⁵⁹ S. B. J. Kan, *PhD Thesis*, University of Cambridge, **2012**.
- ⁶⁰ F. W. Foss Jr., A. H. Snyder, M. D. Davis, M. Rouse, M. D. Okusa, K. R. Lynch, T. L. Macdonald, *Bioorg. Med. Chem.* **2007**, 15, 663.
- ⁶¹ P. Garner, J. M. Park *J. Org. Chem.* **1987**, 52, 2361.
- ⁶² K. Omura, A. K. Sharma, D. Swern, *J. Org. Chem.* **1976**, 41, 957.
- ⁶³ I. Paterson, L. J. Gibson, S. B. J. Kan, *Org. Lett.* **2010**, 12, 5530.
- ⁶⁴ A. Hampton, J. C. Frattantoni, P. M. Carroll, S. Wang, *J. Am. Chem. Soc.* **1965**, 87, 5481-5487.
- ⁶⁵ R. Noyori, T. Ohkuma, M. Kitamura, N. Sayo, H. Kumobayashi, S. Akutagawa, *J. Am. Chem. Soc.* **1987**, 5856.
- ⁶⁶ M. Kitamura, M. Tokunaga, T. Ohkuma, R. Noyori, *Org. Synth.* **1998**, 9, 589.
- ⁶⁷ G. R. Sullivan, J. A. Dale, H. S. Mosher, *J. Am. Chem. Soc.* **1973**, 512.
- ⁶⁸ J. A. Dale, H. S. Mosher, *J. Org. Chem.* **1973**, 2143.
- ⁶⁹ J. M. Goodman, I. Paterson, *Tetrahedron Lett.* **1992**, 33, 7223.

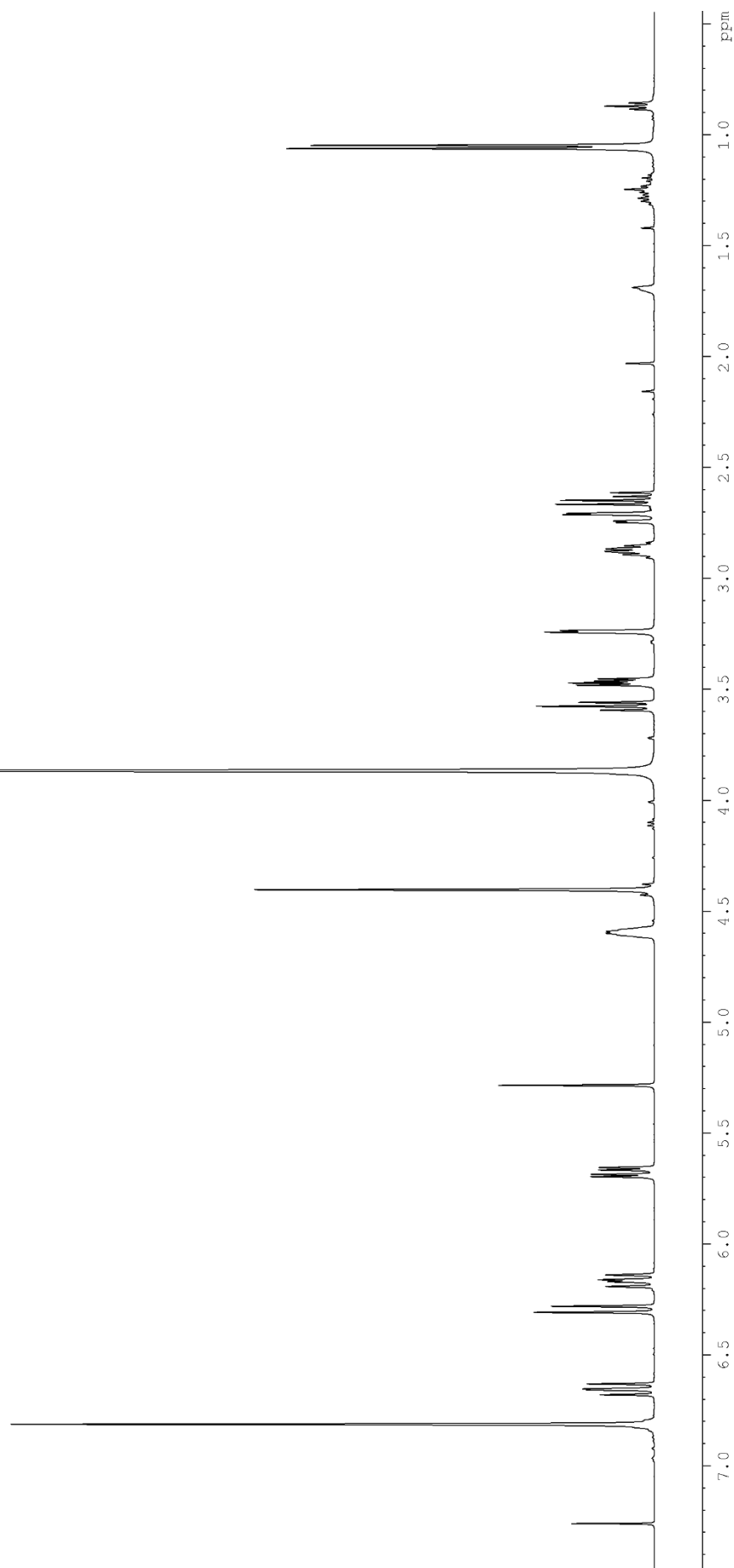
- ⁷⁰ D. B. Dess, J. C. Martin, *J. Org. Chem.* **1983**, *48*, 4155.
- ⁷¹ G. Stork, K. Zhao, *Tetrahedron Lett.* **1989**, *30*, 2173.
- ⁷² A. Aguilar, W. Sun, L. Liu, J. Lu, D. McEachern, D. Bernard, J. R. Deschamps, S. Wang, *J. Med. Chem.* **2014**, *57*, 10486.
- ⁷³ A. Clerici, N. Pastori, O. Porta, *Tetrahedron.* **2001**, *57*, 217.
- ⁷⁴ For a review on the Steglich conditions, see: A. C. Spivey, S. Arseniyadis, *Angew. Chem. Int. Ed.* **2004**, *43*, 5436.
- ⁷⁵ V. S. Prado, A. C. B. Burtoloso, *Synthesis* **2010**, *2*, 361.
- ⁷⁶ E. E. Kwan, J. R. Scheerer, D. A. Evans, *J. Org. Chem.* **2013**, *78*, 175.
- ⁷⁷ B. H. Lipshutz, E. L. Ellsworth, S. H. Dimock, D. C. Reuter, *Tetrahedron Lett.* **1989**, *30*, 2065.
- ⁷⁸ I. Beaudet, J. Parrain, J. Quintard, *Tetrahedron Lett.* **1991**, *32*, 6333.
- ⁷⁹ I. Paterson, S. B. J. Kan, L. J. Gibson, *Org. Lett.* **2010**, *12*, 3724.
- ⁸⁰ (a) S. Shirokawa, M. Kamiyama, T. Nakamura, M. Okada, A. Nakazaki, S. Hosokawa, S. Kobayashi, *J. Am. Chem. Soc.* **2004**, *126*, 13604; (b) M. Shinoyama, S. Shirokawa, A. Nakazaki, S. Kobayashi, *Org. Lett.* **2009**, *11*, 1277; (c) G. Symkenberg, M. Kalesse, *Org. Lett.* **2012**, *14*, 1608.
- ⁸¹ S. Hosokawa, K. Sekiguchi, M. Enemoto, S. Kobayashi, *Tetrahedron Lett.* **2000**, *41*, 6429.
- ⁸² (a) J. Uenishi, R. Kawahama, Y. Shiga, O. Yonemitsu, J. Tsuji, *Tetrahedron Lett.* **1996**, *37*, 6759. (b) J. Uenishi, R. Kawahama, O. Yonemitsu, J. Tsuji, *J. Org. Chem.* **1996**, *61*, 5716. (c) J. Uenishi, R. Kawahama, O. Yonemitsu, J. Tsuji, *J. Org. Chem.* **1998**, *63*, 8965.
- ⁸³ A. Fürstner, J. Funel, M. Tremblay, L. C. Bouchez, C. Nevado, M. Waser, J. Ackersstaff, C. C. Stimson, *Chem. Commun.* **2008**, 2873.
- ⁸⁴ I. Paterson, I. Lyothier, *Org. Lett.* **2004**, *6*, 4933.
- ⁸⁵ Examples of the oxidation of unactivated oxazolines using MnO₂: a) J. Franke, M. Bock, R. Dehn, J. Fohrer, S. B. Mhaske, A. Migliorini, A. A. Kanakis, R. Jansen, J. Herrmann, R. Müller, A. Kirschning, *Chem. Eur. J.* **2015**, *21*, 4272; b) P. Wipf, J. T. Reeves, R. Balachandran, B. W. Day, *J. Med. Chem.* **2002**, *45*, 1901.
- ⁸⁶ S. Williams, J. Jin, S. B. J. Kan, M. Li, L. J. Gibson, I. Paterson, *Angew. Chem. Int. Ed.* **2016**, *56*, 645.
- ⁸⁷ R. Elliott, *Part III Project Report*, University of Cambridge, **2012**.
- ⁸⁸ J. McNulty, J. J. Nair, C. Griffin, S. Pandey, *J. Nat. Prod.* **2008**, *71*, 357.
- ⁸⁹ K. Jones, W. W. Wood, *Carbohydr. Res.* **1986**, *155*, 217.
- ⁹⁰ A. Minami, E. Tadashi, *J. Am. Chem. Soc.* **2007**, *129*, 5102.
- ⁹¹ R. E. Dolle, K. C. Nicolaou, *J. Am. Chem. Soc.* **1985**, *107*, 1691.
- ⁹² K. C. Nicolaou, R. Dolle, D. Papahatjis, J. Randall, *J. Am. Chem. Soc.* **1984**, *106*, 4189.
- ⁹³ L. A. Paquette, L. Barriault, D. Pissarnitski, J. N. Johnston, *J. Am. Chem. Soc.* **2000**, *122*, 619.
- ⁹⁴ A. Findlay, *PhD Thesis*, University of Cambridge, **2008**.
- ⁹⁵ A. K. Ghosh, Y. Wang, J. T. Kim, *J. Org. Chem.* **2001**, *66*, 8973.
- ⁹⁶ B. H. Lipshutz, C. Lindsley, *J. Am. Chem. Soc.* **1997**, *119*, 4555.
- ⁹⁷ I. Paterson, R. Britton, K. Ashton, H. Knust, J. Stafford, *P. Natl. Acad. Sci.* **2004**, *101*, 11986.
- ⁹⁸ J. E. Wrobel, B. Ganem, *J. Org. Chem.* **1983**, *48*, 3761.
- ⁹⁹ D. F. Taber, H. Yu, C. D. Incarvito, A. L. Rheingold, *J. Am. Chem. Soc.* **1998**, *120*, 13285.
- ¹⁰⁰ G. Ho, D. J. Mathre, *J. Org. Chem.* **1995**, *60*, 2271.
- ¹⁰¹ K. C. Nicolaou, Y. Sun, R. Guduru, B. Banerji, D. Y. Chen, *J. Am. Chem. Soc.* **2008**, *130*, 3633.
- ¹⁰² H. H. Baer, H. R. Hanna, *Carbohydr. Res.* **1982**, *102*, 169.
- ¹⁰³ K. Sato, J. Yoshimura, *Carbohydr. Res.* **1982**, *103*, 221.

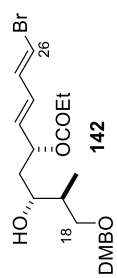
Appendix

Selected NMR Spectra

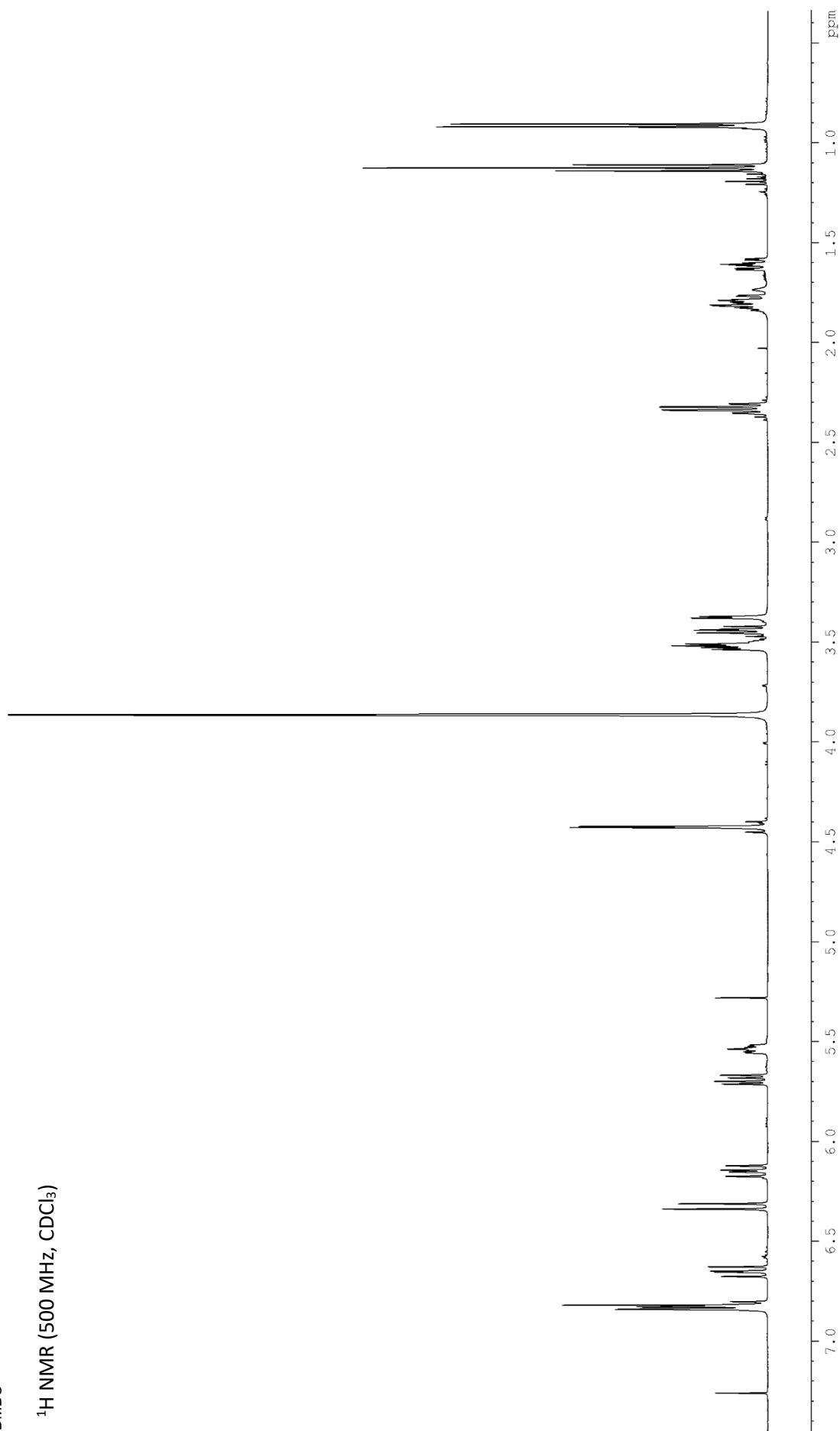


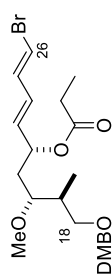
¹H NMR (500 MHz, CDCl₃)





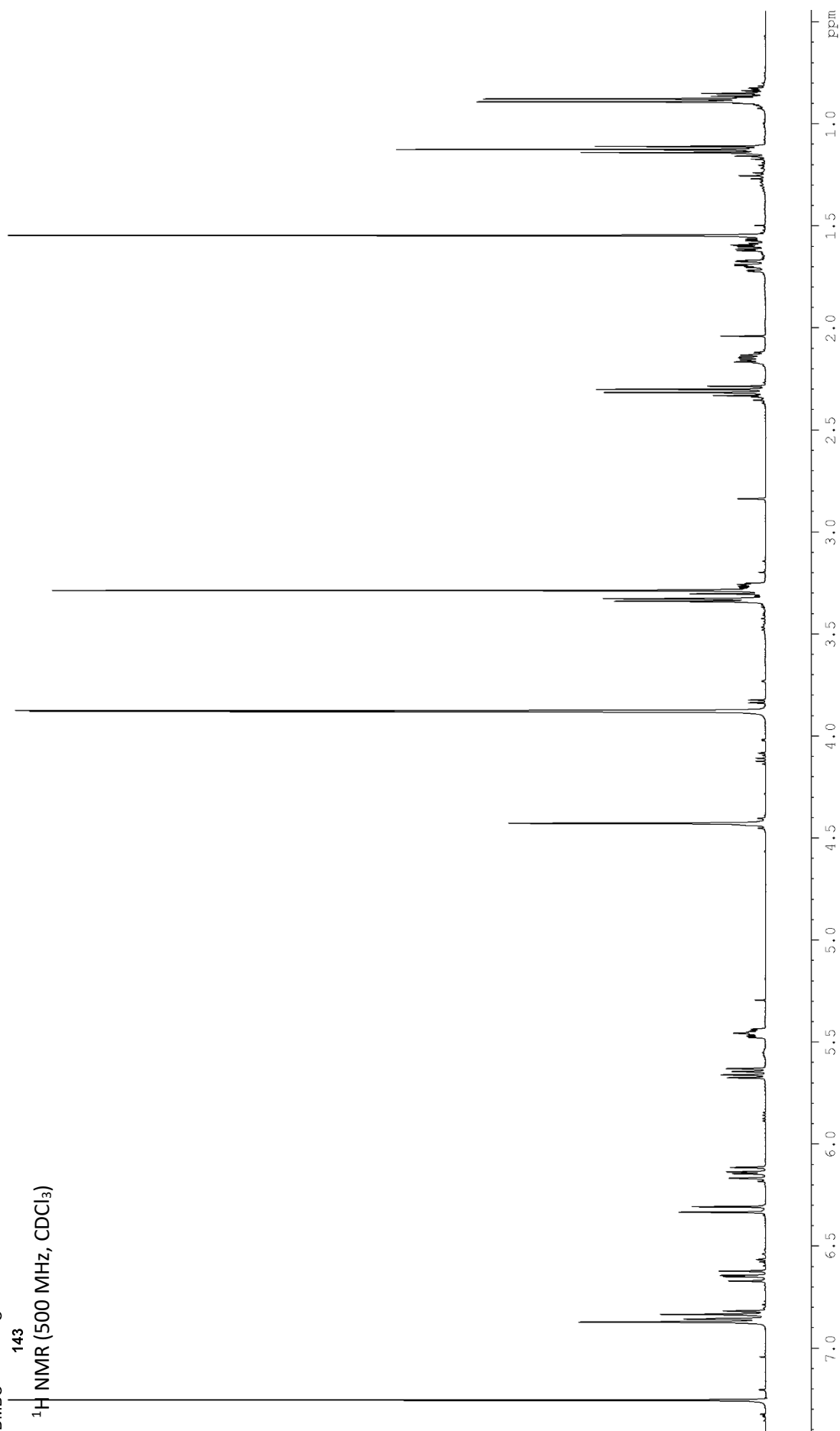
¹H NMR (500 MHz, CDCl₃)

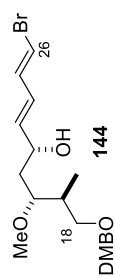




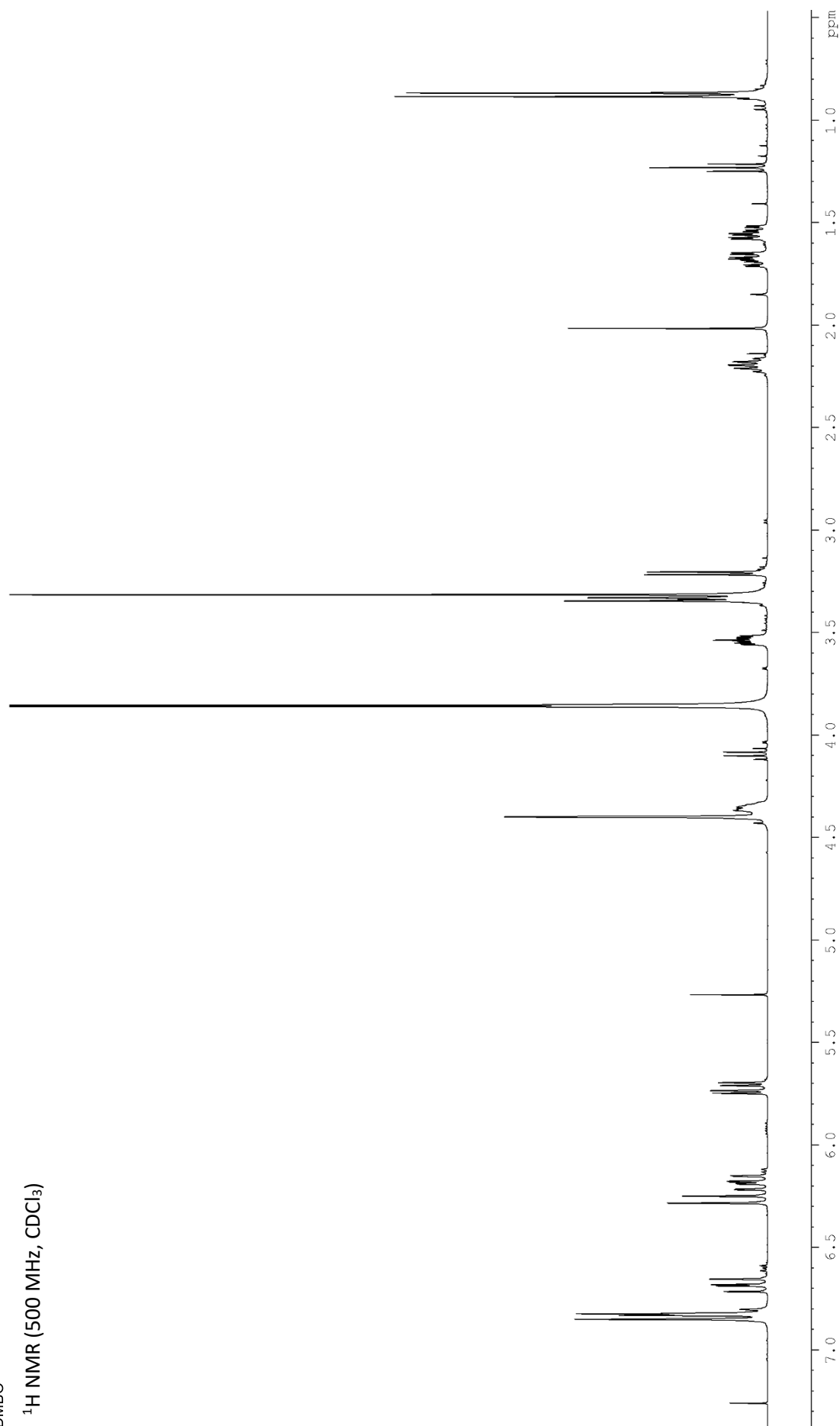
143

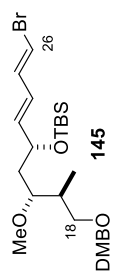
¹H NMR (500 MHz, CDCl₃)



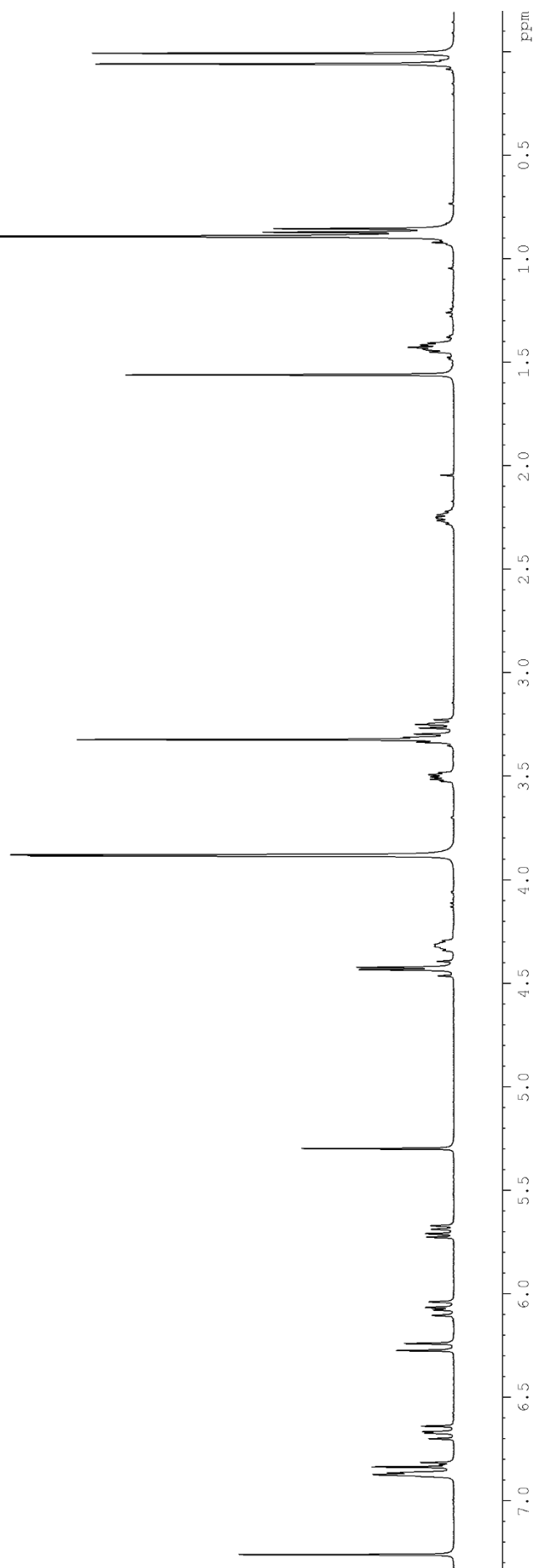


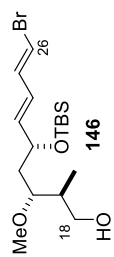
¹H NMR (500 MHz, CDCl₃)



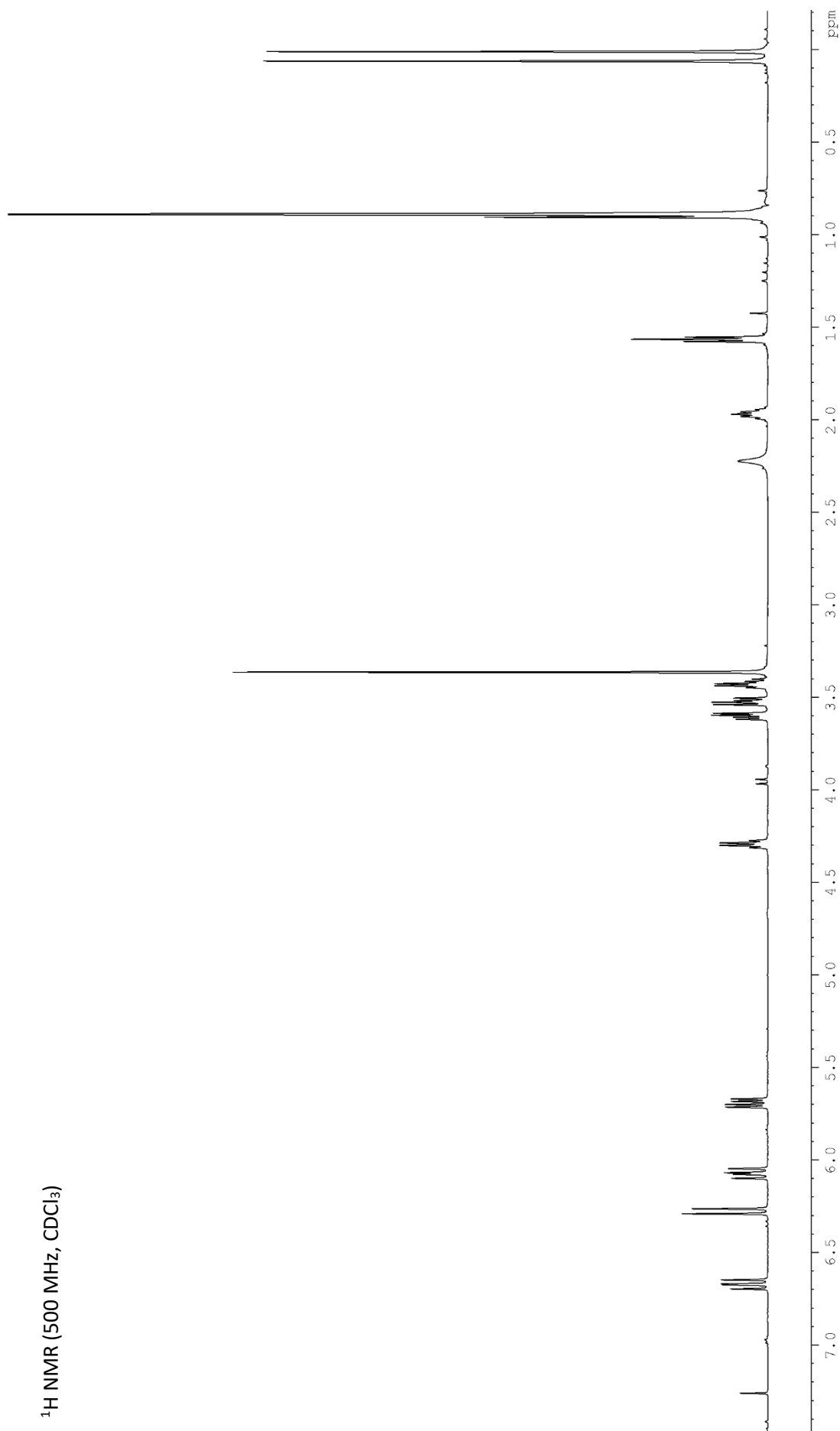


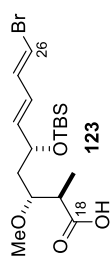
^1H NMR (500 MHz, CDCl_3)



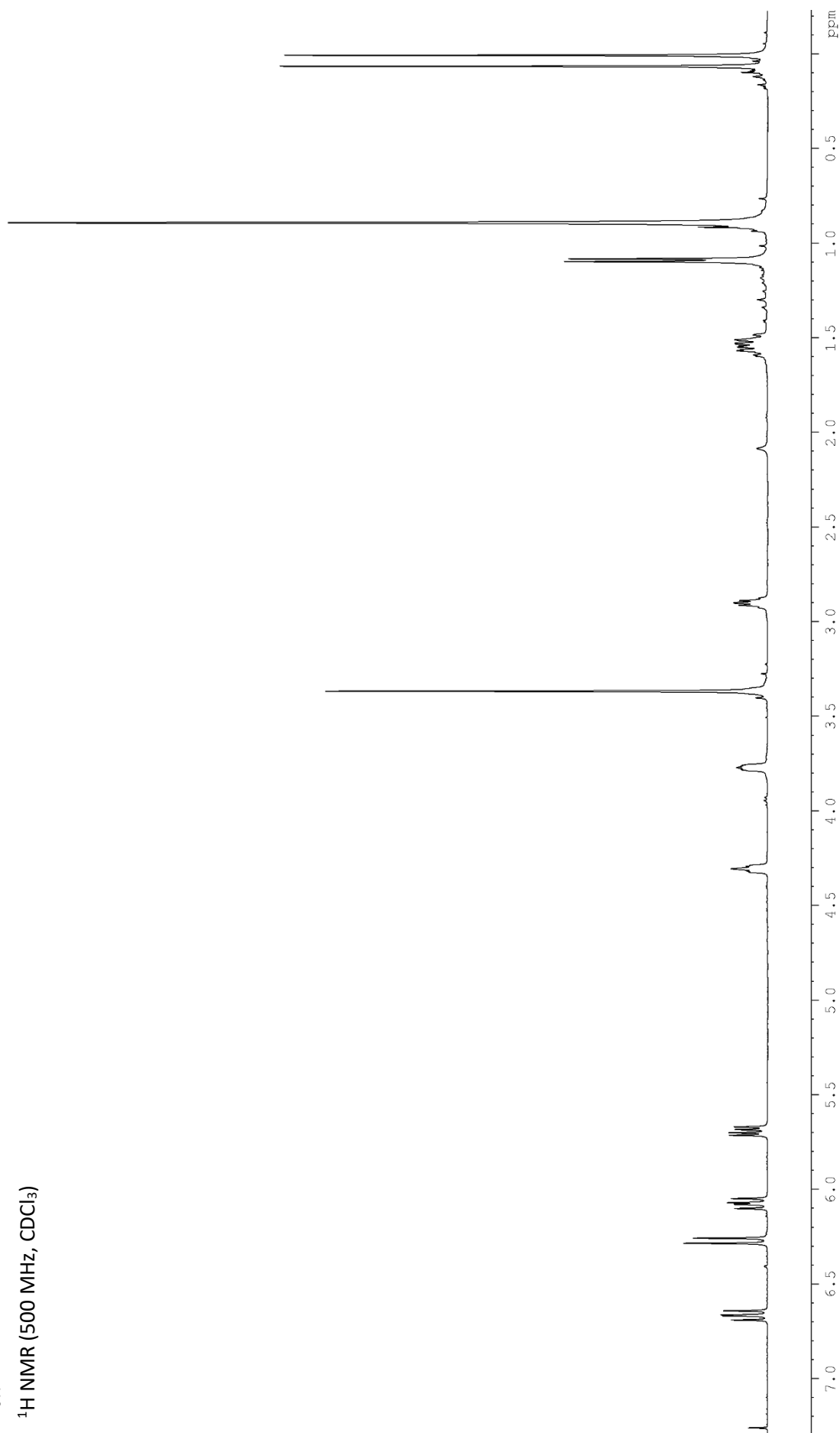


^1H NMR (500 MHz, CDCl_3)

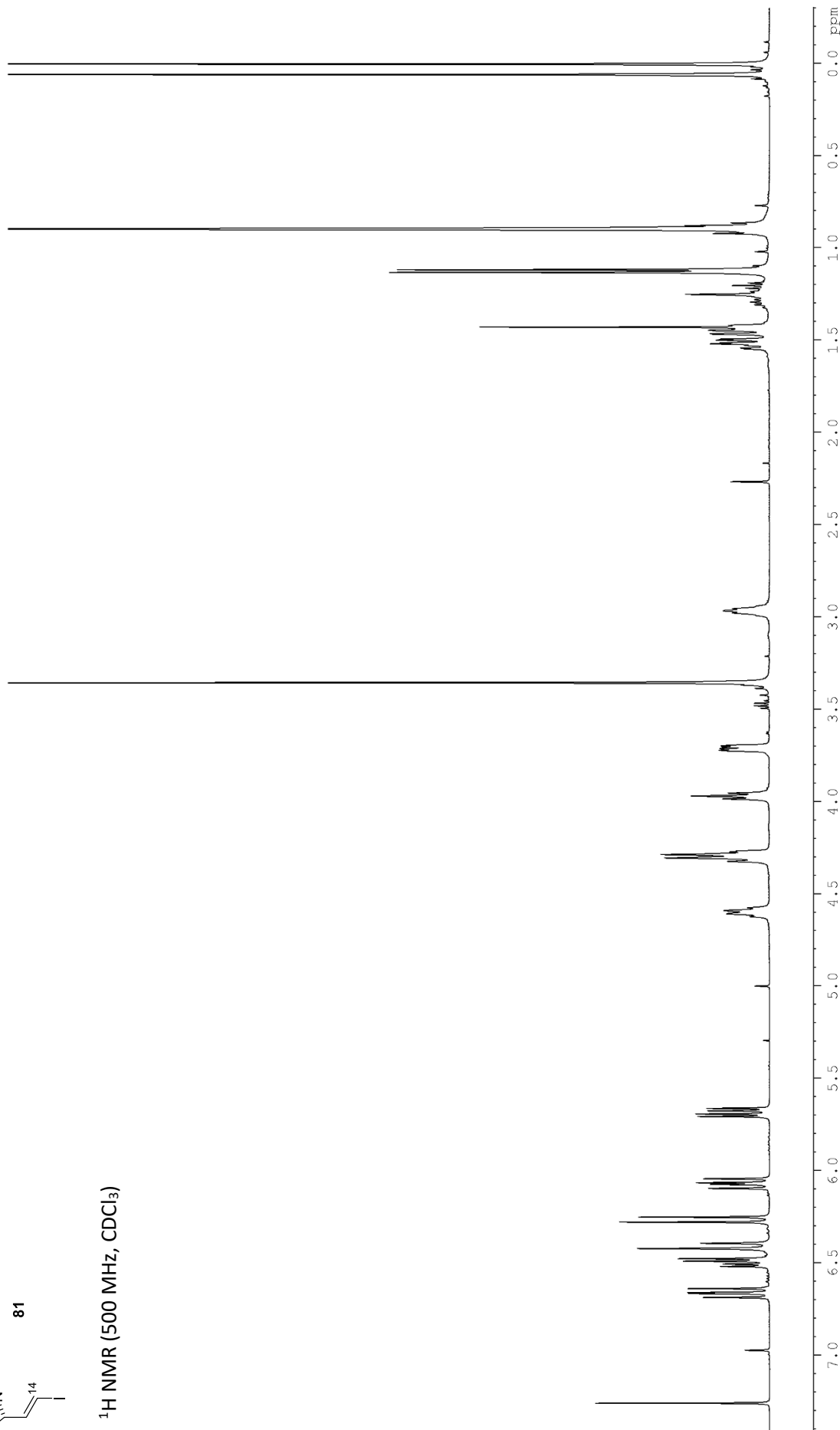
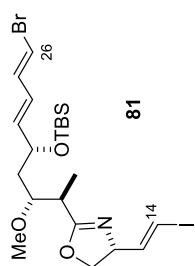




¹H NMR (500 MHz, CDCl₃)



 ^1H NMR (500 MHz, CDCl_3)



^1H NMR (500 MHz, CDCl_3)



165



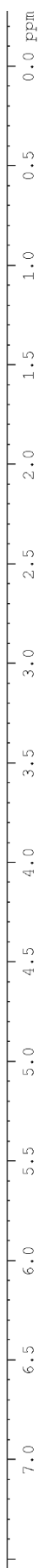


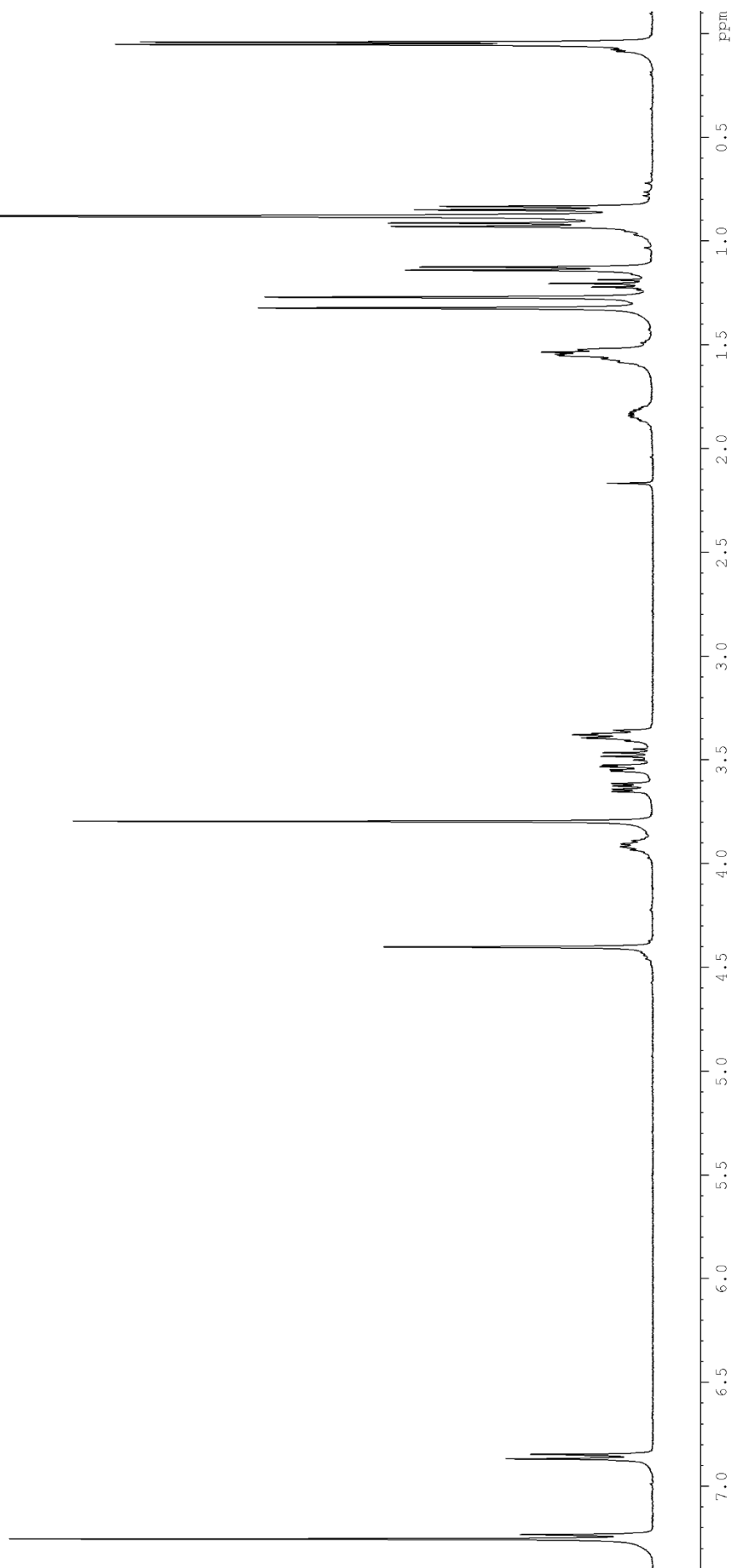
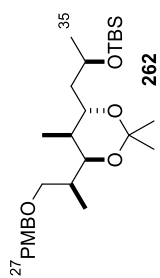
IN





167

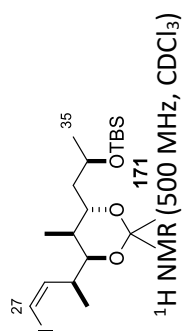


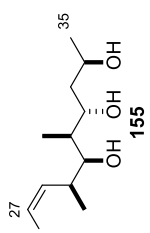




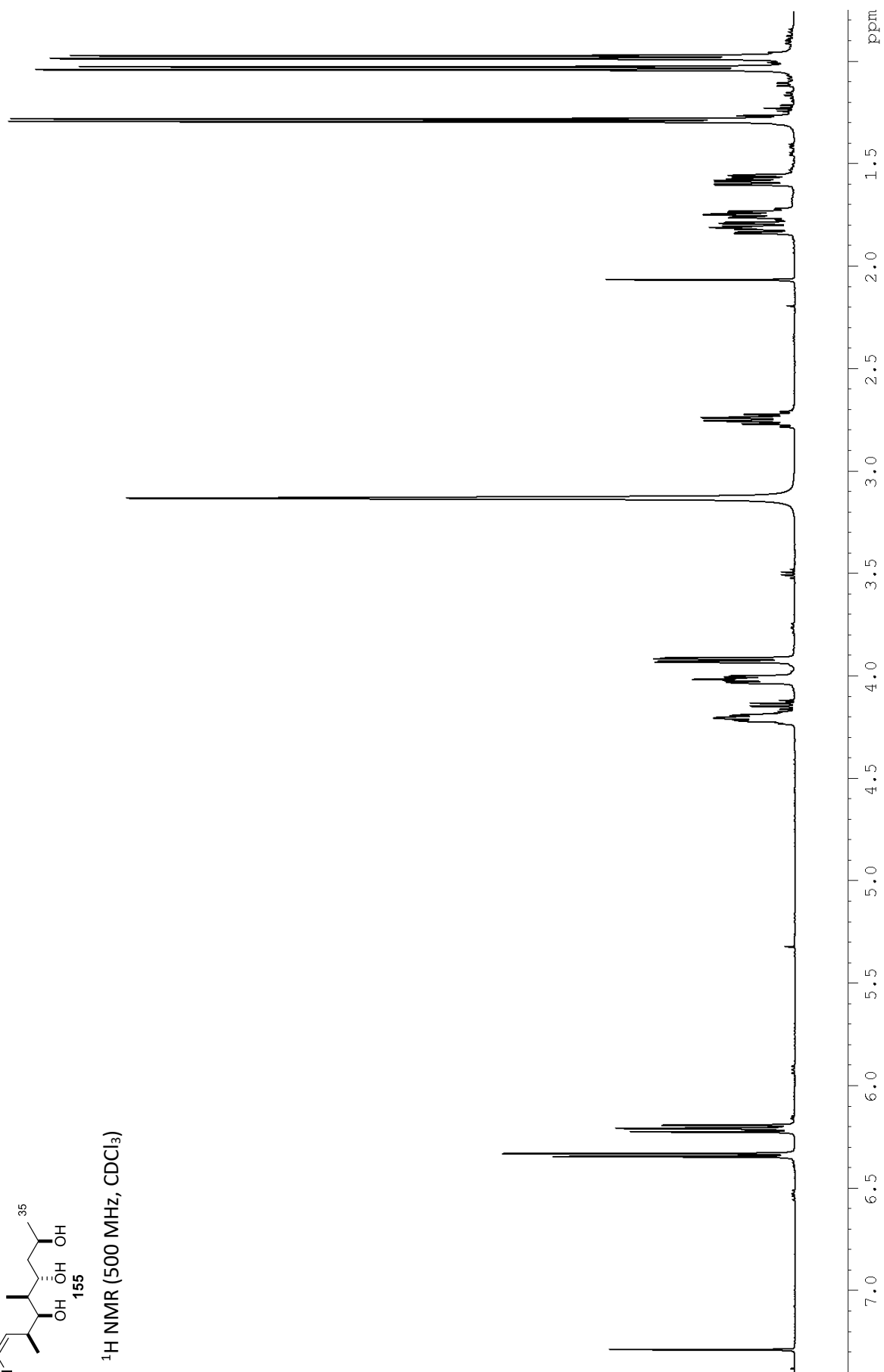
168

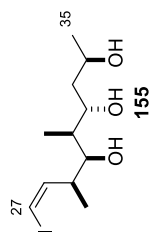




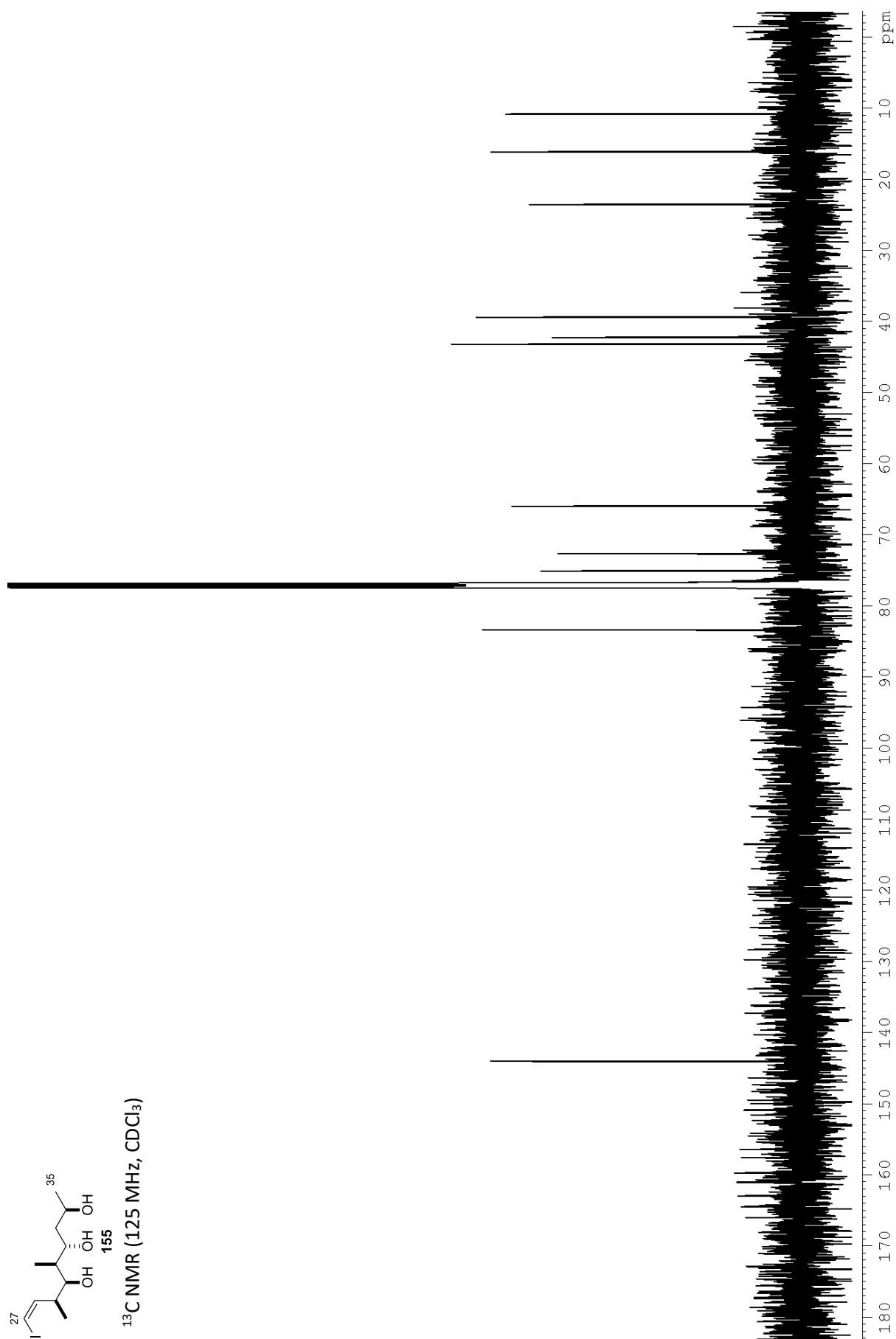


¹H NMR (500 MHz, CDCl₃)





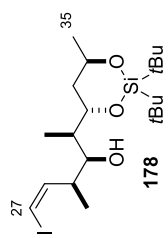
^{13}C NMR (125 MHz, CDCl_3)



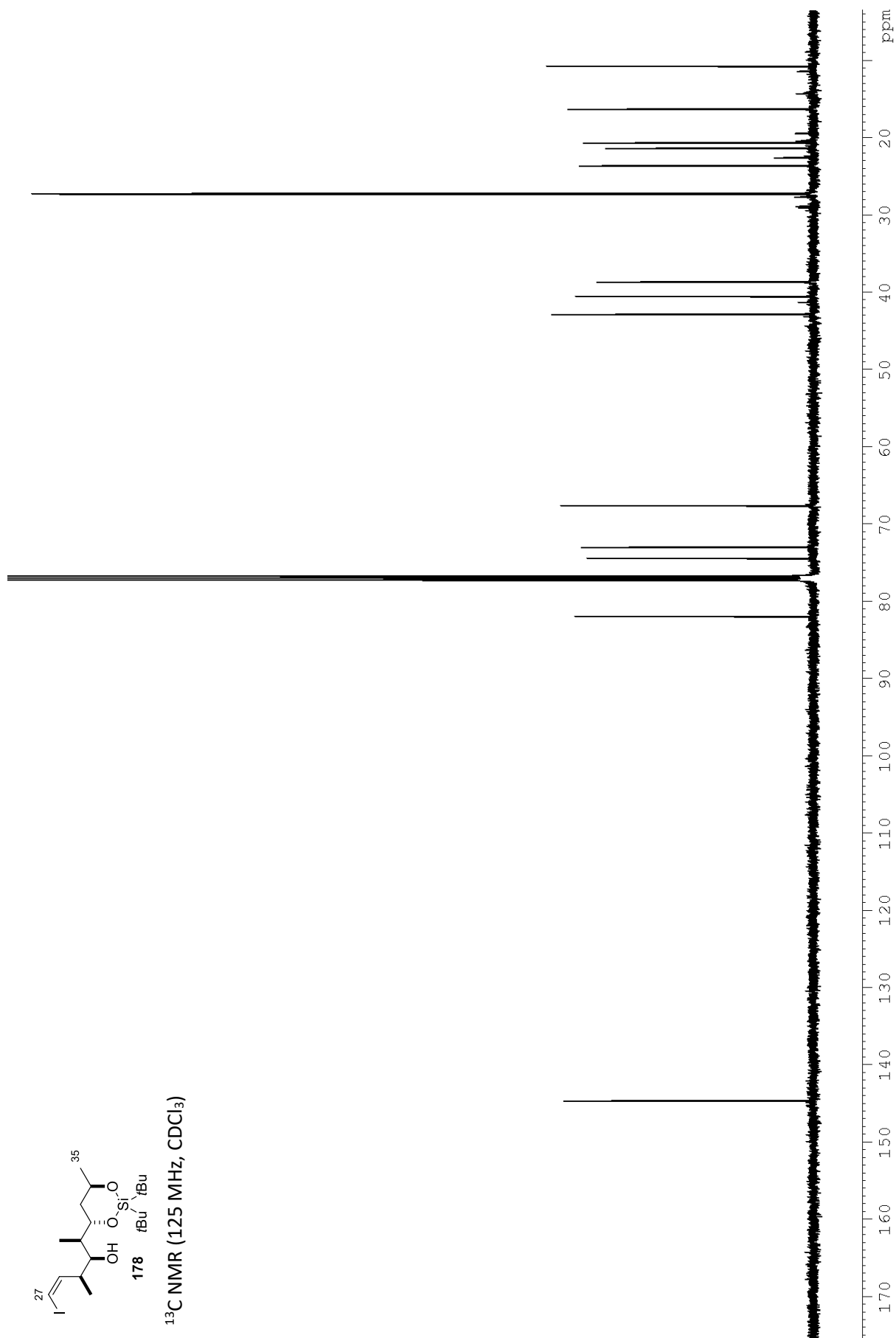


178





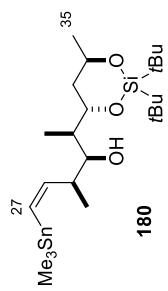
¹³C NMR (125 MHz, CDCl₃)



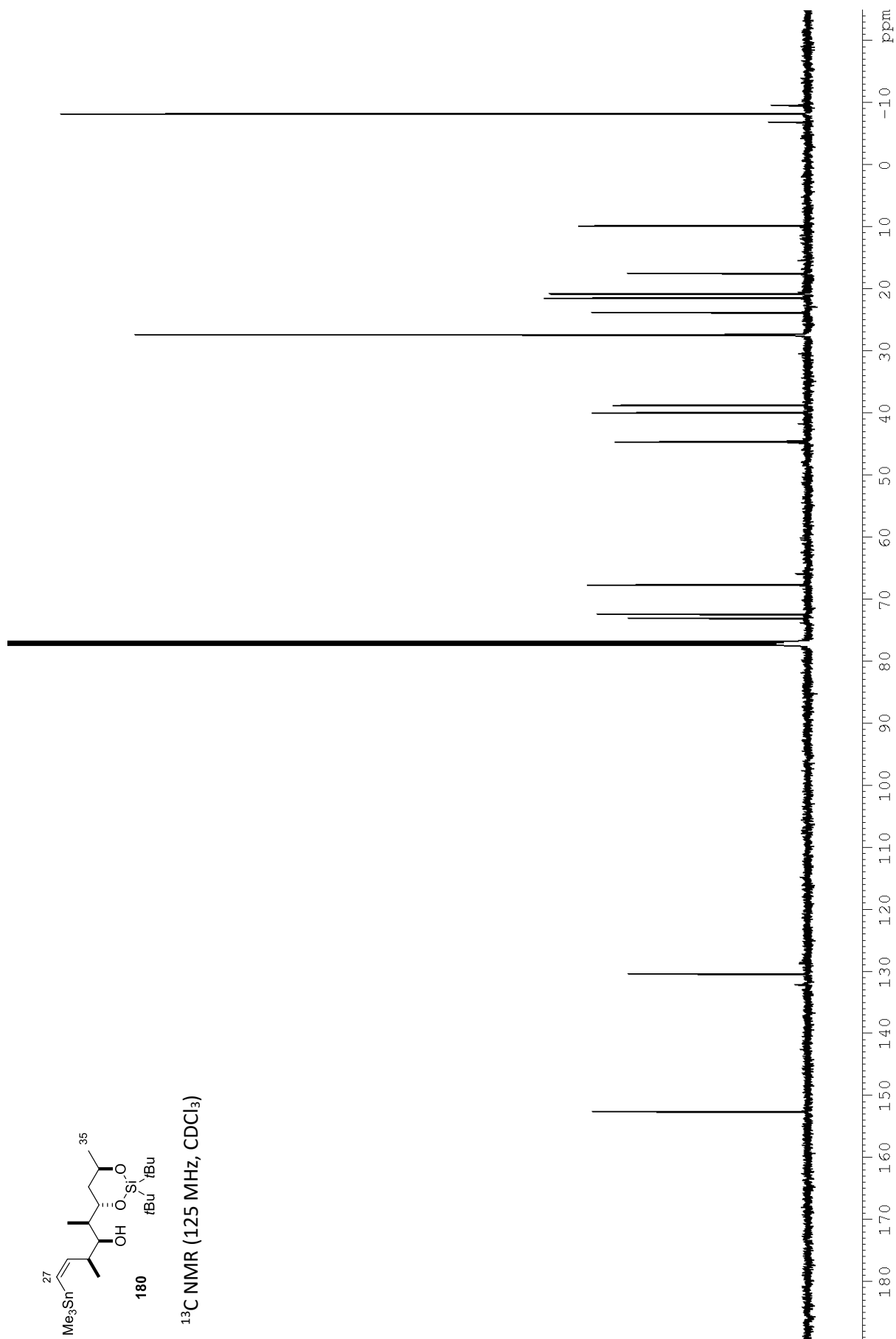

$$\begin{array}{c} \text{Si} \\ \diagup \quad \diagdown \\ t\text{Bu} \quad t\text{Bu} \end{array}$$

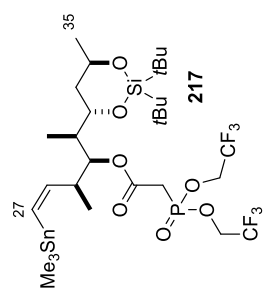
0.15



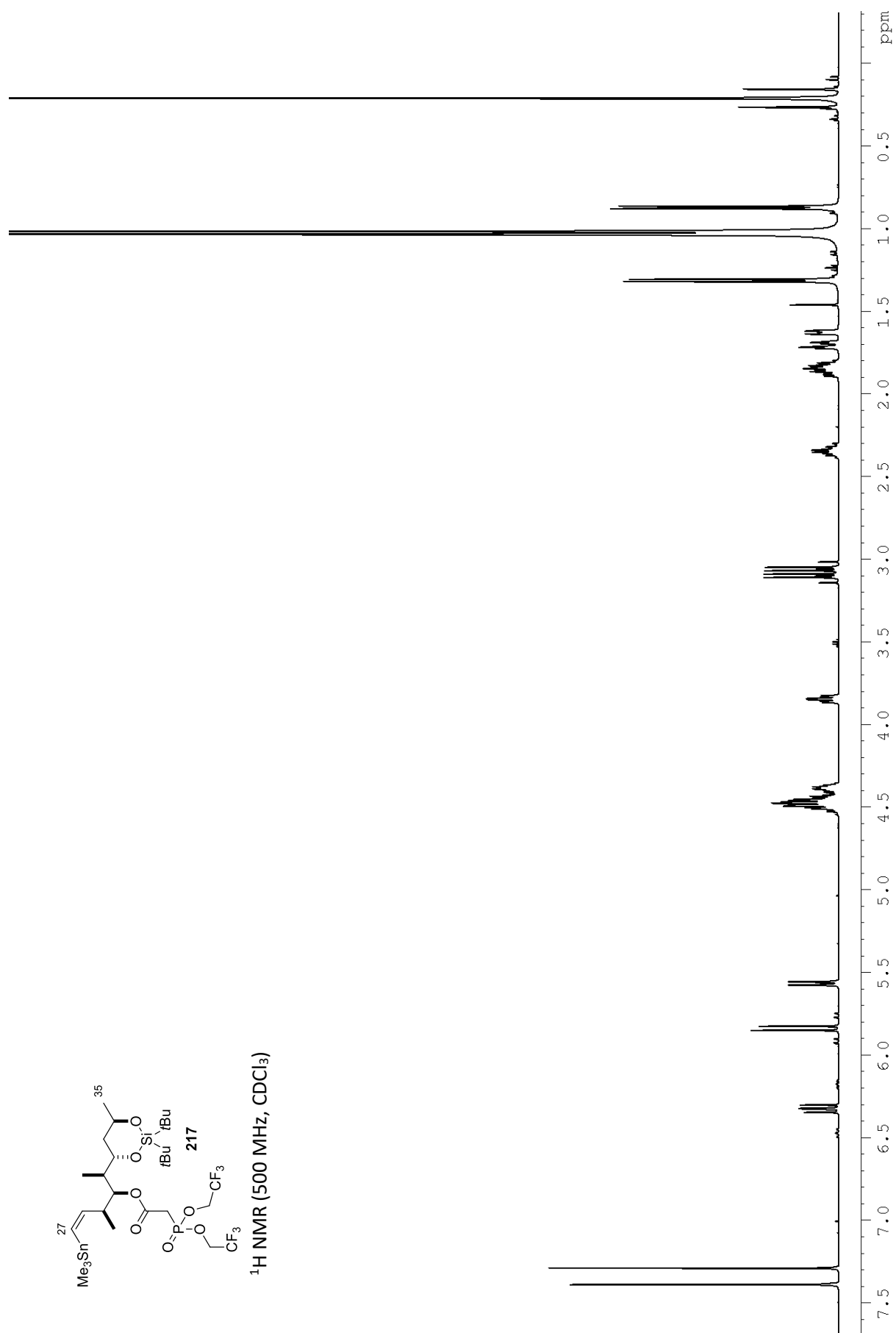


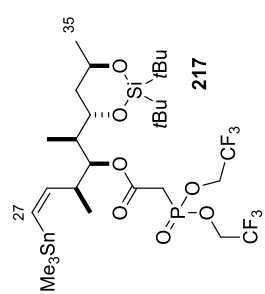
^{13}C NMR (125 MHz, CDCl_3)



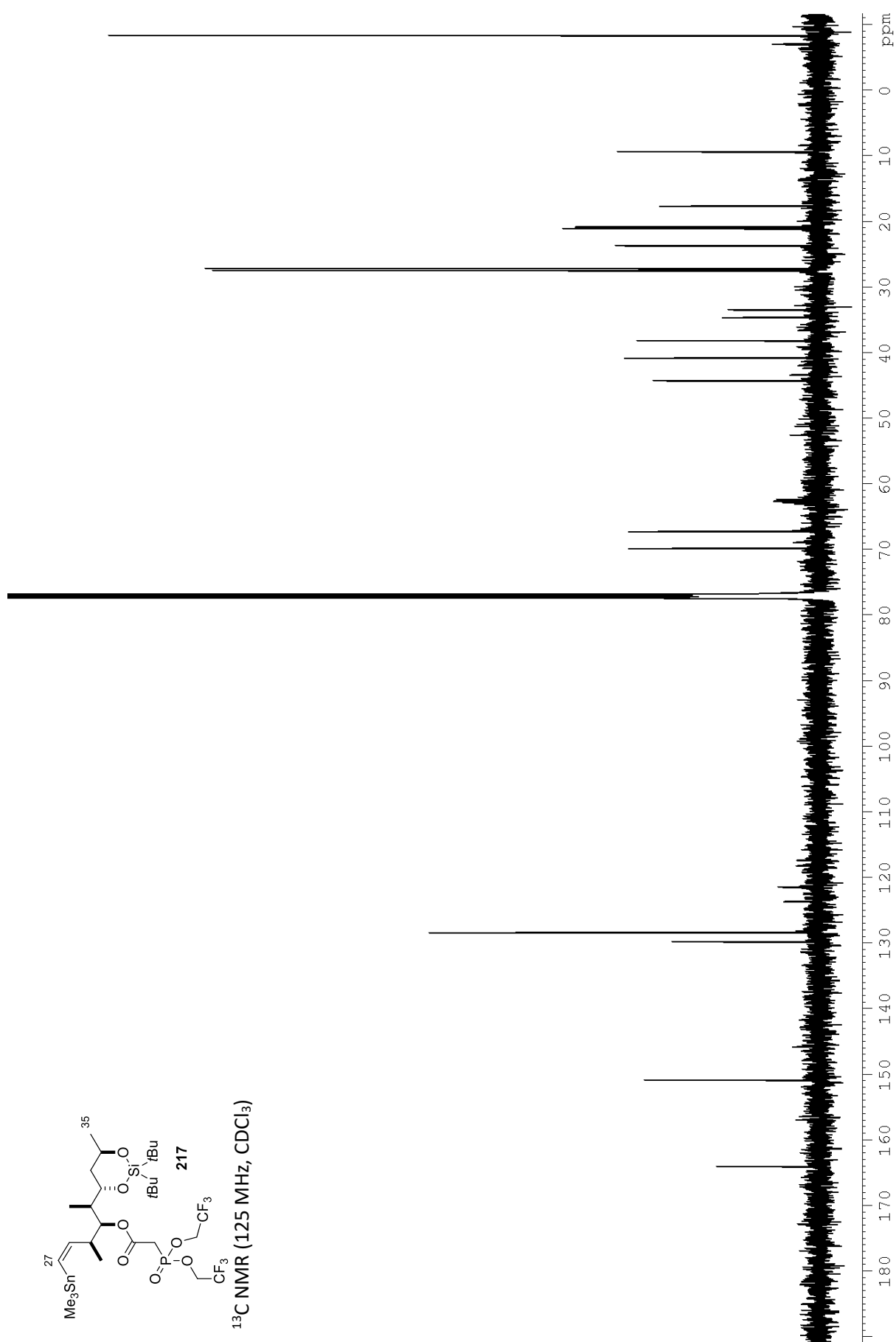


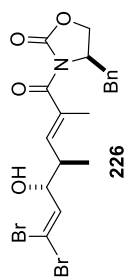
^1H NMR (500 MHz, CDCl_3)



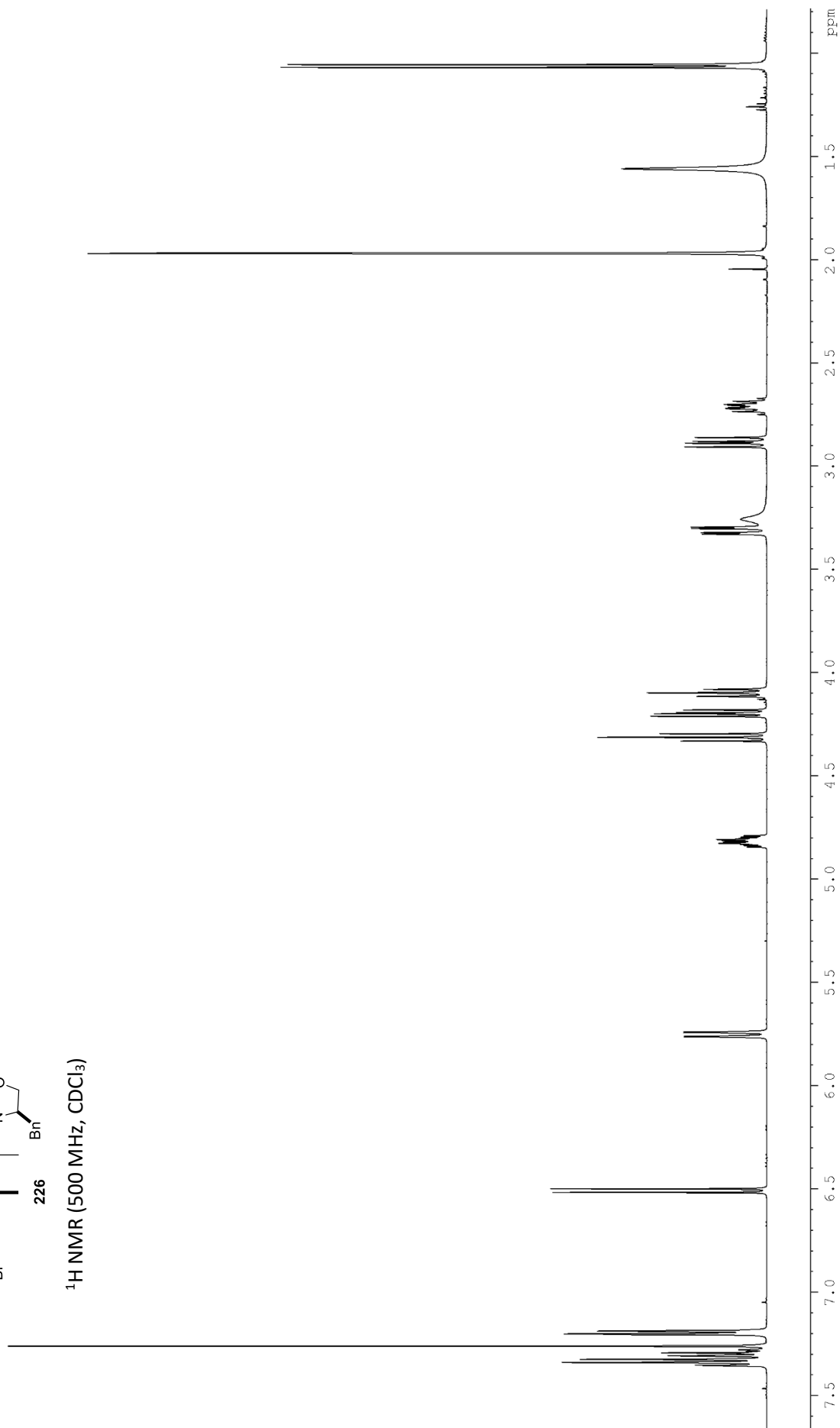


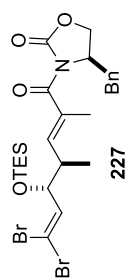
¹³C NMR (125 MHz, CDCl₃)



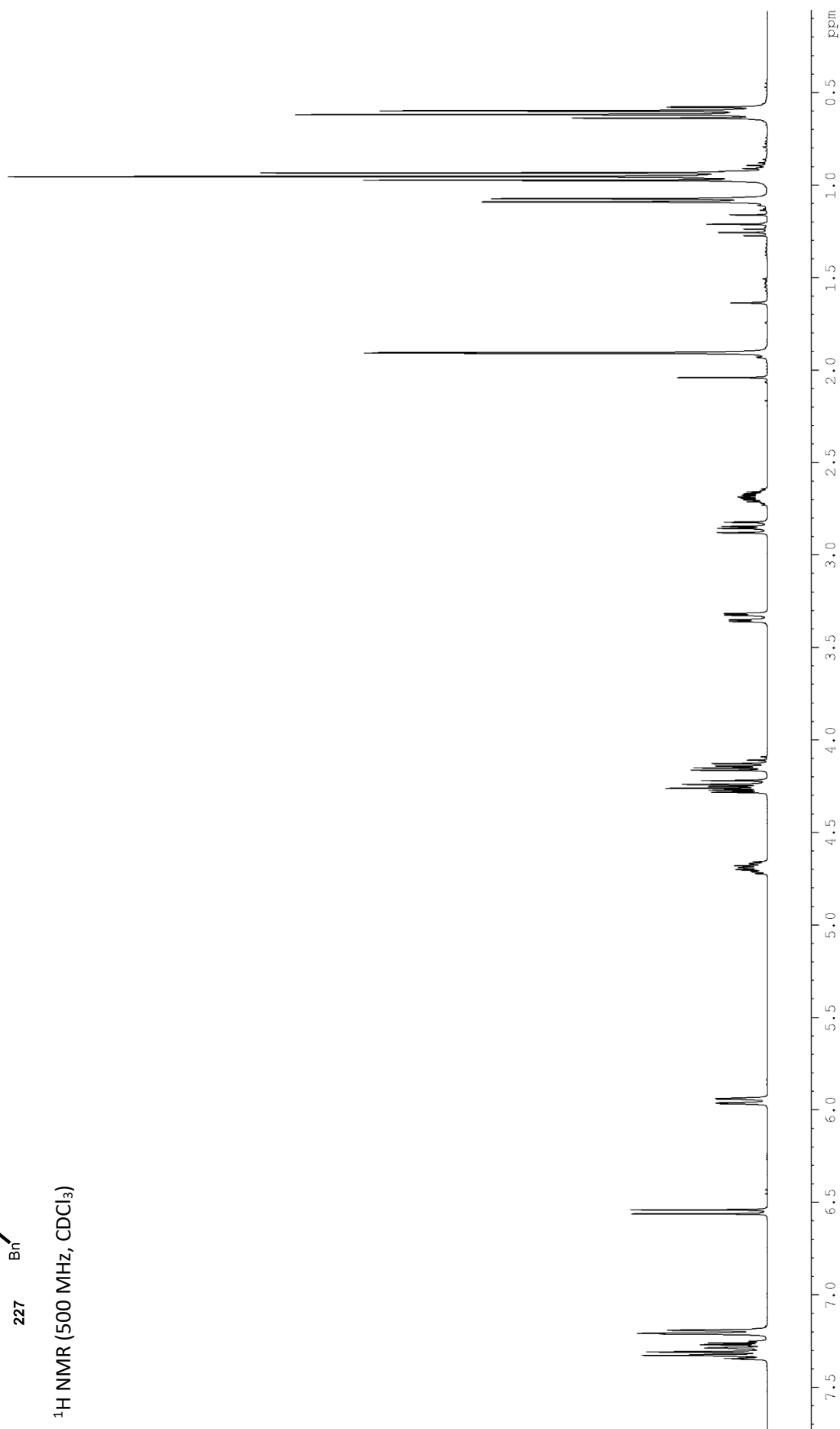


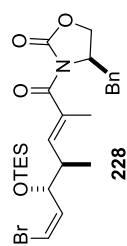
¹H NMR (500 MHz, CDCl₃)



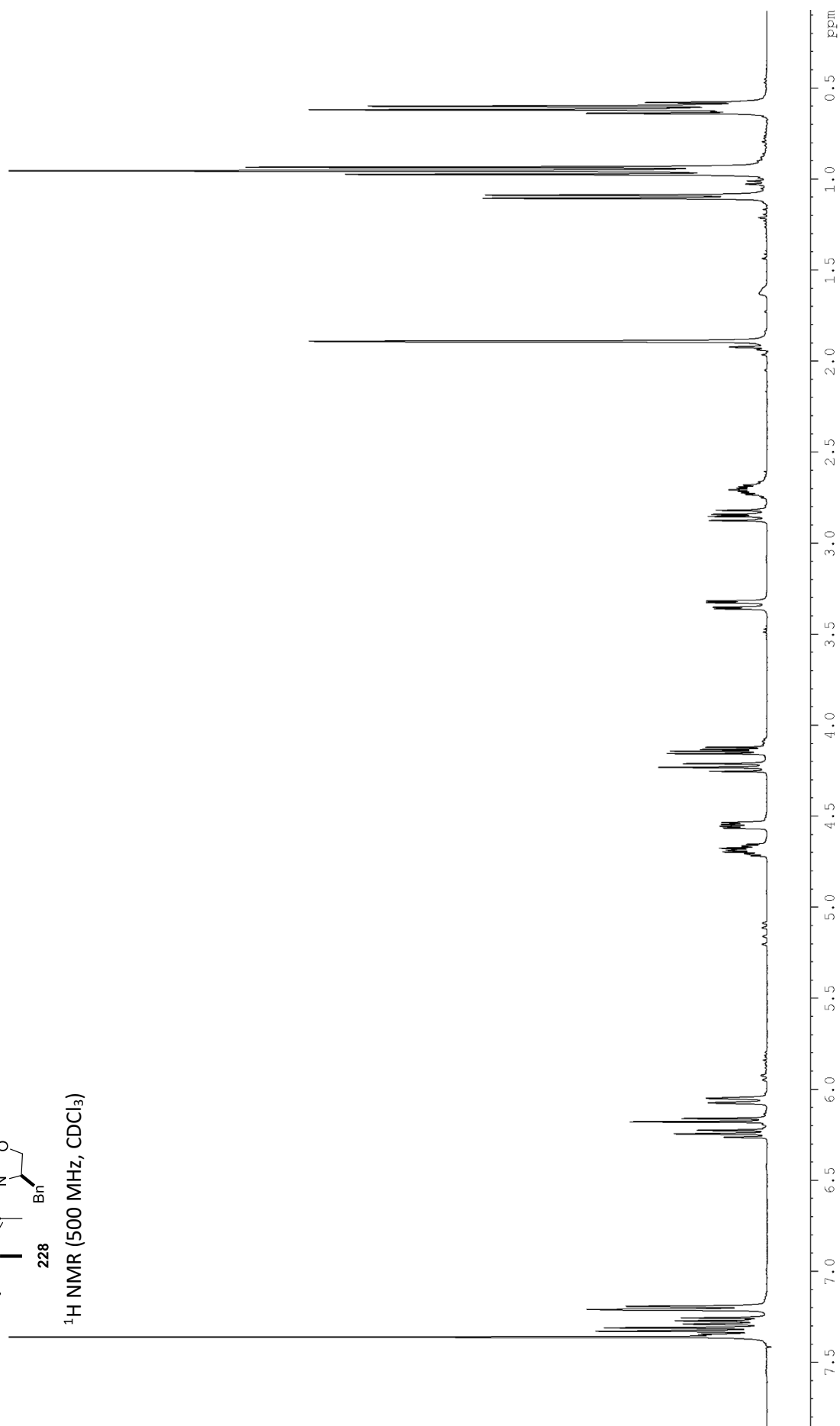


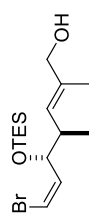
¹H NMR (500 MHz, CDCl₃)





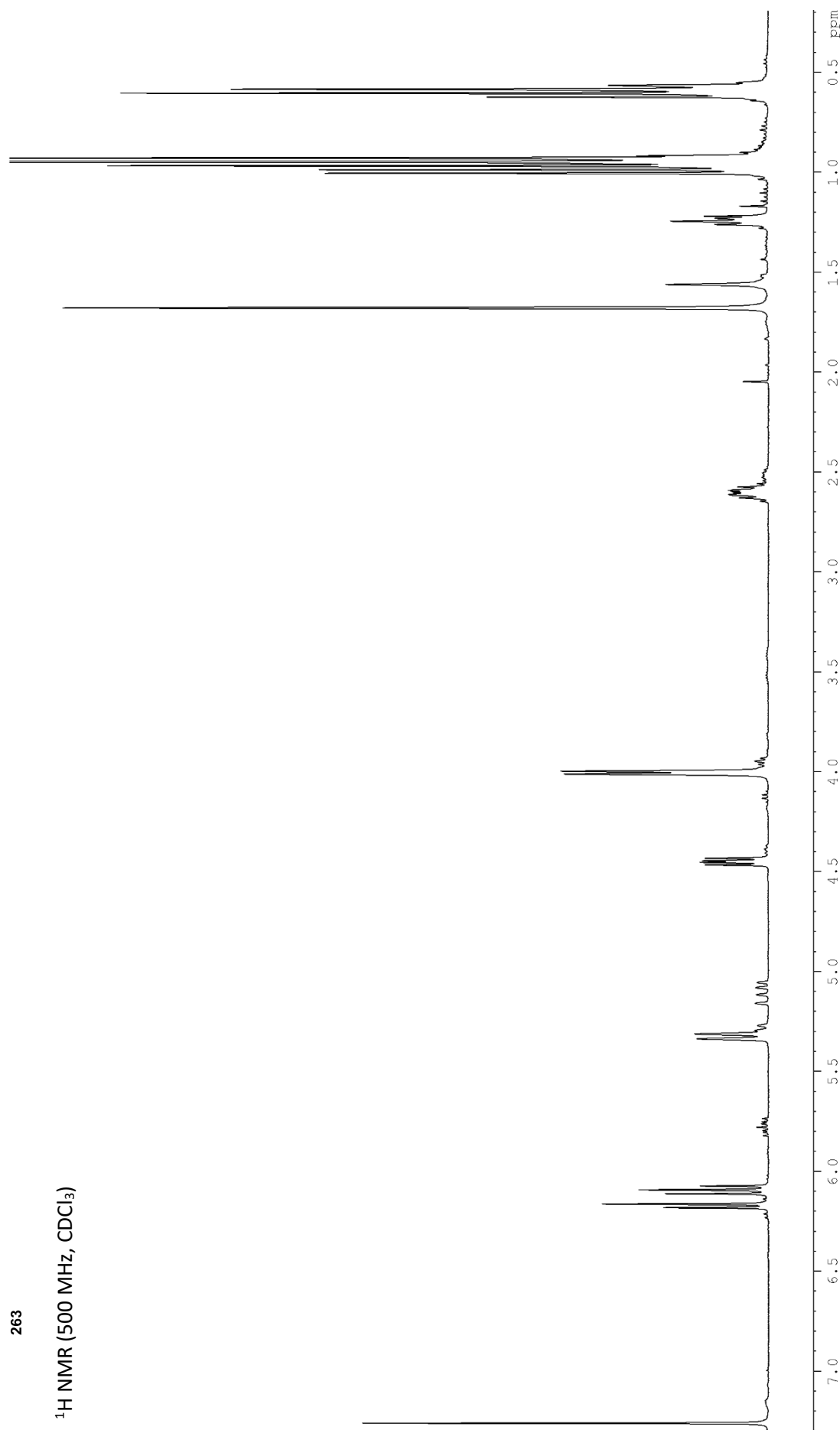
¹H NMR (500 MHz, CDCl₃)

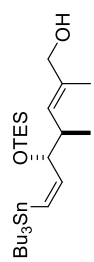




263

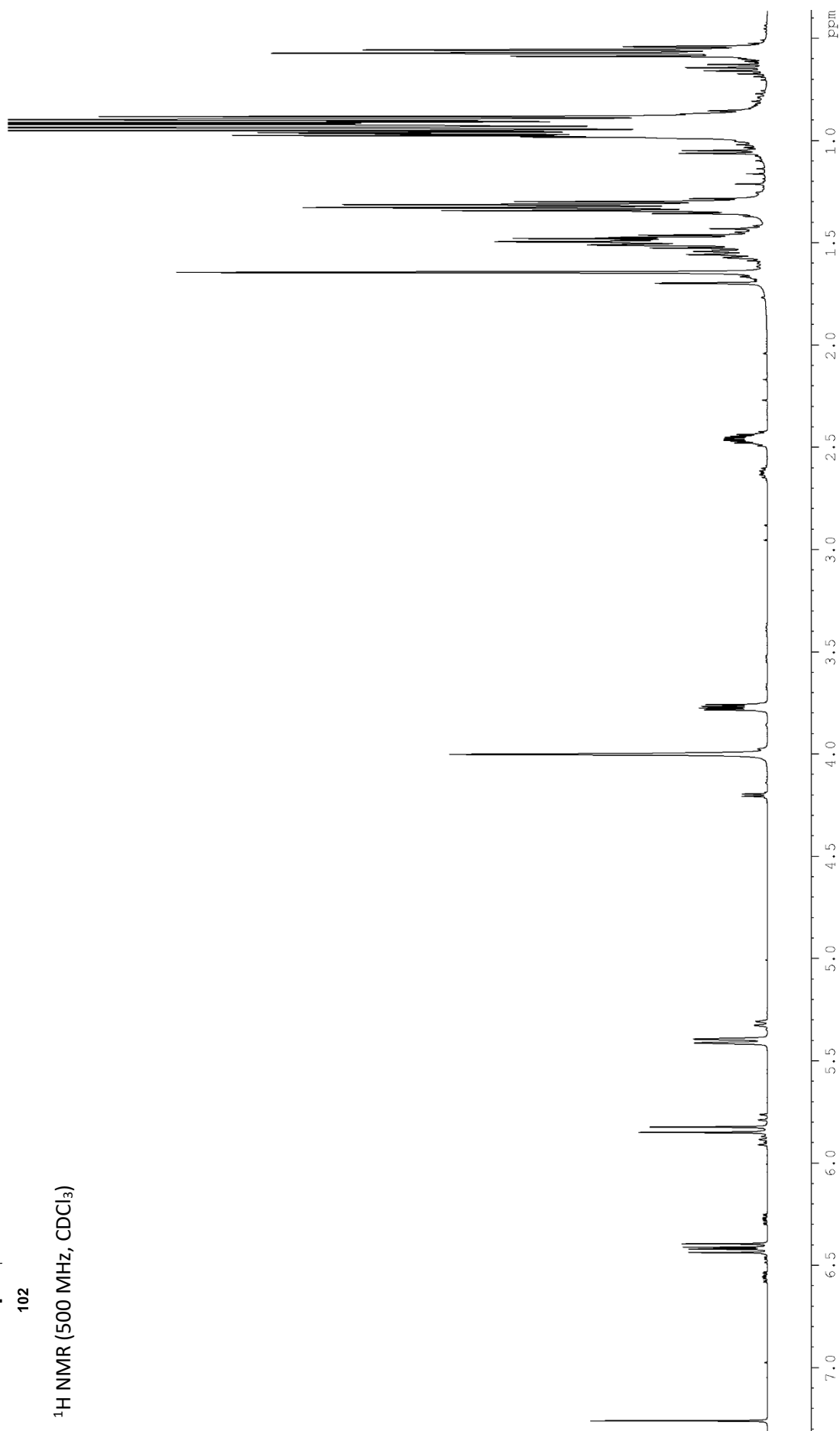
¹H NMR (500 MHz, CDCl₃)

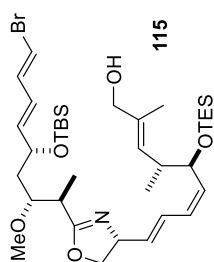




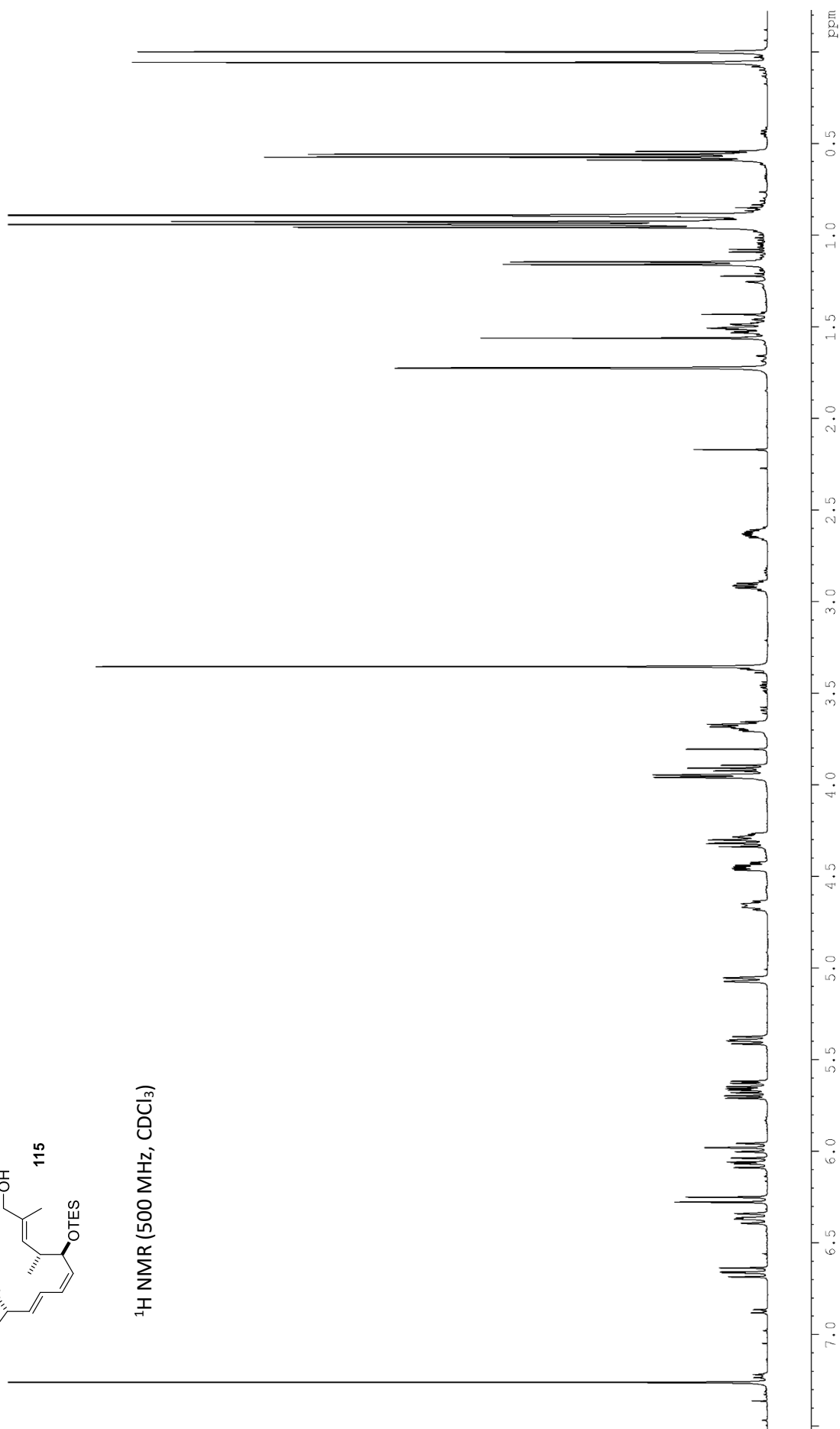
102

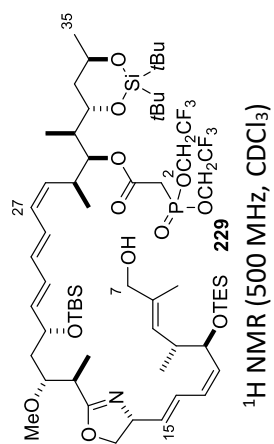
^1H NMR (500 MHz, CDCl_3)



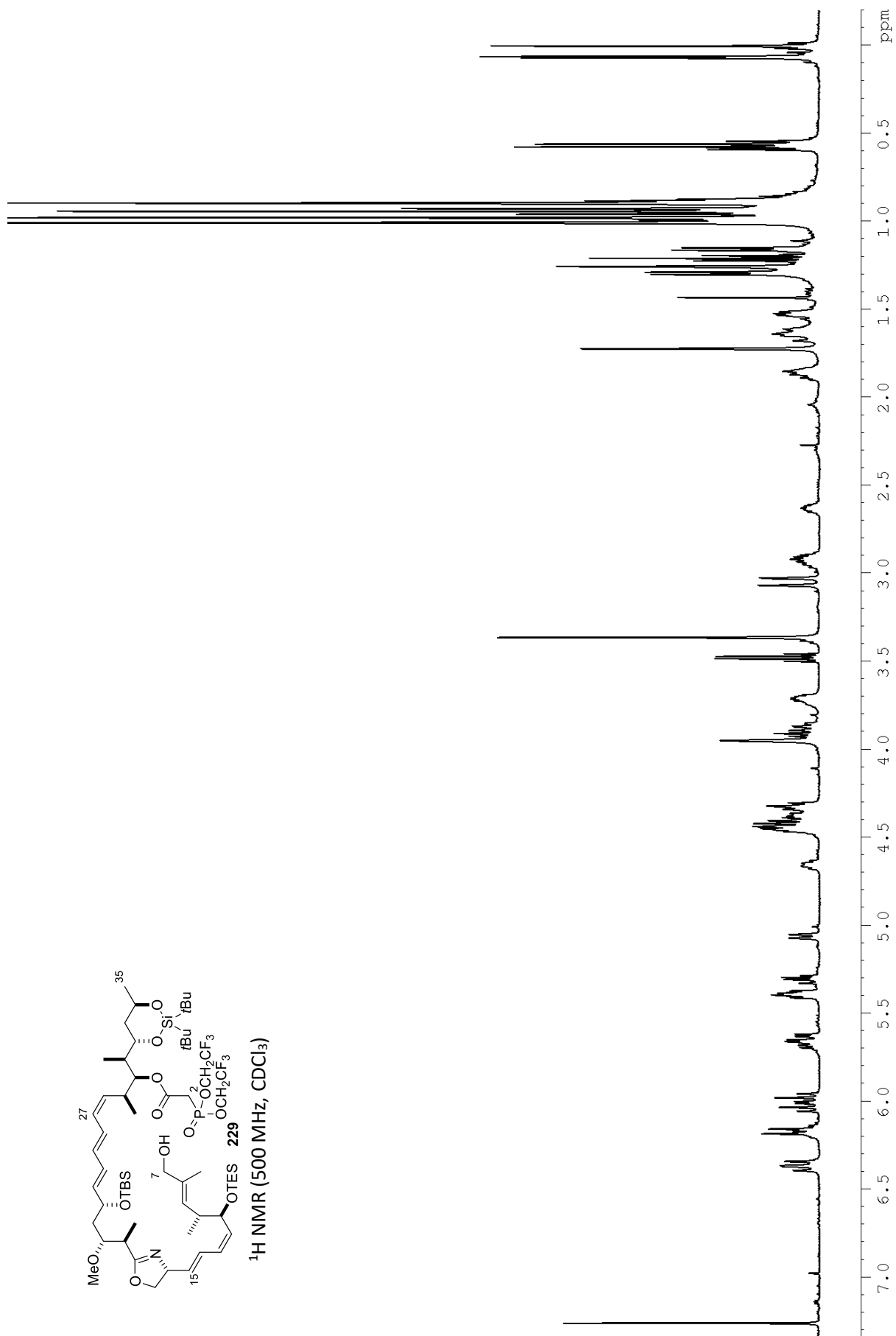


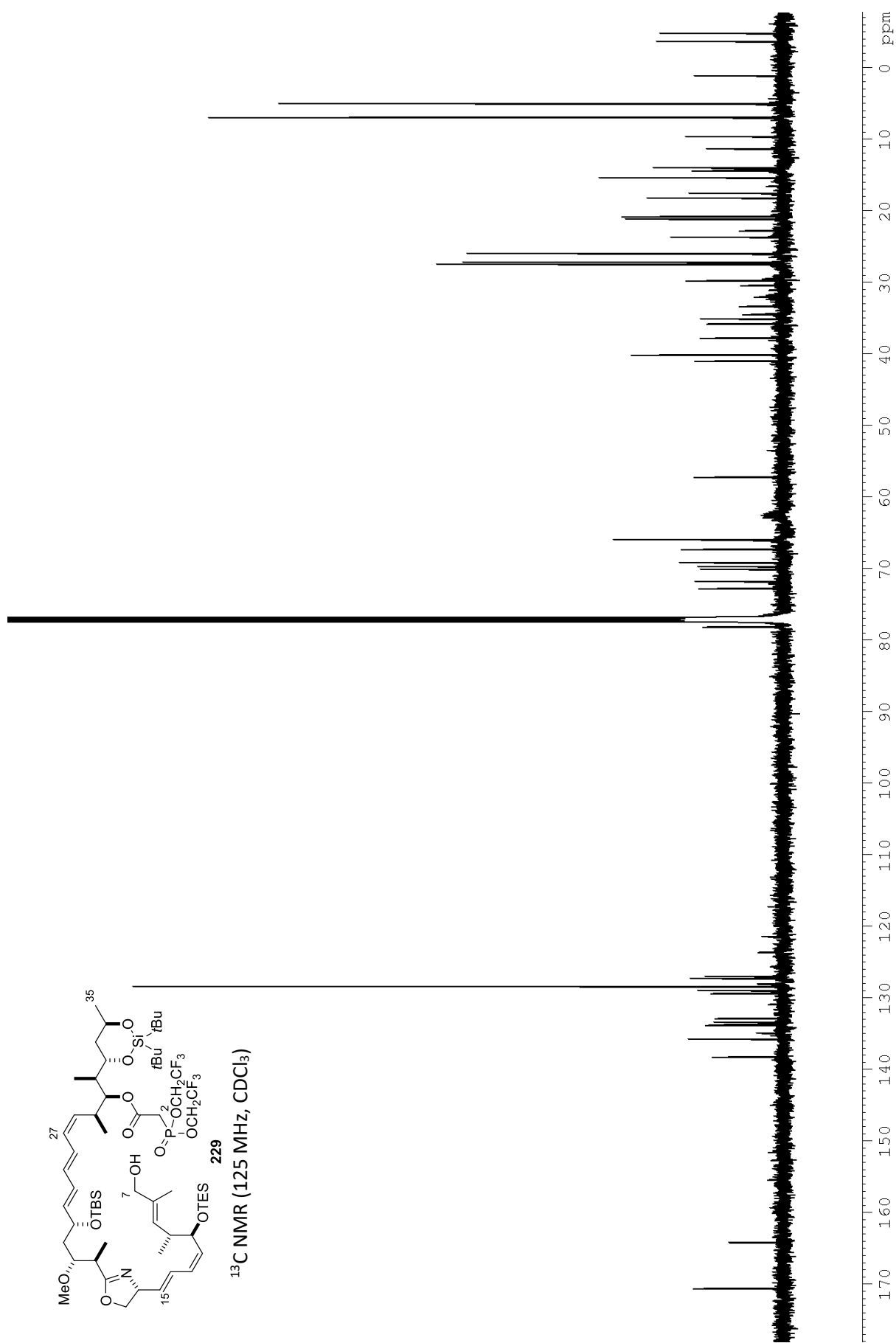
^1H NMR (500 MHz, CDCl_3)

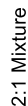




¹H NMR (500 MHz, CDCl₃)

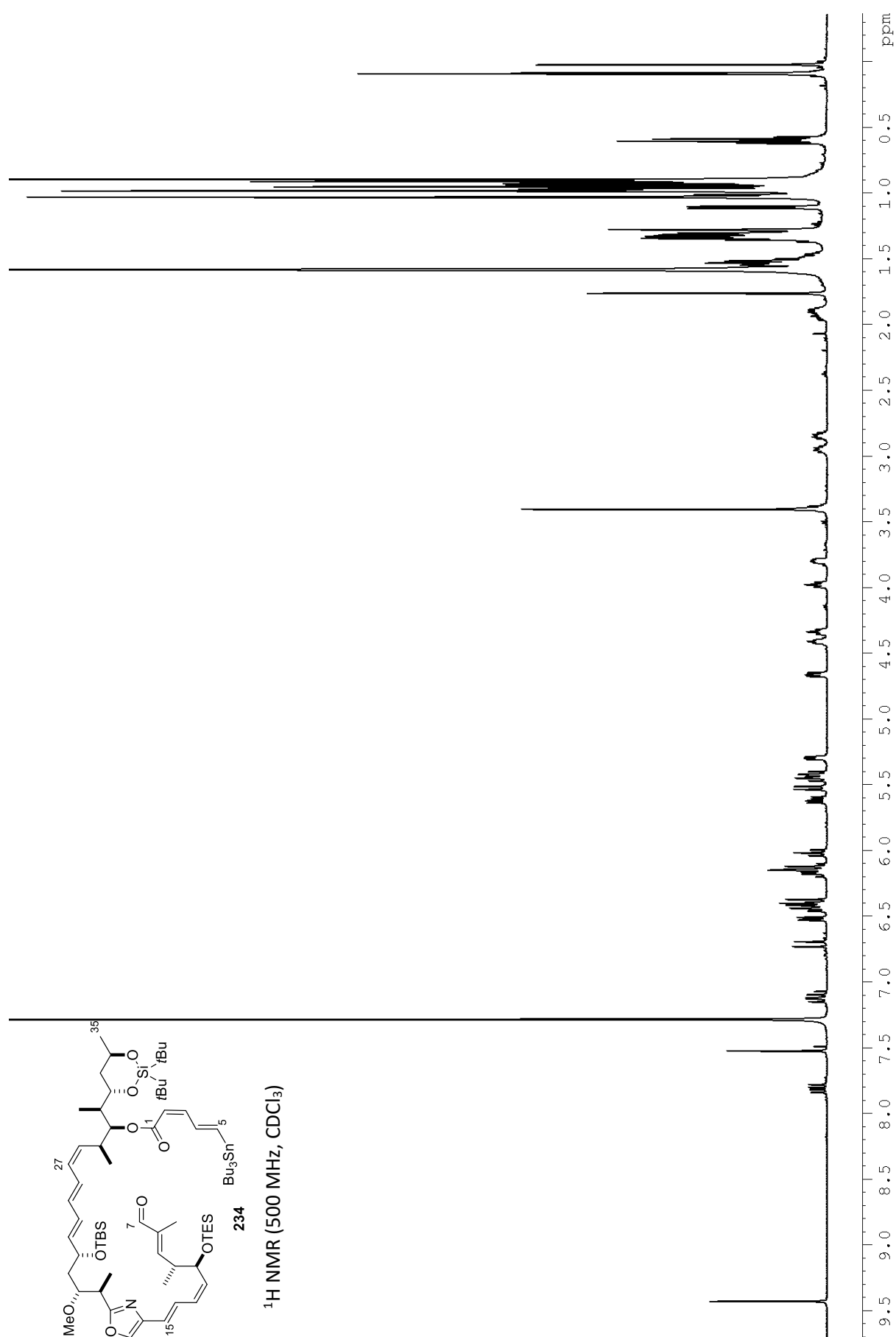


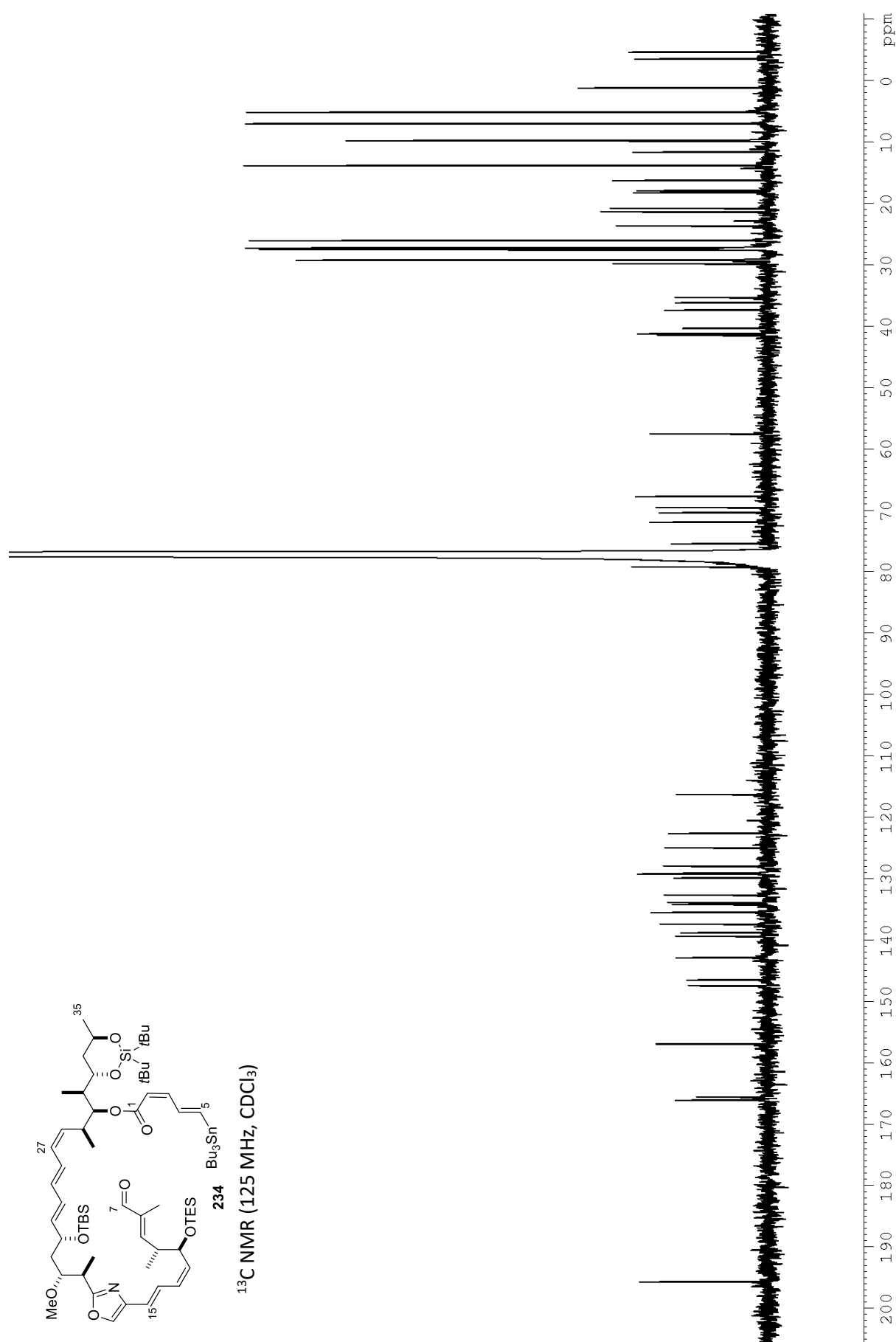


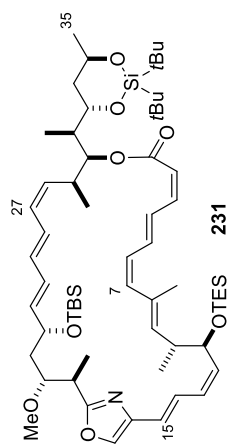


2

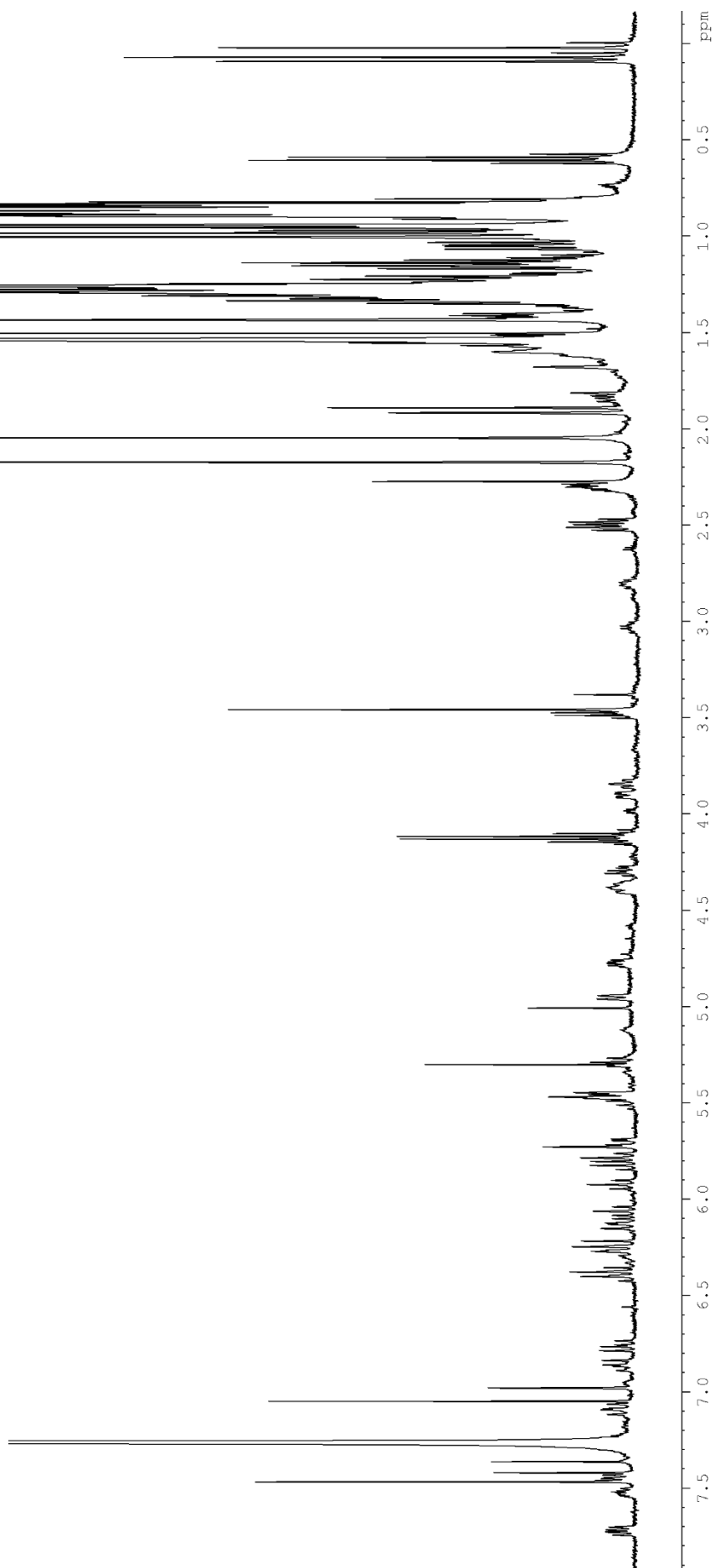


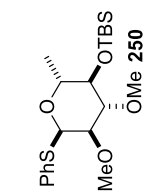




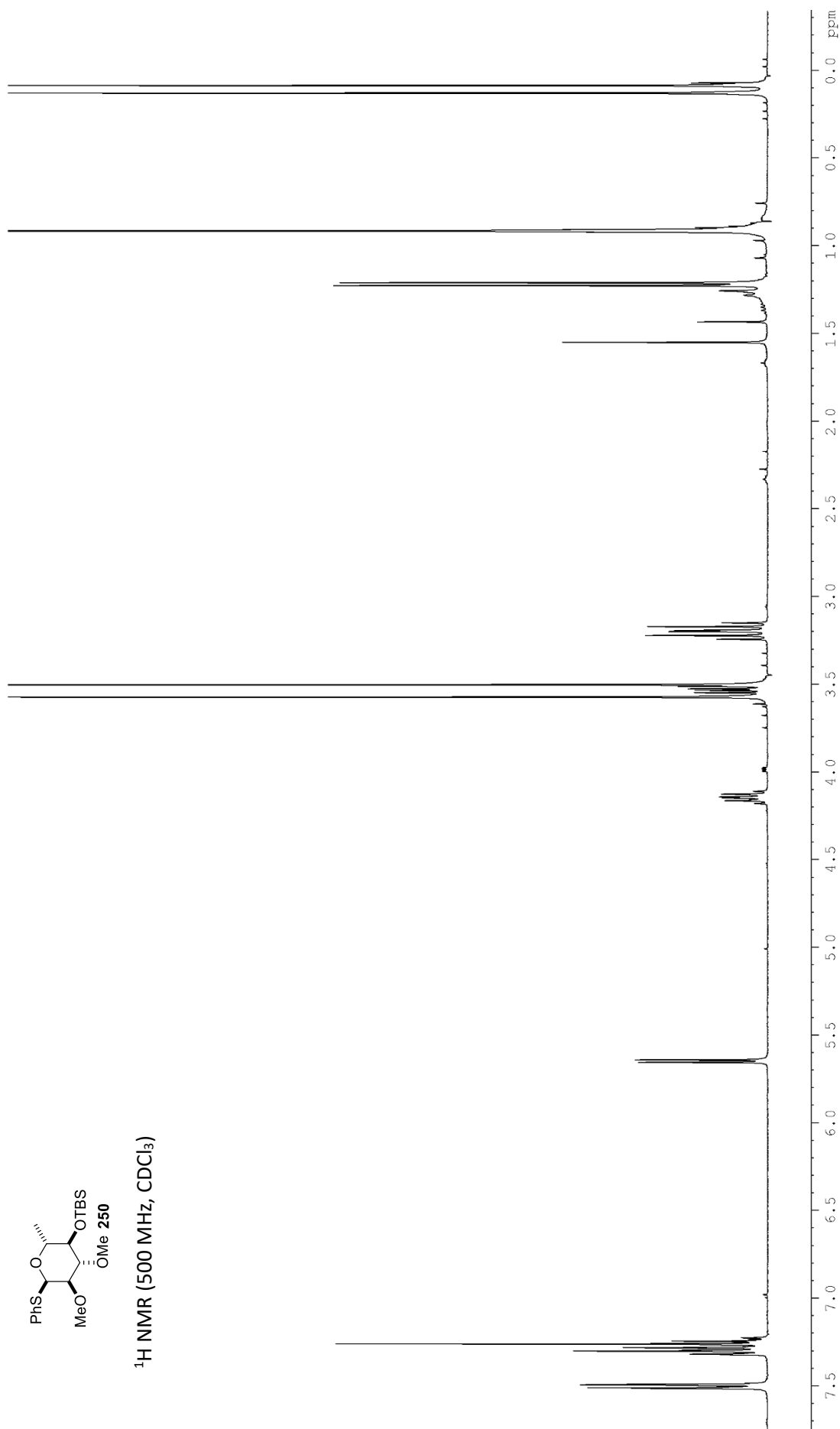


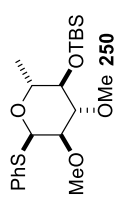
^1H NMR (500 MHz, CDCl_3)



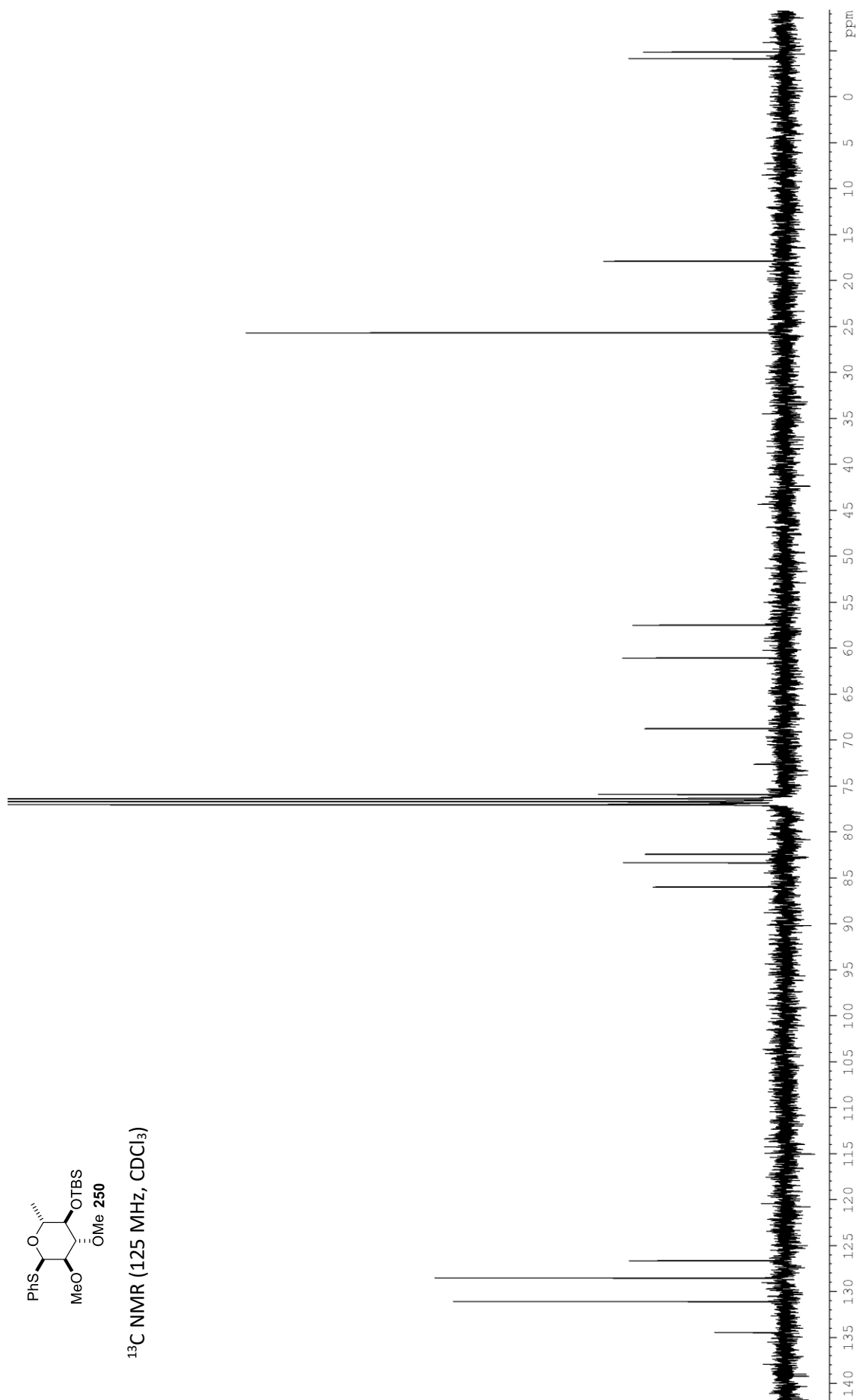


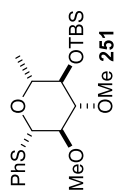
¹H NMR (500 MHz, CDCl₃)



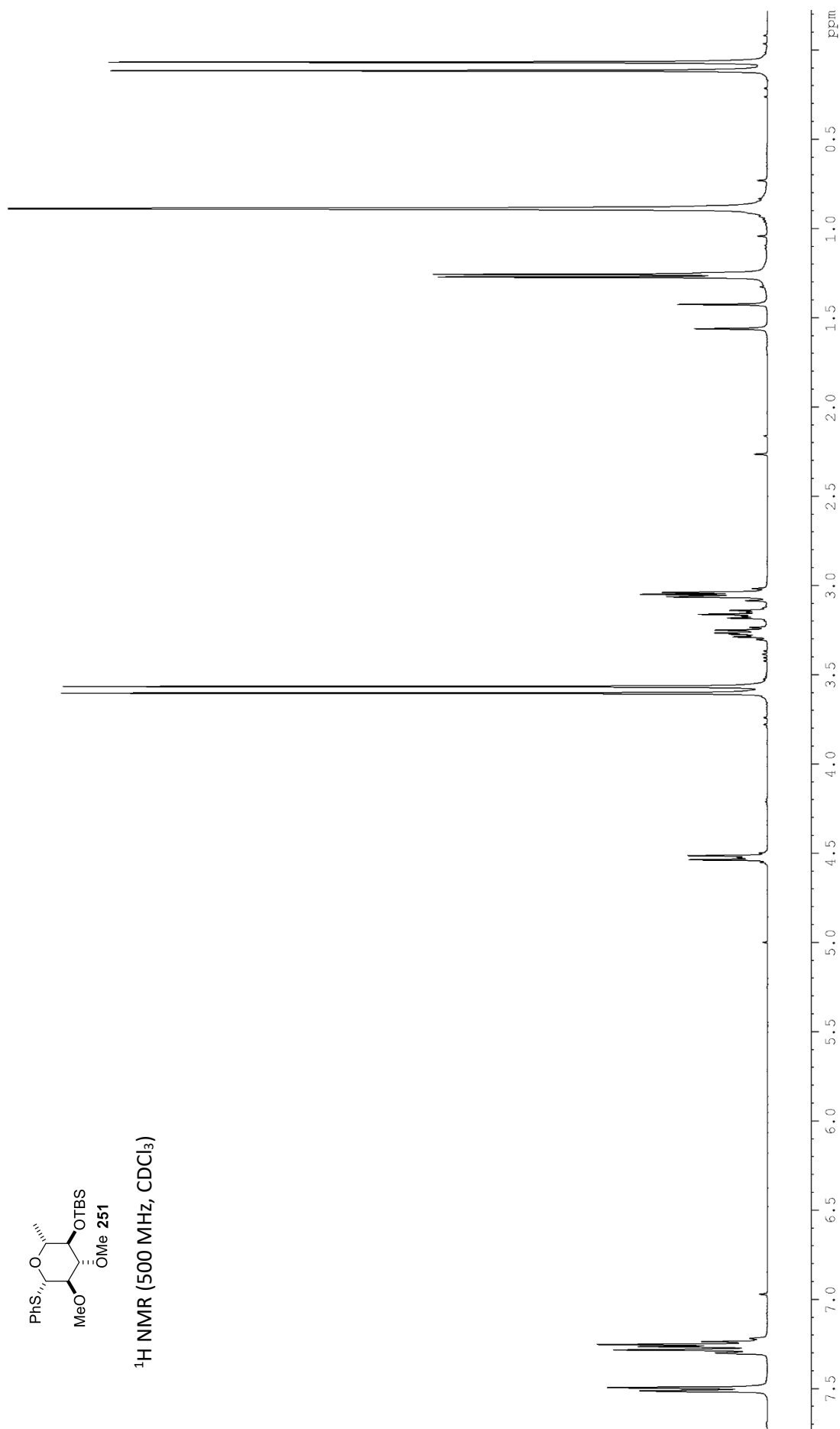


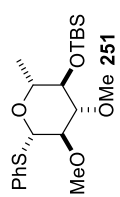
¹³C NMR (125 MHz, CDCl₃)



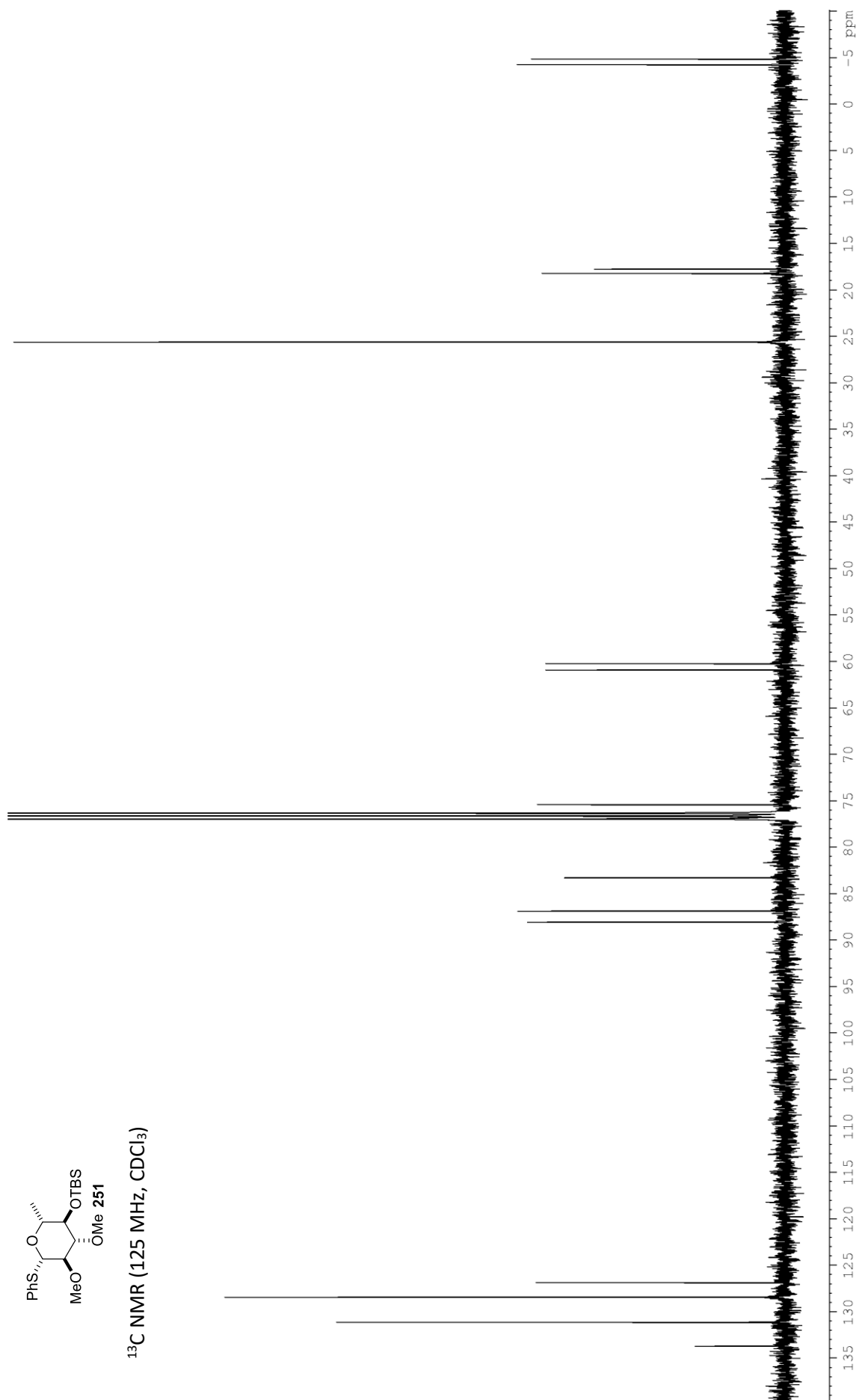


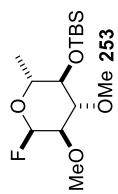
¹H NMR (500 MHz, CDCl₃)



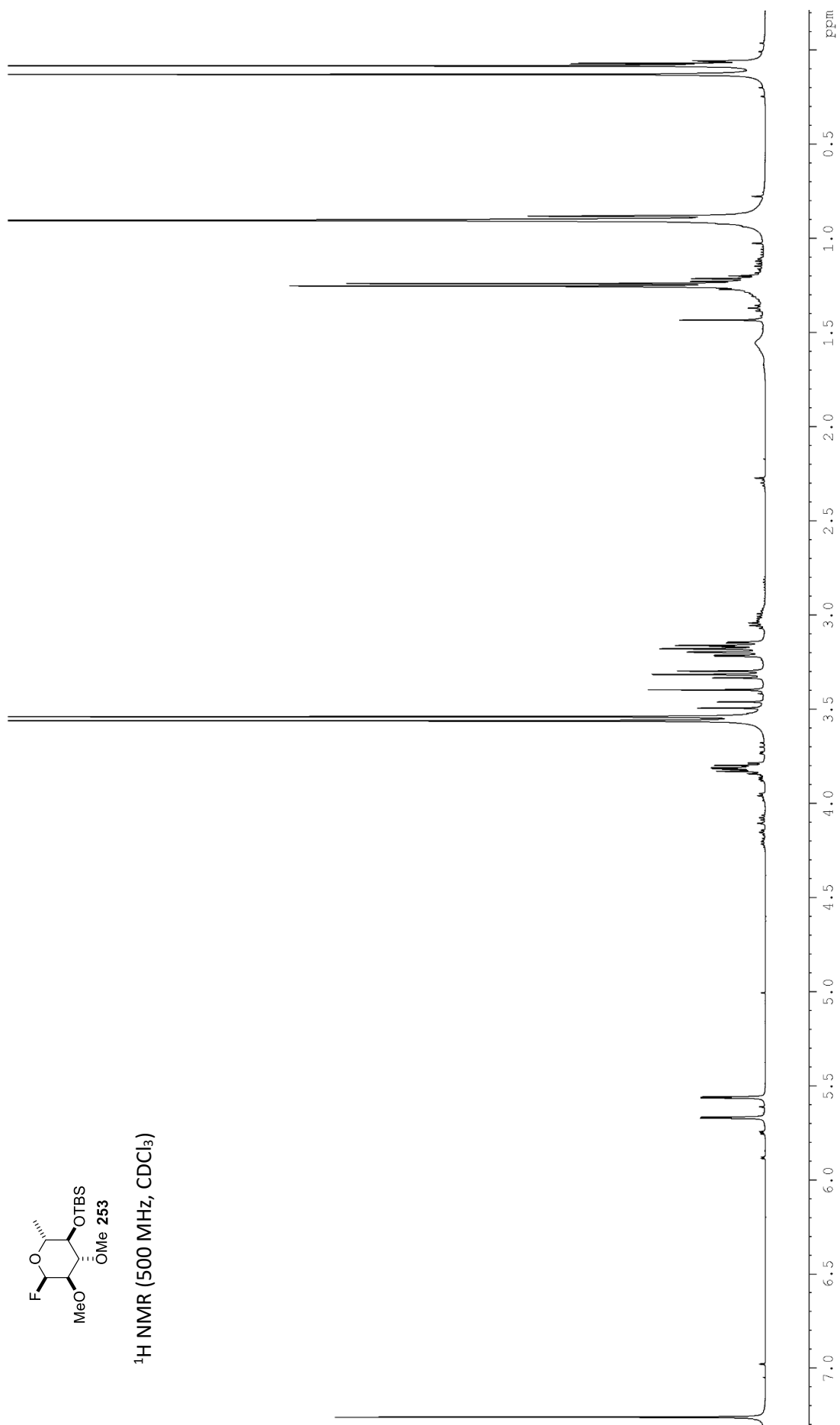


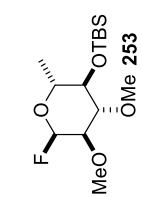
¹³C NMR (125 MHz, CDCl₃)



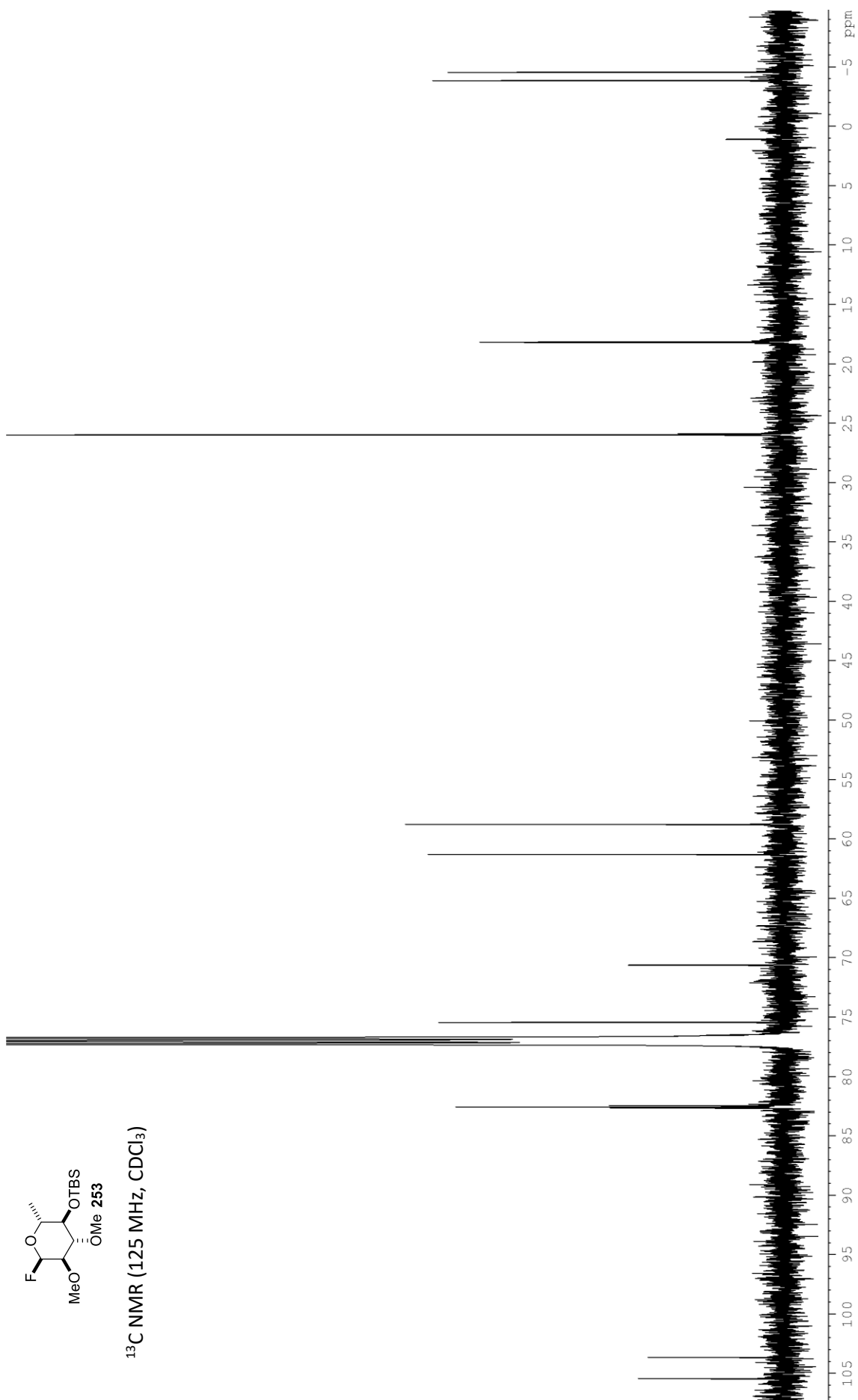


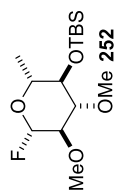
¹H NMR (500 MHz, CDCl₃)



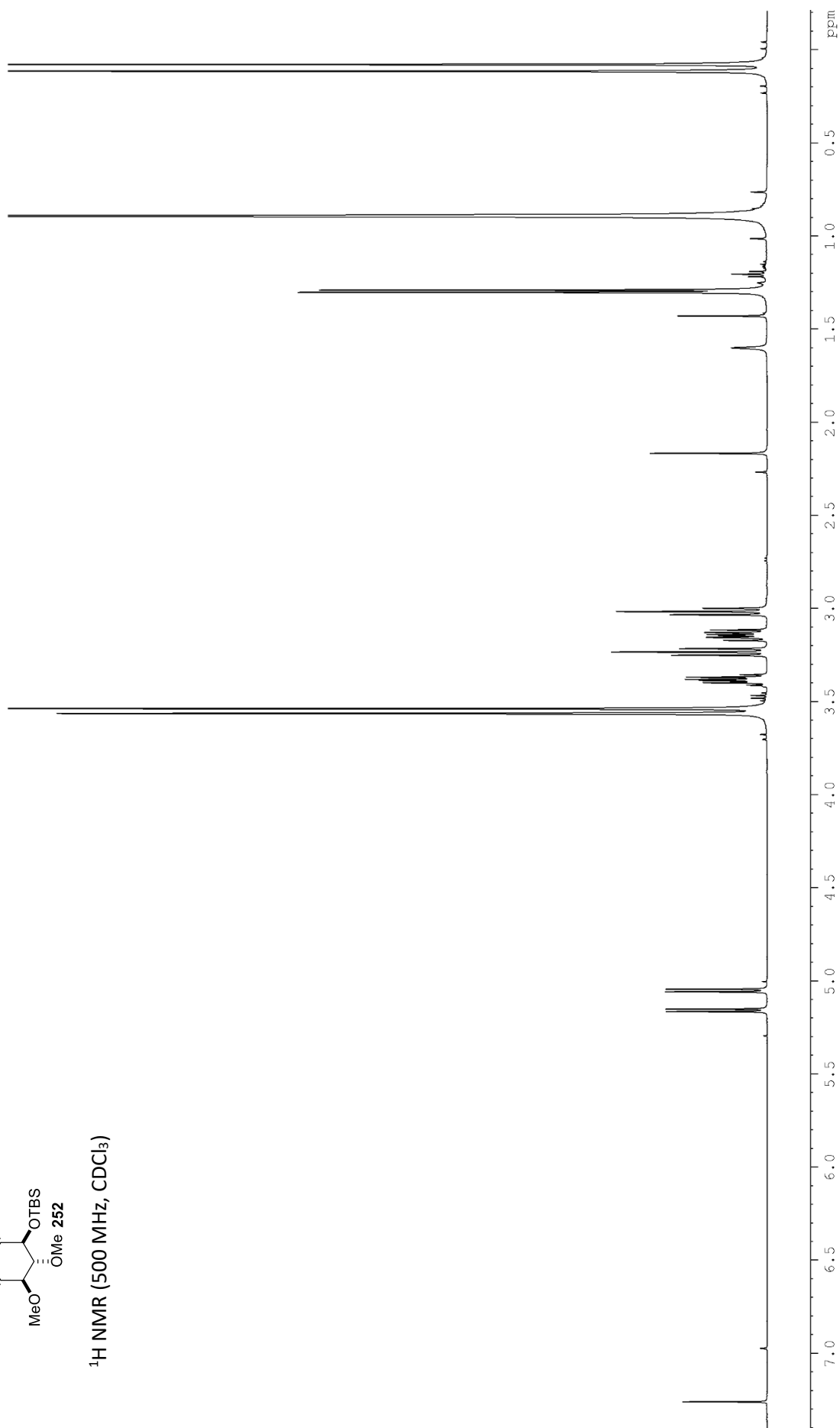


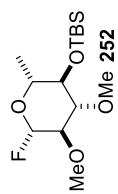
¹³C NMR (125 MHz, CDCl₃)



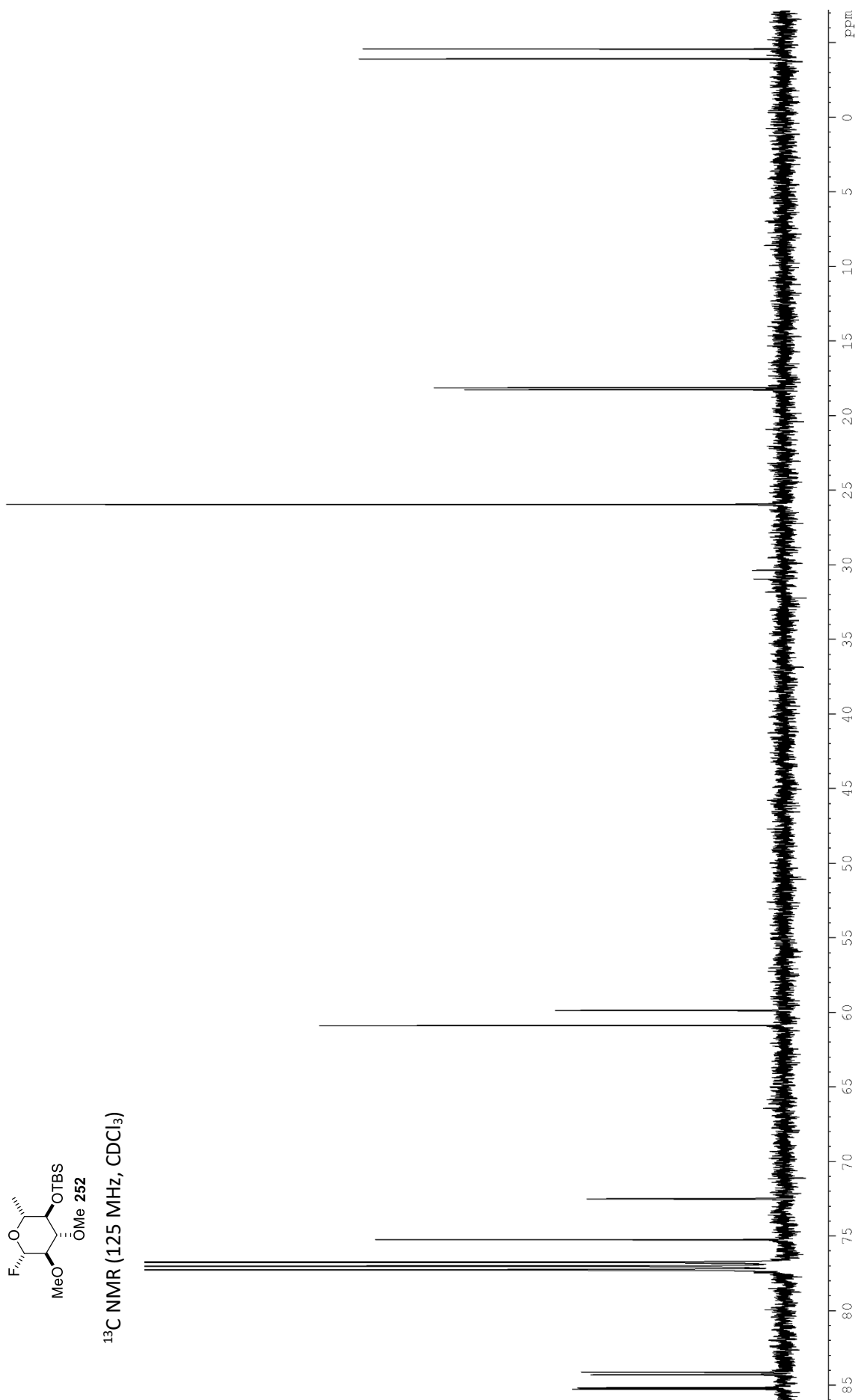


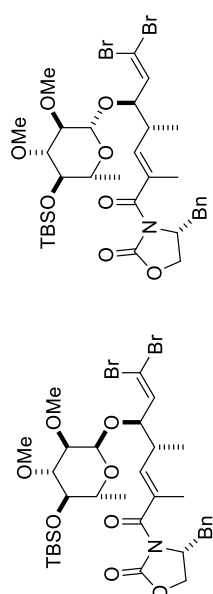
¹H NMR (500 MHz, CDCl₃)





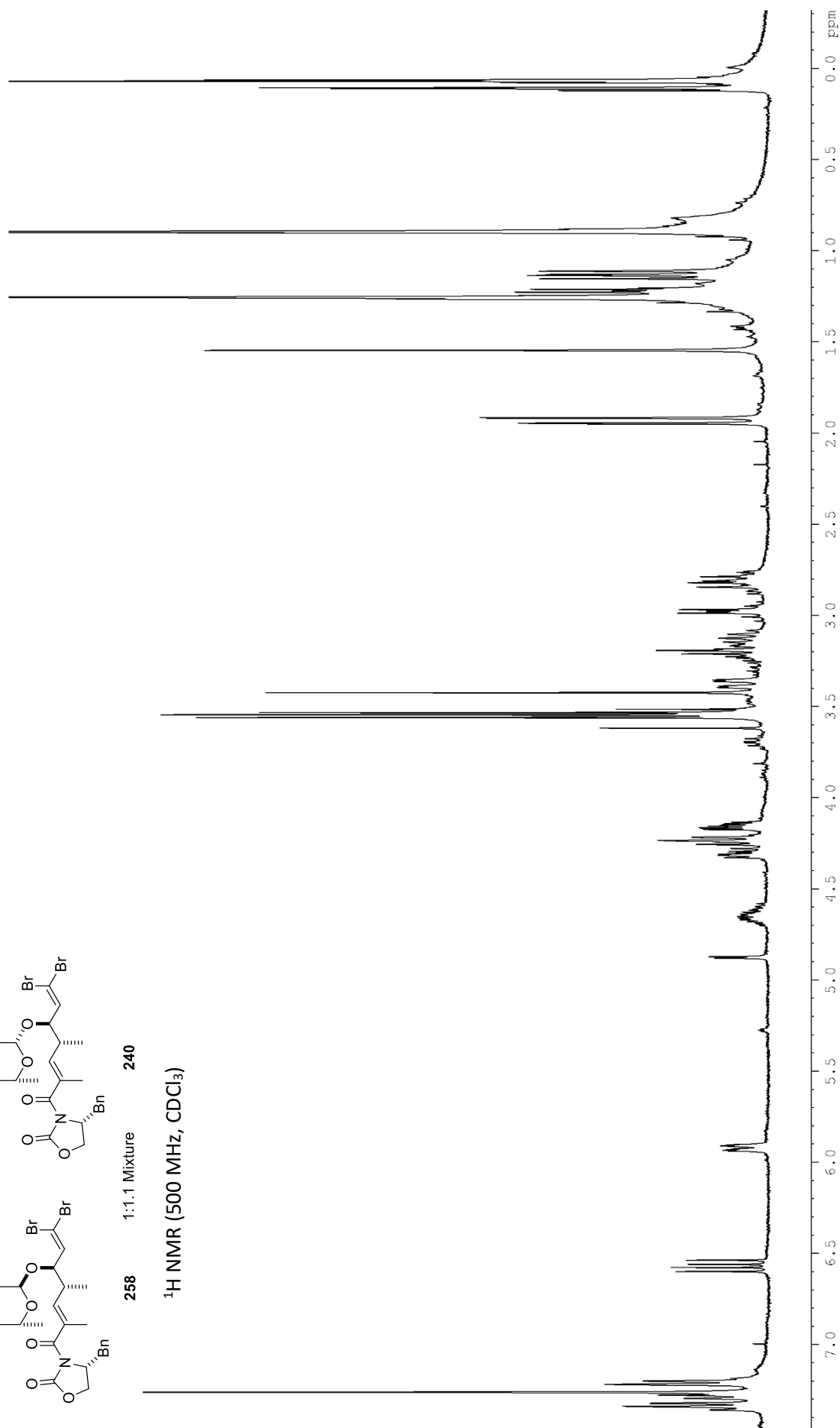
¹³C NMR (125 MHz, CDCl₃)

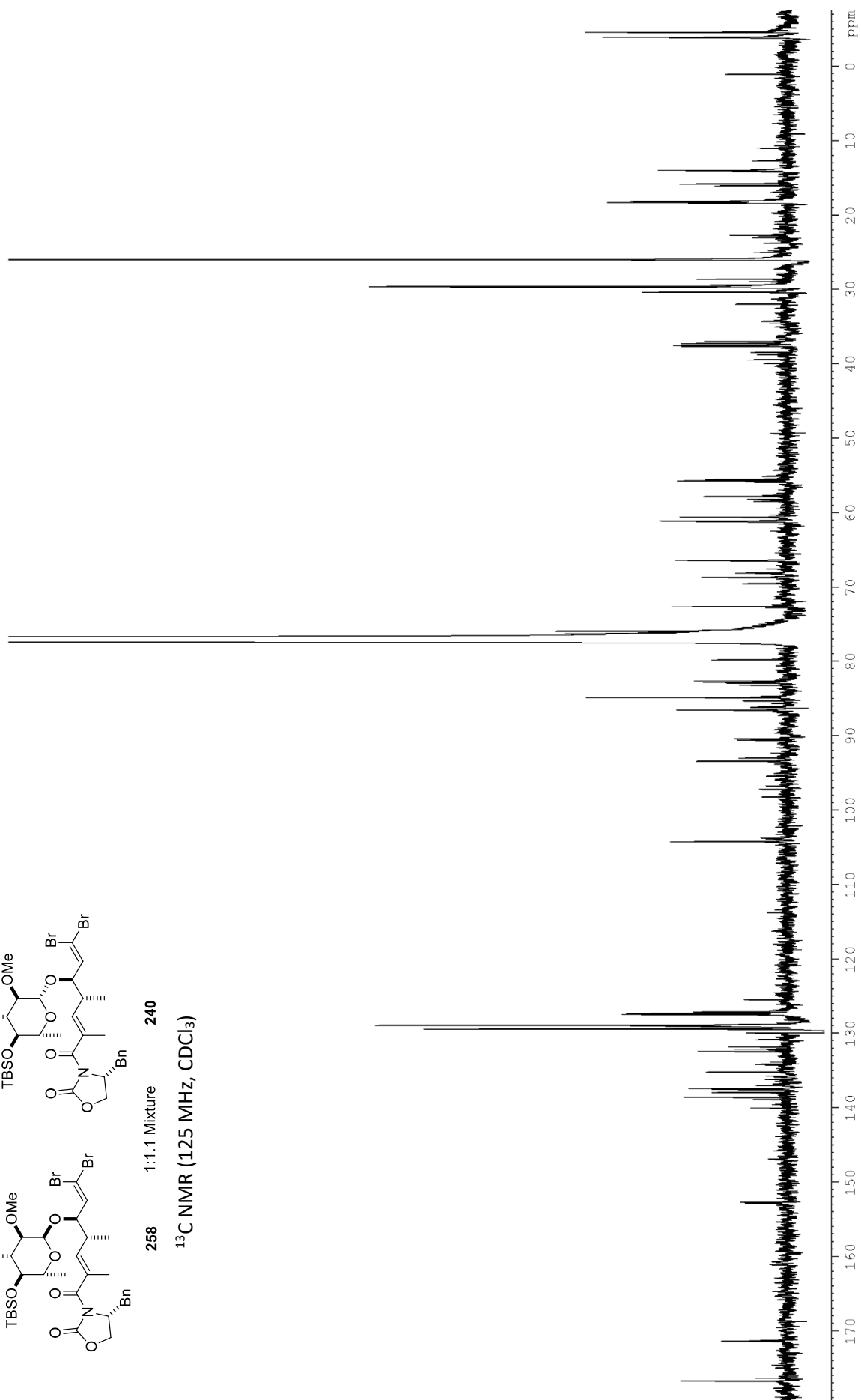
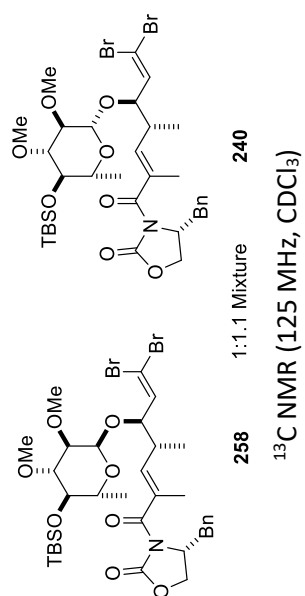


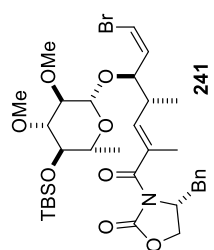


258 1:1.1 Mixture 240

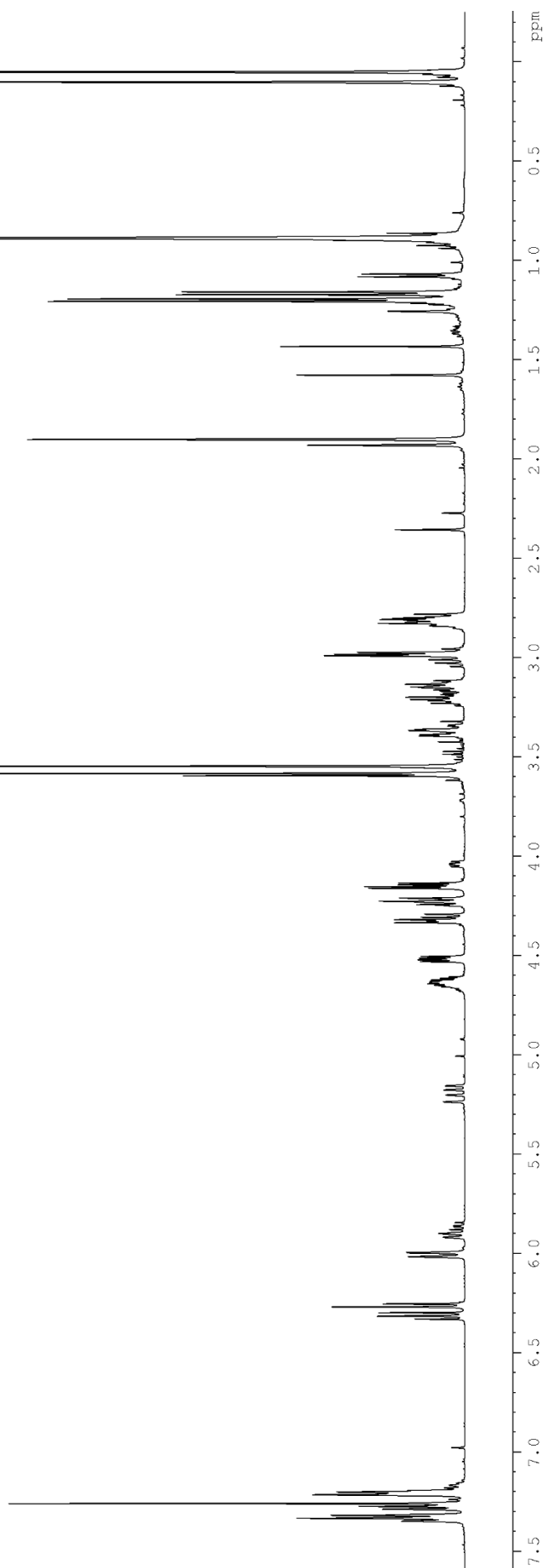
^1H NMR (500 MHz, CDCl_3)

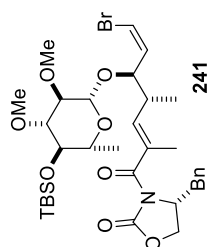






241
¹H NMR (500 MHz, CDCl₃)





241

^{13}C NMR (125 MHz, CDCl_3)

